Homogeneous and Stratified Vented Gas Explosions

by

Sarah Willacy, B.Sc.

Submitted in accordance with the requirements for the degree of
Doctor of Philosophy

Energy and Resources Research Institute
School of Process, Environment and Materials Engineering
University of Leeds

Under the supervision of:
Dr. H.N. Phylaktou, Ph.D., B.Eng., and
Prof. G.E. Andrews, Ph.D., B.Sc., C.Eng, M.I.MechE, SMAIAA, MASME, MSAE

February 2008

Dedicated to family and friends

Abstract

Explosion tests were carried out in four medium-scale test-vessels incorporating closed, vented, duct vented and interconnected vessels. A systematic investigation into the influence of homogeneous and stratified mixtures was undertaken by varying mixture reactivity, ignition position, injection position and mixture composition.

A feature of this work has been the similarities in explosion phenomena between stratified and homogeneous explosions and between partially filled and fully filled geometries to the conclusion that the explosion severity recorded in stratified mixtures towards the lean flammability limit was in many cases much higher than the fuel concentration would normally suggest.

Stratified mixtures with global equivalence ratio around stoichiometric produced significantly lower pressures than their homogeneous equivalents. However, stratified (globally) near-limit mixtures produced overpressures that were several hundred mbar higher than those of the equivalent homogeneous mixtures. Even beyond the flammable range (globally) the stratified mixtures produced significant overpressures.

The phenomena discussed in this thesis illustrate the difficulty in designing adequate protection for such vented, duct vented and interconnected geometries, since even relatively small pocket of weak fuel-air mixtures produced relatively severe explosions. This can have implications for the safety design of inter-connected installations which are not intended to be subject to flammable mixtures.

While it is an important conclusion from the work presented in this chapter that close to the flammability limits the stratified explosion severity was greater than its global concentration would normally indicate, it should be stressed that homogeneous stoichiometric tests still constitute the worst case tests. Therefore, it is not the suggestion of this work that the design of vented vessels should be modified to represent the maxima obtained in stratified work. However, the value of this research in the field of post-explosion investigation is clear.

Publications by the Author

1. Ferrara, G., Willacy, S.K., Phylaktou, H.N., Andrews, G.E., Di Benedetto, A. and Salzano, E. 'Venting of premixed gas explosions with a relief pipe of the same area as the vent.' Proceedings of the European Combustion Meeting ECM2005 (CD format), Louvain-la-Neuve, Belgium. Paper #213, April 2005.

2. Ferrara, G., Willacy, S.K., Phylaktou, H.N., Andrews, G.E., Di Benedetto, A. and Mkpadi, M. 'Duct-vented propane/air explosions with central and rear ignition.' Proceedings of the International Association for Fire Safety Science Symposium IAFSSS2005, Beijing, China, September 2005.

3. Ferrara, G., Willacy, S.K., Phylaktou, H.N., Andrews, G.E., Di Benedetto, A. and Salzano, E. 'Venting of Gas Explosions Through Releif Ducts: Interaction Between Internal and External Explosions' in Journal of Hazardous Materials, 2008, v155, pp358-368.

4. Kasmani, R. M, Willacy, S. K, Phylaktou, H. N and Andrews, G. E, 'Self Accelerating Gas Flames in Large Vented Explosion Volumes That are Not Accounted for in Current Vent Design Correlations.' Proceedings of the 2nd International Conference on Safety & Environment in Process Industry, Naples, Italy, May 2006.

5. Kasmani, R.M, Andrews, G.E., Phylaktou, H.N. and Willacy, S.K., 'Influence of Static Burst Pressure and Ignition Position on Dust-Vented Gas Explosions.' Proceedings of the 5th International Seminar on Fire and Explosion Hazards, Edinburgh, UK, April 2007.

6. Kasmani, R.M, Andrews, G.E., Phylaktou, H.N. and Willacy, S.K., 'Hydrocarbon-air in Duct Vented Explosion.' Proceedings of the European Combustion Meeting ECM2007 (CD format), Crete, April 2007.

7. Kasmani, R.M, Andrews, G.E., Phylaktou, H.N. and Willacy, S.K., 'Vented Explosions with a Vent Duct of Twice the Diameter of the Vent in a Vessel with

an L/D of 2: Extremely Fast Turbulent Flames and High Overpressures in the Vent Duct.' Accepted for publication in the Proceedings of the European Combustion Meeting ECM2009 (CD Format), Vienna, Austria, April 2009.

8. Willacy, S.K., Phylaktou, H.N., Andrews, G.E. and Mkpadi, M.C., 'Explosions in a partially filled interconnected vessel using methane-air in the lean to stoichiometric range.' Proceedings of the European Combustion Meeting ECM2005 (CD format), Louvain-la-Neuve, Belgium. Paper #196, April 2005.

9. Willacy, S.K., Ferrara, G., Phylaktou, H.N., Andrews, G.E. and Mkpadi, M.C., 'Medium Scale Duct Vented Explosions of Stratified Propane-Air Mixtures.' Proceedings of the European Combustion Meeting ECM2005 (CD format), Louvain-la-Neuve, Belgium. Paper #211, April 2005.

10. Willacy, S.K., Phylaktou, H.N., Andrews, G.E., and Mkpadi, M.C. 'Detonation of Hydrogen in a Partially Filled Interconnecting Vessel Following an Initial Period of Pressure Piling' in Combustion Science and Technology, 2006, Vol. 178:10-11, pp1191-1926.

11. Willacy, S.K., Phylaktou, H.N., Andrews, G.E. and Mkpadi, M.C., 'Partially Filled Interconnected Vessel Explosions: Methane-Air in the Lean to Stoichiometric Range' in Journal of the Energy Institute, 2006, Vol. 79:3, pp152-157.

12. Willacy, S.K., Phylaktou, H.N., Andrews G.E., Kasmani, R.M. and Ferrara, G., 'Stratified Propane-Air Explosions of Global Concentration Outside Normal Flammability Limits.' Proceedings of the 2nd International Conference on Safety & Environment in Process Industry, Naples, Italy, May 2006.

13. Willacy, S.K., Phylaktou, H.N., Andrews, G.E. and Ferrara, G., 'Ignition of Stratified Propane-Air Explosions in a Duct Vented Geometry: Effect of Concentration, Ignition and Injection Position' in IChemE B: Process Safety and Environmental Protection, 2007, 85(B2), pp153-161.

14. Willacy, S.K., Phylaktou, H.N., Kasmani, R.M and Andrews, G.E., 'Propane-Air Explosions in a Partially Filled Interconnected Vessel.' Proceedings of the 5th International Seminar on Fire and Explosion Hazards, Edinburgh, UK, April 2007.

15. Willacy, S.K., Phylaktou, H.N., Kasmani, R.M. and Andrews, G.E., 'Comparison Between Simply Vented and Duct Vented Stratified Propane Explosions.' Proceedings of the European Combustion Meeting ECM2007 (CD format), Crete, April 2007.

Contents

List of Figures

List of Tables

Nomenclature

A	Area (m^2)
A_s	Internal surface area of an enclosure (m_2)
A_v	Area of vent (m^2)
c	Speed of sound
C	Venting equation constant
Cp	Specific heat capacity (J/Kg/K)
D	Diameter (m)
(dP/dt)	Rate of pressure change (bar/s)
$(dP/dt)_{max}$	Maximum rate of pressure rise (bar/s)
E	Expansion factor
f	Frequency (Hz)
h	Height (m)
k	Thermal conductivity
K_G	Deflagration index for gases
K_{st}	Deflagration index for dusts
K_v	Vent Coefficient (A/A_v)or ($V^{2/3}/A_v$)
L	Length (m)
Le	Lewis number
m	Molecular weight
Ma	Mach number
Mb	Mass burnt
n	Number of moles

P	Pressure (bar)
p	Porosity
Pa	Ambient pressure (bar)
P_{max}	Maximum overpressure (barg)
P_{red}	Reduced overpressure (barg)
R	Gas Constant (= 8.314 J mol^{-1} K^{-1})
r	Vessel radius (m)
Re	Reynolds number
S_f	Flame speed
S_g	Unburnt gas velocity
S_L	Laminar burning velocity
S_T	Turbulent burning velocity
S_u	Laminar burning velocity (m/s)
T	Temperature (K)
t	Time (s)
t_0	Time of ignition (s)
T_n	Thermocouple (with position number n)
U	Mean flow velocity – steady state
u'	Root mean square (rms) value of the fluctuating component of velocity
V	Volume (m^3)
v	Viscosity
w	Molecular weight
x	Distance (m)

Subscript

a	denotes ambient conditions (not necessarily the same as initial)
b	denotes burnt gas
d	Relating to the dump volume
duct	Relating to the duct
i	not necessarily the same as ambient
max	Maximum value recorded
red	Value reduced by venting
u	denotes unburnt gas
primary	Relating to the primary vessel
in	Entrance to the duct/connecting pipe
out	Exit of the duct/connecting pipe

Greek

Φ	Equivalence ratio
γ	Ratio of specific heat at constant P to that at constant V
ρ	Density (kg/m^3)
ΔP	Pressure differential (bar)
χ	Turbulisation factor

Preface

This thesis presents new experimental research conducted into homogeneous and stratified gas explosions in vented vessels. The Chapters 1 and 2 provide background to the experimental sections of this document. The primary aim or this research was to research the effects of stratified propane-air explosions within a duct vented geometry, which is an area not previously investigated. In order to give this research some basis, tests were also conducted on isolated and simply vented vessels in addition to the duct vented. Furthermore, methane and hydrogen tests were gradually introduced through the configurations. In addition to the stratified tests, homogeneous tests were also performed where possible to give a base line severity by which to compare the stratified tests. As a further pilot study, tests were also conducted on partially filled interconnected vessels which constitutes the next progressive step in this research. A more detailed breakdown of the content of each chapter is provided below.

Chapter 1 provides a brief introduction into the current problem of explosions and explosion research.

Chapter 2 provides a more in depth background to research into the field of explosions, specifically concentrating on stratified gas explosion research conducted to date, and specifically for methane, propane and hydrogen-air mixtures within the vessel geometries investigated in the current research. These include isolated, simply vented and duct vented geometries, along with more complex interconnected geometries. Finally, research into stratified gas explosions is considered

In **Chapter 3**, the experimental and design details for the equipment, instrumentation and methodology used in the research conducted in this lab has been discussed in detail. This chapter also focuses on safety considerations and concerns.

Chapter 4 provides a small study of stratified and homogeneous propane-air explosions within an isolated vessel. The tests presented in this chapter give some baseline data used for assessing the effectiveness of the venting techniques on homogeneous and stratified explosions.

Chapter 5 contains primary experimental research into stratified and homogeneous explosions in a simply vented vessel. The work conducted on this geometry is slightly more extensive than for the isolated vessel. End ignition of initially quiescent homogeneous and stratified propane-air mixtures is the primary concern. Although methane-air mixtures with end ignition are examined briefly. The results presented in this chapter form the basis of comparison between the closed vessel tests in Chapter 4 and the following chapter on duct vented explosions, which is the main focus of this thesis.

Chapter 6 details the work done into stratified mixtures in a duct vented vessel using propane-air mixtures. The reason for the main focus lying with propane is the lack of published experimental data dealing with stratified mixtures within a duct vented geometry. This chapter provides the greatest number of experimental test data and expands variables to include fuel reactivity, overall concentration (including global concentrations which would be out of the flammable range under homogeneous conditions), fuel injection position and ignition position.

Chapter 7 is the final experimental chapter. This chapter is a study of partially filled interconnected geometries using a range of reactivity gases. This chapter deals with another important realistic explosion risk scenario, where an explosive mixture is formed in one chamber of a two chamber vessel. The mixtures for this chapter are homogeneous at this stage.

Finally, **Chapter 8** details the main conclusions of the research and outlines several important research directions for future advancement.

Acknowledgements

I would like to thank my supervisors, Dr Roth Phylaktou and Professor. Gordon Andrews, for allowing me the opportunity to undertake this study. Their advice and encouragement throughout this study is gratefully acknowledged.

Thanks is also expressed to Mr Robert Boreham, for his technical expertise and skill helped to overcome several design problems throughout this project.

I would like to thank the EPSRC for providing a scholarship, without which this research could not have been undertaken.

My deepest thanks go to Dan, who has patiently taken a back seat recently and who has painstakingly produced many of the 3D diagrams which illustrate this work. His unfaltering patience and understanding and proof-reading skills have been invaluable to the completion of this thesis.

Finally, mention is made to my fellow postgraduates throughout the department, who provided a welcome distraction throughout the first three years of the research.

CHAPTER 1:

THE EXPLOSION PROBLEM

1.1. Introduction

Current industrial process plants, both onshore and offshore, are designed in order that any accidental explosion damage should be minimised. Complete elimination of an explosion risk is almost impossible to achieve. Therefore the structures must be designed either to withstand an explosion, or be protected in some manner to reduce the amount of pressure a process vessel needs to withstand. For economic reasons, it is more common to employ pressure reduction or mitigation as methods of explosion protection.

The knowledge of explosion development in homogeneous and stratified explosions, as described in this research, is of importance when developing industrial scale explosion protection measures, such as venting or automatic suppression systems. Indeed, knowledge of the flame path and explosion development is fundamental to suppression system design, in order that minimum safe distances between detection monitors and suppression firing sites are calculated correctly. Experimental research is the most fundamental method for producing the data required to make such calculations, and while modelling techniques play a large part in modern research, the need for validation against experimental data is one that will not soon be replaced.

1.2. The General Explosion Problem

An accidental explosion will take place where the conditions allow, which includes the presence of a flammable fuel in the correct proportion with an oxidant (usually air) and some ignition source. It is very difficult and often impossible to completely prevent ignition sources in all areas which may contain a flammable mixture – for example, in structures which are designed to house flammable gas storage facilities, or where a pipe within a structure fails, thereby creating an unexpected leak. Therefore, it is often necessary when, for example, designing a process plant, to build into the design certain measures to protect the plant or limit the destruction caused in the event that a flammable fuel-oxidant mixture comes into contact with an ignition source. The techniques currently employed include suppression, isolation, containment and venting.

1.3. Recent Industrial Scale Explosions

Throughout the 20th and 21st Centuries, there has been a succession of industrial explosion accidents of varying size and cost. Some of the highest profile accidents include Flixborough, Piper Alpha, Texas Oil and, most recently, Buncefield.

The Nypro (UK) Ltd. process plant explosion at Flixborough on 1 June 1974 was the result of a rupture of a temporary bypass to a process vessel, which allowed a release of heavy cyclohexane vapour to form a cloud at ground level. Subsequent ignition of this vapour resulted in the total destruction of the plant, and the loss of 28 lives.

Over a decade later, on 6 July 1988, an explosion and the ensuing fire caused the loss of 167 lives on the Piper Alpha offshore platform, which was completely destroyed in the incident. Official reports [1, 2] detail that this incident was the result of an accidental release of condensate (light oil) through a temporary flange fitted during maintenance, which had not been designed to take the full working pressure to which it was later subjected. This led to the formation of a combustible condensate cloud, confined by the obstacles within the platform, which was subsequently ignited to cause an explosion. Further destruction was caused by the fire which followed the initial explosion.

This century has seen further such accidental explosions, such as the BP oil refinery in Texas City, USA, where on 25 March 2005 an explosion partially destroyed the plant at a total cost in excess of £1 billion, in addition to the loss of 15 lives. Later the same year, an explosion and subsequent long burning fire at the fuel storage depot at Buncefield (Hemel Hempstead, UK) occurred on 11 December 2005, causing an estimated loss of at least £1.5 billion. While there was no loss of life in this incident there was substantial financial loss to the company and disruption to the lives of those resident in the surrounding areas. Most recently, two persons were killed in the explosion and ensuing fire which occurred at the Sunrise Propane Industrial Gases plant in Toronto Canada on 10 August 2008. The investigation into these latest incidents is still ongoing.

In each of the above cases the incident was caused by accidental ignition of the vapours given off by a liquid fuel leak, which resulted in the formation of a flammable gas cloud possessing some concentration gradient, located within a congested geometry. Despite

the fact that the majority of accidental explosions involve some concentration gradient or 'stratification' of the fuel in air, the research, literature and guidance available on this topic so far is relatively sparse.

1.4. Explosion Protection Techniques

Explosion protective measures involve either preventative or responsive techniques. Preventative techniques involve the removal of one of the three elements necessary for an explosion to occur; i.e. the control of flammable fuel concentration, prevention of all ignition sources or control of oxidant.

Where preventative measures, such as inerting, are impractical or impossible to achieve, protection or mitigation techniques are employed. Mitigation techniques can be split into four broad categories; isolation, suppression, containment and venting.

1.4.1. Isolation

Where a vessel is connected to other equipment through piping or ducts, an explosion can easily be transmitted to the connected geometry. In many cases the consequences of an explosion in a second or third vessel can be much more severe than the explosion in the original chamber [3-5]. Therefore, in order to prevent transmission of an explosion, fast-action isolation mechanisms such as knife gate valves or flame arrestors can be used to prevent flame/explosion transmission into any connected chambers or equipment.

The use of flame arrestors is based upon the principle of quenching, which works by heat loss through thermal conduction to the walls. This can be aided by diluent gases, which will increase the quenching distance required dependent on the flammable mixture and the concentrations involved. Quenching distance decreases with increasing temperature, pressure and oxygen concentration. HSE guidelines (158) state that flame arrestors may fail if the operating pressure or temperature is higher than that specified by the supplier. For example, failure may occur if an arrestor is placed too close to a burner flame or hot surface, causing overheating, or if bends and obstructions

downstream of the arrestor cause pressure increases. Therefore the introduction and placement of a flame arrestor in many industrial installations can be difficult.

With isolation techniques, it is inevitable that some explosion will still occur, therefore isolation techniques should always be used in conjunction with another method of protection, such as containment or venting.

1.4.2. Suppression Systems

Suppression systems work by reducing the speed of the combustion process, and thereby reducing the maximum explosion pressure a vessel must contain. Inert gases or their equivalents – such as CO_2, N_2 and H_2O (vapour) – work by acting as a coolant to the flame, reducing the flame temperature and reactivity of the mixture. The effectiveness of such gases depends upon their ability to absorb heat (specific heat capacity, C_p), therefore where sufficient inert gas is added flame propagation ceases and the explosion is arrested. This method of inerting also displaces the air in the system, reducing the available oxygen concentration.

In order for this method to be effective, however, the activation of the injection of the inerting material (at an injection time, t_i after ignition, governed by a critical activation pressure, P_a) must be early enough, and at a sufficiently high rate, that the quenching reduces the explosion quickly enough, and to a level where structural damage to the confining vessel is avoided.

Alternatively, a very effective method of inerting was to use chemical suppressants such as halogenated hydrocarbons, which worked by decomposing on contact with the flame zone. This reaction liberated free halogen atoms which acted as free radical scavengers, combining with the active hydrogen free radicals, effectively terminating the chain branching reactions necessary for continuing flame propagation. However, the use of such suppression systems are now prohibited due to environmental impact reasons.

In theory, in an inert atmosphere system, no further explosion protection method is required, since a flammable mixture can never be attained. However, such a technique is not infallible and common sense dictates that some other explosion protection device

be used in conjunction with this technique, increasing the expense. Furthermore, inert atmospheres can be hazardous to personnel who may be in the vicinity to maintain, clean or repair such areas, thereby requiring stringent controls.

1.4.3. Containment

Containment of an explosion requires designing a compartment geometry to such a standard that it will easily contain the worst case explosion which could occur from the stoichiometric mixture of the fuel it may contain. This method also requires an element of isolation in order that the explosion may not be transmitted into any connected equipment, and its implementation is often very costly due to the high design pressures required for the total containment of an explosion. In many cases an explosion within such a geometry will often cause permanent deformation to the structure which may require replacement. This method can therefore be very expensive, but necessary where other methods such as venting are unsuitable, for example where toxic products may be released to the surroundings.

1.4.4. Venting

Venting is a widely used explosion protection technique, achieved simply by the addition of a vent onto the geometry requiring protection, thereby releasing explosion products to an external location. Venting involves the prompt opening of a defined aperture on detection of pressure evolution from an explosion. Depending upon the size of the vessel to be protected, several vent openings may be required to alleviate the pressure to an acceptable level. Often used in conjunction with isolation valves where transmission to other pieces of equipment is likely, this method is used to reduce the cost of explosion containment – with respect to total containment – by reducing the amount of pressure the vessel must withstand. Correlations and standards are available for the design of vent size for a given stoichiometric worst case mixture within a specific geometry, as given by NFPA 68 [6] and the European Standard [7]. These standards will be discussed further in Chapter 2.

Similarly to all other methods of explosion mitigation, venting is not applicable for all types of enclosure, for example, venting may not work adequately at larger scales, particularly where there are obstacles present within the enclosure.

Where venting is the chosen protection method for a particular vessel, it is often necessary to direct the explosion products and hot gases to an area which is away from sensitive equipment or personnel, so that cost and hazard to human life is minimised as far as possible. Where an explosion must be directed in this manner there is often the need to add a duct to the vent. However, such manipulation of the geometry can provide further drawbacks, as described in section 1.4.4.1 below.

1.4.4.1. Explosion Venting Through a Duct

It is well documented that while adding a vent to a vessel can significantly reduce the pressure within a vessel, the addition of a duct onto an open vent can increase the severity of the reduced pressure of an explosion (as illustrated in Figure 1-1). This difference can be as much as ten-fold [8] depending upon the parameters involved.

All of the work currently available investigating the effect of a duct on a vented geometry deals with a worst case, stoichiometric, homogeneous mixtures, when in reality, the type of mixture which is more likely to form is a stratified mixture. This area of investigation requires further study in order that safety data can be collated and used to form predictions of realistic worse case scenarios.

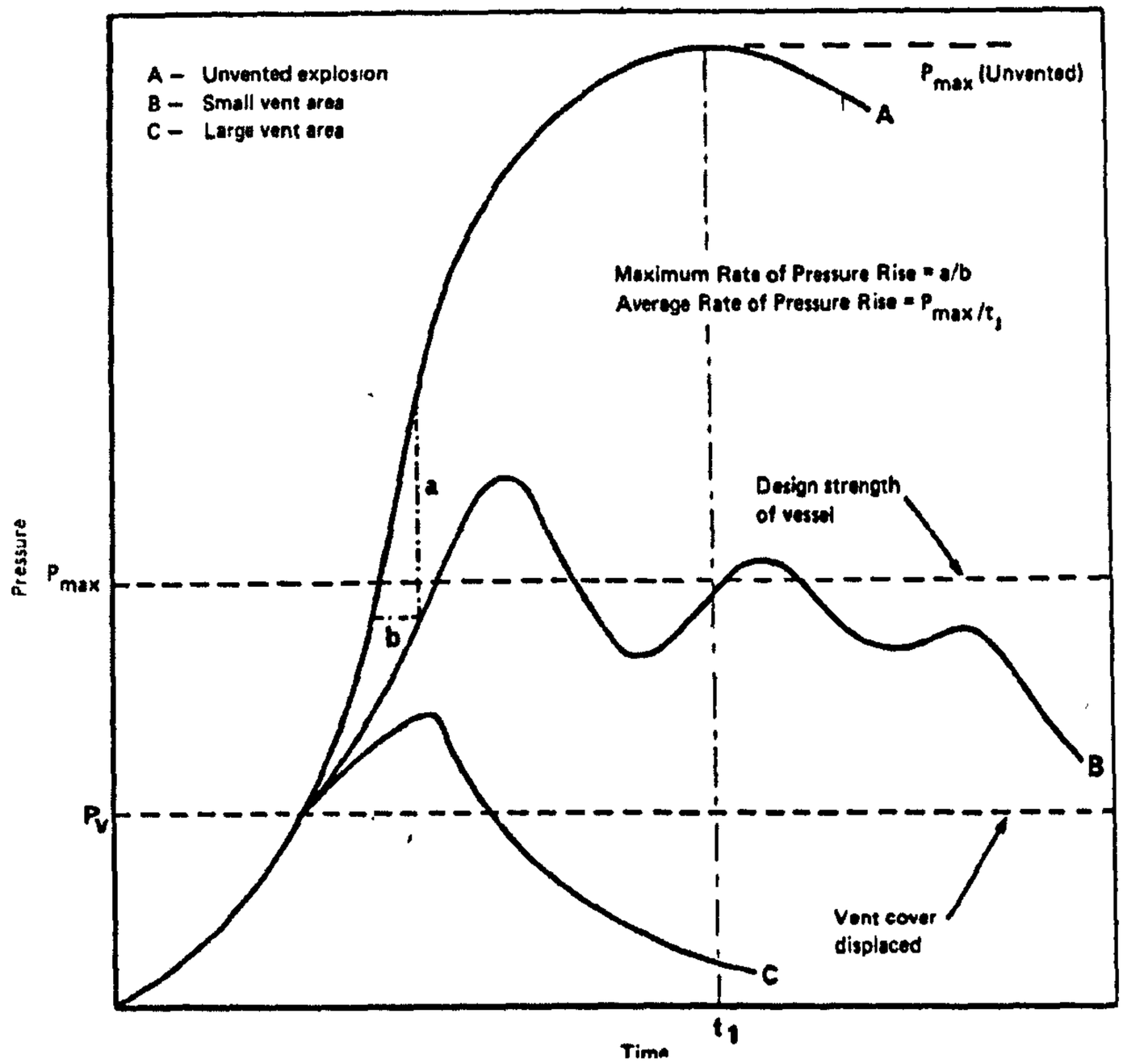

Figure 1-1: Comparison of unvented to vented gas explosions with small and large vent opening. Reproduced from Lunn [9].

1.5. The Stratified Explosion Hazard

A 'real-world' release of gas fuel within an enclosure can occur through either instantaneous, finite duration or continuous release. An instantaneous release may occur where a vessel ruptures completely and all of the fuel contained within it is released almost instantaneously as a vapour 'cloud'. A leak of finite duration may occur where a vessel, pipe or flange has a small crack or fault which releases the fuel contained within at a release rate dependent upon the pressure within the vessel, and where the leak comes from a closed or isolated vessel this will create a 'cloud-like' release.

Finally, a continuous leak is similar to the finite release case, but which continues due to a constant replenishment of the fuel. Such a 'jet' outflow release often occurs in a cracked or poorly sealed/maintained pipe-line with a constant flow of fuel to continue the leak.

The method of release employed within this research is a continuous jet outflow with a consistent pressure and momentum flow into the vessel, which will form a cloud with a concentration gradient inside the test vessel before ignition.

Currently available literature on the research of gas explosions has predominantly focussed on fully premixed/homogeneous fuel-air mixtures, where the concentration of the fuel is evenly distributed in the compartment. In reality, it is more likely that the distribution of fuel within a chamber will be stratified – i.e. having some concentration gradient – being either richer at the top or bottom of the chamber dependent on whether the fuel has a high or low molecular weight. Indeed, many recent explosions (as discussed in Section 1.3) have involved the formation of a concentration gradient in a confined area, usually with a heavier-than-air vapour which accumulates along the ground or lower level of the geometry. In most industrial scale accidents there has been no confinement at the top of the geometry, and explosion severity has been enhanced by obstacles at ground level, increasing turbulence.

Stratified gas explosions of buoyant gases such as methane or hydrogen are also a problem, more so with the rising 'hydrogen economy', therefore some experimental data using hydrogen will also be presented.

Whilst a small amount of data dealing with stratified gas explosions does exist in literature, as discussed in Chapter 2, it would be useful for the design and implementation of standards to have further data where the concentration of the fuel-air mixture is realistic in nature, rather than the homogeneous concentration that is primarily addressed in current literature.

1.6. Significance of the Current Research

Stratified gas explosions are commonplace in a wide variety of real-world situations, as well as providing an interesting subject for scientific academic study. The research presented in this thesis is intended to be of interest not only to the scientific academic community as an extension of research conducted previously on different scales and geometries, but is also intended to be of practical use to the explosion investigation

community by providing some data on realistic explosions which can be referred back to when investigating similar events on industrial scale accidents.

The data presented will hopefully be a valuable source of information to help the investigator work backwards to the amount of fuel released based upon the damage encountered, and not merely have to assume homogeneous gas volumes which, as will be shown later, may actually lead to overestimation of the fuel released, as the stratified explosion produces a more severe event.

The fuels in this research have been chosen for their relevance in the current climate, be that energy or safety. Hydrocarbons are the fuel of the present and therefore research has been undertaken using methane and propane, which have very different properties as hydrocarbon fuels, and also hydrogen as the potential fuel of the future. Much is still not known about the dangers associated with the use of hydrogen, and at least some of these will be addressed in the present research.

By gaining empirical evidence relating to stratified explosions under the relatively simple conditions outlined in this research, a greater understanding of real-world accidental release explosions can be achieved.

1.7. Aims and Objectives of the Current Research

1.7.1. Aims

The aim of this research is to investigate the explosion hazards created by stratified gas layers – including partially filled volumes – in enclosed, vented and interconnected vessels. Through doing this, it is proposed that a better knowledge and understanding of stratified gas hazards can be gained, and this should be a step towards being able to relate experimental data back to real world gas leak situations occurring within enclosed areas.

1.7.2. Primary Objectives

The primary objective of this work is to investigate and produce new experimental data on the hazards of stratified explosions in a medium scale geometry.

The areas of focus within this research are to be:

- The stratified explosion hazard across a range of variable reactivity gases;
- The effect of spark position in relation to leak position of the gas;
- The propensity for stratified gas mixtures to ignite outside of the homogenous flammable limits of the relevant gas;
- The difference in effects from premixed and stratified explosions for the same conditions;
- The effect of time delay from release to ignition in stratified explosions.

CHAPTER 2:

LITERATURE REVIEW

2.1. Introduction

This chapter is intended provide an overview of the fundamental parameters involved in combustion research to date, associated with homogeneous and stratified gas-air mixtures. Data and theory relating to vented, duct vented and interconnected vessel explosions will be discussed.

Due to the abundance of research published on homogeneous gas explosions within the geometry types included in this thesis it is not practical to present all available, so rather a brief overview of key text will be discussed. In each section, a brief summary will be presented, and further information is available from the relevant references.

The presentation and discussion here of some of the works investigating homogeneous mixtures is of importance to the current research, and serves to provide a baseline by which the effective severity of stratified gas explosions can be assessed. Detailing the important literature also serves to demonstrate the validity of this current research as a new contribution to the field of combustion engineering.

2.2. General Explosion Theory

Before discussing the nature of development of explosions within the complex geometries discussed in this research, it is necessary to define and explain some detail of fundamental parameters often used in combustion research.

2.2.1. Flammability Limits

The flammability limits for a given combustible material are physical measurable parameters which define the concentration of the fuel, when mixed with an oxidant, outside of which a sustained flame cannot propagate. The lower flammability limit (LFL) and upper flammability limit (UFL) are measures of these concentrations, expressed as a volume ratio (%) or equivalence ratio (Φ). Often in literature, the upper and lower flammability limits may be referred to as explosive limits (UEL and LEL respectively), these terms are interchangeable and have no difference in meaning [10].

Flammability is dependent upon a number of variables, including initial conditions (specifically pressure and temperature), and ignition energy. In simple terms, the higher the temperature or pressure at the time of ignition, the easier the reaction will propagate [11]. Furthermore, the properties of the individual gases particularly, the relative diffusivity of the fuel and an oxidant close to the flammability limits can influence those limits [12].

Knowledge of flammability limits is important to industries which deal with combustible materials, within which a potentially flammable or explosive mixture may form, in order that quantitative risk analyses can be carried out effectively.

There has been a significant amount of research into the determination of the LFL and UFL for most flammable fuel-air mixtures. Consequently, there is slight variation in literature as to the exact values of these limits. The overall trend with time has seen a gradual widening of the flammability limits [10, 12-18]. This widening may be attributed to differences in measurement criterion, or to an increased sophistication measurement techniques and equipment. For the purposes of the current research, the limits which will be followed are those of Zabetakis [19], shown in Table 2-1, which match those most widely used. It is, however, acknowledged that variability is probable, dependent upon the equipment and measurement guidelines.

Table 2-1: Flammability limits for homogeneous methane, propane and hydrogen-air mixtures at standard ambient initial conditions [19]

	LFL	Stoichiometric	UFL
Methane	5.0	9.5	15.0
Propane	2.1	4.02	9.5
Hydrogen	4.0	29.5	75.0

From a safety perspective, the lower flammability limit is of greater importance. This is because the concern in an accident situation is for a flammable fuel to leak and form a flammable mixture approaching and exceeding the lean limit as it mixes with air. The rich limit may also be of importance where air or oxygen may leak into a storage vessel,

vapour extraction system or vacuum extraction lines, where the UEL can be approached. However, this is less common in accident scenarios.

2.2.2. Equivalence Ratio

The equivalence ratio (Φ) is defined as the ratio between the actual amount of fuel present in a system and the theoretical stoichiometric fuel concentration for that fuel. This relationship can be expressed in simple terms by:

$$\Phi = \left[\left(Air/Fuel\right)_{Stoichiometric} \Big/ \left(Air/Fuel\right)_{Actual}\right] \qquad \text{Eq. 2-1}$$

where $\Phi < 1$ is lean, $\Phi = 1$ is stoichiometric and $\Phi > 1$ is a fuel rich mixture. A stoichiometric mixture can be defined as the balanced combustion of a fuel and an oxidiser, such that none of either remains at the end of combustion [6]. The stoichiometric value is often taken to be the worst case scenario in terms of explosion protection calculations, when in actuality, for most gases, the most severe explosion for a given gas will typically occur to the rich side of stoichiometric where an excess of fuel is available for participation in the combustion reaction.

Following ignition of a flammable mixture, the flame, providing it is not extinguished, will propagate away from the ignition source in one of two regimes; either subsonic (deflagration), or supersonic (detonation), relative to the unburned gas. The theory of propagation in these two regimes is discussed briefly below.

2.2.3. Deflagration

In accident scenarios, deflagrations are the most common type of explosion. A deflagration will propagate at subsonic speeds, that is, the burning velocity of the unburned gas in the system is slower than the speed of sound [20]. The pressure of a deflagration may be as low as a few mbar up to several bar, dependent upon the confining nature of the surroundings. As a general rule, for most combustible materials the ratio of initial pressure to peak pressure within an enclosure will not exceed a ratio of approximately 8:1 [19]. However, in some cases, the explosion may accelerate to

detonation where the ratio can exceed 40:1 [19]. Some details of unconfined explosion development are given in the following sections, followed by details of explosion development specific to closed, vented, duct-vented and interconnected vessels in Sections 2.3, 2.4, 2.5 and 2.6 respectively.

2.2.3.1. Flame Speed and Burning Velocity

Flame speed, S_f, and burning velocity, S_u, are two fundamental parameters used to characterise premixed combustion propagation, however in literature these terms are sometimes used interchangeably [20]. To avoid uncertainty relating to these terms, the definitions used in the present work are given below.

Burning velocity, S_u, is defined as the velocity of the flame relative to the unburned gas movement ahead of the flame, this can either be laminar, S_L, or turbulent, S_T. Flame speed, S_f, then is defined as the velocity of the flame relative to some static or fixed observer; in the current work flame speeds are calculated with respect to flame passage detection on the fixed position thermocouples, generally along the axial plane of the geometry.

S_f is always greater than S_u due to the expansion of the hot burned gases which pushes both the flame front and the unburned gas ahead of the flame forward. The relationship between flame speed, burning velocity and the unburned gas velocity, u, can then be expressed as:

$$S_f = S_u + u \qquad \text{Eq. 2-2}$$

If the flow field is laminar then the propagating flame front is smooth, whereas if the flow field is turbulent then the propagating flame front is wrinkled, defined by the relationship:

$$S_T = \left(A_T / A_o\right) S_L \qquad \text{Eq. 2-3}$$

where A_o is the flame area based on the mean flame profile and A_T is the turbulent flame area [21].

For a premixed flame:

$$\rho_u S_u = \rho_b S_b \quad \text{(mass)} \qquad \text{Eq. 2-4}$$

$$P_u + \rho_u u_u^2 = P_b + \rho_b u_b^2 \quad \text{(momentum)} \qquad \text{Eq. 2-5}$$

$$h_u + \tfrac{1}{2} u_u^2 = h_b + \tfrac{1}{2} u_b^2 \quad \text{(energy)} \qquad \text{Eq. 2-6}$$

$$P = \frac{\rho R T}{W} \quad \text{(Gas Law)} \qquad \text{Eq. 2-7}$$

where ρ is the gas density, P is pressure, h is the specific enthalpy per unit mass, R is the universal gas constant, T is the gas temperature, W is the molecular weight and subscripts b and u refer to burned and unburned species respectively. By rearranging Eq. 2-7 to give:

$$\frac{R}{W_u} \rho_u T_u = \frac{R}{W_b} \rho_b T_b \qquad \text{Eq. 2-8}$$

Then

$$\rho_u T_u = \rho_b T_b \qquad \text{Eq. 2-9}$$

And

$$\frac{\rho_u}{\rho_b} \approx \frac{T_u}{T_b} \Rightarrow S_b = \frac{\rho_u}{\rho_b} S_u \qquad \text{Eq. 2-10}$$

The volume which the burned and unburned gases occupy is significantly different, represented by the expansion factor, or expansion ratio, E, defined as the ratio of unburned to burned gas densities. For most flammable hydrocarbon gases and vapours the value of E is between around 7 and 8. E can be expressed with the relationship:

$$E \equiv \rho_u / \rho_b \qquad \text{Eq. 2-11}$$

At constant pressure, taking into account the Gas Law (Eq. 2-8), with

$$W = \frac{m}{n} \qquad \text{Eq. 2-12}$$

Where m is the mass of the gas and n is the number of moles, then

$$n_u \rho_u T_u \approx n_b \rho_b T_b \qquad \text{Eq. 2-13}$$

and E can be given by [22]:

$$E = \left(\frac{T_b}{T_u}\right)\left(\frac{n_b}{n_u}\right) \qquad \text{Eq. 2-14}$$

The relationship between expansion ratio and burning velocity is:

$$S_f = ES_u \qquad \text{Eq. 2-15}$$

For an initial ambient pressure (~ 1 bar), and an expansion factor in the range 7-8, an explosion within a closed volume would create a maximum overpressure of 7-8 bara. Where turbulence-inducing obstacles are present, the explosion severity in terms of S_f and $(dP/dt)_{max}$ can be increased, and in some cases the explosion can run to detonation.

Table 2-2: Characteristic laminar burning velocity, S_L, flame speed, S_f, deflagration index for gases, K_G, and expansion ratio, E, for stoichiometric methane, propane and hydrogen under standard ambient conditions (25°C, and 1atm).

	Methane	**Propane**	**Hydrogen**
S_L (m s^{-1}) [23]	0.45	0.52	3.5
S_f (m s^{-1}) [23]	3.5	4.0	28
E [23]	7.4	7.6	8.0

The rate of pressure rise within a confined explosion can provide a measure of the burning rate, with the relationship [22]:

$$V(\mathrm{d}P/\mathrm{d}t) = \mathrm{d}m_b/\mathrm{d}t\,[RT_b/M_b - RT_u/M_u] \qquad \text{Eq. 2-16}$$

where $\mathrm{d}m_b/\mathrm{d}t$ is the mass burning rate, given by the general equation:

$$dm_b/dt = A_f \rho_u S_u \qquad \text{Eq. 2-17}$$

where A_f is the area of the flame, and S_u is the burning velocity, either laminar or turbulent. In a closed system, (dP/dt) is directly proportional to S_u, with the relationship [22]:

$$(dP/dt) = (A_f / V)\, P\,.\,(E\text{-}1)\, S_u \qquad \text{Eq. 2-18}$$

Some fundamental characteristics for the gases used in this research are presented in Table 2-2, including laminar burning velocity, flame speed, deflagration index and the expansion factor.

2.2.3.2. Minimum Ignition Energy

Within the flammability limits, the closer a mixture is to stoichiometric the easier the mixture is to ignite; i.e. the minimum ignition energy required for ignition is lower. Figure 2-1 shows the minimum ignition energy for a methane-air mixture, and demonstrates that even approaching the flammability limits 3 mJ is sufficient energy to ignite a methane-air mixture. As the concentration tends further towards the flammability limits 10 J is sufficient to ignite a methane-air or butane-air mixture [24]. Similar results are available for propane-air and hydrogen-air mixtures. Therefore, an ignition energy of 16 J, as employed in the current research, is sufficient energy for tests where the fuel-air mixture close to the flammability limits.

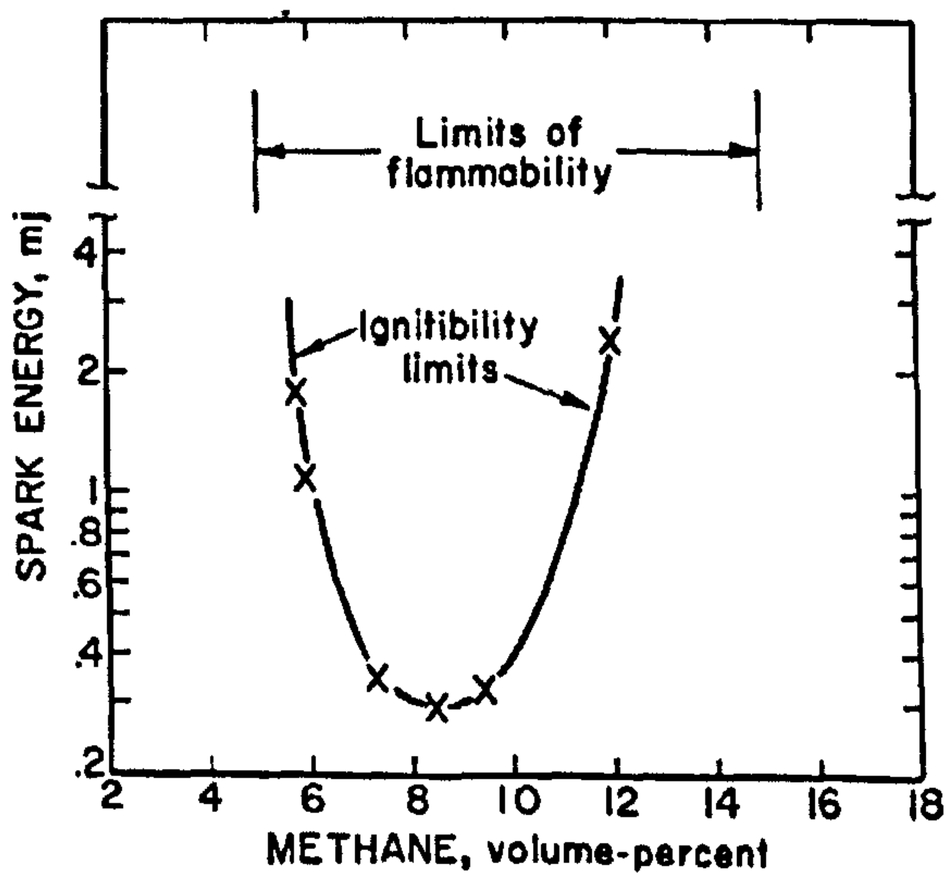

Figure 2-1: Ignitability curve and the limits of flammability for methane air mixtures at atmospheric pressure and T=26°C [19]

2.2.3.3. Pressure Development in Unconfined Explosions

An explosion in an unconfined area will generally produce a flash fire – a ball of flame which rises vertically due to buoyancy effects. Where the flame comes into contact with some flammable material or fuel this may become ignited, resulting in a subsequent fire. This is often the case in many accidental explosions at fuel refining or storage facilities, as discussed previously.

Since there are no geometry constraints influencing the development of an unconfined explosion, the resulting overpressure is governed by the inertia of the gas ahead of the flame. Based upon simplified acoustic theory, this gives:

$$P = P_a\left(\frac{2\gamma Ma^2}{1+Ma}\right) \qquad \text{Eq. 2-19}$$

where P is the overpressure, P_a is the ambient pressure, γ is is the ratio of the heat capacity at constant pressure, C_P, to heat capacity at constant volume, C_V (taken to be 1.4), and Ma is the flame speed mach number (flame speed / speed of sound).

2.2.4. Detonation

The study of the detonation phenomenon dates back over a century. The presence of a detonation wave in a combustible gas was first observed in 1881 by Berthelot & Vieille, and independently Mallard & le Chatelier [14, 25-27]. Since this date the phenomena of detonation waves has attracted much attention, from the initial theory of supersonic combustion provided by Chapman in 1899, and independently by Jouguet in 1905 [16] (currently recognised as the C-J model), and later improvement by independent researchers Zel'dovich, von Neumann and Döring during World War II (known as the ZND theory), who offered a reasonable postulation of the wave structure [16, 20, 27, 28]. There is an abundance of research available on the further refinement of these theories, with the most significant advances towards the understanding of detonation waves emerging since the late 1950's [27].

For the purposes of the current research a brief description of some of the main theories and mechanisms which will be referred to in later text are presented here. This section

is not intended to be a comprehensive review of detonation literature as this is not the main focus of the research, but the knowledge of such mechanisms may prove critical in determining how to prevent such events from occurring. Should more in-depth information be required, the reader is directed to the cited literature.

2.2.4.1. Detonation Theory

Detonation is the term used to describe a combustion wave propagating at supersonic burning velocities, and is the propagation of a shock wave followed by a reaction front [6, 28]. A detonation wave typically propagates at velocities in the range 1500 to 2000 ms^{-1} (relative to the unburned gas), with peak pressures in the region of 15-20 bar [20].

The fundamental difference between a deflagration and a detonation is that while in a deflagration the heat release rate and/or number of molecules per unit volume increases approximately uniformly with time over the course of the explosion, in a detonation the wave is spatially non-uniform and propagates through the unburned mixture as a 'shock front' behind which changes occur in such a way that that the chemical heat release can be utilized to support further propagation of the detonation wave [14].

Detonations can be initiated by direct or indirect means. Direct initiation is created by strong rapid ignition sources such as high explosive charges, which have sufficient energy to result in the immediate emergence of a detonation in a suitable fuel mixture. Indirect initiation occurs when an existing deflagration becomes accelerated due to external influences such as confinement or obstacles, and subsequently undergoes acceleration or transition to detonation (DDT) [27] (this method of initiation is discussed further in Section 2.2.4.5). The ignition energy required for direct initiation of a detonation wave is generally many orders of magnitude larger than that required to initiate a deflagration [19].

2.2.4.2. Detonation Limits

Similarly to the limits governing flammability, a detonation may only be maintained between certain concentration limits. These limits are distinct from, but lie within, the flammability limits [10, 14], and are therefore generally narrower. Not all flammable

mixtures can lead to detonation, those of interest to this research are 2.57-7.37% for propane [16], and 18.3-58.9% for hydrogen [10, 16]. The apparent detonation limits for a particular combustible mixture are not strongly dependent upon the method of ignition [14].

2.2.4.3. C-J and ZND Detonation

The Chapman-Jouguet detonation model as discussed above was formulated at the turn of the 20th Century, and was the first model to offer an explanation of the propagation of the newly discovered detonation wave. The theory is a one-dimensional model which treats the detonation wave as a discontinuity with infinite reaction rate [20], involving simple considerations of the coupling of the leading shock front, the velocity of which is dictated by the composition of the fuel and the following reaction zone [16]. The model incorporates an energy conservation term which, when employed into the traditional Rankine-Hugoniot analysis, provides a tangential plane to the Rankine-Hugoniot curve shown in Figure 2-2. Shock energy is generated in the zone between this plane and the shock front by thermal expansion, and it is this expansion process which governs the detonation velocity [10]. The point at which this plane intersects the curve, labelled as the 'Upper CJ point' in Figure 2-2 provides the theoretical value for the CJ pressure and velocity and can be calculated from [14]:

$$P_{CJ} = P_o \frac{(1+\gamma) \pm \sqrt{(1+\gamma)^2 - 4\gamma(T_o/T_b)}}{2\gamma(T_o/|T_b)} \qquad \text{Eq. 2-20}$$

and

$$v_o^2 = c_o^2(1+\gamma)^2 \frac{\left[1+\sqrt{1-\left[4\gamma(T_o/T_b)/(1+\gamma)^2\right]}\right]^2}{4\gamma^2(T_o/T_b)} \qquad \text{Eq. 2-21}$$

where γ = 1.4, T_o and T_b denote the initial and burned gas temperatures and c_o is the speed of sound in the unburned mixture.

The derivation of these formulae along with the associated governing conservation and state equations can be readily found in literature [10, 14, 16, 20, 27, 28]. Table 2-3

presents the C-J pressure and velocity for the fuel-air mixtures of interest under standard ambient conditions, assuming stoichiometric concentration.

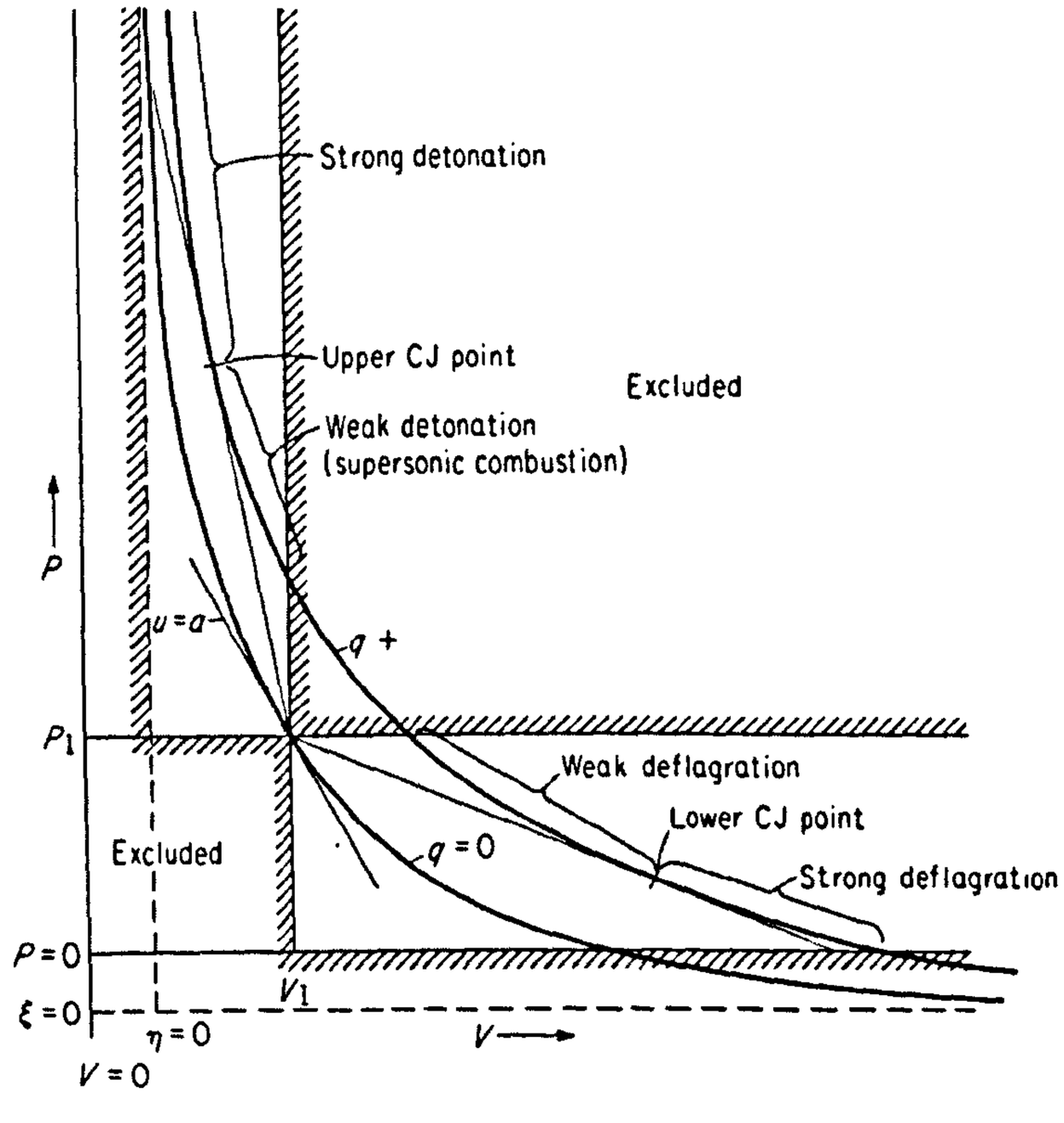

Figure 2-2: Pressure-volume plot of end states for a one-dimensional steady process with heat addition, indicating Chapman-Jouget states [29].

Table 2-3: C-J pressure and velocity for some fuel air mixtures at standard ambient initial conditions [20]

	Methane	**Propane**	**Hydrogen**
C-J Pressure (bar)	17.4	18.6	15.8
C-J Velocity (ms^{-1})	1802	1804	1968

The ZND theory builds upon the original detonation theory by Chapman and Jouguet as mentioned above, and offers improvement by means of the addition of a method for accounting for the rate of reaction. In the ZND-model, a detonation is considered to be a non-reactive shock wave followed by a reaction zone [28]. The leading shock wave triggers exothermic chemical reactions in the reaction zone which continues until the

flow becomes sonic for a C-J detonation [16, 28]. The thickness of this reaction zone is governed by the reaction rate [20]. The ZND theory gives exactly the same detonation pressures and velocities as the C-J theory, the only difference between the two models being the thickness of the wave. Further details on this theory are available in literature [16, 20, 28].

2.2.4.4. Rarefaction Waves

A steady detonation wave is followed by an unsteady rarefaction wave [14]. Thus, rarefaction refers to the area of relative low pressure following a shock wave[27, 30]. Figure 2-3 illustrates the one-dimensional propagation of a detonation wave propagating along a tube which is open at one end, and with ignition at the closed end ($x = 0$) [20]. In this situation the pressure and density decreases for approximately half the distance travelled by the rarefaction wave, which is then followed by quiescent gas [14], i.e. $u = 0$ *m/*s, and hence when the detonation front is at the position $x = L$ as shown, the tail of the rarefaction wave will be at around $x = L/2$ for the conditions shown in Figure 2-3 below.

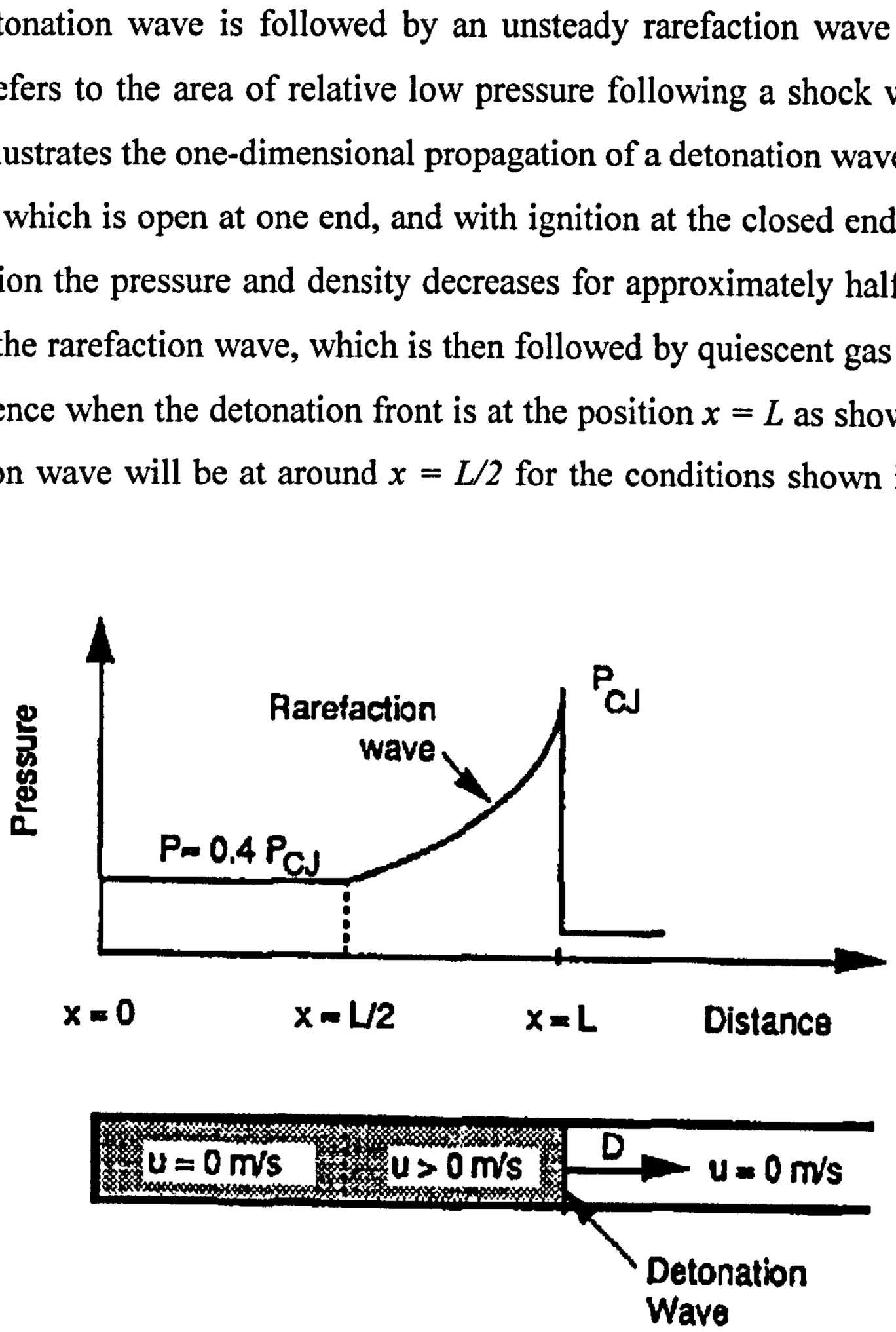

Figure 2-3: Pressure-distance profile for the propagation of a detonation wave along a tube, with ignition at the closed end ($x = 0$) [20].

2.2.4.5. Deflagration to Detonation Transition (DDT)

In confined or partially confined geometries there is the possibility that deflagrating explosions may run to detonation. Triggering mechanisms for DDT initiation include obstacles and changes in geometry. Detonation under these circumstances can be described in terms of an accelerating flame coupling with the shock wave. The result is an instantaneous release of heat and a fast propagating, high pressure region over a transition distance. This phenomenon has been particularly observed in very reactive mixtures such as stoichiometric acetylene-air, hydrogen-air, and many less reactive mixtures with oxygen as the oxidant [20].

The distance required for DDT to occur depends upon many factors including the flammable mixture, temperature, pressure, geometry, and ignition source [19, 20]. DDT is difficult to achieve in the open since an unusually large flame acceleration would be required. However partial confinement greatly enhances the likelihood of DDT occurring [14, 20, 27].

Strehlow [28] reports three mechanisms responsible for flame acceleration to detonation transition, the first being the Taylor-Markstein mechanism, where an instability is created by the acceleration of flow in the direction of the less dense medium; secondly, formation of a turbulent boundary layer at the surface of an enclosure caused by the unburned gas motion ahead of the flame, which causes a marked increase in the rate of heat release; and thirdly the impulsive flow generated by the flame causes the separated flow region of every obstacle to shed a vortex as a result of which as the flame enters the area, similarly to the second mechanism, the heat release rate increases rapidly. These three mechanisms have been shown to cause the flame acceleration necessary for transition to detonation to occur [28].

In addition to the basic theoretical and older literature mentioned above, there has been an abundance of recent experimental literature dedicated to this topic which the reader is directed to for further information [14, 27, 31-35].

2.2.4.6. The SWACER Mechanism

The Shock Wave Amplification by Coherent Energy Release (SWACER) mechanism was proposed to account for the direct formation of a spherical detonation [36], but can also be used to account for confined detonation formation [16]. This mechanism refers to the fast turbulent mixing of hot burned gases with the unburned gases, which can lead to the onset of detonation in very short distances [37]. More specifically, this mechanism involves the evolution of active species and temperature gradients ahead of the flame, triggered by the initial ignition event, and it is the release of chemical energy from these species coupling to the leading front which results in an rapid amplification of the front to C-J velocity [16].

This mechanism is significant in terms of detonation transition as it does not require the presence of a strong shock wave, but offers a chemical mechanism for generating an accelerating shock wave which quickly approaches C-J velocity [28].

2.3. Explosions in Enclosed Vessels

Where an explosion takes place in a closed vessel, no volume expansion is possible, therefore there must be an increase in overall maximum pressure (P_{max}). Assuming adiabatic expansion, as discussed in Section 2.3.1, the maximum pressure which can be expected in a closed volume is related to the expansion factor and initial pressure with the relationship:

$$P_{max} = EP_i \qquad \text{Eq. 2-22}$$

where P_i is the initial pressure in the vessel before ignition, and E is given in Eq. 2-11.

For most common gas and vapours ignited at ambient pressure and temperature, the maximum adiabatic pressure expected is of the order of 7-8 bara (relating to the adiabatic expansion factor E with a value of between 7 and 8). Actual values for the gases used in this research are given in Table 2-2. The value of P_{max} is then almost independent of the vessel volume.

The ignition of a gas at the centre of a closed vessel produces an initial spherical flame front initially of flame speed S_f, which is related to the burning velocity, S_u, by:

$$S_u = S_f \frac{\rho_b}{\rho_u} = S_f n \frac{T_u}{T_b} \qquad \text{Eq. 2-23}$$

where ρ is the density, T is the temperature and n is the molar ratio of unburned to burned gas, and where b and u refer to the burned and unburned gas respectively.

This expanding flame front pushes ahead the unburned gases at a velocity, S_g, where:

$$S_g = S_f - S_u \qquad \text{Eq. 2-24}$$

Further, the rate of pressure rise, $(dP/dt)_{max}$, is significantly dependent on both the vessel geometry (specifically volume) and the type of gas mixture it contains. The value of $(dP/dt)_{max}$ can vary widely from gas to gas, and can be characterised by the *Cubic Law* which states a relationship between the volume of the vessel and the maximum rate of pressure rise obtained, which is equal to some constant, K_G, specific to the gas involved. The Cubic Law is given by the relationship [11]:

$$K_G = const = (dP/dt)_{\max} \cdot V^{1/3} \text{ (bar.m s}^{-1}\text{)} \qquad \text{Eq. 2-25}$$

where V is the vessel volume, and the values of the constant K_G for the gases discussed in this research are given to be 5.5, 100 and 550 for methane, propane and hydrogen respectively [38].

The cubic law has been calculated and employed for spherical volumes where the flame can expand in all directions equally without contact with the vessel walls. Where an explosion initiates from the centre of a cylindrical vessel, the flame will initially behave as a spherical explosion until there is some interaction with the walls. On contact with the walls the flame surface area is suddenly reduced, and the flame will then propagate axially in both directions along the cylinder, into the unburned mixture ahead of the flame, with a near hemispherical flame front. The expansion of burned gases in a confined explosion causes an adiabatic compression of the unburned gases ahead of the flame, resulting in a rise in pressure and temperature within the system.

The overall severity of the explosion can therefore be decreased, and in some cases oscillations are superimposed over the pressure trace [11]. It is therefore very important when designing process vessels and protection measures for safety systems that the shape of the vessel is taken into consideration.

2.3.1. Adiabatic Pressure at Constant Volume

The calculation of adiabatic maximum explosion pressures will be used to compare with the experimentally recorded pressure rise, in order to assess the effects of heat losses to the vessel walls. The maximum pressure which occurs at constant volume may be calculated using Eq. 2-26 [10].

$$P_{\max} = P_i \times \frac{T_e}{T_i} \times \frac{\Sigma n_b}{\Sigma n_u} \qquad \text{Eq. 2-26}$$

where P_{max} is the final explosion pressure, P_i and T_i the initial mixture pressure and temperature, T_e the adiabatic flame temperature at constant volume, n_b is the number of moles of product at adiabatic flame temperature calculated from constant pressure or volume basis and n_u the moles of reactants.

An adiabatic maximum pressure can only be obtained where there are no heat losses to the confining walls of the geometry (i.e. taking place without heat leaving or entering the system). This will only be the case where the explosion takes place within a spherical vessel, ignited at the centre, therefore it is expected that the values for a closed cylindrical volume – as used in the present research – will be much lower than those predicted by the adiabatic pressure calculation.

2.3.2. Factors which Influence the Maximum Pressure and Rates of Pressure Rise in Enclosed Explosions

The severity of an explosion is typically characterised by two fundamental parameters; the maximum pressure attained in the explosion (P_{max}), and the rate of pressure rise, including either the maximum rate of pressure rise ($(dP/dt)_{max}$) or the average rate of pressure rise [9]. Measurement of these parameters is reasonably simple, but care must

be taken in their interpretation as both values can be influenced by a range of factors. In addition to those already discussed, the chemical composition of the fuel, the initial conditions, the volume which the flammable mixture occupies, the ignition source, the nature of the confining geometry, and any turbulence can affect P_{max} and $(dP/dt)_{max}$.

Initial Conditions

An increase in initial pressure within the system increases both the maximum pressure and rate of pressure rise. It is noted in literature that the relationship is linear over a small range of initial increasing pressure. In contrast, whilst the initial temperature has little or no effect on the rate of pressure rise, as the initial temperature increases, the maximum explosion pressure decreases. This is due to a reduction in the density of the fuel-air mixture at elevated temperatures, and hence the available energy output [9].

Volume or fraction occupied by the fuel-air mixture

Where the fuel-air mixture occupies only a fraction of the volume, it may seem logical to assume that the maximum pressure is reduced accordingly. Indeed, once again a linear relationship is noted between the amount of flammable mixture available within the vessel and the resulting maximum pressure [9, 15]. However, given that in certain circumstances the explosion pressure recorded from partial volume or stratified explosions can be higher than the total amount of fuel that is present in the system dictates, this is not necessarily a relationship which can be strictly adopted. The nature of stratified explosions is discussed further below.

Ignition Source

The ignition source characteristics, specifically its type, strength and position, are important in explosion development, particularly in initiation close to the flammability limits. In addition, the position of the ignition position can affect the measurable explosion parameters by changing the path of the flame from the ignition, which in turn alters the surface area of the flame. Where the ignition is closer to the wall, the flame surface areas is impeded by flame attachment to the wall. The greater the flame attachment to the wall, the greater the heat transfer through the walls of the vessel and hence the greater the impedance on explosion development. It is widely accepted that the least heat transfer occurs where the ignition is central to the vessel. It is widely

accepted that an ignition source located close to the centre of a compact vessel will also produce the most severe explosion, however this alters once a vent is added to the vessel the relationship changes and end ignition is actually shown to be the worst case.

The Confining Geometry

The geometry within which an explosion takes place is an important factor in explosion severity and development. Indeed, both P_{max} and $(dP/dt)_{max}$ are affected by changes in the physical environment, including the size and shape of the confining geometry. More specifically, heat transfer from the flame and hot gases to the walls of the confining geometry reduces the maximum values which can be expected. It is understood that the highest values of P_{max} and $(dP/dt)_{max}$ are produced when the ignition is positioned centrally within a spherical enclosure [9], thereby providing the largest distance for explosion development in all directions before the flame and hot gases become cooled by the walls of the vessel. Since accidental explosions are more likely to occur within a non-spherical vessel, with an ignition source most likely close to one of the walls, the maximum worst case is unlikely to occur in reality, and it is likely that there will always be some reduction from the adiabatic maximum which can be expected from a centrally ignited explosion within a homogeneous mixture within a spherical vessel.

Turbulence

Turbulence within an enclosure can be generated by obstructions to the smooth flow of air/flame through the enclosure, including internal fittings and even rough surfaces which can have the effect of increasing flame surface area by stretching and tearing the flame apart.

Depending upon the nature of the vessel, the effect of turbulence can serve to increase the maximum rate of pressure rise, but has a differing effect upon the maximum pressure attained. For compact vessels where L/D < 3, a minimal increase in maximum pressure has been reported [9], whereas for longer vessels, with an L/D > 3, the effect is more pronounced. In longer vessels, faster flame speeds caused by turbulence decreases the amount of time available within which the flame can transfer heat to the walls of the vessel, and therefore the overall maximum pressure within the vessel tends to increase with relation to the same explosion in a quiescent state [9]. The effects of turbulence

are known to vary dependent upon concentration within the flammability limits, and are most marked where S_u is low.

Oscillatory Combustion and Pressure Wave Interaction

The presence of oscillatory combustion superimposed over a pressure trace has been well documented in literature [17, 29, 39]. Such oscillatory behaviour can be significant in terms of structural responses as large transient pressure fluctuations can cause damage to the confining geometry [29]. In some cases where the onset of a cellular flame structure occurs in the early stages of an enclosed explosion, it can promote acceleration of the flame front resulting in an increased rate of pressure rise within the vessel [39]. Leyer & Manson [40] showed that in the onset of oscillatory combustion within short, closed vessels can be triggered by the interaction of the flame front with the side walls of the vessel. They argued that the expansion waves generated as a result of this interaction induced a hydrodynamic instability in the flame front which served to further increase these waves. Taylor instabilities are triggered where the density interface between the burned and unburned gases, i.e. the flame front, is accelerated in the unstable direction of the higher density medium, which can be cause by the interaction of these waves with the flame front. Finally, oscillatory combustion has been linked to the longitudinal acoustic vibrations of the vessel, the flame front instabilities and changes in the burning rate (i.e. Rayleigh's criterion) [17, 30].

Phylaktou *et al* [17] have noted the presence of oscillatory combustion occurring with all three gases used in this research. They reported upper and lower limits within which such oscillations were more readily observed, these as being 7.5-11.5% for methane-air mixtures, 2.75-6.25% for propane-air mixtures and 9.0-61.5% for hydrogen-air mixtures. They go on to argue that whilst some authors have noted that such pressure oscillations occur preferentially in rich mixtures for fuels with a heavier than air molecular weight, and in lean mixtures for fuels with a lighter than air molecular weight, no such preferential behaviour was observed in their work.

2.4. Explosions in Vented Enclosures

The technique of adding a vent to an enclosure is not intended to suppress or prevent an explosion from occurring, but to reduce the explosion pressure contained within a vessel, such that the design pressure of that vessel is not exceeded, and also to control the direction which the explosion products are directed. This is achieved by venting burned *and* unburned gases through the vent, therefore the amount of energy available for combustion inside the vessel is correspondingly reduced, as is the maximum explosion pressure. Vent positioning is particularly important in plant design, where the vent is designed to be an aperture through which burned and unburned gases may be released to a safe location to prevent destruction of the containing vessel and danger to hazardous or manned areas. The addition of a vent to a vessel with a known explosion risk is also a means by which the design strength, and thereby the associated costs, can be decreased.

NFPA 68 [6, 38] provides official guidance for the sizing of vents within an enclosure, based upon the maximum reduced pressure, P_{red}, the vessel can withstand and the L/D ratio of the vessel. For high strength enclosures with $L/D < 2$, the required vent area can be calculated using:

$$A_v = \left[(0.127\log_{10} K_G - 0.0567)P_{red}^{-0.582} + 0.175P_{red}^{-0.372}(P_{stat} - 0.1)\right]V^{2/3} \qquad \text{Eq. 2-27}$$

where A_s is the internal surface area of the enclosure, K_G is the deflagration index, P_{stat} is the vent burst pressure (≤ 0.5 bar) and V is the vessel volume. For vessel L/D between 2 and 5, the vent area calculated in Equation 2-13 should be increased by an amount, ΔA, calculated by:

$$\Delta A = \frac{A_v K_G (L/D - 2)^2}{750} \qquad \text{Eq. 2-28}$$

However, it has been noted that the equations offered in NFPA 68 are conservative [41] and not generally applicable to all situations including vessels with an L/D > 5 or stratified mixtures.

The pressure-time profile for a vented explosion is different to that of a completely confined explosion. Dependent upon ignition position, the large single peak typically

observed for an enclosed explosion becomes several peaks in a vented explosion, dependent on vent size, ignition position and whether the vent is covered. Several authors report the presence of either three or four peaks, dependent upon the geometry [9, 39, 42-44], relating to vent burst, interaction between outflow through the vent and external combustion, interaction of the flame with the vessel geometry and an acoustic oscillatory peak. Peaks may be absent from the pressure trace where elements are lacking, for example where no vent cover is employed, or appear to be absent where two peaks may have merged, usually where the acoustic peak is superimposed over one of the earlier peaks. Where the vent area is very large the peak may reduce to a lower single peak, or increase to multiple smaller peaks where the vent is very small. More details can be found with relation to each individual study in the references listed.

2.4.1. Additional Factors Which Affect the Maximum Pressure and Rates of Pressure Rise in Vented Enclosures

Explosions in vented vessels are subject to the same factors governing explosion development as closed vessels, such as mixture composition, volume and reactivity, turbulence, ignition strength and position, initial/ambient conditions, and confining geometry, as discussed in Section 2.3 However, the addition of a vent to a geometry also has some influence on the development of an explosion, particularly with reference to vent size, area and position.

2.4.1.1. Oscillatory Combustion and Pressure Wave Interactions

Similarly to the closed vessel explosions, the presence of oscillatory combustion within vented explosions has been noted by several authors to be present on vented pressure traces [39, 45, 46], particularly with relation to central ignition and rich mixtures. Acoustic oscillations have been linked to the generation of a strong pressure peak in vented vessels [46].

Following ignition, the unburned gas flow through the vent serves to accelerate the flame towards the vent, in the direction of the more dense medium, i.e. the unburned gases, thus satisfying the criteria for Taylor the instability Figure 2-4. This instability

serves then to further accelerate the flame towards the vent. As the flame reaches the vent opening, it ignites the unburned gas cloud pushed out of the vent by the expanding gases behind the flame front, giving rise to an external explosion. Such behaviour has been studied mathematically [47, 48]. This external explosion event triggers the onset of Helmholtz oscillations – that is the pocket of burned gas within the vessel undergoes bulk motion towards and away from the vent opening, triggering a predominantly oscillatory peak which is eventually dampened down as the flame expands and reaches the vessel walls, decreasing the rate of production of burned gases due to a sudden reduction in flame surface area. The burning rates during this phase are enhanced by the turbulence generated between the burned gases flowing out through the vent, and the unburned gases remaining in the vessel. Oscillatory combustion has been shown to stretch and tear the flame front such that the surface area becomes increased, leading to faster flame speeds.

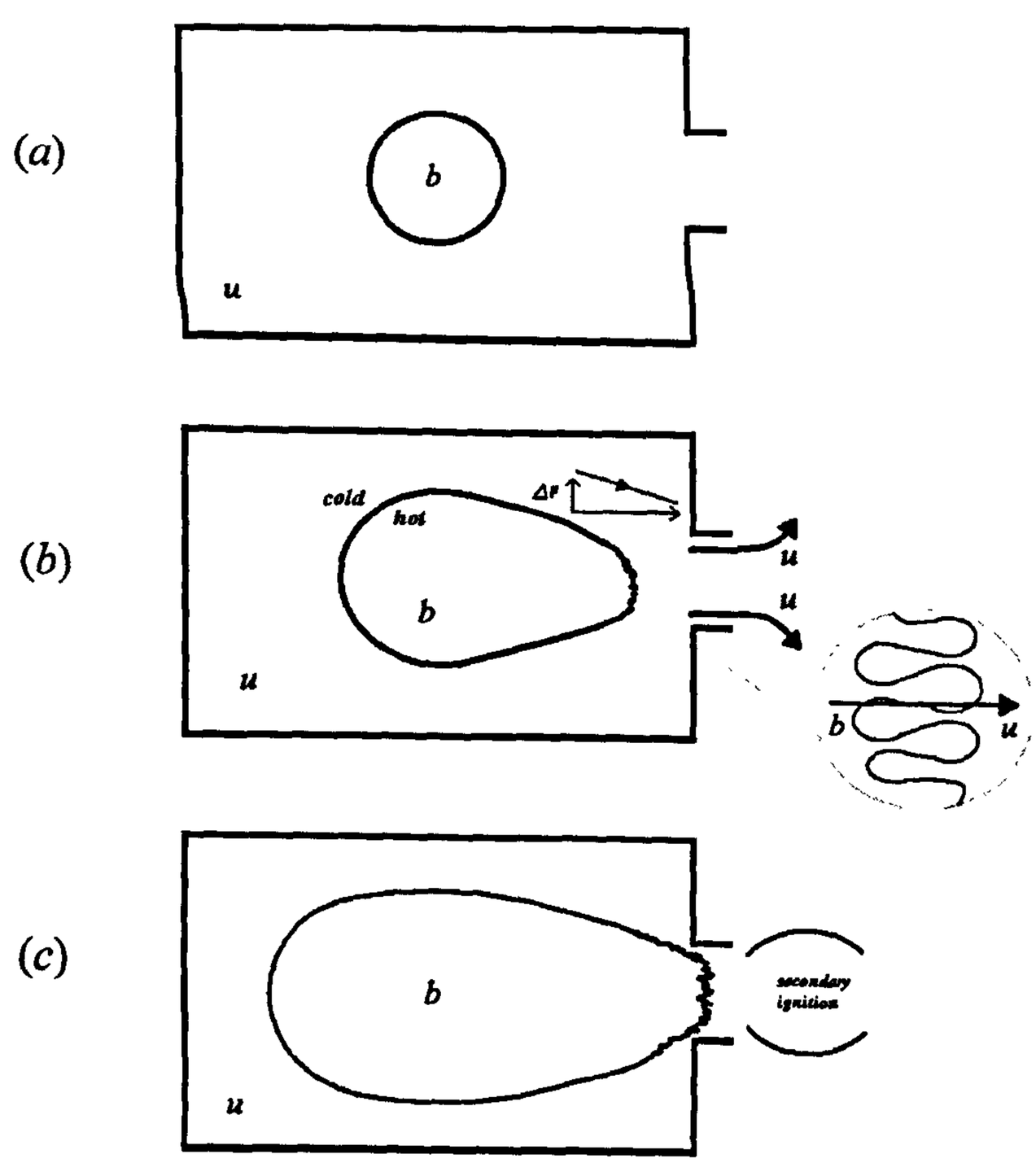

Figure 2-4: Schematic representation of a vented explosion, showing (a) initial spherical flame propagation, (b) acceleration of the leading edge of the flame front towards the vent, and the onset of Taylor instabilities, and (c) external explosion of the unburned gas pushed out of the vent.

The oscillatory peak occurs as the pressure within the vessel continues to fall from the flame interaction with the geometry, until a high frequency oscillatory pressure peak occurs, generated as pressure waves resulting from the combustion process couple with the acoustic modes of the vessel and set up sustained pressure oscillations (thus satisfying the Rayleigh criterion). It is reported that this final acoustically-enhanced combustion phase is associated with burning into isolated pockets of gas, located in the corners of the vessel [43]. It is further reported that this final peak most readily occurs in fuel rich mixtures for methane, propane and ethylene, with the maxima recorded well to the rich side of stoichiometric. This is consistent with the findings of other authors [46, 49]. The fact that maximum values of this acoustic peak occur to the rich side of stoichiometric in propane and ethylene supports the contention that gas mixtures exhibiting a spontaneous cellular structure are most sensitive to pressure effects, and therefore are most likely to exhibit acoustically enhanced flame instabilities [30, 46]. However, the results of Cooper *et al* [43] detract from this theory – they observed the same oscillatory combustion in rich methane mixtures, despite the fact that methane mixtures apparently exhibit this spontaneous cellular structure in lean mixtures.

2.5. Explosions in Duct Vented Vessels

Duct vented geometries are common-place in industrial installations where it is necessary to direct explosion products and hot gases away from sensitive or manned areas. However, it has been shown that the presence of a duct on a vent opening can readily increase the severity of an explosion [11, 50] and in some highly reactive mixtures can shorten the distance of deflagration to detonation transition (DDT) [51], or even induce an upstream directed detonation in the primary vessel [52]. Such increases will therefore increase the reduced pressure (P_{red}), which poses a further safety problem that should be accounted for in the design and implementation of the installation.

Recent works involving vented gas explosions have tended to focus upon the effects of geometry, ignition position, initial turbulence and pressure vent deployment [8, 45, 53]. A point raised repeatedly in this literature is that central ignition is observed to be the worst case. Ponizy & Leyer [8] discuss the effect of spark position within a simply vented vessel. They report that for ignition central to the chamber the maximum

pressure profile is achieved, with the relationship *central > end > proximity to the duct*. In practice, however, this scenario may be an underestimation.

The works of Ponizy & Leyer [8, 50] and later Ponizy & Veysseriere [54, 55], were based on small scale geometries (3.6 litre), and due to the complications of scale effects it is not possible to know whether the results are applicable to larger, more industrially-relevant geometries.

Many vent calculation methods exist and have been discussed in literature [9, 15, 23, 38, 56, 57]. Where a duct is added to a vent, the effective increase on the expected reduced pressure, P_{red}, (expressed in barg) can be estimated for a homogeneous explosion based upon the equations given by NFPA 68 [57] for duct lengths below 3m, and <4 duct diameters, given by:

$$P'_{red} = 0.779\ (P_{red})^{1.161} \qquad \text{Eq. 2-29}$$

and for duct lengths between 3m and 6m

$$P'_{red} = 0.172\ (P_{red})^{1.936} \qquad \text{Eq. 2-30}$$

2.5.1. Additional Factors Which Affect the Maximum Pressure and Rates of Pressure Rise in Duct Vented Enclosures

Duct vented explosions are subject to many of the same influencing factors as mentioned above for vented vessels, including the phenomenon of acoustic oscillations on the pressure records. Indeed, Kordylewski & Wach [45] reported such oscillations in their work on small scale duct vented explosions, and suggested that this phenomenon could be somehow responsible for the unusual pressure rise in the primary chamber. However, given that they also observed strong pressure rises (with respect to vented vessels without a duct) in the absence of any oscillatory behaviour, then this link is tenuous.

A 'burn-up' event in the duct – that is the turbulent mixing of burned and unburned gases in the initial sections of the duct which promoted violent burning within this area – has been addressed by several authors as the main event responsible for the dramatic

increase of pressure in the primary vessel [8, 50, 58]. Such an event, it is argued, produces a pressure impulse from the duct into the primary vessel, which induces turbulent flow either by means of backflow of unburned gases or blockage of effective venting from the primary vessel into the vent. Other authors have attributed pressure drops due to the resistance of the gas flow through the primary vessel and duct as being responsible for large differences between vented and duct vented vessels [59, 60]

An additional hazard associated with hydrogen (and propane) is its susceptibility to DDT [20]. A study by Medvedev *et al* [52] used a small (4 litre) cylindrical vessel connected to a ducted vent, to investigate hydrogen-oxygen-nitrogen and acetone-oxygen-nitrogen explosions. They observed that even with a short duct there was a detonation or detonation-like event occurring in the ignition chamber after the flame had entered the duct. However, they argue that considering that the explosion was triggered by only a weak ignition source, there was a very low probability that the observed detonation could be formed in the usual manner similar to that in elongated tubes. In fact, they concluded that the event was due to the SWACER (shock wave amplification by coherent energy release) mechanism – this refers to the fast turbulent mixing of hot burned gases with the unburned gases, which can lead to the onset of detonation in very short distances. They referred to this phenomenon as 'upstream-directed detonation' as it appeared to initiate in the duct, or at the vent opening, propagating back into the vessel.

2.6. Explosions in Interconnected Vessels

Interconnected compartments are common in a wide range of situations, including two adjacent rooms with a linking corridor, two linked reactor vessels, and two adjoining tanks with connecting pipe work. Connected chambers with potential flammable gas leaks have a potential for accidental release which can be caused by many factors, including inadequate maintenance of equipment, design weaknesses, material defects, corrosion, and so on. In many cases this release will occur in only one of the connected volumes, as it is unlikely that two simultaneous leaks will occur in two connected volumes at the same time. It is this situation of a leak in one compartment connected to another containing no flammable gas that is investigated in Chapter 7 of the present

work. Furthermore, the extreme example is investigated whereby if the leak had mixed with the volume in both vessels then no ignition could occur as the amount of flammable gas studied is insufficient to form a flammable mixture. The present work was undertaken to provide data for the testing of computer models [3] as well as for experimental evidence on this practical risk scenario.

Research already conducted in this area has predominantly focussed upon linked compartments where both compartments and the connecting duct were filled with flammable mixtures [3-5, 61]. This demonstrated that interconnected vessels can display a phenomenon referred to as pressure piling, a mechanism specific to interconnected vessels, which causes faster rates of pressure rise *(dP/dt)* and higher maximum pressures (P_{max}) in the second vessel when compared to an isolated vessel of the same size [4]. Additionally, more severe explosions have been found in the second vessel compared to the ignition vessel [3, 61]. It is usual for the more severe explosion to occur in the secondary vessel, but there are differences observed for different ignition positions within the primary chamber.

For central ignition, higher P_{max} was observed in the secondary vessel and it occurred slightly earlier in the explosion development than the maximum pressure in the primary vessel [61]. For end ignition, it was found that the secondary vessel had slightly higher P_{max}, but much higher $(dP/dt)_{max}$. End ignition led to more severe explosion in the second vessel, which may be attributed to increased turbulence and gas compression factors [4, 61, 62]. Razus *et al* [4] concluded that the most important factors in interconnected vessel explosions were the connecting tube diameter, flame direction, volume ratio of vessels and the distance between the spark and connecting pipe. They also concluded that no matter what configuration was used, the highest maximum pressure was always observed in the second vessel. The results from the above research on fully filled premixed interconnected vessel explosions clearly suggest that explosion severity makes effective protection of such systems difficult. However, it is not currently known whether similar conclusions can be drawn when considering the more realistic scenarios of partially filled interconnected vessels. Alexiou, Phylaktou & Andrews [62] were the first to investigate this scenario with three linked vessels, with only the first (smallest) vessel containing a flammable mixture. They showed that high

overpressure could still occur in the third vessel, even though the overall mixture was not flammable.

2.6.1. Factors which Influence the Maximum Pressure and Rates of Pressure Rise in Interconnected Vessels

The compression of gases in the secondary vessel of an interconnected geometry before the time of flame arrival and the turbulence induced in both vessels by the flow in the connecting pipe plays a major role in interconnected vessel explosions.

Explosions in interconnected geometries typically experience higher pressures and rates of pressure rise than single closed vessels of the same volume. As discussed, current published literature regarding interconnected vessel explosions has predominantly focused on a flammable mixture filling the entire geometry [3-5, 61]. Such experimental researchers report a number of common findings, including that when an explosion occurs in an interconnected vessel, greater severity can be achieved than in an isolated vessel of equivalent size/volume. Also, for most fuel-air mixtures, the second chamber displays higher rates of pressure rise and peak pressures than the primary chamber due to a predisposition of interconnected vessels to pressure piling. The fact that most enclosures are only able to withstand tenths of a bar overpressure [60] indicates that the pressure piling phenomenon, whether it occurs in partially- or fully-filled vessels, may cause damage to the confining geometry.

In interconnected geometries, it has been shown that pressures in the second vessel experience higher maxima (P_{max}) and slightly faster rates of rise (dP/dt_{max}) than the primary vessel for central ignition, and in addition, these phenomena occurring in the second vessel also tend to appear earlier than for the primary vessel [3]. For end ignition in the same configuration, however, it is reported that often the secondary vessel displays slightly higher P_{max}, but much higher dP/dt_{max} (in the region of 4x higher compared to only 1.07x for central ignition using stoichiometric methane-air mixture) [3]. It is also reported that end ignition leads to more severe explosion in the second vessel, which may be attributed to increased turbulence and gas compression factors [3-5].

2.6.1.1. Pressure Piling

The presence of a connecting pipe between two vessels, such as connections by pipelines, can produce especially high explosion parameters due to an effect known as pressure piling [9]. Pressure piling is a mechanism specific to interconnected vessels which causes faster rates of pressure rise (dP/dt) and higher maximum pressures (P_{max}) in the second vessel when compared to an isolated vessel of the same size [4]. The literature consistently reports a more severe explosion in the second vessel [3, 61] compared to the ignition vessel.

The term pressure piling refers to a situation where the maximum pressure recorded in a connected vessel is higher than the adiabatic pressure expected, based on the assumption of a uniform starting pressure throughout the vessel. This has been attributed to the pre-compression of the mixture in the non-ignition chamber, prior to flame arrival, resulting in an effective starting pressure for this vessel higher than that of the system as a whole at the time of ignition, thereby causing higher than predicted rates of pressure rise and maximum pressures. The degree of pressure piling observed in any configuration is dependent on many system parameters including system geometry, mixture reactivity and size of the linking geometry [61].

Major influences on the behaviour of explosions within interconnected vessels include pipe diameter and vessel volume ratio [4]. Razus *et al* [4] conducted an in-depth investigation into the effect of the major influencing factors within an interconnecting geometry. They concluded that the most influential factors included initial pressure and tube diameter, and other important factors included flame direction, volume ratio of vessels and distance between spark and connecting pipe. They concluded that no matter what configuration was used (including upward and downward propagation), the maximum pressure (and the pressure piling phenomenon) was always observed in the second vessel. This supports the evidence that in an interconnected vessel, the second vessel is likely to experience a more severe explosion and a higher pressure irrespective of the exact configuration or initial pressure.

Studies have reported a specific interaction between interconnected vessels (in the case of two interconnected vessels linked by a duct) [61, 63]. Figure 2-5 (from Di Benedetto *et al* [63]) illustrates such an interaction for two unequal cylindrical vessels connected

by a pipe. The black line represents the pressure in the (larger) primary vessel and the red line the pressure in the (smaller) secondary vessel. The figure displays an initial slow pressure rise throughout the whole vessel before the flame enters the second vessel. During the initial stages of the explosion in the primary vessel unburned gases were pushed ahead through the connecting pipe and into the secondary vessel, increasing the pressure in the secondary vessel to P_1 marked on Figure 2-5 at time t_1. In addition to this increased initial pressure in the secondary vessel, the flame injection from the connecting pipe serves to generate increased turbulence which causes increased flame propagation velocity. This is eventually culminated in the maximum pressure recorded in the second vessel (P_k), which is consistently reported to be higher than the maximum pressure from the primary vessel (P_m), and where pressure piling is evident P_k will also exceed the adiabatic value.

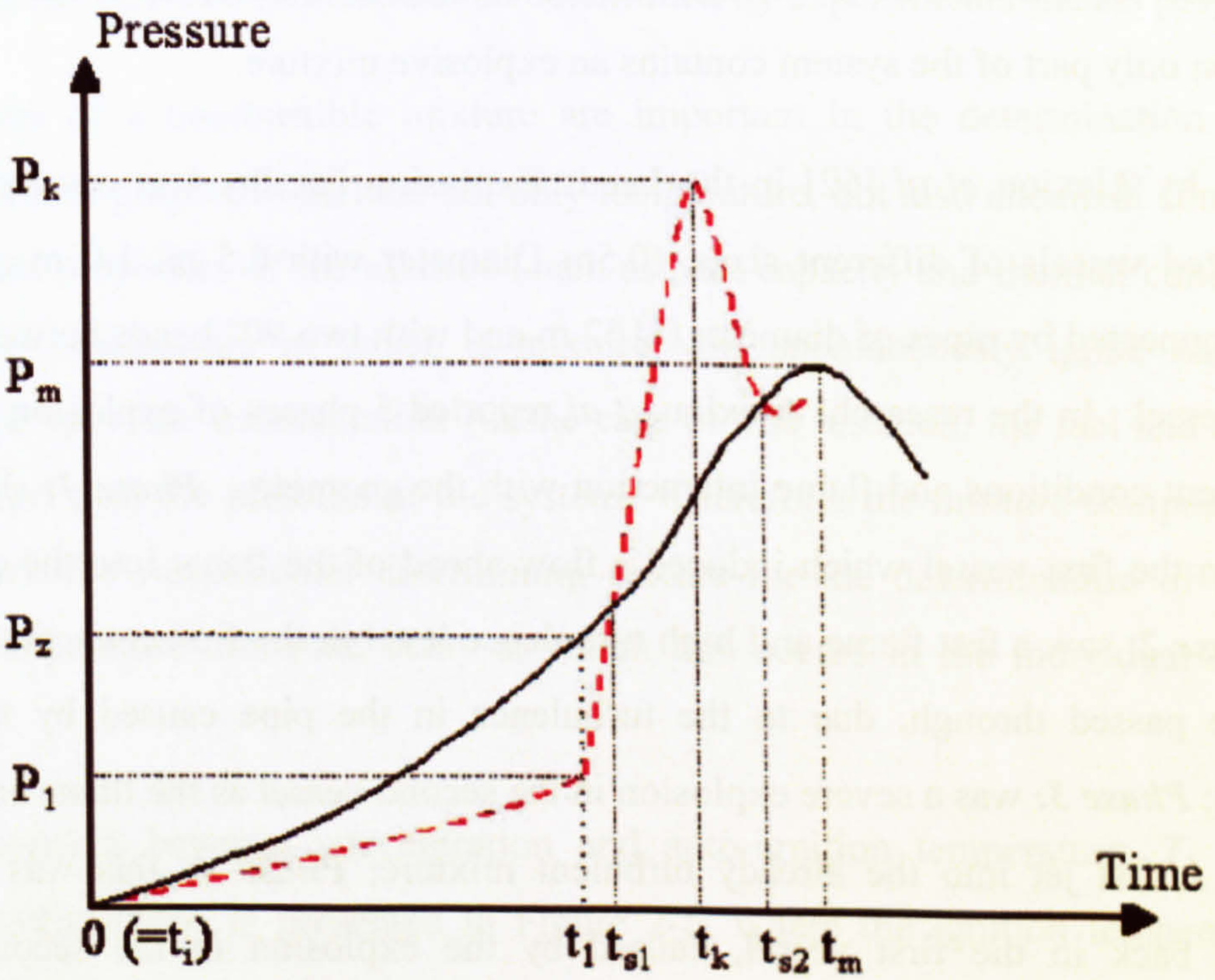

Figure 2-5: Quantitative trend of pressure as a function of time in a two vessel interconnected geometry [63].

The specific value of pre-compression in the secondary vessel is a direct consequence of the reaction and venting of the laminar explosion initiating in the primary vessel. It follows from this that since the final maximum pressure is determined by the initial

conditions, so the final value of pressure in the secondary vessel (P_k) should be determined by the initial pressure in the secondary vessel when the jet flame exits the connecting pipe and ignites the unburned mixture [63]. Bartknecht [11] and Singh [61] carried out small-scale and medium-scale methane-air experiments in interconnected geometries. They concluded that the main features of importance in terms of severity were ignition position, pipe diameter and volume ratio between connected vessels.

2.6.2. Partially-Filled Interconnected Vessel Explosions

The above research on fully-filled premixed interconnected-vessel explosions clearly suggest that explosion severity makes effective protection of such systems difficult. This returns the focus to the more realistic scenario of the partially-filled interconnected vessels, and the question as to whether similar behaviour is observed when at the time of ignition only part of the system contains an explosive mixture.

Research by Alexiou *et al* [62] in the Leeds Explosion Facility was conducted using three linked vessels of different sizes, (0.5m Diameter with 0.5 m, 1.0 m and 2.0 m length) connected by pipes of diameter 0.162 m and with two 90° bends between the 2nd and 3rd vessel. In the research, Alexiou *et al* reported 5 phases of explosion related to the different conditions and flame interaction with the geometry. ***Phase 1:*** slow initial burning in the first vessel which induced a flow ahead of the flame into the connected pipe; ***Phase 2:*** saw a fast flame and high turbulence level in the first connecting pipe as the flame passed through, due to the turbulence in the pipe caused by the initial explosion; ***Phase 3:*** was a severe explosion in the second vessel as the flame entered the vessel as a fast jet into the already turbulent mixture; ***Phase 4:*** this was a severe explosion back in the first vessel, caused by the explosion in the second vessel expanding and inducing a backflow of gas turbulence into the first vessel, in addition to venting into the third vessel, creating a first pressure peak there; and finally ***Phase 5:*** was a second rapid pressure rise in the second vessel which was attributed to the fast burning of phase 4 in the first vessel which is then discharged into the second vessel and adding to the turbulence already generated in this vessel. Following these five phases, there was a further explosion reported in the third vessel which was a consequence of

the burning of the remains of the unburned gas displaced by the first five phases of the explosion.

2.7. Autoignition Phenomenon

Autoignition is a term used to describe the mechanism whereby a mixture undergoes spontaneous ignition in the absence of an external ignition source. The lowest temperature at which the mixture is able to sustain such combustion is known as the autoignition temperature (AIT). Autoignition behaviour of a mixture is determined by the relative reactivities of main propagating free radicals of a fuel [64]. Where the AIT of a mixture cannot easily be derived from any simple physiochemical basis, for example where the fuel contains impurities such as the presence of up to 8% ethane in natural gas, the AIT of a mixture can be determined by experimental means [64].

The features of a combustible mixture are important in the determination of auto-ignition. These properties include not only temperature, but also chemical composition and physical properties of the mixture (such as heat capacity and thermal conductivity) [26]. The temperature at which a mixture will spontaneously ignite has a high dependence upon the concentration (in the case of this research, the fuel and air as the oxidant), and also the pressure of the system. Therefore, the mixture composition and pressure are the fundamental determining factors for the determination of the auto-ignition temperature and time delay at which this occurs in the individual explosion [26].

The relationship between concentration and auto-ignition temperature, T_b (°C), for various hydrocarbons is presented in Figure 2-6, where the ignition temperature was determined using the Le Chatelier method involving injection of a previously prepared cold mixture into a heated evacuated vessel (further details on this and other methods of auto-ignition temperature determination are not entered into here, but are available in [26]). This figure assumes that the body of gas is initially at rest, and does not account for time delay between initiation and ignition.

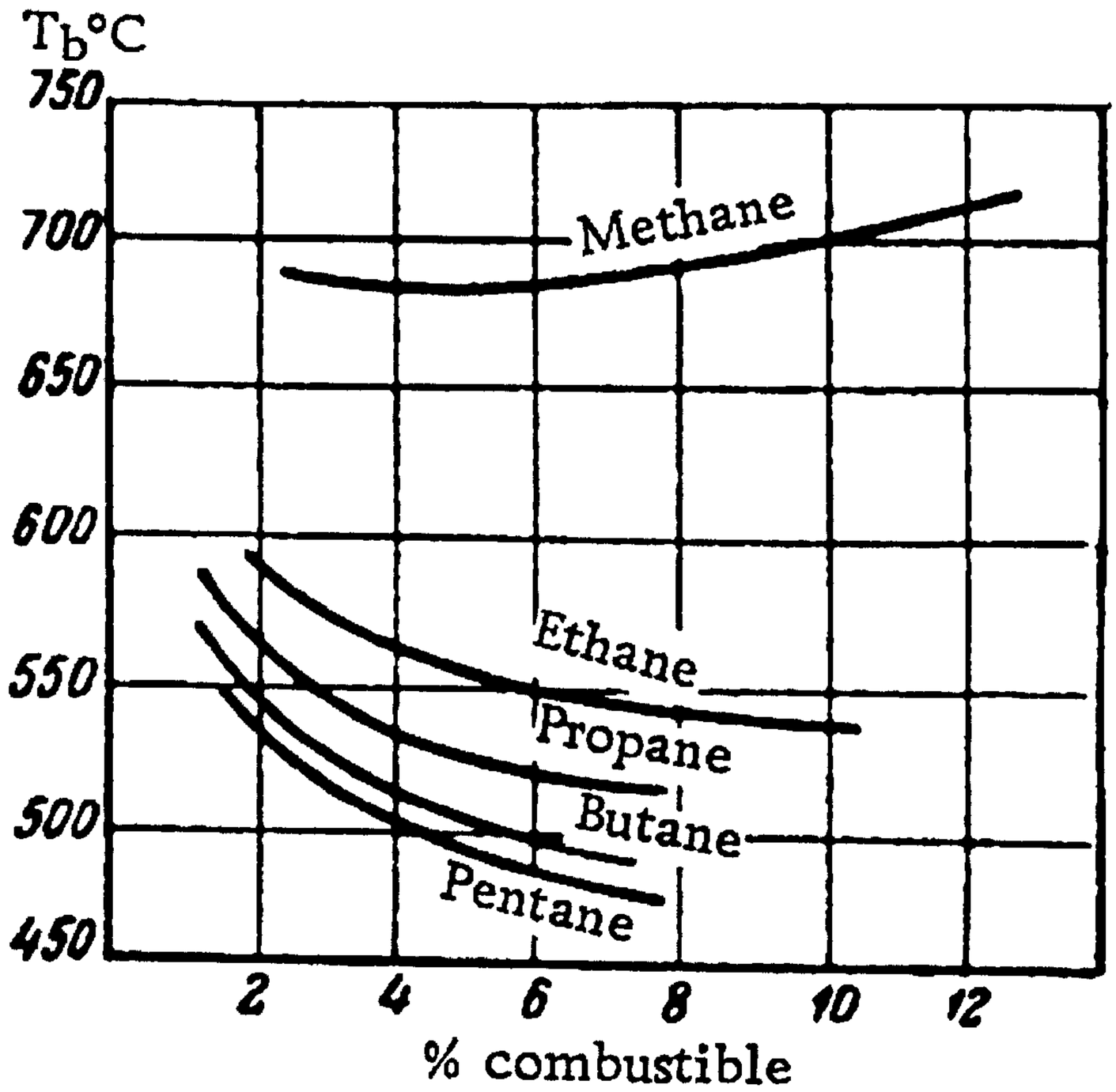

Figure 2-6: Auto-ignition temperature as a function of hydrocarbon concentration (from [26])

Figure 2-6 shows the auto-ignition time delay or lag associated with propane at different concentrations and different initial temperatures. It is shown that as the temperature and concentration of the mixture increases, the ignition delay time reduces. The graph presented does not extend to the initial ambient temperatures, starting at a temperature of 521°C and steadily increasing. However, the temperature of the medium with the onset of auto-ignition will not be at ambient temperature.

In ignition delay experiments conducted by Williams [27], the ignition delay τ was defined as the ratio between the distance downstream at which detectable luminous emissions began, and the convective velocity, V. Since in the present work, it is not possible to measure luminous emissions, the time of onset of the detonation-like peak was used. With an extrapolated temperature from Figure 2-6 and ignition-time delay from Figure 2-7, the triggering event can be approximated from the values obtained.

Lewis [10] reports that in a pipe, several autoignition events may occur in regular succession and that they are likely to occur in the space between the forming shock wave and the ensuing flame front, before the flame front is able to close the gap.

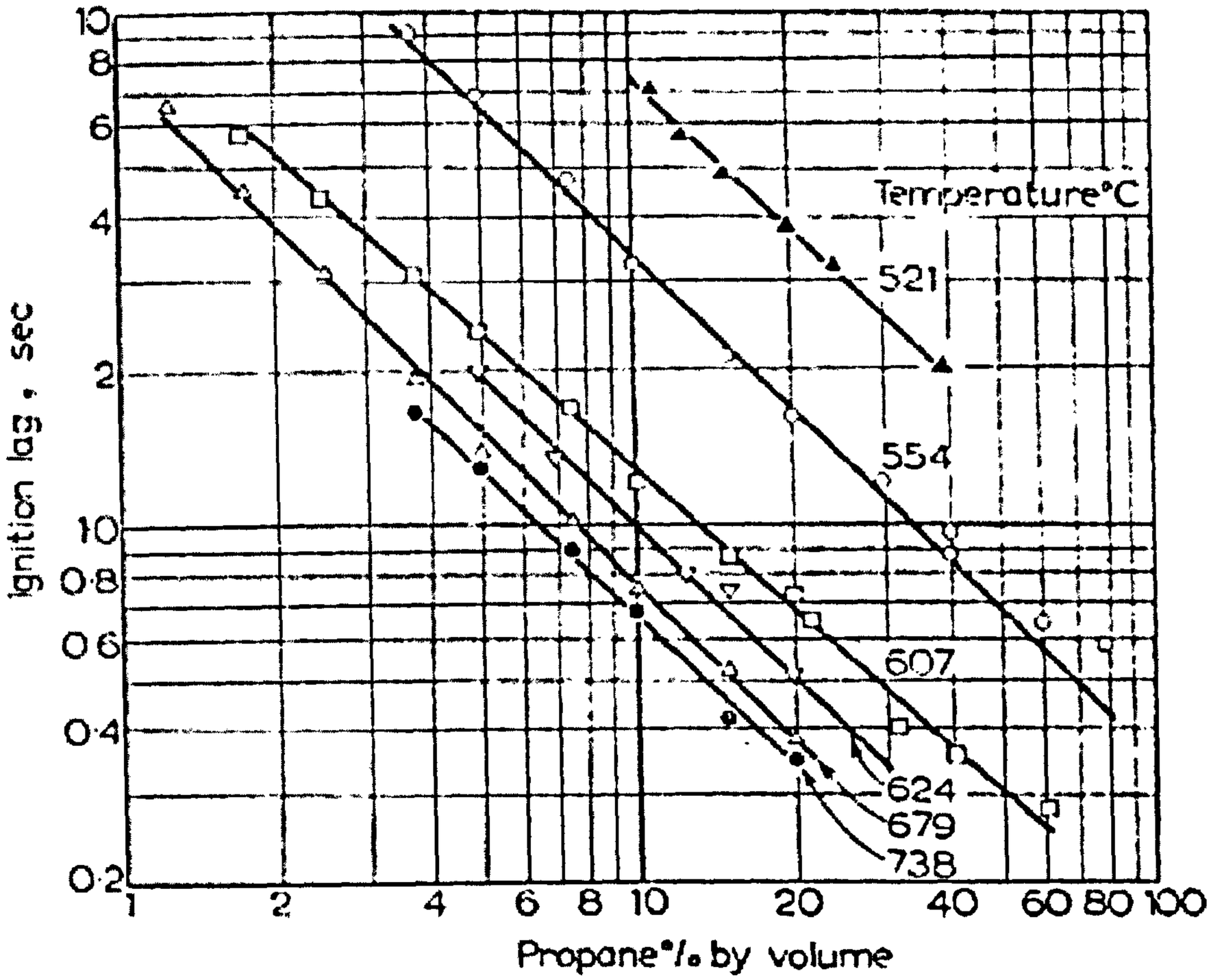

Figure 2-7: Ignition delay data as a function of propane concentration, (from Mullins and Penner [14])

2.8. The Stratified Gas Explosion Hazard

The above-mentioned research into duct vented gas explosions has concentrated (as indeed have many other explosion studies) on homogeneous gas mixtures only. A more realistic mixture would be stratified (having a concentration gradient), normally created by some accidental leak. In the laboratory, a lot of attention is paid to ensuring that the mixture is completely homogeneous before ignition, using methods such as fans, recirculation pumps and partial pressure techniques. However, in reality, the likelihood of explosions resulting from a stratified fuel-air mixtures is high, especially with regard to a particularly buoyant or heavier than air fuel leak within a confined area or structure.

The investigation of stratified fuel-air combustion is significant to many industries where the possibility of a fire or explosion can arise from an accidental leak of a flammable fuel from storage tanks, pipelines and transportation tanks. The implementation of controlled energy release from a confined gas-air explosion has been

at the forefront of industrial development throughout the past century, including development of technologies such as internal combustion engines (using stratified charges) [65, 66]. Conversely, there have also been a significant number of uncontrolled releases as discussed previously, where uncontrolled gas or vapour releases led to the partial or total destruction of several plants, and the loss of lives. In the wake of such events, research into stratified gas-air explosions can provide a step towards the advancement of scientific knowledge which will ultimately be aimed at the prediction and mitigation of such incidents.

Stratified explosions may inherently produce lower overpressures than the equivalent homogeneous mixtures. However, they still pose a concern as it has been noted that the resulting overpressures can easily exceed what a structure can tolerate [67].

Investigation into stratified gas explosions has not only been centred around the development of technologies such as the internal combustion engine, but also directed towards understanding a wide range of combustion phenomena, including oil spill / vaporising pool explosions [68, 69] and combustion of methane layer in coal mines [55, 70, 71]. Whilst in the past a lot of attention has been paid to the research of methane layer explosions pertaining to coal mines, in more recent years the focus has begun to shift towards industrial safety in flammable liquid process/dispensing areas [67].

2.8.1. General Theory

A stratified mixture is formed where fluids of different densities try to arrange themselves in distinct layers due to the forces of gravity. If a gas is released into the atmosphere, typically it will mix and disperse under its own momentum and buoyancy (for low molecular weight gases). However, where the release is within some confined geometry, a concentration gradient will form as there is a smaller volume available for dispersion [72]. In practical situations, a concentration gradient, also referred to as a heterogeneous or stratified mixture, will almost always form when two gases or vapours are allowed to mix freely without external influence. Indeed, literature has brought attention to the fact that stratified explosions tend to be more prevalent than those of an entirely homogeneous nature [19].

In general terms, a stratified explosion will tend to be less severe with respect to maximum pressure (P_{max}), rate of pressure rise (dP/dt) and flame-speed (S_f) than the equivalent 'global concentration' homogeneous mixtures (total concentration of fuel injected as a % of the total volume). However, as noted in literature [19, 55, 70], it is important to remember that stratified mixtures can ignite at global concentration well outside the accepted flammability limits if the equivalent mixture were homogeneous.

Unlike the equivalent homogeneous mixture, in stratified mixtures the whole of the leak area is generally not a 'danger zone' all of the time – the release usually forms a gradient where there will be a rich portion of the mixture (concentration above the UFL), and a lean portion (concentration below the LFL), with a flammable fraction in between. Therefore an ignition source present when the release begins may not ignite the mixture until the flammable fraction reaches that point.

There are a number of approaches to predicting the formation of a leak within a structure and out in the open atmosphere which offer an estimation of which portions of the release will be within the flammable fraction, usually as a function of time. It is not the intention of the current research to investigate stratified gas *formation*, rather it is the *effect* of the stratified mixture in comparison to the equivalent homogeneous which is of importance. Therefore, while a brief summary of the techniques and theories adopted is given below, this does not purport to be a comprehensive review of literature in this area. If the reader requires further information on a particular theory or technique, they are directed to the relevant text references offered in each section.

2.8.2. Formation of a Stratified Gas Mixture

Gas accumulation generally occurs over time and is a function of the gas type, release rate, momentum, buoyancy flux and leak position/direction within the confining volume. Where the fuel has a high molecular weight without some external mixing force, there will be a low lying concentration of the fuel air mixture, which may be characterised in explosion investigation as producing more damage to the bottom of confining geometry [73], whereas where the molecular weight of a fuel is low, the majority of the damage will be towards the top of an enclosure.

The release of a flammable gas within an enclosure can occur in several different ways, with two readily-identifiable extremes of fuel release. Slow/low momentum releases can often go undetected for a period of time since sensors or pressure detectors will not necessarily detect the release immediately. Unless acted upon, such releases can build up over time to form a flammable mixture within a room or closed process vessel which may make contact with an ignition source at some point. Conversely, the rupture of a vessel may create a high momentum or instantaneous release of fuel into an enclosure or system which will quickly reach flammable concentrations.

Forced ventilation is often employed where flammable gases are housed indoors or in a sealed compartment. In such cases, natural or forced ventilation systems can often train low momentum leaks to an external location. Often, however, where an instantaneous release is involved or where there is no enclosure ventilation, a leak can quickly form into a flammable cloud. Any possible leak rate between the aforementioned extremes are possible.

2.8.3. Laboratory Techniques for Formation of a Stratified Mixture

In considering the preparation required to achieve a stratified mixture using reactive gases, there are several methods described in the literature in which a degree of stratification has been achieved. These vary from very simple to excessively complex, and are achieved using a variety of equipment. The most well documented methods proposed by current literature include direct injection of fuel into a vessel [74], preparation of concentric spheres contained by 'soap bubbles' [75, 76], use of a pre-ignition partitioned compartment [55, 77], roof layers [70], and evaporation from a pool of liquid fuel [69, 73]. The complexity of these methods varies wildly, each having their own individual merits and weaknesses from both a practical and theoretical perspective. The major methods of stratified mixture preparation are here considered in turn.

Simple Injection Method

The simple injection method is perhaps at face-value one of the simplest and most realistic approaches. This mixture preparation method has been used by Whitehouse *et*

al [74], who conducted a series of stratified hydrogen tests using an air-filled $10m^3$ vertical test cylinder with hydrogen allowed to leak in at the top to form a variety of concentration gradients equating to stratified layers. This method is advantageous in that it is fast, simple, and comparatively inexpensive to implement. Difficulties arise as the stratification within the vessel may not be repeatable in every case, and may only be accurate to within loose error bounds. In this case, results may require standardisation to become comparable.

The Soap-Bubble Method

Considering the 'soap bubble' method, this technique appears to be ideal for the stratification purpose. On closer inspection, however, it becomes apparent that there are many flaws. In this method concentrations of gas are separated by filling concentric soap bubbles with the required concentration. Using a single bubble, simulation is not quite realistic, as there is a separating barrier preventing a premixed section mixing with an air layer, which gives rise to questions regarding the applicability of the results obtained. The soap bubble method has been used to varying degrees of sophistication. Simple scenarios, such as that used by Furuno *et al* [76], deal with a single soap bubble containing a fuel concentration within a larger combustion chamber containing either a lower concentration mixture or air. In this research, Furuno *et al* [76] suggest that there is no difference in premixed trials with and without the soap bubble, but since the pressure is equalised and the concentrations are identical, no difference would be expected, therefore this is a flawed argument. However, in the stratified scenario, there is a high concentration of gas separated by a thin membrane to a lower concentration area or air only area. The barrier itself prevents realistic mixing along the interface.

Experiments which use a series of concentric spheres of soap bubble mixtures, in decreasing gas concentration outwards [75], are a little better in their simulation of concentration gradients, however even these experiments are subject to some of the same constraints. Such experiments are designed to give a good approximation of vapour cloud explosions and were developed to validate the numerical models which deal with such scenarios [75]. However, it is not very often that a perfectly hemispherical leak of constant concentration gradient occurs when gas is released into a room, as the mere action of a gas being released allows the fuel to entrain some air with it thereby becoming slightly mixed on exit from the leak site. This mixing occurs along

the interface between fuel and air, and is prevented from occurring naturally in the soap bubble method. The results, therefore, are limited in their applicability to real life situations. They are still very useful, however, for approximation and for general interest and simple modelling technique testing.

Partitioned Compartment Method

Partitioned compartment mixture preparation involves partitioning the test vessel using a retractable partition which is normally withdrawn immediately before or at a given time delay before ignition [55]. This method has been used with both small scale and large scale apparatus [55], and limited published material spanning many decades is available. Advantages of this method include its simplicity, however, similarly to the 'soap bubble' method, this technique has issues relating to its comparability to real situations. It would be rare for a layer to form completely isolated from the surrounding area, and only mixing along a plane of retracting membrane. This technique produces a simulation whereby a layer is formed of uniform concentration above a layer of differing uniform concentration, completely ignoring the possibility of complexities such as pockets of varied concentration gas which inevitably form in real stratified mixture preparation. This method is not perfect, but, as described in the previous and current work sections below, this method has been utilised within this research to simulate a gas pocket in an interconnected compartment scenario.

Roof Layer Method

Considering roof layers, this range of experiments have predominantly involved the use of methane. In the main, work in this area has taken place to investigate explosions in coal mines. It has been a common consensus that a layer of methane forming at the roof of a coal mine can be particularly dangerous, especially if this dislodges settled dust and creates a secondary dust explosion heightening the severity [70]. The work undertaken by Phillips [70] indicated that the burning velocity of a stoichiometric stratified methane air mixture is independent from fuel concentration and gradient at the interface of the layers. However, despite this early work, there has since been a consensus that experimental data regarding flame dynamics in stratified mixtures in real chambers has been lacking [75], and at present, this situation has not been fully rectified.

While this method reproduces one of the most realistic scenarios, the practicalities are unfortunately somewhat different. The method of gas introduction through a porous roof to allow an injection of gas across the whole length of the roof layer is a very attractive approach, which will give a reasonably uniform stratified layer. Many of the experiments conducted using this technique involve open gallery experiments [70] or open ended, which requires outdoor tests or allows only small scale tests indoors. This method lacks the ability to perform heavy and light gas stratification using the same equipment which adds extra expense.

Evaporation from a Liquid Pool

Finally, the use of liquid pool fuel evaporation. This technique is reasonably simple to perform, and has been exploited by a variety of researchers in the past [73, 78]. This technique generally involves a shallow metal tray containing the liquid fuel, floated upon a variable temperature water bath. Advantages of this method include its relative simplicity; however, scale and repeatability from test to test could be a problem. Drawbacks associated with this method again include the imprecise nature of the evaporation, and repeatability in this technique may be difficult, even using the same conditions or preparations.

2.8.4. Overview of Experimental Studies

The current literature on stratified explosions deals predominantly with buoyant gases [55, 70, 73]. To the authors' knowledge, the only work which has combined the investigation of stratified mixtures and vented vessels was conducted in a large scale, simply vented (without a duct), rectangular geometry [67, 68, 79, 80]. This work provides useful data, but may not be as useful to process vessels which are often cylindrical. Additionally, many process vessels are fitted with duct vents to direct explosion products away from sensitive areas. It has already been shown in literature that the presence of a duct can induce a more severe explosion than a simply vented case [11, 50].

In general terms, stratified gas explosions tend to be less severe with respect to maximum pressure (P_{max}), maximum rate of pressure rise $(dP/dt)_{max,}$ and flame-speed

than homogeneous explosion tests, but there is the added danger that even when a leak would be outside the flammable region when fully homogeneous it can be ignited under stratified conditions. For example, in an early study conducted by Liebman *et al* [55], a 50% methane-air mixture was successfully ignited under stratified conditions. This trend also applies where the concentration is below the lower flammability limit, showing that in some cases the explosion can be more severe than the partial pressure concentration of fuel would suggest [70].

Buoyant Gases

Early studies on stratified gas explosions were dominated by research into methane roof layers in mines [55, 70]. Such research highlighted the danger of the possibility of ignition of a mixture outside the normal flammable range. Indeed as previously discussed in the research conducted by [55], a 50% methane-air mixture was successfully ignited in an open gallery chamber confined only at the top.

These early works reported a 3-phase flame consisting of an initial 'premixed flame' which burns as a 'U' shaped flame through the flammable fuel layer (bounded by the UFL and LFL), followed by a diffusion flame close behind where the fuel rich layer and the air rich layer mix through a process of diffusion in the wake of the premixed flame and subsequently burn, and finally a convection flame (described as a ragged burning of the remaining fuel, mixed by buoyancy factors) which can follow these flames by some distance.

The flame structure associated with the flame passing through the interaction of stratified methane-air layers is consistently described throughout the literature [55, 70, 81]. The conceptual model is that the flame has a specific 3 zone structure, (illustrated in Figure 2-8);

1) A 'U' shaped premixed advancing flame at the front, burning through the established flammable zone;

2) A diffusion flame burning in the wake of the premixed flame forming as the fuel and air coning together in the wake burns; and

3) A convection flame following up to 300 mm behind the diffusion flame [55, 70]

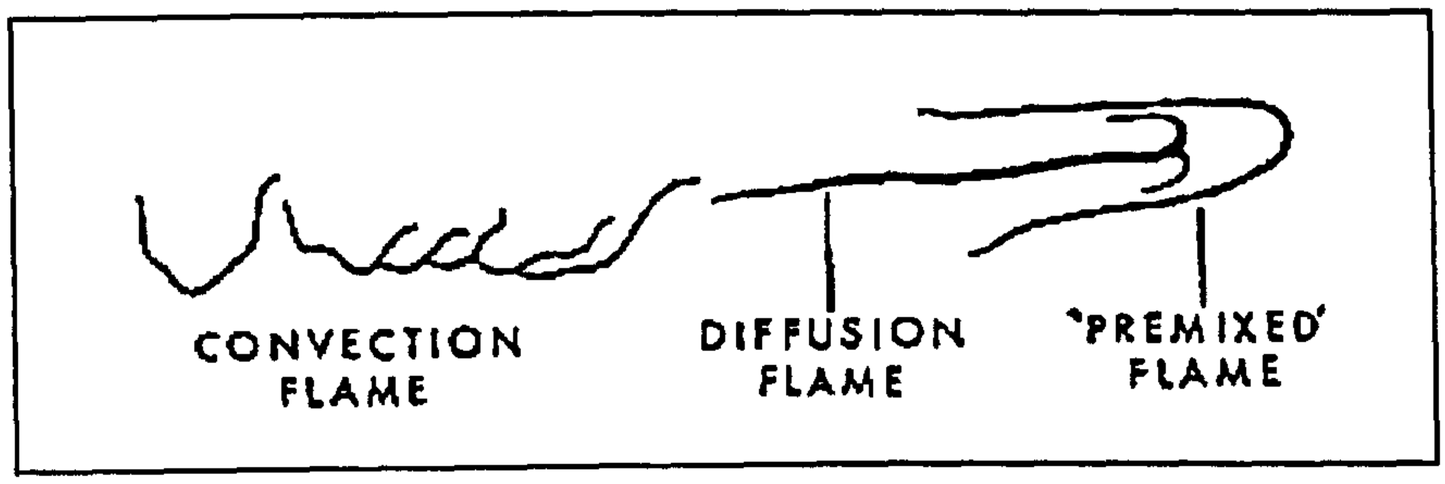

Figure 2-8: Three zone flame structure [70]

Attempts have been made to quantify the differences above through observation. Jiménez [66] reports that there are four main effects which occur when a flame propagates into a stratified mixture, contributing to a change in the rate of heat release:

- Differences in the composition of the mixture and equivalence ratio give rise to local differences in the reaction rate, producing a deformation of the flame front as the segments of the flame front propagate at different speeds through these instabilities. This effect increases the flame surface area in comparison to a homogeneous mixture;

- These differences in local reaction rate then allow local variations in the heat released per unit area of the propagating flame – this effect can either increase or decrease the global heat release rate relating to the specific non-homogeneities;

- The local reaction rate can decrease as the flame surface aligns with the tangential strain of the mixture – this can have the effect of locally reducing the reaction rate according to the non-homogeneities; and finally,

- The local temperature and concentrations can vary, both increasing and decreasing in a non-homogeneous flame, to a greater extent than a homogeneous one [66].

However, despite all of the differences in local reaction rate and heat release rate discussed by Jiménez [66], the overall conclusion offered by this work is that there is very little difference between the global heat release rate in comparable homogeneous and stratified gas explosions.

Finally, there is the issue of increased severity and unexpected explosions, which are a problem in stratified mixtures, but which may not be so for homogeneous mixtures. It has been shown in literature concerning stratified mixtures that even concentrations outside the normal flammable range can be ignited when allowed to stratify within an air-filled compartment. For example, in an early study conducted by Liebman *et al* [55], using the partitioned compartment method (see section 2.8.3), a 50% methane-air mixture was successfully ignited when the partition was removed and the gas allowed to mix for a set period of time. This was a mixture at approximately 35% above the maximum flammability limit for methane. This trend also applies where the concentration is below the lower flammability limit. Phillips [70] reports that in some cases the explosion can be more severe than the partial pressure concentration of fuel would suggest it should be. Moreover. Whitehouse *et al* [74] conducted stratified hydrogen combustion experimental research using a 10.3m^3 vertical cylinder. Their main concern was the investigation of combustion pressures, burn fractions and flame speeds, the results of which were compared to homogeneous mixtures of the same average concentration.

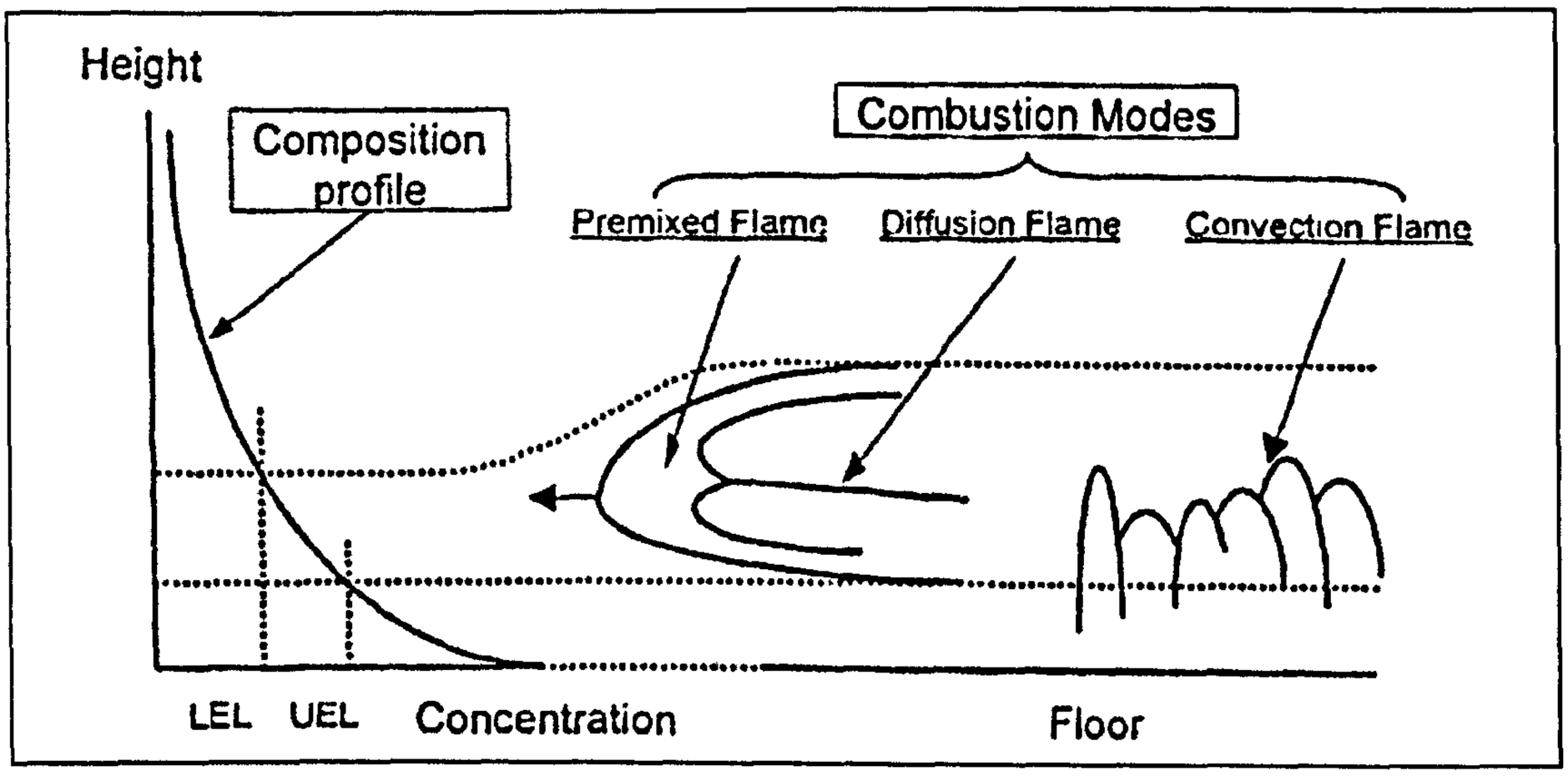

Figure 2-9: Graphical representation of 3-phase flame propagation through heavier than air fuel/air mixtures [67]

Conversely, a large proportion of accidental gas or vapour releases will involve a high molecular-weight compound, which is then likely to lead to the formation of an inhomogeneous stratified mixture in the lower region of a confining geometry. There has been limited work in this area and in many scenarios this is likely to result in

reduced overpressures, in which case our protection measures may be over-engineered. Despite this, the published literature on this topic is quite sparse.

A similar 3-structure flame to that discussed in section 2.8.4 has been described for propane explosions in the works of Tamanini [67, 79, 80, 82]. In this research, a very large 63.7m^3 chamber was used to form stratified mixtures of propane-air, ignited using a travelling ignition source, initiated on the ground and travelling upwards until a flammable mixture was encountered. This work offered a very useful graphical representation of the propagation of this 3-phase flame through the concentration gradient, reproduced in Figure 2-9. Also illustrated on figure 2-6 are 3 fractions; air-rich, flammable and fuel-rich. In his work, Tamanini proposed that a volume containing a stratified mixture can be treated as three separate fractions; oxygen-rich (non-flammable), flammable (which Tamanini refers to as the premixed fraction) and fuel-rich (non-flammable). It is reported that only the flammable and rich fractions play a significant part in the evolution of pressure in the vessel. This makes sense given that any lean (non-flammable) fraction requires the addition of fuel to become integral to the explosion – in fuel-rich fractions the fuel is already present, and can therefore be accounted for in any calculations.

Figure 2-9 illustrates well the importance of the 'flammable' layer where the initiation and main primary burning begins, but also shows the levels of air-rich and fuel-rich portions still available for mixing once the initial flame front has passed, giving rise to the diffusion flame and subsequently to the convection flame. The higher pressure and temperature (provided here by the premixed and diffusion flame burning) are known to affect the flammability limits of the mixture, allowing the ensuing flame structures to initiate and propagate more readily where the residual unburned portion is further outside the flammability limits. In addition to the heat (convective mixing reported in previous literature [55, 70]) producing this flame, the increased levels of pressure and temperature may reach a critical point for the particular mixture which leads to the initiation of the subsequent burning as a convective flame at a determined time delay. This theory may help to explain the sometimes significant time delay observed between the premixed/diffusion flames and the ensuing convective flame, and account for its absence in some tests where the correct conditions were not reached. It can also be argued that the diffusion flame may be assisted by the same mechanism.

Building on the earlier works, several authors have modelled the progression of the flame structure through non-homogeneous mixtures [83, 84], which has been referred to as a 'triple flame' structure, shown schematically in Figure 2-10. In this figure, Z represents the mixture fraction, which determines the local equivalence ratio, and subsequently the value of the burning velocity. Z_{st} then represents the stoichiometric mixture line above and below which the fuel-air mixture is rich and lean respectively. Of course this would then be reversed for heavier-than-air fuels. The diffusion flame is then formed in the wake of these flames as the residual unburned fuel from the rich flame and residual oxygen from the lean flames mix together and burn [85].

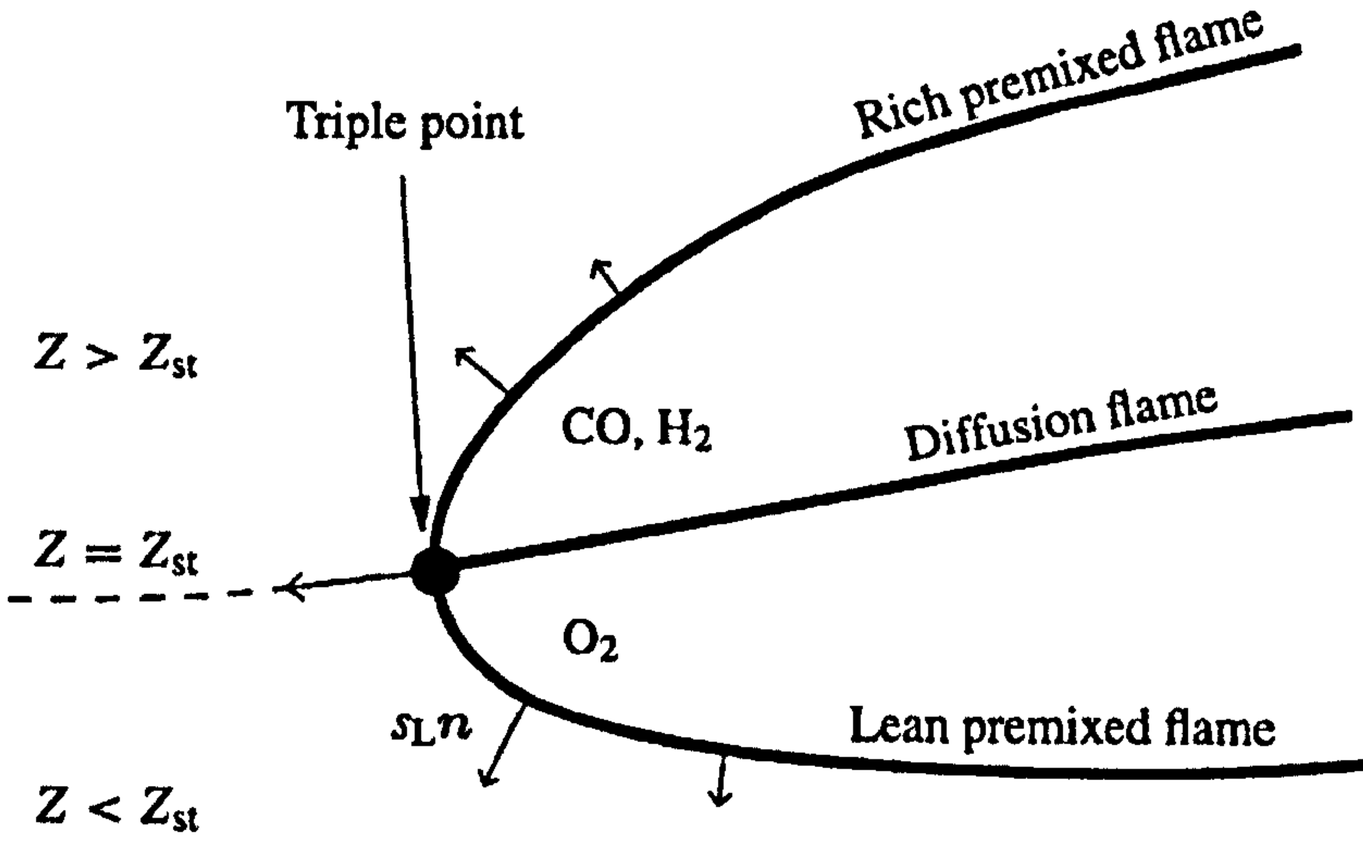

Figure 2-10: Schematic representation of a triple flame, with the arrows representing the local burning velocity [85].

In modelling these flames in this way, estimations over time of the flame propagation through a non-homogeneous gas-air mixture can be obtained. Further details on this model can be found in the cited literature.

2.9. Implications to the Objectives of the Present Study

The methods which have previously been used in literature, and the outcomes from them, have allowed a more informed choice of the methods and techniques to be used in this project. Assessing the current available means in our laboratory, it has been

possible to select the most appropriate methods for our purpose in terms of equipment used, processes and procedures adopted.

Regarding stratification mixture preparation, it has been decided to use a combination of the simple release method and partitioned compartment to separate the test vessel from the duct. The current work incorporates this chamber separation technique using a solid partition to keep a single chamber isolated from the rest of the vessel during the mixture preparation phase. Furthermore, a combination of standard homogeneous mixture preparation (using the partial pressure method) and direct leak methods were utilised to create stratification within this single compartment on a medium scale. These techniques and their combination were chosen mainly because of the simplicity, cost effectiveness and availability of existing equipment within the lab. Additionally, from the literature, it has been indicated that these methods and the respective combinations hold the best technique for the scenario that is being attempted.

2.10. Summary

The research covered by the available literature has done little to address variables in stratified gas explosions such as duct venting and the relative ignition position, leak position and volume of ignitable gas/vapour.

The current research will present new experimental data covering the above points in duct vented stratified gas explosions, including similar tests using the same primary vessel under unvented and simply vented conditions in Chapters 4 and 5 respectively.

Current design specifications as set out in the NFPA 68 venting standards [6] are based upon the assumption that stoichiometric homogeneous mixtures are consistently worst case, which is accepted to be so. However, as the global concentration of a stratified mixture approaches the flammability limits, stratified mixtures can produce a more severe explosion in terms of P_{max}, $(dP/dt)_{max}$ and flame speed S_f [86]. It is not disputed that the design of a vessel should be based upon the worst case explosion which a vessel may be required to contain (i.e. stoichiometric homogeneous), but there is no doubt that prediction of stratified mixture explosion severity would be a useful tool. More recently, the Draft European Standard on Venting [7] was produced, which offers some

small attention to stratified mixtures, including a correction factor for calculation of the severity of an explosion based on a correction factor from the equivalent homogeneous mixture that the vessel may contain.

CHAPTER 3:

EXPERIMENTAL SET-UP AND MEASUREMENT TECHNIQUES

3.1. Test Facility

The tests for this work have been conducted in the 'Explosion Hazards – High Pressure Test Facility' situated in room B11 of the Houldsworth Building at the University of Leeds. This test facility has been operational since 4th March 1997, and consists of a main 'Test room' and smaller 'Control room' (a schematic of this is shown in Figure 3-1). A concrete partitioning wall between these two areas was installed as a safety consideration and access between the two was only possible through one of two interlocked doors. The doors are linked to the interlock circuit which controls the ignition.

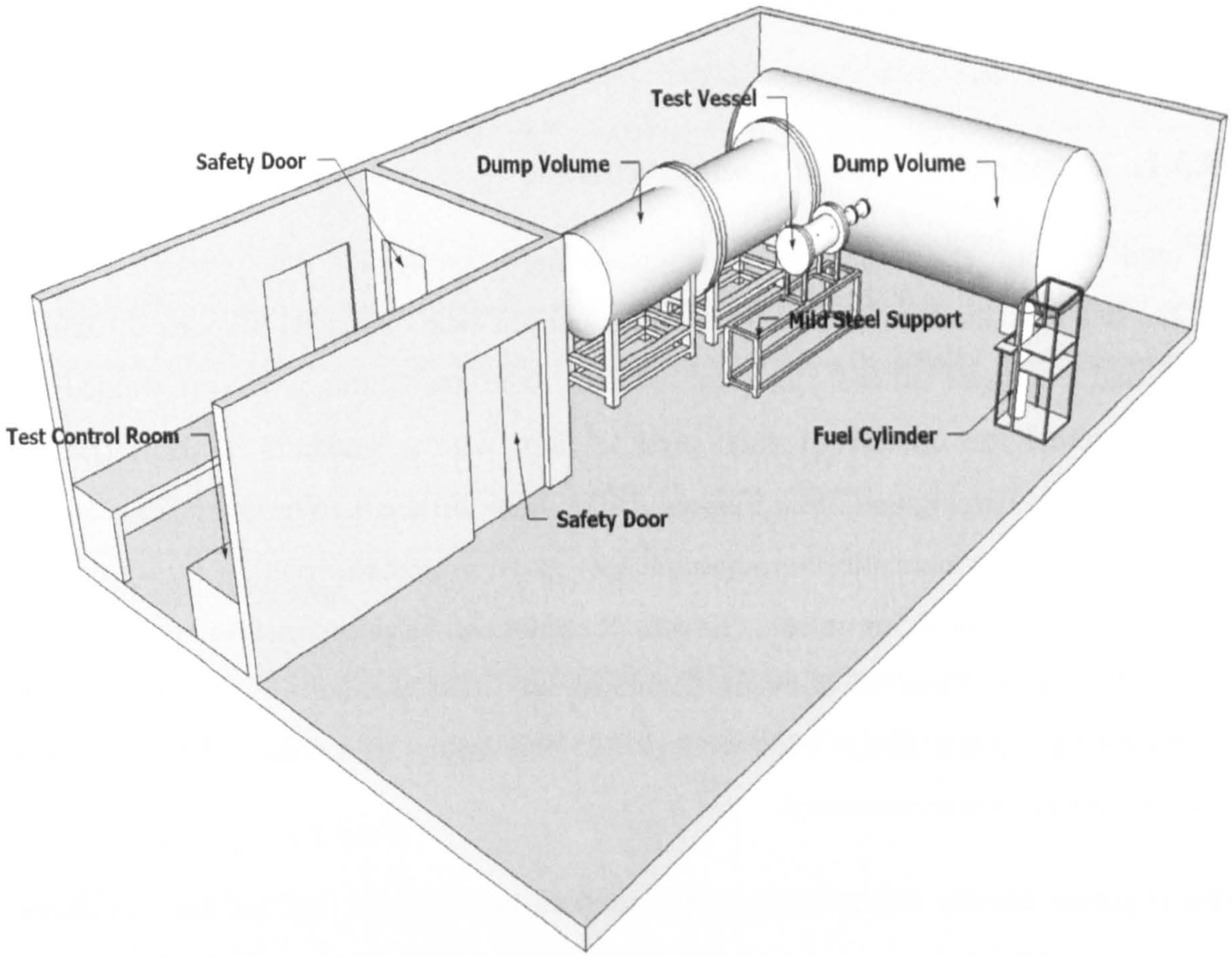

Figure 3-1: Test facility schematic

3.2. Factors Governing Test-Vessel Design and Instrumentation

Previous work conducted at the University of Leeds' Explosion Hazards – High Pressure Test Facility has shaped to some extent the work conducted within this thesis. Much of the equipment has been used prior to the current test program and has been designed to be interchangeable and therefore accommodate a wide range of possible geometry scenarios.

The work presented in this thesis includes an extensive test program involving vented and duct vented vessels. In order to achieve this indoors, a large 'dump' volume with a total volume of at least 250x that of the primary vessel volume has been employed to allow an approximation of vessel venting into the atmosphere, as is the case in most industrial explosions.

3.3. Explosion Geometries

3.3.1. Apparatus Design Considerations

A total of four explosion geometries were used throughout this research. These geometries were made up from existing pipe sections with diameters of either 0.162m or 0.5m, and lengths of either 0.5m, 1.0m or 2.0m. Instrumentation ports were welded and tapped around the outside of each pipe section, with a standard ½" BSP (British Standard Pipe) tapping and 3mm internal drilled hole. In the 0.162m diameter sections, a mild steel frame held the thermocouples in place to ensure accurate measurements between tests. In the 0.5m vessels this was not practical, therefore instrumentation ports were widened to 5mm to allow a sheath to be fitted around the outside of each thermocouple. Blank flange ends were drilled and tapped to accommodate additional instrumentation where necessary.

The decision to use the existing pipe sections was taken due to the functional requirement of the test-vessel design and the objectives of the project. These were:

a. The vessels needed to be in manageable sections which could be connected up to form a variety of vessels of different length and configuration;
b. Provision was required for partition of the test vessel from the rest of the vessel during mixture preparation;
c. A sufficient number of ports in the correct orientation were required for vessel instrumentation including thermocouples, pressure transducers, gas sampling ports, air inlet, outlet and spark igniters;
d. The vessel needed to be easily assembled at floor level and of manageable weight to be lifted using block and tackle lifting equipment for connection with the dump volume;
e. Use of removable, modifiable end flanges was necessary to allow for the provision of additional instrumentation ports and sharp diameter changes into and out of ducts;

f. The vessel needed to be capable of withstanding the adiabatic pressure of the gases involved despite the vented configuration and also any potential detonation pressures which were experienced in certain areas.

Existing pipes were of Austenitic Chromium-Nickel (low-carbon) stainless steel construction (304L). This material was originally chosen due to the better anti-corrosion properties and slightly better stress characteristics than mild steel construction pipes [87].

3.3.1.1. Vessel Shape

The cylindrical shape of the vessels used in this research was decided above other possible section shape such as triangular or square due to the following reasons [88]:

a. Ease of manufacture;
b. The cylindrical shape allows more uniform distribution of wall stress due to internal pressure rise;
c. The construction of a cylindrical vessel requires less welding that the same area square shaped vessel;
d. Equidistance of the internal surfaces from the ignition point ensures the vessel shape has minimal influence on flame front characteristics;

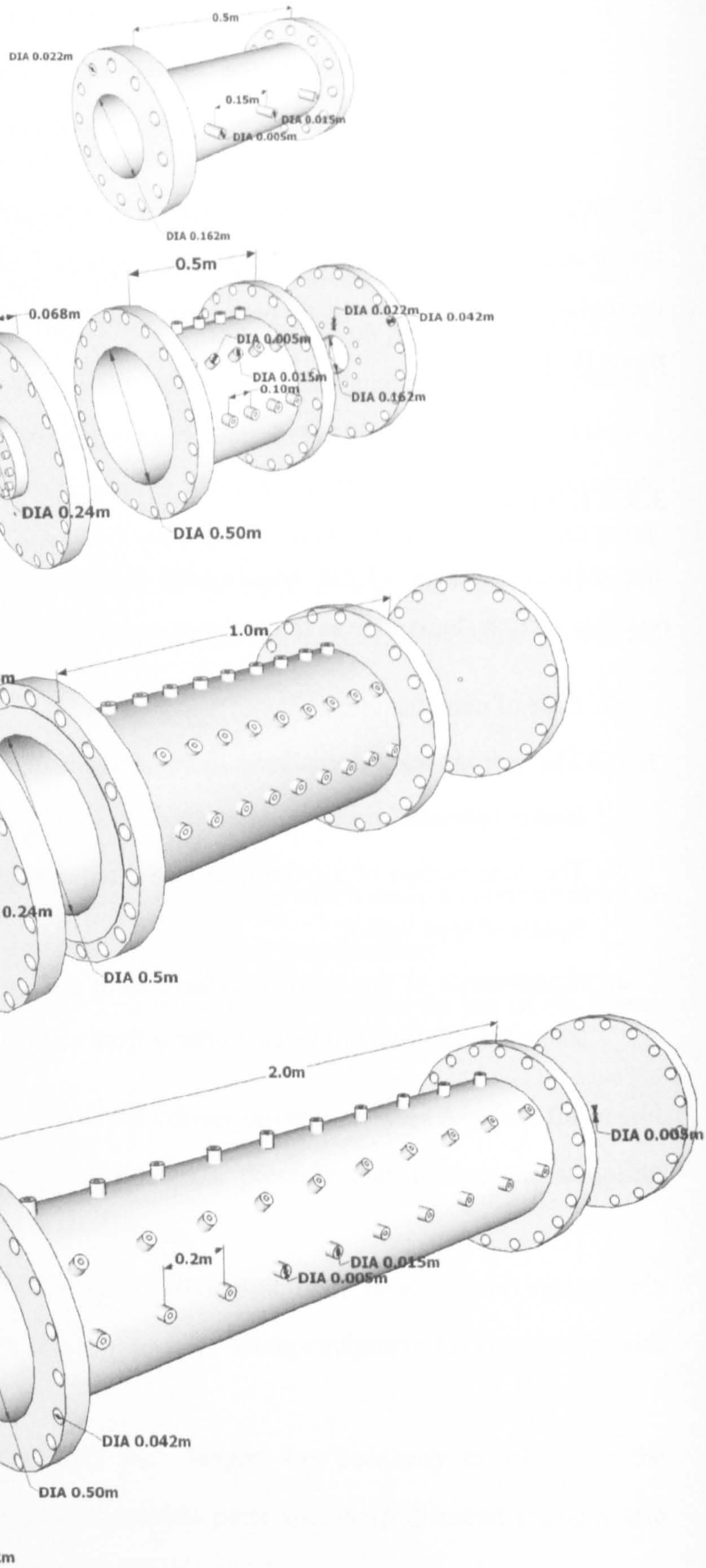

Figure 3-2: Scaled drawings of the pipe sections used in this research. (a) 0.5m/0.162m, (b) 0.5m/0.5m, (c) 1.0m/0.5m, (d) 2.0m/0.5m with associated end flange closures.

e. Similarity of cylindrical vessels to the geometries found in industrial equivalents.

In the current research, a total of four pipe section sizes were employed, as shown in Figure 3-2.

3.3.1.2. Selection of End Closures

It was necessary to interchange the equipment with sections of different diameter and introduce further instrumentation throughout the life of the project, therefore removable blank flanged ends were implemented to seal the open pipe sections. These were necessary only on the 0.5m diameter vessels and were designed with a vent hole the same diameter as the vent attached (0.162m). Such flange ends facilitated connection both to vent pipes and to interchangeable blank plates bearing a variety of instrumentation ports dependent upon requirement. Specific examples of the end flanges are shown in Figure 3-3.

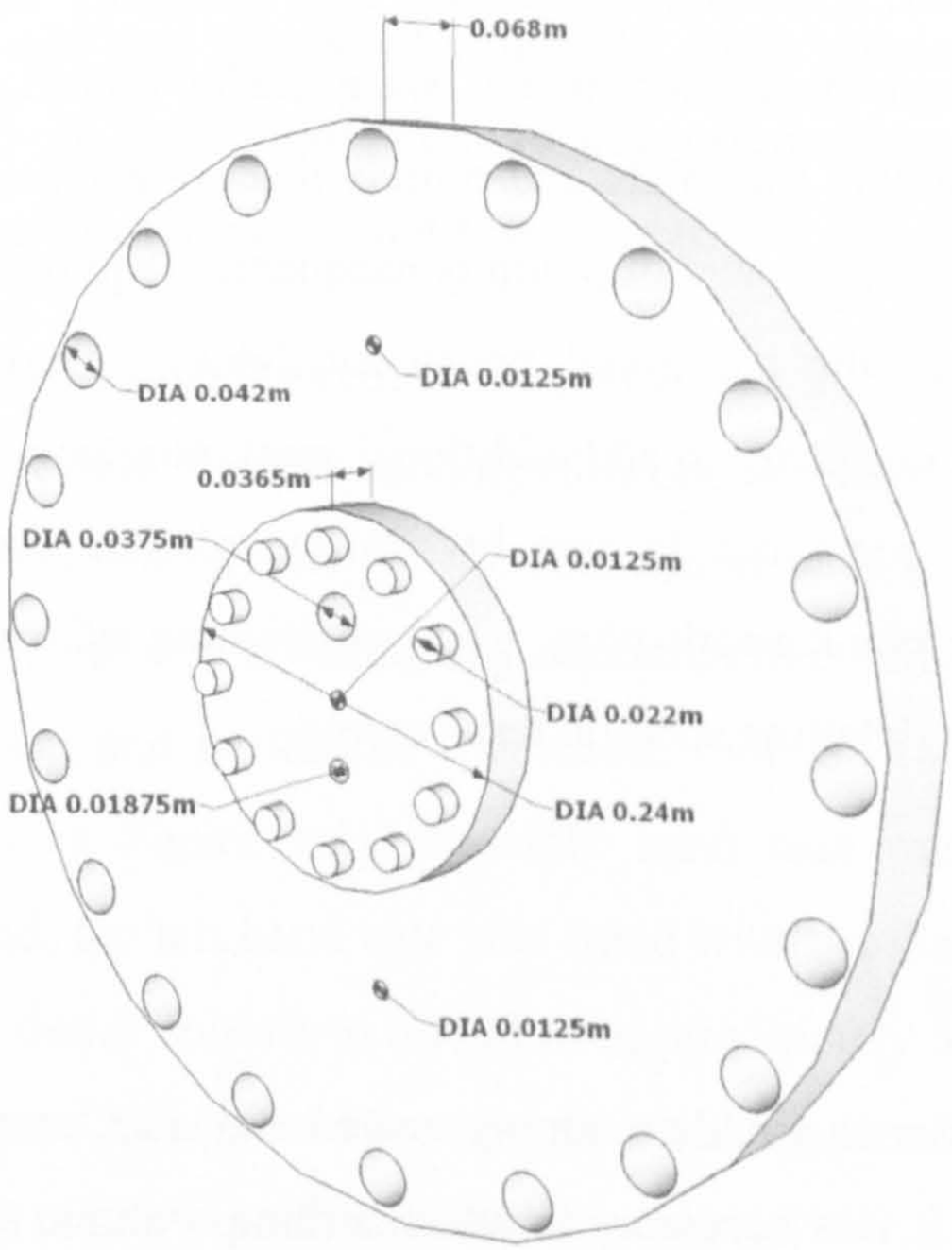

Figure 3-3: Flange end for all test vessels.

3.3.1.3. Selection of Gaskets

Flat ring gaskets were positioned between vessel face sections and endplates. These gaskets were made from pressed asbestos and were designed to prevent the leakage of explosion products from pipe joints by providing a semi-plastic seal between surfaces which will seal irregularities. Gaskets experience deformation under load which seals the connections and provides an air tight seal, thereby increasing safety.

3.3.1.4. Instrumentation and Access Ports

The initial designs of the vessels in this test facility were governed by a number of concerns, including the ability to cater for the work at the time in addition to potential future projects which would use the same equipment. These included the present project. Such design considerations led to arrays of instrumentation ports, and drilled and tapped bosses being emplaced along the lengths of all of the vessels. For larger diameter (0.5m) vessels, spark plug ports were also available. In addition, a variety of blank end flanges were purchased which were easily modifiable in the university workshop to accommodate the inlets and outlets that were required (for example, the later introduction of a larger vacuum pump consequently required larger piping in order to make proper use of the additional power available). During the course of the research, as it became necessary to add additional spark plug ports, this was done before testing began. Any ports not in use by instrumentation were blanked with the appropriate 'bung' or blank spark plug. The positioning of instrumentation ports is shown in later sections detailing specific test-vessels.

3.3.1.5. Dump Vessel

As noted above, in order to simulate simply vented and duct vented explosions within the indoor test facility it was necessary to attach a dump volume to the open end of the vent. This method allowed safe venting of burned and unburned gases ejected from the vent, and ensured that these were safely contained until being purged to the atmosphere after the end of each test.

The dump volume was designed that a variety of vessels can be attached to the front face; the flanged openings shown in Figure 3-4 were designed to match the existing equipment allowing connection to 1.5m (N1), 0.5m (N2), 0.162m (N3) and 0.076m (N4) diameter pipes and vessels. The final design of the dump vessel was limited by space restrictions in the test facility. The vessel was designed to specification and manufactured by Hustlers of Yeadon Ltd., and was constructed from 15mm thick rolled steel plates which were welded together on site in the test room. Two torispherical dished ends of nominal 10mm thickness were welded to either end of the 2.5m diameter vessel to give a total length of 8m and a volume of approximately $40m^3$. The specific details of internal diameter, enclosure strength, geometry details and governing standards used (BS4504 and BS1560) are given in

Table 3-1.

Instrumentation ports (¼" BSP) were added in order that conditions within the dump vessel could be monitored using pressure transducers or thermocouples. For the current research, only the pressure was monitored within the dump volume to ensure that there was no pressure build-up; the investigation of any external explosion is beyond the scope of this research and has therefore not been extensively investigated.

Tests-vessels were connected to the central flange (shown in red in Figure 3-4) to give the maximum length opposite the vent opening (this position having full diameter length ~ 2.5m), thereby reducing the impact of the interaction with the vessel walls on the explosion development, and also avoiding any obstacle effects from the internal support frame located at the top and bottom of the vessel. Of the two large 1.5m flanged openings (labelled N1 in Figure 3-4), the right hand side was fitted with a blank torispherical dished end, the left hand side was fitted with two 3m long, 1.5m diameter vessels increasing the dump volume to a total of approximately $52m^3$ to further reduce any interconnected vessel effects which may occur. All other flanged openings were blocked with flat blank plates to seal the vessel.

Table 3-1: Dump vessel design details

Section	Dimension
Shell:	
Internal diameter (m)	2.470
Length (m)	6.720
Shell Thickness (mm)	15
Torispherical (2:1) Dished Ends:	
Outer diameter (m)	2.500
Nominal plate thickness (mm)	10
Assembled Structure:	
Total Length (m)	8.000
Design Pressure (bar)	9.00
Certified pressure (hydraulic test) (barg)	11.25

Flanged Openings:

Type	Internal Diameter	Neck Thickness	Flange	Number of bolts	Bolt-hole PCD (mm)	Rating
N1	1.5m	20 plate	Special	52	1759	Special
N2	0.49m	10 plate	RFSO	20	635	BS 4504 40/3
N3	0.162m	SCH 40	RFSO	12	269.9	BS 1560 Class 300
N4	0.0762m	SCH 40	RFSO	8	168.3	BS 1560 Class 300
N5	¼ " BSP	COUPLING			-	Special

A mobile support frame of 2m length was used to support test-vessels for connection to the central port of the dump volume. The frame was fabricated from 5mm thick, square section mild steel. 150mm diameter heavy-duty jacking castors were bolted to each of the four corners of the frame allowing the vessel to be moved into position and aligned accurately before bolting to the dump vessel.

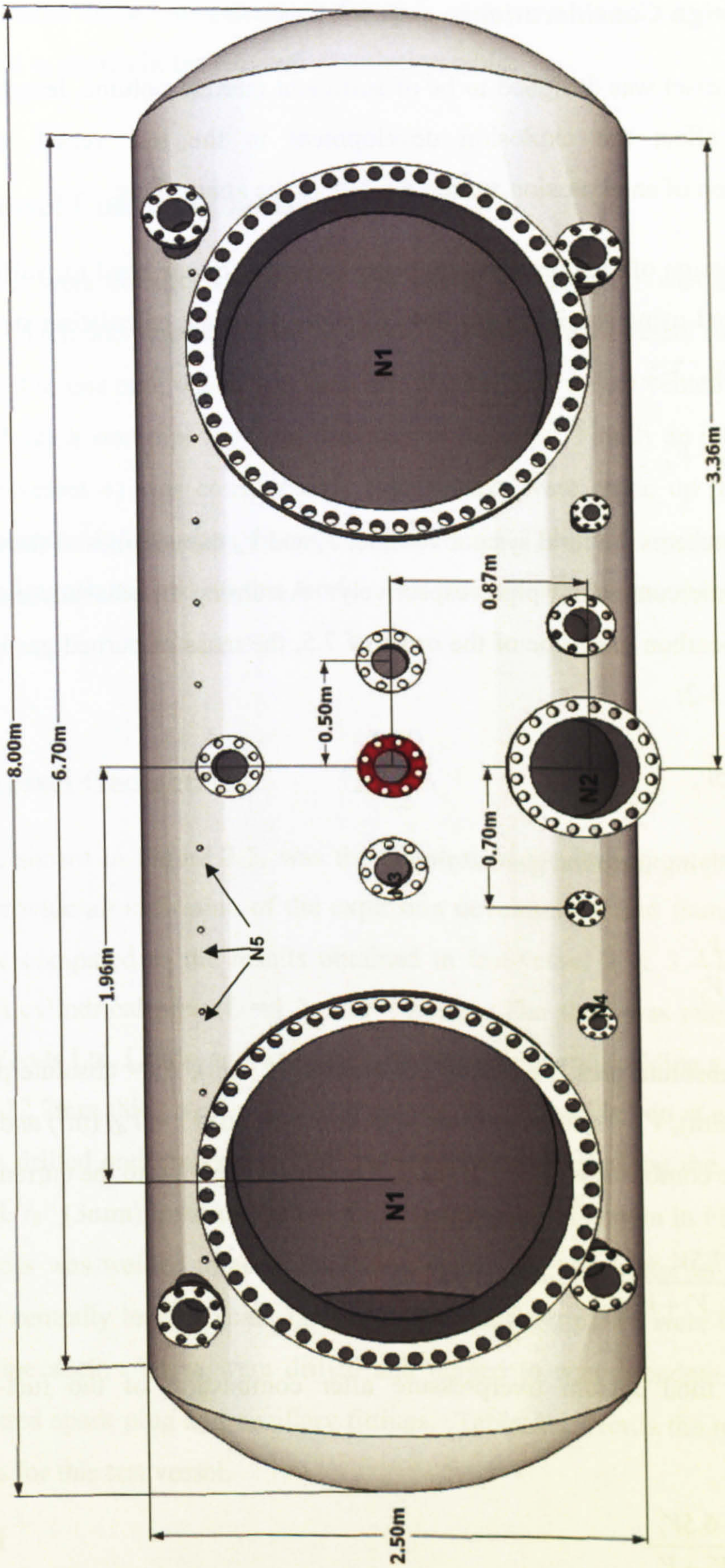

Figure 3-4: Scaled drawing of the dump volume, front face, with the connection port used shown in red.

3.3.1.6. Design Considerations

The dump vessel was designed to be of sufficient internal volume, length and diameter as to not affect the explosion development in the test vessel, and allow an approximation of an explosion vented directly to the atmosphere.

The initial design of the dump vessel, being governed by the need for sufficient volume, was calculated using the ideal gas law [87] following the calculation steps outlined in Eq. 3-1 to Eq. 3-5.

$$V_T = V_t + V_d \qquad \text{Eq. 3-1}$$

where V_T represents the total system volume, V_t and V_d the volumes of the test and dump vessel plus interconnecting pipe respectively. Assuming an adiabatic expansion for a typical hydrocarbon gas to be of the order of 7.5, the mass of burned gas is equal to V_b, given by Eq. 3-2:

$$V_b = 7.5V_t \qquad \text{Eq. 3-2}$$

therefore, applying the ideal gas law,

$$P_2 = P_1 \frac{V_1}{V_2} \qquad \text{Eq. 3-3}$$

Where P_1 = absolute pressure before combustion (1 atm), P_2 = absolute pressure after combustion (atm), V_1 = system volume after combustion ($V_b + V_d$) (m^3) and V_2 = system volume before combustion ($V_t + V_d$) (m^3). Therefore, applying to the current work:

$$P_2 = 1 \times \frac{7.5V_t + V_d}{V_t + V_d} \qquad \text{Eq. 3-4}$$

therefore the total system overpressure after combustion of the fuel-air mixture becomes:

$$P_{sys} = \frac{6.5V_t}{V_t + V_d} \qquad \text{Eq. 3-5}$$

The system pressure value was calculated for each of the test vessels connected to the dump vessel and is shown in the relevant description table.

3.4.Test –Vessel Construction Details

Four geometries were constructed for this test series; test-vessel 1 was a completely closed vessel, which was later modified to create a simply vented vessel (test-vessel 2) by adding a vent to one end, which was then transformed into a duct vented vessel (test-vessel 3) by adding a vent pipe the same diameter as the vent. Finally an interconnected geometry (test-vessel 4) was constructed. Test vessels were made up of cylindrical flanged pipe sections (of the sizes discussed in Section 3.2) bolted together to form the individual configurations used on this work. Test vessels are discussed individually in Section 3.5.

3.5. Test-Vessel Geometries

Test-vessel 1, shown in Figure 3-5, was the simplest of the four geometries, and was designed to provide an indication of the explosion development and flame path which could then be compared to the results obtained in test-vessel 2 & 3. The geometry consisted of a cylindrical pipe (L = 1.0m, D = 0.5m). The shell was manufactured by Vierod and Woods Ltd, Leeds, and was fabricated by rolling and welding a seam along a 1m length of 12.7mm thick steel plate, with slip-on flanges welded on at each pipe end. Arrays of ten drilled and tapped ½" BSP bosses were welded along the length of the vessel around $^1/_8$" (3mm) instrumentation holes (positioned as shown in Figure 3-5). In addition, a boss was welded to accommodate a spark plug used later in test-vessels 2 and 3 for the centrally located spark ignition. Flat blanking plates were bolted at each end of the pipe shell. These were drilled and tapped to accommodate fittings for a centrally located spark plug and ancillary fittings. Table 3-2 details the relevant vessel design details for this test vessel.

Table 3-2: Test-Vessel design details for test-vessels 1 & 2.

	Test-Vessel 1	**Test-Vessel 2**
Pipe Sections:		
Internal diameter (nominal) (m)	0.482	0.482
Section length (nominal) (m)	1	1
Number of sections	1	1
Wall thickness (mm)	12.7	12.7
Design Pressure (bar)	28	28
Flanges:		
Class (BS1560, 1989)	300	300
Flange thickness (mm)	68	68
Number of bolts	20	20
Bolt hole diameter (mm)	42	42
Bolt Hole PCD (mm)	670	670
Diameter of bolts (mm)	38	38
Vent diameter (m)	-	0.162
Vent area (m^3)	-	0.0206
Assembled test-vessel:		
Hydraulic pressure rating (barg)	40	10
Volume, V_t (m^3)	0.182	0.182
Ratio of total system volume to test vessel volume, V_T/V_t	-	286.71
System overpressure due to adiabatic combustion , P_{sys} (bar)	-	0.02267

Test-vessel 2, shown in Figure 3-6, utilised the same 1.0m long, 0.5m diameter rolled steel pipe as described for test-vessel 1. In addition to the details described for test-vessel 1 above, a vented flange end with vent diameter = 0.162m replaced one of the blank flange ends. A vacuum gate valve was fitted to this vent opening, which was then connected directly to the dump vessel. The gate valve was required to partition the primary vessel from the dump vessel during mixture preparation. Further details of the gate valve and the dump vessel can be found in sections 3.6.9 and 3.3.1.5 respectively. Table 3-2 details the relevant vessel design details for this test-vessel.

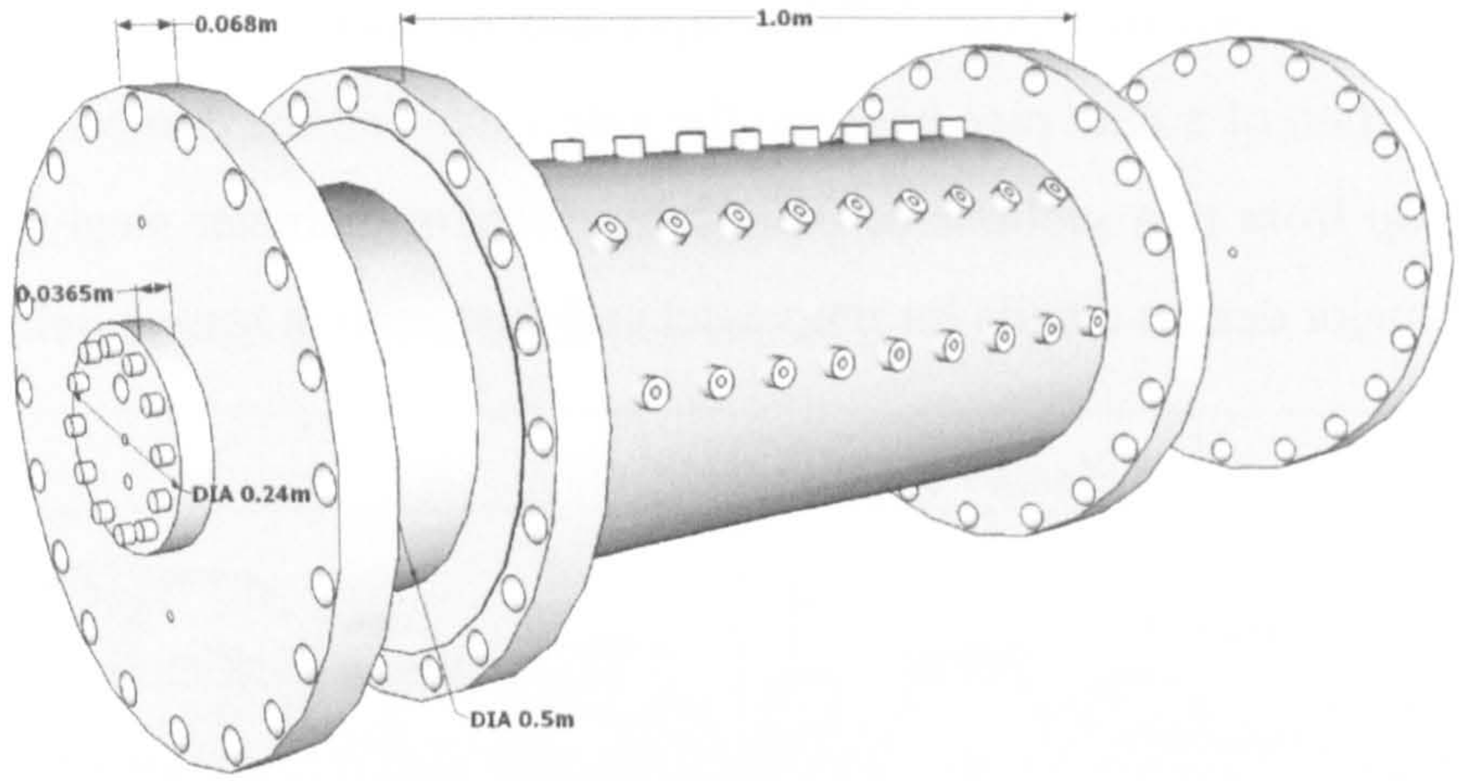

Figure 3-5: Schematic drawing of Test-vessel 1: Closed vessel geometry.

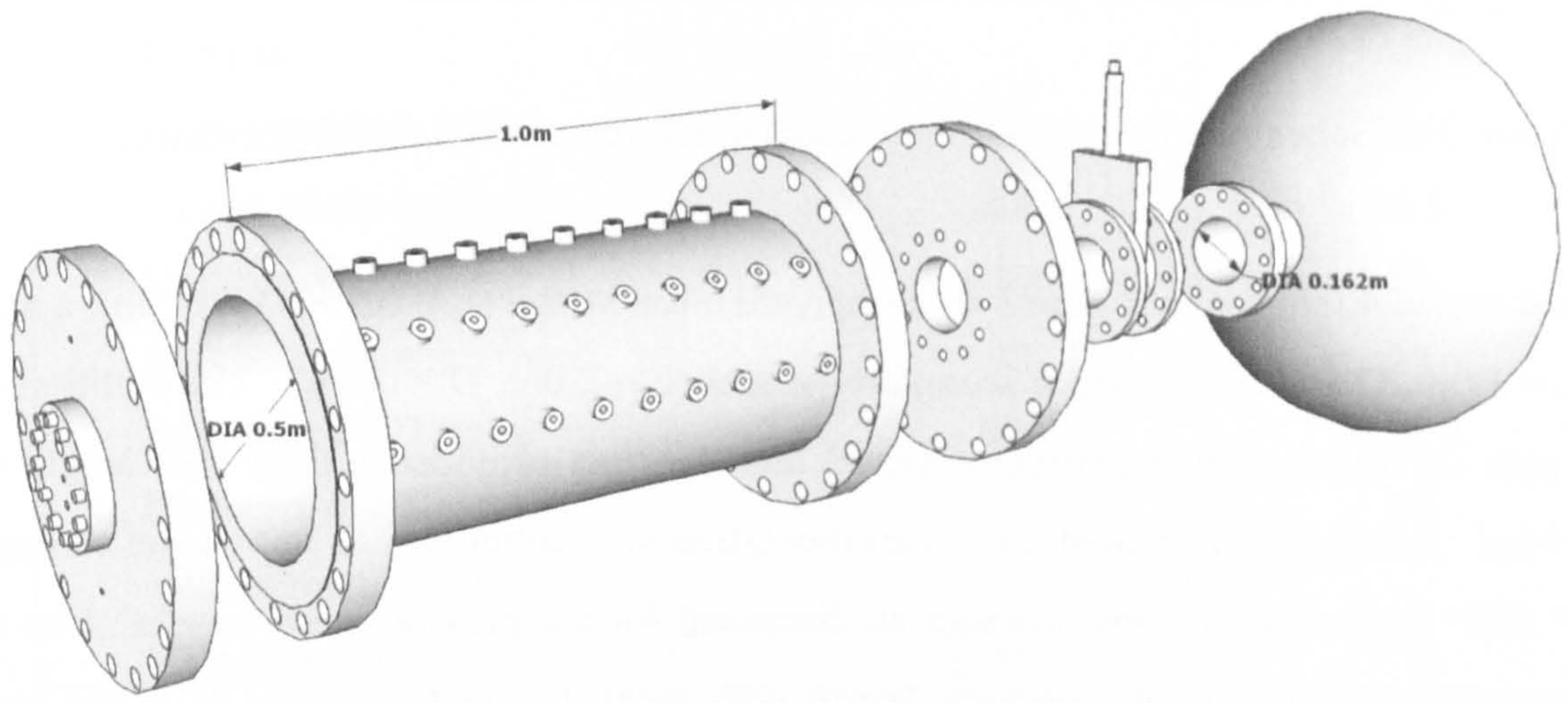

Figure 3-6: Schematic drawing of test-vessel 2: Vented vessel geometry.

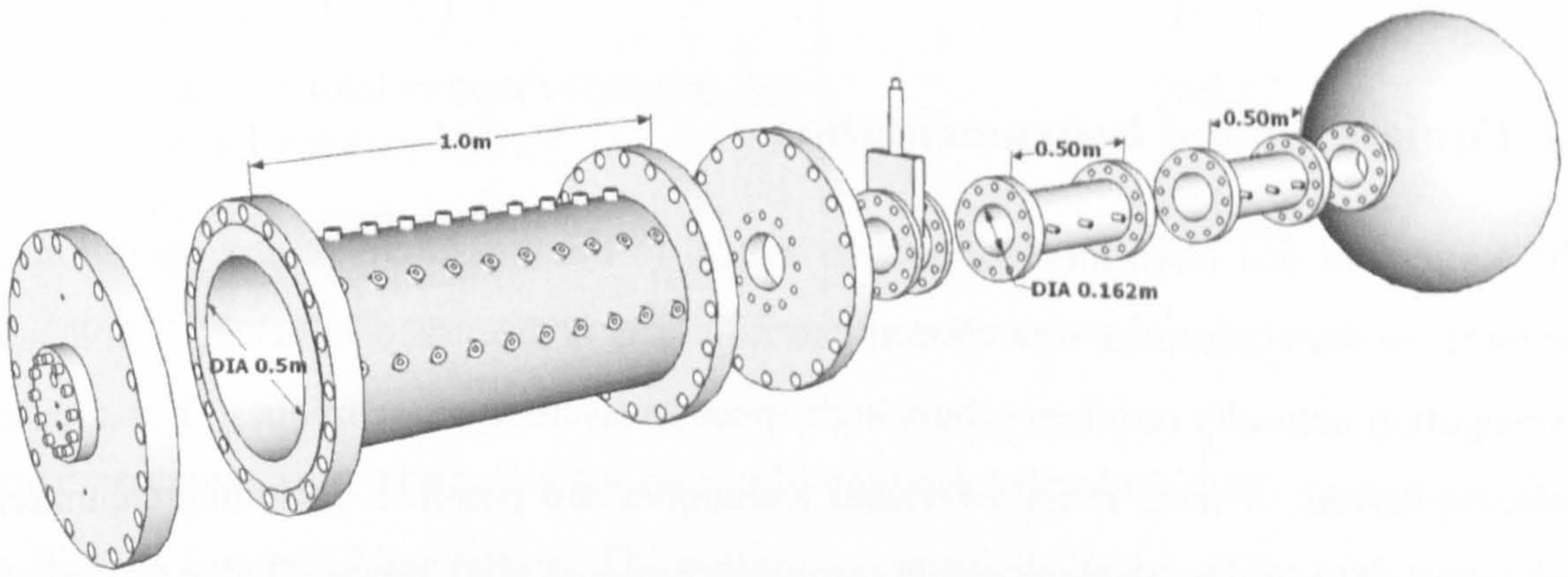

Figure 3-7: Schematic drawing of test-vessel 3: Duct vented geometry.

Test-vessel 3 (shown in Figure 3-7) incorporated the same geometry as test-vessel 2, with the addition of a duct pipe between the gate valve and the dump volume. The duct was made up from two sections of 0.5m long, 0.162m diameter steel pipe. Table 3-3 details the major design details for the vessel and duct used in test-vessel 3.

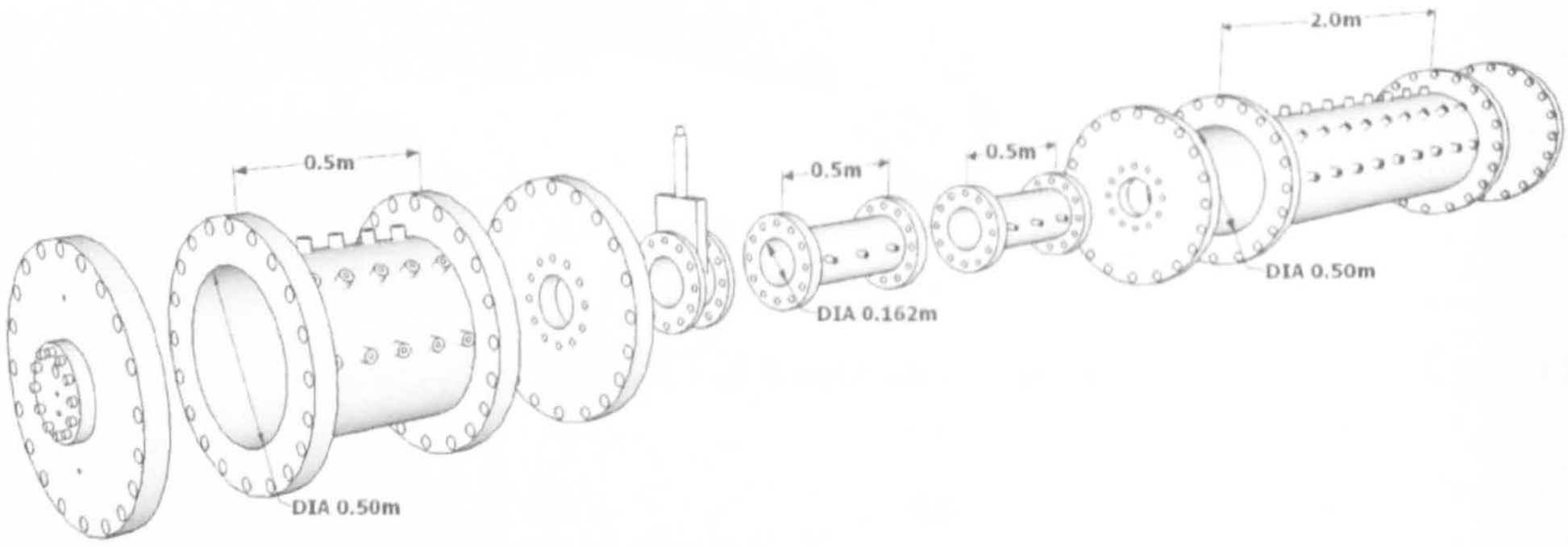

Figure 3-8: Schematic drawing of test-vessel 4: Interconnected vessel geometry.

Test vessel 4 (shown in Figure 3-8) comprised a test vessel (L = 0.5m, D = 0.5m), a duct (L = 1.0m, D = 0.162m) and a secondary vessel (L = 2.0m, D = 0.5m). The addition of a gate valve between the primary vessel and the duct provided a total duct length of 1.14m. Ancillary equipment and instrumentation was connected to this vessel through ½" BSP bosses in the same manner as discussed for the previous test vessels. Due to the reduced volume of the primary vessel with respect to test-vessels 2 & 3, the vent coefficient, K_v (= $V^{2/3}/A_v$), was reduced to 10.3. Design specifications for test-vessel 4 are detailed in Table 3-4.

3.6.Equipment and Instrumentation

The equipment and instrumentation were critical to the measurement and operation of the tests, so the equipment was chosen carefully and is discussed in detail. Explosion investigation naturally requires robust high speed measurement techniques. For smaller scale explosions, a wide range of visual techniques are possible, including Schlieren photography to monitor flame travel through low pressure glass tubes. Due to the nature and severity of the explosions in the current larger scale equipment, the thermocouple

and pressure transducer instrumentation described in the following sections was implemented.

Table 3-3: Test-Vessel design details for test-vessel 3.

	Test vessel	Duct
Pipe Sections:		
Internal diameter (nominal) (m)	0.482	0.162
Section length (nominal) (m)	1	0.5
Number of sections	1	2
Wall thickness (mm)	12.7	3.4
Design Pressure (bar)	28	35.5
Flanges:		
Class (BS1560, 1970)	300	300
Flange thickness (mm)	68	36.5
Number of bolts	20	12
Bolt hole diameter (mm)	42	22
Bolt Hole PCD (mm)	670	269.9
Diameter of bolts (mm)	38	19
Vent diameter (m)	0.162	-
Vent area (m^3)	0.0206	-
Assembled test-vessel:		
Hydraulic pressure rating (barg)	10	
Volume, V_t (m^3)	0.182	
Volume, V_T (m^3)	52.21	
Ratio of total system volume to test vessel volume, V_T/V_t	286.87	
System overpressure due to adiabatic combustion , P_{sys} (bar)	0.02266	

Instrumentation was wired directly into a 34-channel Microlink 4000 system supplied by Biodata Limited, Manchester. The system was specially designed for high speed data capture with a sampling frequency of up to 200 kHz per channel. The system was capable of monitoring a total of 34 analogue inputs including thermocouples, UV

detection units and up to 12 pressure transducers. The conversion of the analogue input signals into digital signals for processing was via a 12 bit ADC (Analogue-Digital Converter), giving a resolution of 1 part in 2^{12} (=4096). The voltage measurement range for thermocouples was -100 to +100 mV, and for pressure transducers 0 - 200 mV, therefore for pressure transducer of range 0-5 bar, the resultant resolution was ± 1.2 mbar.

Table 3-4: Design details for test-vessel 4.

	Primary Vessel	**Duct**	**Secondary Vessel**
Pipe Sections:			
Internal diameter (nominal) (m)	0.482	0.162	0.482
Section length (nominal) (m)	0.5	0.5	2
Number of sections	1	2	1
Wall thickness (mm)	12.7	3.4	12.7
Design Pressure (bar)	28	35.5	28
Flanges:			
Class (BS1560, 1970)	300	300	300
Flange thickness (mm)	68	36.5	68
Number of bolts	20	12	20
Bolt hole diameter (mm)	42	22	42
Bolt Hole PCD (mm)	670	269.9	670
Diameter of bolts (mm)	38	19	38
Vent diameter (m)	0.162	-	0.162
Vent area (m^3)	0.0206	-	0.0206
Assembled test-vessel:			
Hydraulic pressure rating (barg)	10		
Volume, V_T (m^3)	0.4767		

The data samples were stored in a cyclic manner; where the memory is full, the signal was overwritten from the beginning until a signal was received to mark the start of required data. This marker was synchronised to coincide with the spark ignition using the specialist software package Windspeed Wavecap. The Wavecap package was

capable of variation in pre- and post-trigger sampling times and sampling frequency. Once stored, the data was read from each channel and saved as a waveform. Processing and signal conditioning of the large amounts of waveform data was carried out using the IMC data processing package FAMOS (Fast Analysis and Monitoring Of Signals).

3.6.1. Thermocouples

The thermocouples used in this research were type K, mineral insulated, exposed junction thermocouples supplied by TC Ltd, UK. The shaft of the thermocouple was 3mm with a 0.6mm diameter exposed junction. Arrays of thermocouples were generally positioned along the axial centre-line of the test-vessels. Standard thermocouple extension cable conforming to BS EN 60584.3 was used to connect each thermocouple to the data acquisition system. The measurement of flame temperature was of secondary consideration to the recording of the time of initial flame passage for flame position and flame speed calculations, therefore the type-K thermocouple was deemed adequately robust for this use.

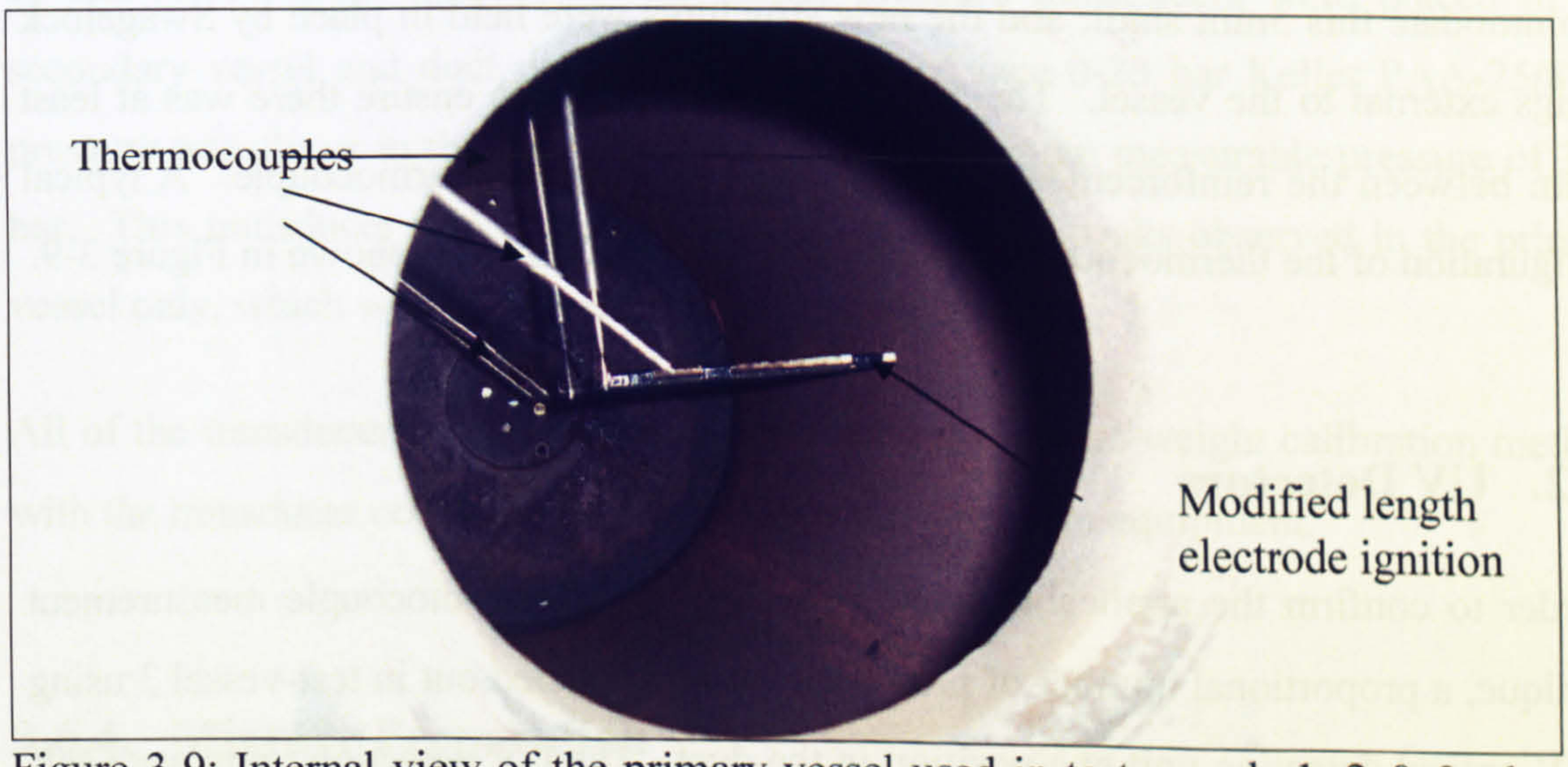

Figure 3-9: Internal view of the primary vessel used in test-vessels 1, 2 & 3, showing thermocouples along the axial centreline, with steel sheaths, plus central modified length electrode ignition is also displayed.

Thermocouples were inserted into the vessels through 3mm instrumentation holes within the instrumentation ports, and either sized to run along the central axial line of the vessel or close to the vessel wall to detect flame arrival in unburned gas pockets. All

thermocouples were fixed in place and sealed using threaded Swagelock compression fittings.

The thermocouples were used to determine the time of flame arrival, signified as a sudden temperature rise on the thermocouple output. There was no significant dead time in the thermocouple response, but there was a large thermal lag due to the 0.6mm diameter thermocouple bead that was used. This limited its applicability for temperature measurement, but was deemed adequate for time of arrival measurement as the thermocouple was sufficiently robust to survive the explosion. Furthermore, measurement techniques such as ionisation probes or UV detectors were inadequate for use with hydrogen tests, therefore thermocouples were the most logical choice.

Where the dynamic load of the explosion was likely to be high, internal frames were used to ensure position integrity between tests. Duct lengths were fitted with a thin steel frame, which held the thermocouple tip at least 20mm from the exposed junction. In the primary vessel, a frame was not practical due to multiple ignition sites. This problem was overcome by reinforcing the shaft of the thermocouple with a 5mm steel sheath (internal diameter = 3mm). The effected instrumentation ports were modified to accommodate this 5mm shaft, and the new structures were held in place by Swagelock fittings external to the vessel. The sheaths were measured to ensure there was at least 20mm between the reinforcement and the exposed tip of the thermocouple. A typical configuration of the thermocouple placement for test-vessels 1-3 is shown in Figure 3-9.

3.6.2. UV Detectors

In order to confirm the applicability and reliability of the thermocouple measurement technique, a proportional number of propane tests were carried out in test-vessel 3 using an UV optical detection unit at a position in the duct. The UV detection units were self contained sealed units which could be fitted to the existing ½" BSP instrumentation ports on the vessel or the duct. The passage of a flame was confirmed by a steep increase in voltage output recorded on the data acquisition system. The UV radiation given off by the reaction zone of a flame (short wavelength < 440 nm) was detected by the detection unit and was recorded as a steep increase in voltage output. In the tests

which used both detection techniques, the times of flame arrivals were compared and found to be in excellent agreement [87].

3.6.3. Pressure Measurement

In order to measure the pressure within the vessel at the time of the explosion it was necessary to use robust equipment that was able to measure the fast explosion pressures without loss of sensitivity or equipment integrity. Two different types of Keller pressure transducers were used in the course of this research. In test-vessels 1, 2 and 3, Keller type PAA-11/10bar/80059.2 pressure transducers were employed with a 0 - 10 bar measurable range, and a maximum measurable pressure of 15 bar. These transducers were of an internal diaphragm construction and were placed in the instrumentation ports; 3 in the test vessel, and 3 in the duct (where attached). Finally, an internal diaphragm Keller type PAA-11/5bar/80059.2 0-5 bar transducer (maximum measurable pressure 7.5 bar) was placed in the dump vessel above the vent exit, to measure the overpressure in the dump vessel during and following the explosion.

In test-vessel 4, the same 0-10 bar Keller pressure transducers were placed in the secondary vessel and duct, in addition to a closed face 0-25 bar Keller PAA-25/8735 pressure transducer in the primary vessel with a maximum measurable pressure of 37.5 bar. This transducer was chosen to measure detonation peaks observed in the primary vessel only, which will be discussed later in chapter 7.

All of the transducers were calibrated using a standard dead-weight calibration method, with the transducer connected to the datalogging waveform equipment.

3.6.4. Mixture Preparation

The partial pressure theory was used to create an accurate known mixture within the test vessel, therefore the accurate measurement of the test-vessel pressure whilst under vacuum was required. This was achieved using an Edwards Barocel Pressure Sensor type 600AB Trans 100MB, with a working pressure range of 1000 mbar and accuracy of 0.15%. The unit was integral to the system within the test vessel filling track and

enabled accurate measuring of the vacuum pressure during fuel injection. Operational principles of this sensor were to transduce absolute vacuum pressure into a DC output voltage precisely proportional to the input pressure. The unit was connected to an Edwards Diametrics type 1500 digital output display, which gave a reading accuracy of ±0.05 mbar. Assuming a final pre-ignition pressure of 1013.2 mbar, a 10% methane/air mixture could therefore be prepared to within an accuracy of 0.05%. The Barocel was capable of measuring the pressure within the primary and the secondary vessel/dump volume present in test-vessels 2, 3 and 4 by the addition of a two way valve on the control panel, connected to the test vessel either side of the gate valve.

Where pressures inside the vessel were to exceed normal atmospheric, an analogue display Budenburg pressure gauge with a measurement range of 0 to 2.5 bara was employed. This gauge was also fitted in parallel to the Barocel sensor during mixture preparation as an additional safety feature to prevent the explosion starting pressure being above standard atmospheric.

3.6.5. Spark Ignition System

Ignition was actuated by means of a standard combustion engine spark plug (16 J). The electrodes were extended by welding stainless steel strips of similar dimensions to the existing electrodes to the lengths required. Figure 3-10 shows a typical extended electrode internal combustion engine spark plug. To prevent arcing of the spark at any location other than the designated spark gap, the central electrode was passed through ceramic beads and secured using electrical tape.

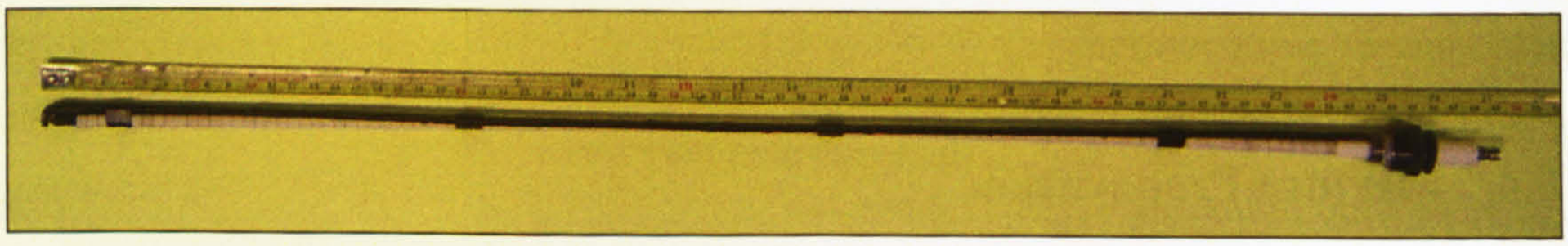

Figure 3-10: Internal combustion engine spark plug with extended electrodes.

Ignition was possible from any one of four positions, including top, centre, bottom and end, as shown in Figure 3-11. The end ignition was at a position such that it was flush with the position of the end flange of the primary vessel. The remaining three ignition

positions were approximately half way along the vessel between the end wall and the vent.

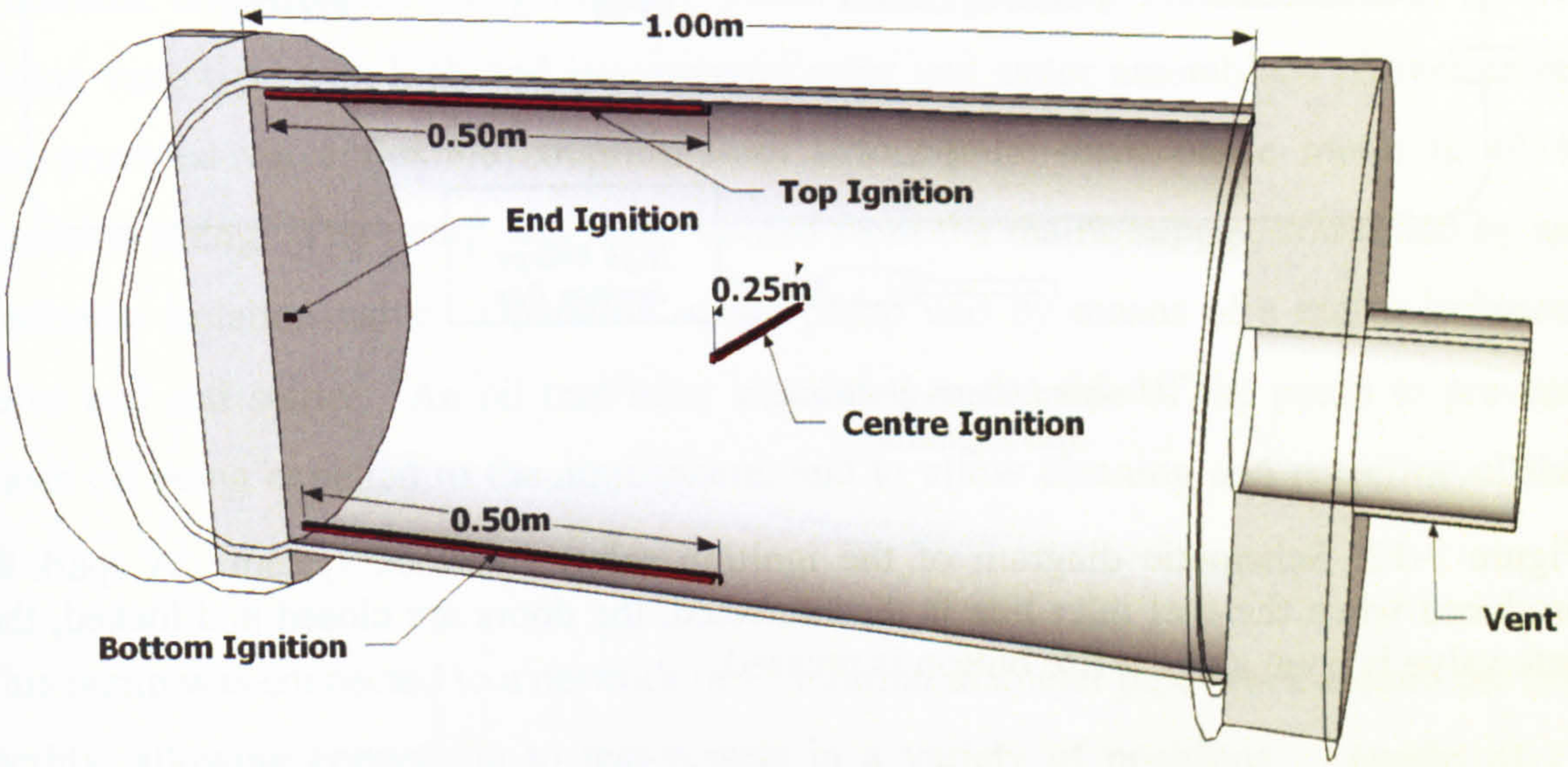

Figure 3-11: Ignition position in the test vessel of test-vessels 1 - 3.

The spark energised using the mains electricity supply, which passed through a capacitor and released a consistent amount of energy upon ignition, provided all conditions of the ignition circuit were met. The ignition circuit incorporated a number of safety features which in turn controlled an interlock system designed to ensure the safety of the operators and maintain the integrity of the equipment. The ignition safety interlock system, shown schematically in Figure 3-12, energised the ignition circuit only when the following criteria were met:

i. Fuel line DISCONNECTED from test vessel,
ii. Interlocking doors CLOSED,
iii. Interlocking doors LOCKED,
iv. Gate valve OPEN.

Once the above conditions are met, the spark ignition circuit was live, and successful ignition would be actuated on depressing the 'fire' button. Conversely if any of the conditions were not met, the circuit was broken and the spark ignition circuit was rendered inactive.

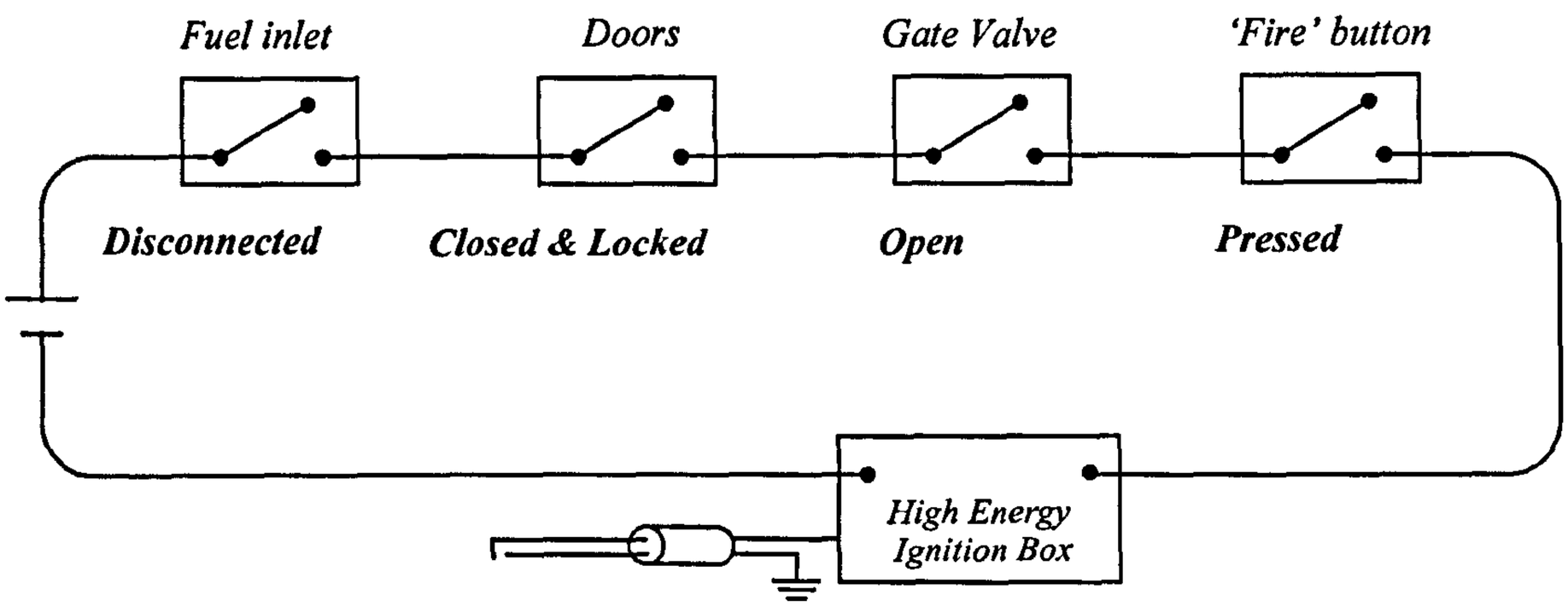

Figure 3-12: Schematic diagram of the ignition safety interlock system. A spark is produced when the fuel inlet line is disconnected, the doors are closed and locked, the gate valve is open and the fire button is pressed.

3.6.6. Evacuation System

Vessel evacuation is an important part of the mixture preparation cycle and purging procedure for all geometries investigated in this research. Two evacuation pumps were available for use in the test facility; a small vacuum pump (Vac A) was used for smaller vessels and where additional evacuation was required. A larger vacuum pump (Vac B) used for the main evacuation and purging of all vessels.

3.6.6.1. Vacuum Pump A

Vacuum pump A was a small 'Edwards E1M18' single direct-drive, rotary vacuum pump, with a nominal displacement rating of 340 l/min. The pumping mechanism was of the slotted rotor/sliding vane type. Direct-drive was provided via a flexible coupling from a totally enclosed fan-cooled motor. Operation of vacuum pump A was by means of an on/off switch on the mixture preparation apparatus.

3.6.6.2. Vacuum Pump B

Vacuum pump B was a larger 'Edwards E2M175' two-stage, rotary vacuum pump with a nominal displacement rating of 2967 l/min. The pumping mechanism was of the sliding vane type with high and low vacuum rotor and stator assemblies. Direct drive was provided via a flexible coupling from a four-pole, three phase motor to IP54 enclosure rating. The pump was water cooled from the mains supply, controlled by an electronic isolation valve. Operation of the pump was by means of a mains isolation valve and soft starter. An oil trap/filter was fitted to the side of the pump to prevent waste oil being expelled to the atmosphere, and to allow cleaning and recycling of the oil.

This pump was connected to a network of 1" internal diameter pipe-work around the test facility, allowing connection to test-vessels in a variety of positions. Lengths of 1" internal diameter, vacuum-rated flexible hose were used to connect the individual test vessels to vacuum pump B, with the exception of the dump volume which was connected via a series of 2" internal diameter pipework.

3.6.7. Mass Flow-Meter

For stratified explosion mixture preparation it was necessary to monitor the flow rate of the fuel injection into the test vessel. For this reason, a Brooks Smart Series (Thermal Mass Flow) Mass Flow Meter, model 5851S, was positioned along the fuel inlet line in order to provide accurate measures of gas flow injection into the vessel. The mass flow meter used a thermal mass flow sensor to produce an output signal corresponding to the specific flow rate. The flow meter was used in conjunction with a Brooks Microprocessor Control and Read-Out Unit Model 0154. The read-out unit had a four channel input module which converted the electrical signal produced by the flow meter into a read-out in l/min.

The flow meter was calibrated using Nitrogen, and therefore a simple conversion was necessary due to the scale shift which would occur between the signal and output actual mass flow rate based upon the difference in heat capacities between the reference gas and the gas of interest (i.e. Methane, Propane or Hydrogen). This is achieved by

employing the sensor conversion factors (shown in Table 3-5) in Eq. 3-6.

$$\textit{Actual gas Flow rate} = \textit{Output Reading} \cdot \frac{\textit{Factor of the new gas}}{\textit{Factor of the calibrated gas}} \qquad \text{Eq. 3-6}$$

Table 3-5: Gas conversion table for gases of interest for use with Brooks Smart Mass Flow Meter.

Gas Name	Formula	Gasfactor
Nitrogen	N2	1.000
Hydrogen	H2	1.008
Methane	CH4	0.763
Propane	C3H8	0.343

3.6.8. Pipes, Valves and Fittings

The selection of pipes, valves and fittings for each test-vessel depended largely upon the purpose of the connected equipment. Fuel lines were of flexible stainless steel construction with an external diameter of ¼", and mixture preparation monitoring line was of similar construction with a ½" external diameter. Both lines were connected to the vessel via Swagelock click-lock fittings so that the lines could be detached from the vessel prior to ignition. With the exception of the vacuum lines, all other pipework was ¼" or ½" external diameter copper piping, with Swagelock compression fittings used at all connections. In order to maintain efficiency, vacuum pipe-work – which comprised 1" or 2" fixed mild steel piping, and 1" flexible reinforced rubber hosing – connected vacuum pump B to the test-vessels and dump volume. A network of piping which allowed vacuum pump B to be connected to a test vessel anywhere in the test facility was also of mild steel construction, with a 1" internal diameter. Where vacuum pump A was used ½" copper pipe work was sufficient, as test volumes were generally lower.

On the control panel, a Whitey four-way valve was used to select between fuel, compressed air and ambient air injection. This was accompanied by a selection of Whitey ball valves and needle valves, which were used to regulate the flow. On the test vessel, ambient air-filling valves were ½" diameter and all other access ports (fuel,

sample withdrawal ports and nitrogen inlet) were ¼" diameter. Compressed air could be introduced to the system from a 4 bar line via the control panel, and was connected via a ¼" diameter nylon pipe.

Swagelock brass and steel pressure fittings – connectors, adapters, elbows, tees etc. – were employed for all of the ¼" and ½" pipelines, and also for all access ports. On/off control was via Swagelock ball valves, and Swagelock compression fittings were used for all ¼" and ½" fittings.

3.6.9. Vacuum Gate Valve

In test-vessels 2, 3 & 4, a one-sided vacuum gate valve was employed to separate the test vessel from the remainder of the vessel during mixture preparation. The gate valve measuring 0.14m long and 0.162m internal diameter, was constructed from a light weight aluminium body with Viton seals.

The vacuum gate valve was a series 12 model DN160 (6") with pneumatic actuator, supplied by VAT Vacuum Products, London (see Figure 3-13). The pneumatic actuator was a double acting cylinder with solenoid valve controlling a 4 bar compressed air supply feed. The gate valve was controlled remotely from the control room.

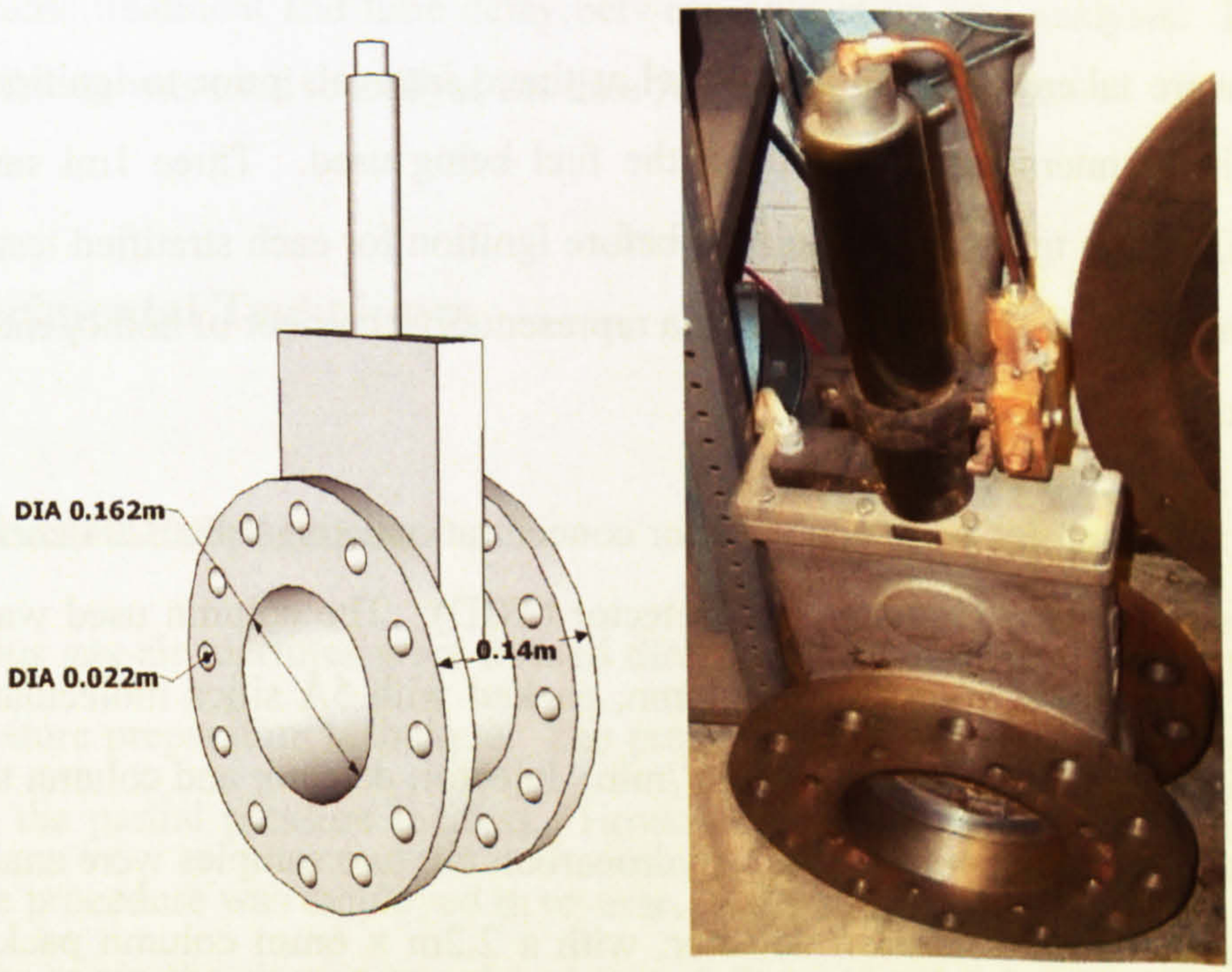

Figure 3-13: The 0.162m diameter vacuum gate valve

The valve was not supplied with an explosion pressure rating, therefore before commencing work on test-vessels 2, 3 & 4, a certified hydraulic test was performed on the valve section (with valve open) to a pressure of 10 barg. This effectively limited the maximum pressure within the duct to a maximum of 10 barg.

3.6.10. Selection of Fuels

The investigation of fuels in this research is limited to propane, methane and hydrogen. Propane was the main focus of this research, and was chosen because the explosion behaviour of a propane-air mixture is similar to those of many higher fraction hydrocarbons, which typically have K_G values in the range of 40-70 bar.m.s^{-1} [11]. In many situations, a heavier fuel will collect at low points in the confining geometry or terrain, making research into such fuels invaluable. Methane was selected because of its common nature, buoyant properties in air and (relatively) low reactivity. The buoyant nature of hydrogen lends itself to the investigation of stratified gas concentrations well, and the current move towards a hydrogen economy provides a true need for the data presented in this thesis.

3.6.11. Gas Chromatography

Samples were taken from the test vessel at timed intervals prior to ignition, and were analysed in manners dependent upon the fuel being used. Three 1ml samples were removed from the test-vessel 1 minute before ignition for each stratified test to confirm the concentration gradient, and also for a representative number of homogeneous tests to confirm homogeneity.

Hydrogen fuel samples were analysed for concentration using a Pye 204 chromatograph which uses a Thermal Conductivity Detector (TCD). The column used was a 1.8m x 6mm (6ft x 0.25in) stainless steel column, packed with 5Å silica molecular sieve and argon carrier gas at a flow rate of 24cm^3/min. Injector, detector and column temperature in this system were all set to 100°C. Hydrocarbon mixture samples were analysed using a Pye-Unicam flame ionisation detector, with a 2.2m x 6mm column packed with *n*-octane Poracil C of 80-100 mesh size, with nitrogen carrier gas.

The analysed gas content returned two variables; the retention time, and the response of the injected fuel-air mixture in mV. The retention time of the peak was used to distinguish between gases; this was typically 132sec, 80sec, and 60sec for propane, methane and hydrogen respectively. The concentration was calculated as a function of the area beneath the response curve, in addition to the height of the peak. This value was used in conjunction with the known samples to calibrate the instrument, and this calibration curve was then used to calculate the percentage concentration of the unknown stratified mixture samples. The instruments were checked daily and recalibrated (where necessary) using standard calibration gases. Calibration ranges for the three gases were propane (0 - 20 %), methane (0 - 20 %) and hydrogen (0 - 50 %).

Mixtures of known (homogeneous mixtures) or unknown (stratified mixtures) concentration were prepared within test-vessels 1, 2 and 3. Gas samples were then withdrawn using a series of 1ml gas-tight luer lock syringes fitted with 12" luer lock needles. The needles were inserted into the vessel via Swagelock on/off ball valves capped with self sealing bungs at the appropriate position (10 mm from the top of the vessel, 10 mm from bottom of the vessel and 50 mm above the axial centre-line). Self-sealing septas were used to seal the tip of the needle to prevent leakage prior to analysis. Samples were then analysed immediately using gas chromatography as discussed above. In addition, the same syringe/needle combination was used for calibration mixtures to ensure the same treatment and time delay between extraction and analysis. Dedicated specialist software was used to analyse the data from each instrument.

3.7. Experimental Techniques

3.7.1. Mixture Preparation

Homogeneous gas-air mixtures were formed directly in the test vessel using the partial pressure mixture preparation technique. The preparation of stratified mixtures was also based upon the partial pressure method. However, in order to create a concentration gradient, the procedure was employed in reverse. Rather than inducing thorough mixing by fast intake of air, the air was introduced first, followed by the fuel injection at one of

three positions, dependent upon the gradient required. This technique was found to produce an adequate and repeatable concentration gradient within the vessel. The flow rate for each gas was calculated to create a turbulent jet inlet where the Reynolds number, calculated by Eq. 3-7, should be >4000.

$$\mathrm{Re} = \frac{\rho U D}{v} \qquad \text{Eq. 3-7}$$

by rearranging Eq. 3-7 to evaluate with respect to velocity, the equation becomes:

$$U = \frac{\mathrm{Re}.v}{\rho D} \quad \text{(m/s)} \qquad \text{Eq. 3-8}$$

where ρ is density (kg/m^3), U is velocity (m/s), D is orifice diameter (m) and v is viscosity. Values of v and ρ for each gas are given in Table 3-6.

Table 3-6: Values for employment into Eq. 3-7 and Eq. 3-8

	v (m^2/s)	ρ (Kg/m^3)
Methane	1.17×10^{-5}	0.6512
Propane	8.0×10^{-6}	1.87
Hydrogen	8.90×10^{-5}	0.0838

A turbulent injection flow did not create a stratified mixture for methane, therefore it was necessary to reduce the flow rate accordingly until a satisfactory and repeatable concentration gradient could be formed. This was not finalised until after test-vessel 3 had been constructed, therefore while it was the original intention to present stratified methane data within test-vessel 2, it was not possible. However, this may provide a direction for valuable further research.

3.7.2. Flame Position Measurement

The thermocouples that were arranged along the axial centre-line in each test-vessel were used to detect the path of the flame as it travelled away from the point of ignition.

The passage of the flame through the primary vessel was recorded as a distinct change on the output signal from each thermocouple (Figure 3-14). The timing of this distinct change, in comparison to that measured on an adjacent thermocouple, allowed the average flame speed between two fixed points to be calculated. This technique has been used previously at the University of Leeds [87, 89], and has been validated in comparison to photographic techniques in a closed spherical vessel.

Measurement of the flame passage through the duct was more complicated. Pre-compression caused preheating of the unburned gas ahead of the flame front which also manifested as a change in gradient along the signal output. Implementation of a UV optical detection unit in a representative number of tests, confirmed that the first change in signal output did not correspond to the passage of the leading edge of the flame front, whereas the second change in signal output did. Therefore accurate measurements of flame passage through the duct could be obtained by measuring the timing of this second gradient change. In many of the duct vented tests, the flame passage through the duct was very fast, therefore the arrival times at all six thermocouples within the duct could not be accurately resolved. In these cases it was necessary to measure the timing of flame passage at the first and last thermocouples only, thereby providing an average flame speed through the duct.

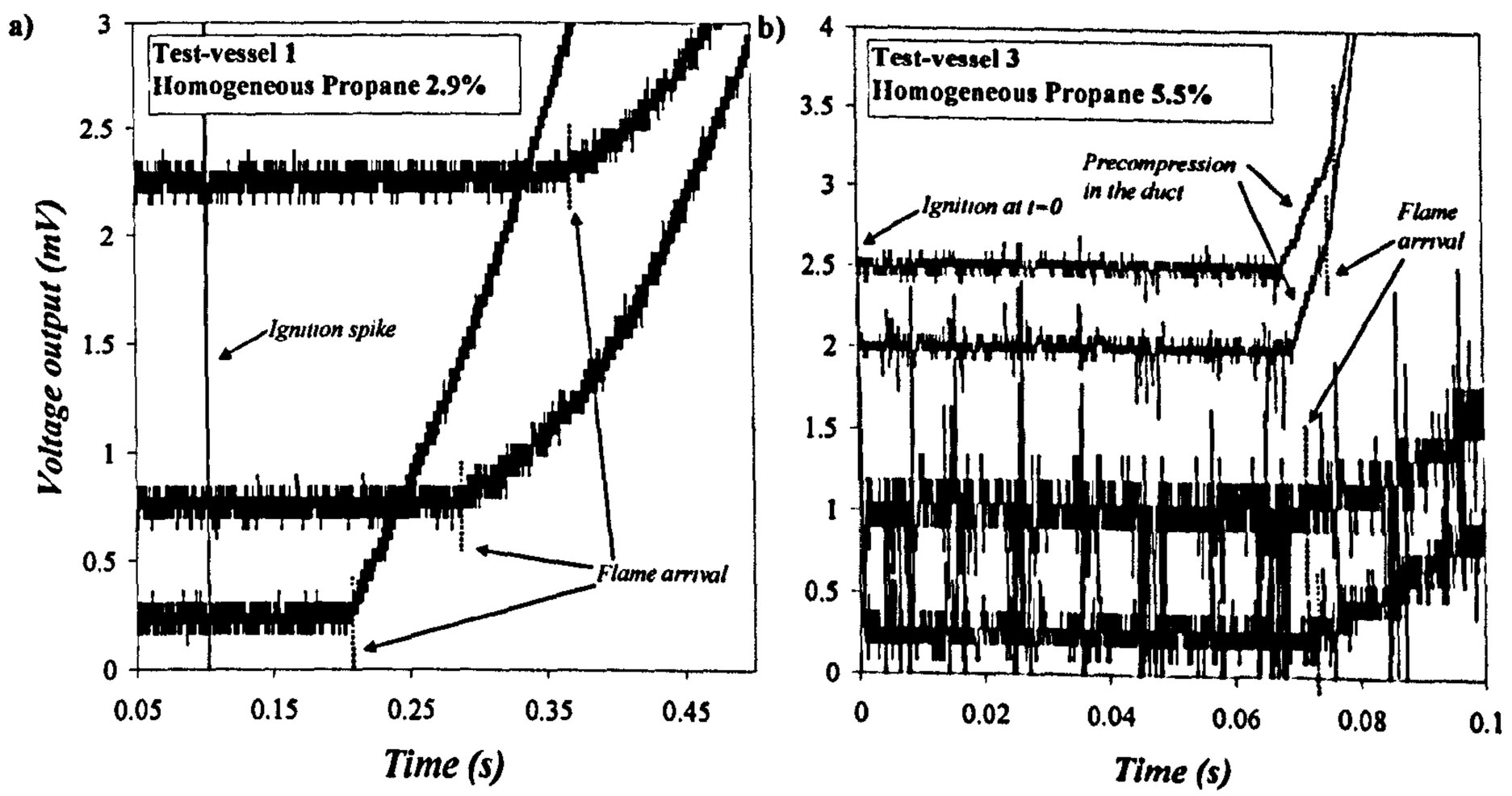

Figure 3-14: Typical thermocouple output traces for (a) test-vessel 1 and (b) test-vessel 3, showing the pre-compression within the duct.

3.7.3. Flame Speed Calculation

Flame speeds were calculated by measuring the time taken for the flame to travel between two adjacent thermocouples with respect to the distance travelled, with the relationship:

$$S_f = \frac{x_{T_n} - x_{T_{n-1}}}{t_{T_n} - t_{T_{n-1}}} \quad \text{(m/s)} \qquad \text{Eq. 3-9}$$

where S_f is the flame speed, x is the distance from the spark ignition, t is the time of flame arrival and T_n corresponds to a numbered thermocouple in each case.

This method was successful in the laminar phase before the flame entered the duct. However, once the flame reached the contraction region and was accelerated through the duct the flame speed became much faster, such that for highly reactive mixtures the flame appeared to be recorded at several thermocouples simultaneously. For this reason, measurements along the entire length of the duct are presented, as an average between the first and last thermocouples in the duct.

3.7.4. Explosion Pressure Measurement

The pressure of an explosion was measured using an array of piezoresistive pressure transducers as discussed in section 3.6.3. On many of the pressure traces, there was a significant amount of oscillation relating to acoustic noise present on the pressure signals, both in the test vessel and the duct. In order to make useful comparisons between tests, pressure traces were first normalised to ignition at t=0 and then a smoothing function was applied. The principle of the smoothing function was to reduce the influence of the oscillations on the individual pressure traces. This allowed a more realistic measurement of maximum pressure to be obtained without the high frequency oscillations superimposed, and also to allow clearer presentation of the results. Figure 3-15 illustrates the difference between the 'raw' pressure-time trace and the smoothed curve. It is clear that the smoothing function does not alter the shape of the curve, but does alter the height of the maximum to be in line with approximately the centre of the acoustic frequency.

The smoothing process involved an averaging over a set time frame. For example, in test-vessel 3, a smoothing interval of 5ms meant that that the pressure would be averaged over a 5ms period, beginning with the first data point, and the result placed at a point central to the averaged data points. This was repeated on a point by point increment throughout the trace. The smoothing function was also a necessary pre-requisite to obtaining a realistic rate of pressure rise for each test. Without smoothing, the $(dP/dt)_{max}$ values would relate to the individual oscillations and not the general trend.

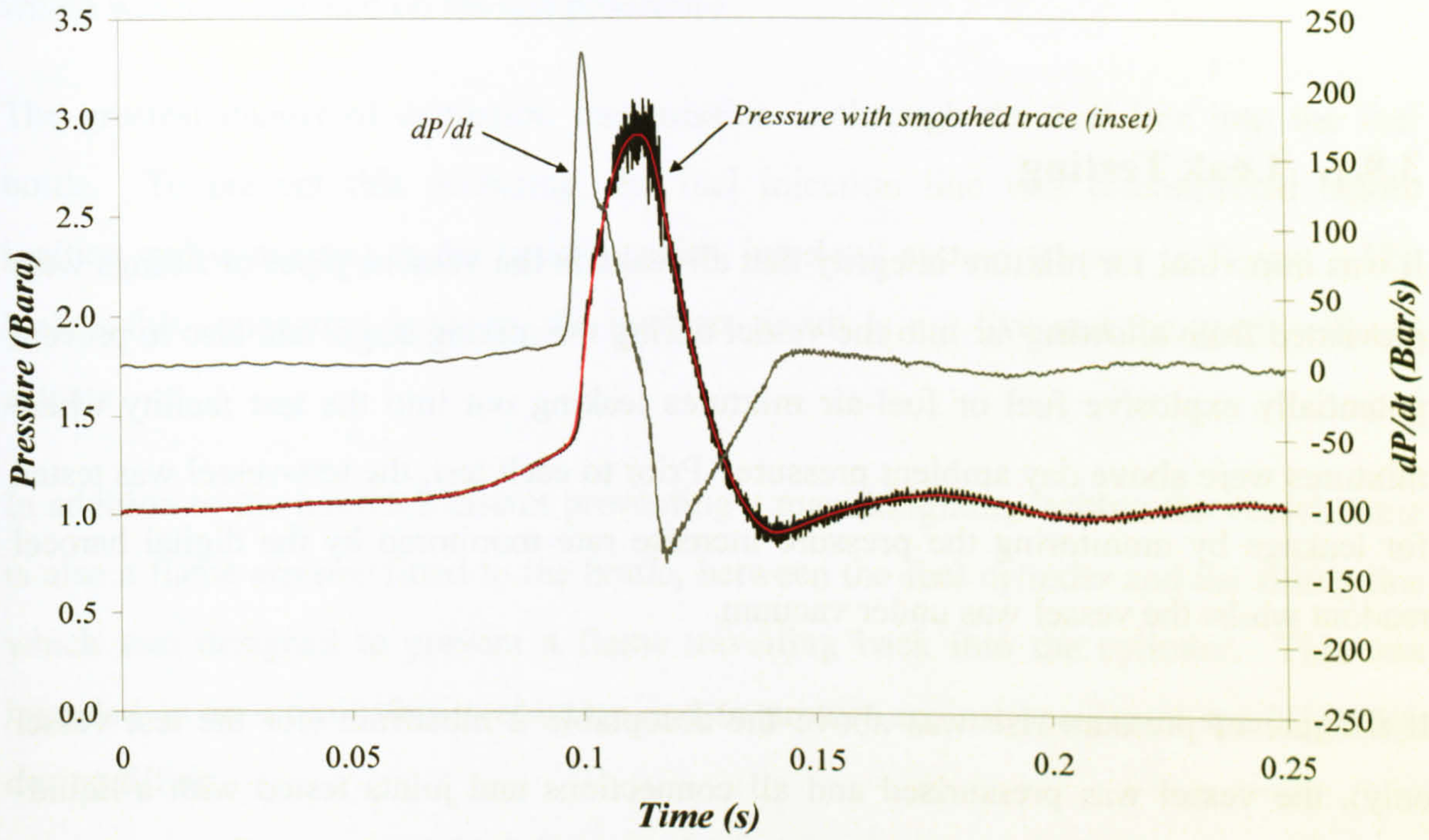

Figure 3-15: Comparison between raw and smoothed pressure signals with dP/dt trace added.

When comparing maximum recorded pressures between tests with variable starting ambient pressures, the recorded maximum was normalised with respect to the measurement of room atmospheric pressure at the exact time of the test, using the simple correction factor shown in Eq. 3-10.

$$P'_{Red} = P_{Red} / P_i \qquad \text{Eq. 3-10}$$

Where P'_{Red} is the normalised reduced pressure, P_{Red} is the measured reduced pressure and P_i is the initial ambient pressure.

3.8. Operating Procedures and Safety Considerations

For safety reasons, an operating procedure was required for each individual explosion test. A separate operating procedure form was devised for each test-vessel, and a separate sheet completed during each test. This procedure was constantly revised to account for minor modifications and improvements to the working test-vessels, and completely revised between geometries. For each test-vessel, the operating procedure followed a similar method, assuming bolting up and commissioning of the test-vessels. This is outlined in the steps detailed in Appendix 1 for test-vessels 2 & 3.

3.8.1. Leak Testing

It was important for mixture integrity that all leaks in the vessels, pipes or fittings were prevented from allowing air into the vessel during the mixing stage, and also to prevent potentially explosive fuel or fuel-air mixtures leaking out into the test facility where mixtures were above day ambient pressure. Prior to each test, the test-vessel was tested for leakage by monitoring the pressure increase rate monitored by the digital barocel readout whilst the vessel was under vacuum.

If the rate of pressure rise was above the acceptable 2 mbar/min (for the test vessel only), the vessel was pressurised and all connections and joints tested with a liquid-surfactant / water mixture, highlighting any leaks within the system. The leaks were then corrected and the test-vessel re-tested. Generally the leak-rate was maintained well below 1 mbar/min in all cases.

3.8.2. Comments and Recommendations on Safety

Before the commissioning of each test-vessel, a risk assessment was carried out to determine any potential risks, in order to minimise the possibility that a problem would occur and to put procedures in place should anything unintentional happen. Several safety points which were addressed during the course of this research are outlined below.

Transmission of an explosion to auxiliary equipment

Where there needs to be permanent connections to equipment such as vacuum pumps and barocel (from secondary/dump volume) there is the risk of transmission of an explosion to the equipment. This is avoided using a series of isolation valves close to the vessel so that the volume remains unchanged, but also remains isolated. This is controlled by sequential checking and recording onto the tick sheet test procedure for every individual explosion test conducted. The main connection from the test vessel to the barocel is protected by removing the pipe (male/female connector) before each test, which was also checked on the test procedure.

The greatest danger of explosion transmission is through the fuel line into the fuel bottle. To prevent this occurring, the fuel injection line was disconnected before ignition and connected to the ignition safety interlock system (shown in Figure 3-12). Unless this connection is made, the ignition circuit is not live and the spark will not actuate.

In addition to the interlock circuit preventing a manual ignition within the vessel, there is also a flame arrestor fitted to the bottle, between the fuel cylinder and the filling line which was designed to prevent a flame travelling back into the cylinder. This was intended as an extra safety precaution and to protect against accidental spark ignition during filling.

Creation of a gas/air mixture with an initial pressure exceeding 1 bar

For homogeneous mixtures prepared in test-vessels 2 & 3, the initial mixture pressure would never exceed day ambient pressure under the standard test procedure, since ambient air filling is used to top up the vessel. For stratified mixtures prepared in test-vessels 2 & 3 and for all mixtures prepared in test-vessels 1 & 4, over filling was avoided by careful monitoring of the injection of the fuel and compressed air. This was backed up by an audible alarm fitting within the control panel system which sounded when the pressure in the test vessel significantly exceeded standard ambient pressure. No tests during this research were conducted at elevated pressure, so this alarm was connected and switched on for the duration of the project.

Spark ignition failure

The spark ignition was tested prior to each test to check integrity. In the unlikely event that the spark did not ignite the mixture, the safest way to deal with the flammable mixture was to ignite from another position. In order to do this there was a secondary spark plug present in the vessel. For central, top and bottom ignition, the back-up spark plug was connected to the ignition box and then the mixture ignited. Following this the faulty spark was removed, given maintenance and replaced where necessary. Where secondary ignition was not possible, the test vessel was isolated from the secondary/dump vessel, and the test vessel inerted using N_2 gas to a pressure > 1.5 bar. In this case the digital barocel was isolated to prevent damage, and the analogue readout used to measure the pressure. Once inerted, the test vessel could be evacuated using vacuum pump B, followed by standard purging procedures as outlined in Appendix 1.

Creation of a non-ignitable mixture

It was often the case in stratified explosion mixtures that the mixture was out of the flammable range at the spark, especially where global concentrations outside the normal flammable range were prepared. Where this was the case, the back-up spark or mixture inerting procedure was used as described for spark failure above. In addition, to determine whether the problem was due to the mixture being out of the flammable range at the spark, or due to spark failure, the gas samples withdrawn from the vessel were analysed using gas chromatography and the issue addressed accordingly.

Release of a combustible gas into the test room

The danger associated with allowing release of a combustible gas into the test room was a consideration both for this facility and for the whole building. The fuel cylinders were isolated by three valves, and safety procedures are in place to prevent accidental leaks. In the unlikely event that a flammable fuel-air mixture did form in the test room, and an accidental spark ignited this, the large cross section windows were the weakest structure and were designed to act as a vent in the event of significant pressure build-up. It was intended that the windows would fail and release the pressure before any structural damage was done to the supporting walls and beams. The window glass was covered with a thin plastic sheet to limit glass fragmentation on breaking.

CHAPTER 4:

CLOSED VESSEL: HOMOGENEOUS AND STRATIFIED EXPLOSIONS

4.1. Introduction

Phylaktou *et al* [17] point out the importance of the investigation of the initial stages of an explosion in a long L/D vessel in terms of considerations for pressure relief venting of the vessel. Such considerations are also important in the case of shorter L/D vessels, as researched in the current work. By gaining an understanding of pressure development during all stages of the closed vessel explosion, both for homogeneous and stratified mixture compositions, a better understanding of the phenomena observed in vented and duct vented test programmes can be gained.

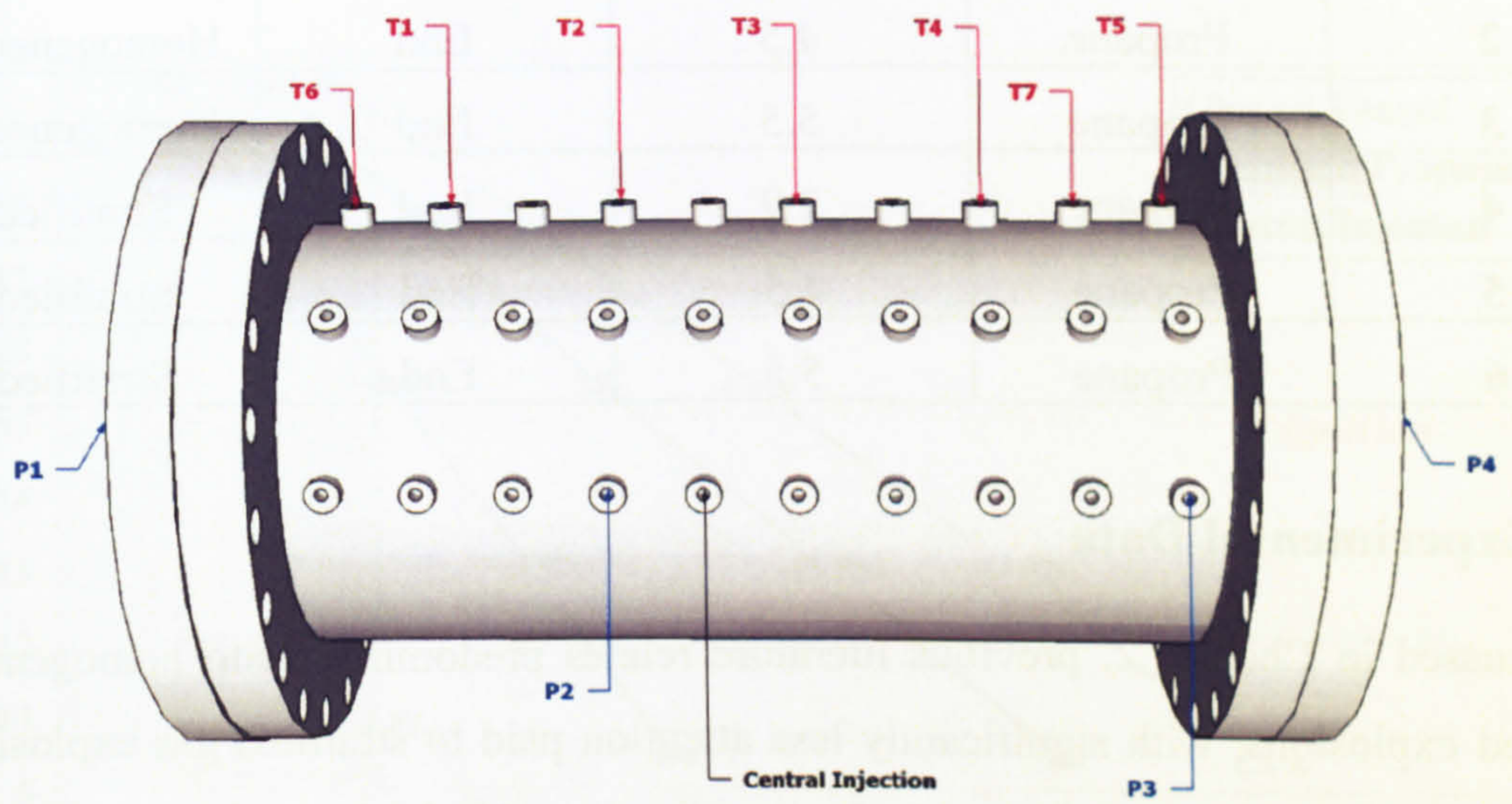

Figure 4-1: Rig 1, closed vessel test geometry. Items labelled P & T denote the location of the pressure transducers and thermocouples respectively.

The test programme presented in this chapter represents a small study of closed vessel propane-air explosions, in a cylindrical vessel of length (L) = 1.0 m, diameter (D) = 0.5 m, volume (V) = 0.196 m^3. The vessel employed in the current test programme also forms the primary chamber for the vented and duct vented test programmes discussed in Chapters 5 & 6. The results from this chapter may therefore be used as a simple reference by which the effectiveness of the venting process for homogeneous and stratified gas explosions may be determined.

The main fuel used throughout this experimental work is propane, therefore it is on this that the current chapter will focus. The tests in this section have been conducted in Rig 1, shown in Figure 4-1. More detailed technical specifications of this rig can be found in Chapter 3. The various test configurations investigated in this test programme are listed in Table 4-1

Table 4-1: List of explosion characteristics for all explosion tests discussed in this chapter.

Condition	Fuel	Concentration (%)	Ignition Position	Composition
1	Propane	2.9	End	Homogeneous
2	Propane	4.5	End	Homogeneous
3	Propane	5.5	End	Homogeneous
4	Propane	2.9	End	Stratified
5	Propane	4.5	End	Stratified
6	Propane	5.5	End	Stratified

4.2. Experimental Data

As discussed in Chapter 2, previous literature relates predominantly to homogeneous premixed explosions, with significantly less attention paid to stratified gas explosions, despite the fact that in an accidental leak scenario, a stratified mixture is more likely to form. The current test programme presents experimental data collected using propane-air mixture under homogeneous and stratified composition. Three concentrations were investigated; lean (2.9%), rich (5.5%), and 'worst case' (slightly to the rich side of stoichiometric at 4.5%). The basic results and explosion dynamics are presented here, including flame development, maximum pressures, rates of pressure rise and flame speeds, and results are compared to theoretical adiabatic values for closed vessel explosions.

In all cases, the starting pressures for both homogeneous and stratified mixtures were close to standard ambient pressure (~1.0132 bar), and injection of the fuel was via the central injection port on the outer wall of the cylinder. Mixtures were prepared as discussed in Chapter 3.

4.2.1. Stratified Mixture Composition

The concentration gradients measured by gas chromatography for the concentrations of interest here are presented in Figure 4-2, giving an estimation of the concentration gradient through the vessel as a function of the non-dimensional parameter *h/D*, where *h* is the height in the vessel where the sample was taken and *D* is the diameter of the vessel.

Of the three concentrations investigated, all are below the LFL at the top of the vessel, and 2.9% is very close to this limit along the centre line of the vessel where the ignition is situated (as indicated on Figure 4-2).

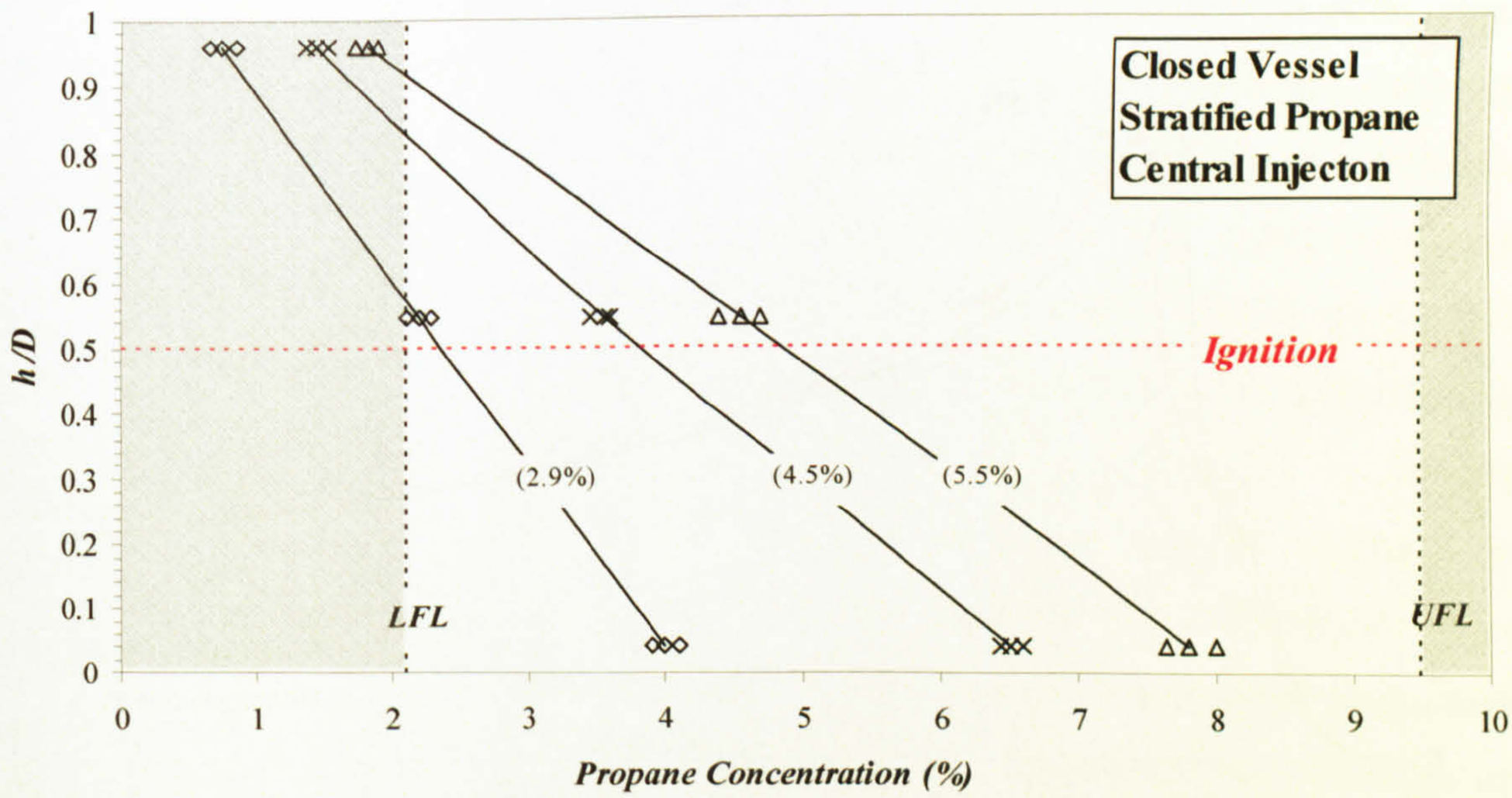

Figure 4-2: Propane-air concentration gradients measured by gas chromatography with (inset) global concentration injected.

4.2.2. General Observations

In order to best present the explosion development in this closed vessel, typical pressure traces for propane-air explosions, with end ignition at 2.9% and 4.5% global volume concentration are shown in Figure 4-3a, and 5.5% global volume is shown separately in Figure 4-3b. For all tests the pressure rise was fairly evenly distributed in the vessel, with all transducers recording similar maximum pressures and rates of pressure rise, the lowest level having been measured by Pt_1 (closest to the spark).

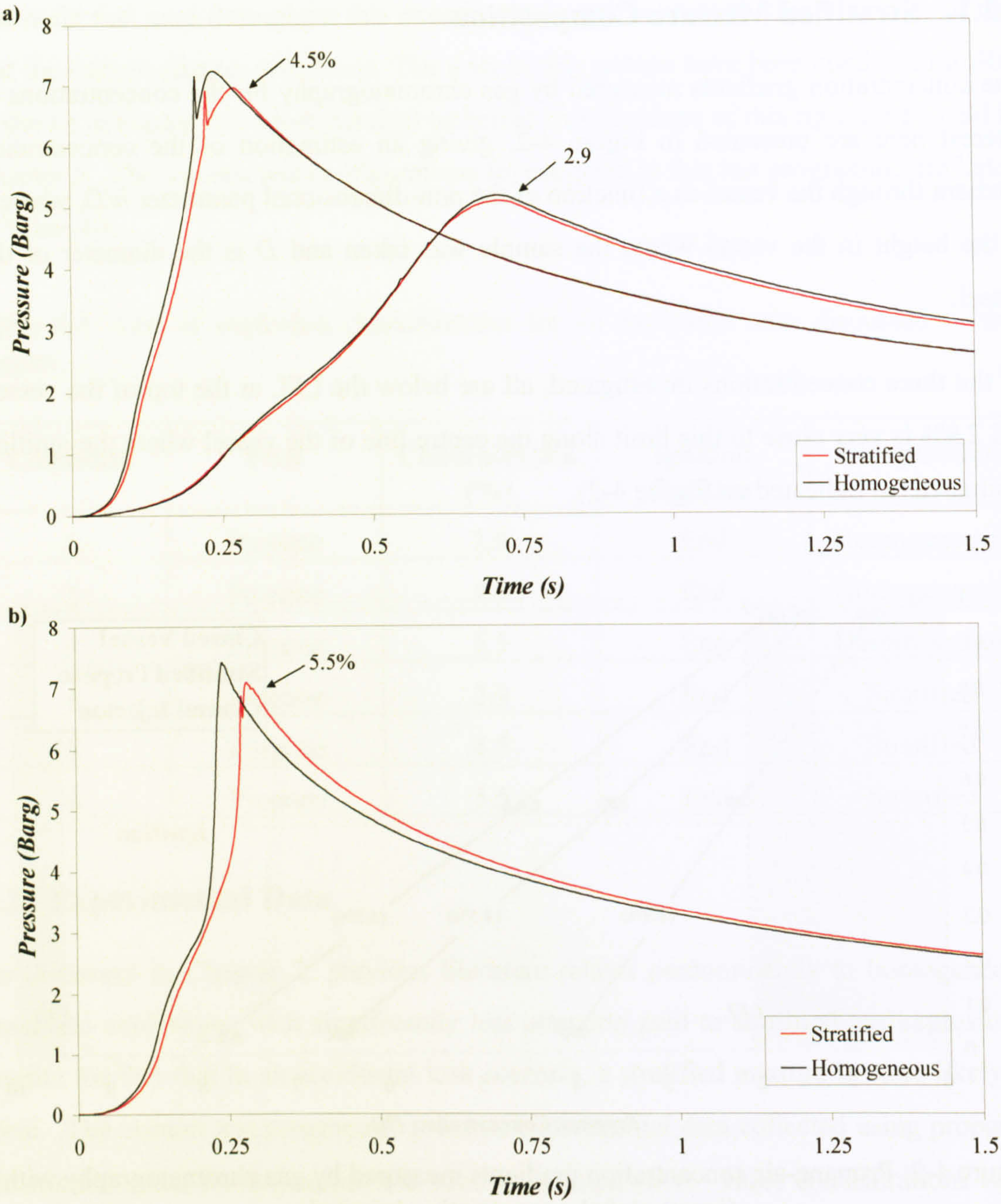

Figure 4-3: Typical (smoothed) pressure traces for homogeneous and stratified explosion tests for end ignition recorded at Pt_2 for a) 2.9% and 4.5% global concentration and b) 5.5% global concentration

The pressure-time curves exhibited by homogeneous and stratified explosions were reasonably similar in magnitude, shape and acceleration. At 2.9% both curves show a smooth increase with a small decrease in gradient close to 275 ms, then a rounded peak reaching a maximum of ~5 bar(g) before decaying slowly. At 4.5%, the curves show a much faster initial pressure rise and also a short duration 'spike', corresponding to high rates of pressure rise, $(dP/dt)_{max}$ up to ~ 575 bar/s, just prior to the main burning peak,

which had a much lower rate of pressure rise; $(dP/dt)_{max}$ ~ 65 bar/s. This 'spike' phenomenon was also evident at 5.5% for stratified mixtures, but not homogeneous as displayed on Figure 4-3b. The possible origin of this 'spike' behaviour will be discussed further in Section 4.2.6.

In general, the stratified tests showed slightly slower initial stages and reduced maximum, which were most likely to be due to the starting composition of the fuel in the chamber. However, as the explosion progressed, the mixture became more thoroughly mixed due to the effects of turbulent and diffusive mixing as the flame advanced. This mixing in the unburned gases would then have created a mixture closer in composition to the homogenous, as the fuel rich portion at the bottom of the vessel became mixed with the air rich portion at the top of the vessel. Therefore, since an equivalent amount of potential energy was available in both homogeneous and stratified composition mixtures, it is not unexpected that as the stratified mixture became quickly close to the homogeneous composition, a pressure curve of similar shape and magnitude resulted. Based on their stratified hydrogen-air mixture research, Whitehouse *et al* [74] suggested that the differences in peak pressures between homogeneous and stratified gas explosions of the same global concentration were due to differences in combustion completeness and that differences in rates of pressure rise could be attributed to the mass burn rate associated with the local hydrogen concentration. This theory may also be applied to the current work. The effect of the concentration gradient formed within the vessel will be investigated further in Chapter 6, where the injection position of the fuel has been used to successfully vary the concentration gradient.

By looking at the pressure-time curves alongside the time of flame arrival, measured by the fixed position thermocouples, it was possible to infer the flame shape and position to give a prediction of when the flame interacted with the geometry. Figure 4-4 shows the pressure-time traces for 4.5% with (a) homogeneous and (b) stratified mixture composition. The time of flame arrival at thermocouples Tc_1 to Tc_5 is shown with respect to axial distance (x m) from the spark ignition. The dotted vertical lines represent the time at which the flame is recorded at the thermocouples located in the top corners of the vessels (labelled Tc_6 and Tc_7 in Figure 4-1). The time of flame attachment to the vessel wall is marked (*) in each case.

Comparison between the flame arrival time at the axial thermocouples and arrival times to the radial thermocouples indicates that the flame did not develop as a true hemisphere flame from the point of ignition, but propagated as an elongated flame up until the point at which it touched the cylindrical walls of the vessel. As the flame interacted with the walls of the cylinder, it suffered a significant loss in both surface area and heat, which served to retard the flame, this corresponded to a slight reduction in rate of pressure increase at the points marked (*) in Figure 4-4.

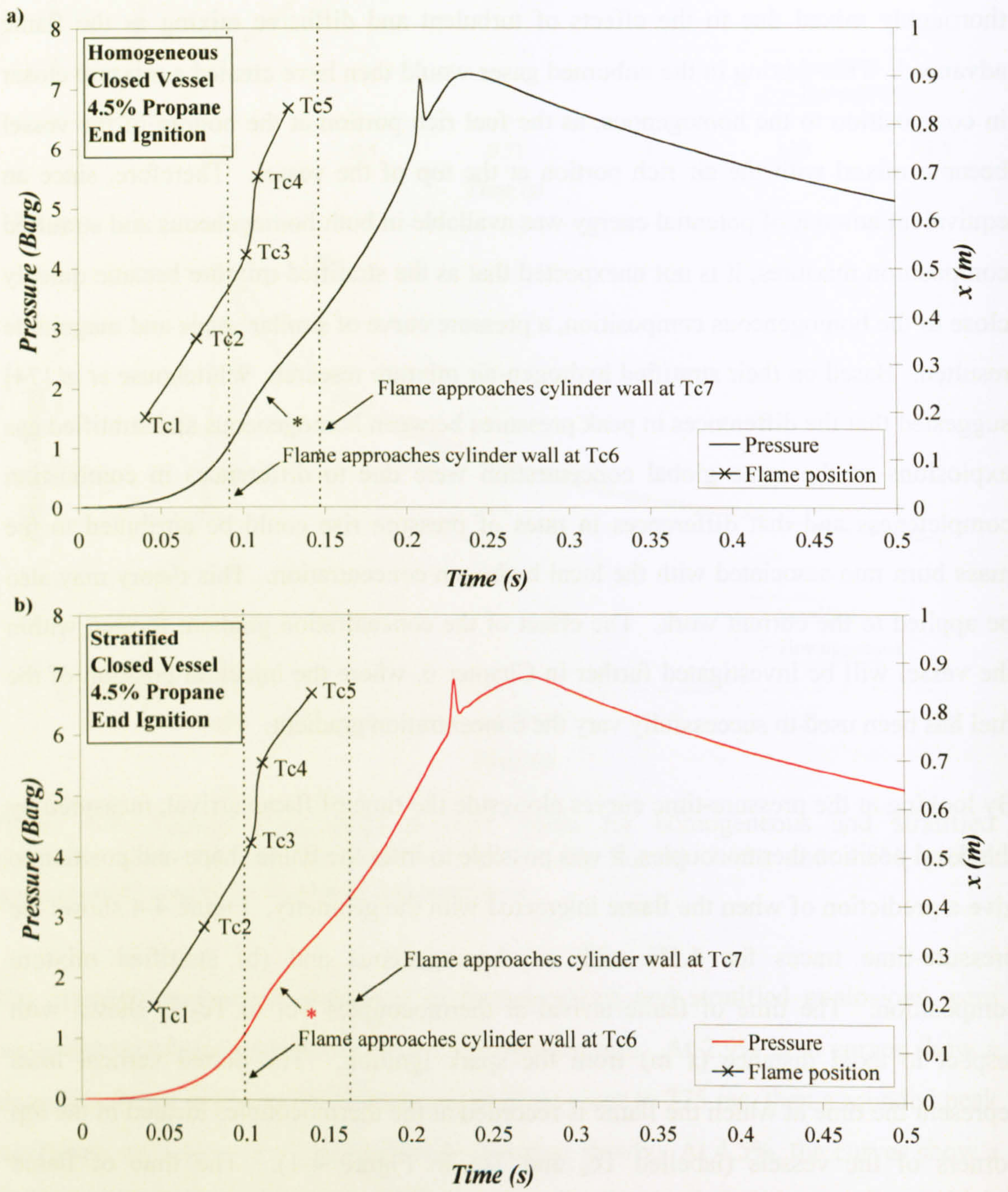

Figure 4-4: Pressure-time curves for end ignition, 4.5% propane with (a) homogeneous and (b) stratified mixture composition.

4.2.3. Flame Development

The explosion development in this closed vessel follows the mode of combustion previously observed by other researchers for longer L/D ratio cylindrical vessels. The previous research reports between 2 and 4 phases of combustion which an explosion in a closed cylindrical vessel would follow. Early works [25] tended to describe the combustion of a closed vessel explosion in just 2 phases, whereas more recent works have broken this down further, into a total of four phases [17, 40]. Where only two phases are described, the four phase regime can also be fitted to the experimental results as shown in Figure 4-5, which shows Schlieren photographs taken at four key stages of the combustion development for a cylindrical chamber of L/D = 2.5.

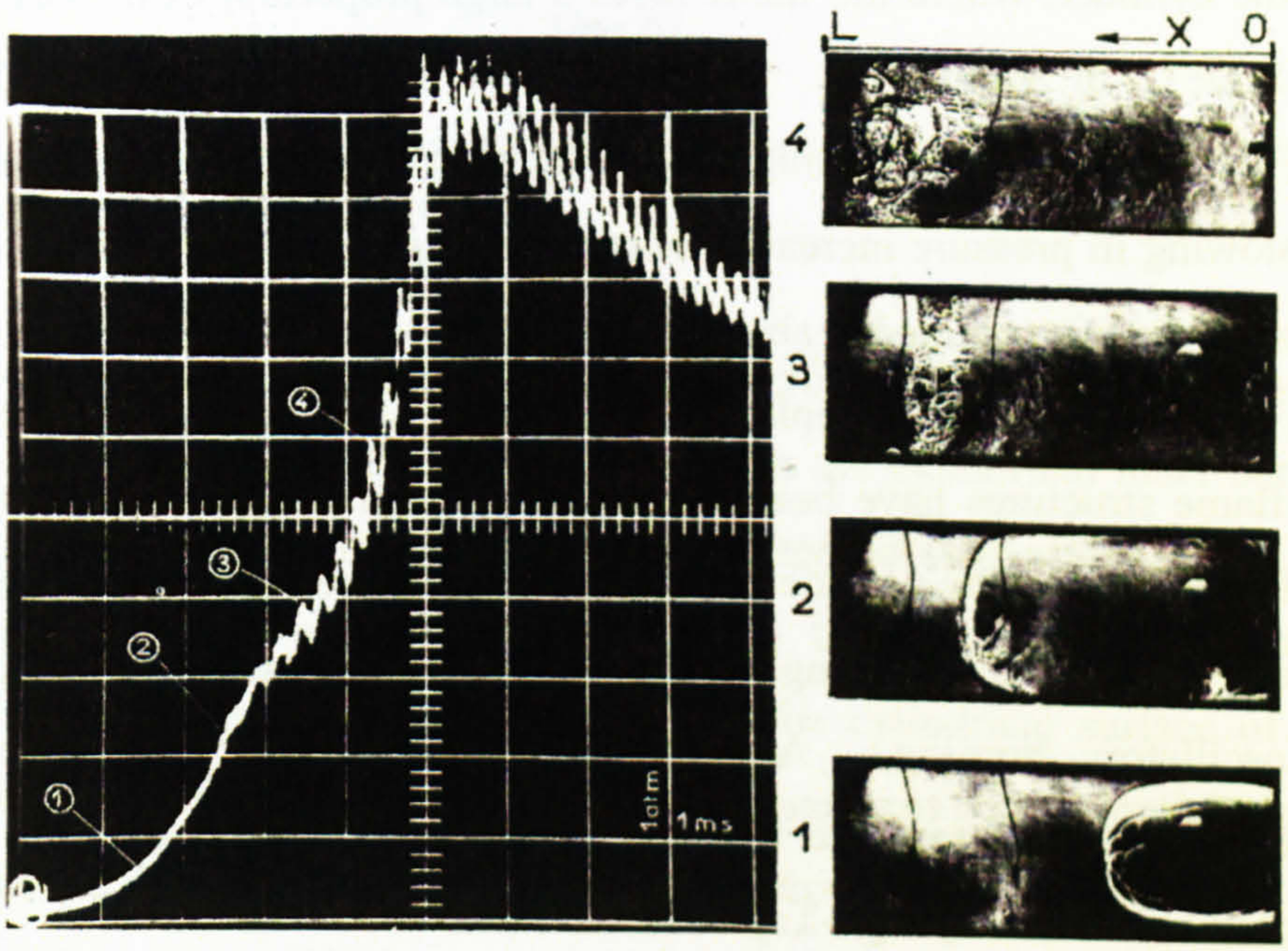

Figure 4-5: Typical flame development for a closed vessel explosion (reproduced in Leyer & Manson [40]).

Where a four-phase explosion is detailed, the following phases of combustion are reported [17], and the corresponding phases in the current work are labelled on Figure 4-6 for comparison.

Phase 1: A very short phase which lasts from the point of ignition up until the point at which the flame has grown to approximately half the radius of the cylinder, during which time the flame is growing as a hemisphere. There is very little pressure rise associated with this period.

Phase 2: This phase corresponds to the period as the flame begins to elongate axially along the cylindrical vessel growing more slowly in the radial direction as the unburned gases are compressed by the expanding flame front. The elongated shape of the flame during this phase, shown in Slide 1 of Figure 4-5, has been observed experimentally by several authors [40, 90]. Phylaktou *et al* [17], using a long L/D cylindrical vessel, reported that this phase continued for up to four vessel diameters, where maximum flame speeds were recorded. In compact vessels, expansion of up to four vessel diameters is impossible, therefore this phase is foreshortened and the explosion severity reduced accordingly.

Phase 3: Phase 3 is initiated by the interaction of the flame with the curved inner surface of the cylinder, where the flame loses a large proportion of its surface area, as shown in Slide 2 of Figure 4-5. Combustion is slowed significantly due to this interaction, and therefore exhibits much lower flame speeds, rates of pressure rise and a plateau or slowing in pressure increase. This stage could be as long as half of the total explosion time, and is reportedly absent in the case of fast combustion regimes (for example in a 7.5% ethylene/air explosion) [17]. The onset of oscillatory combustion and 'tulip' flame structures have been associated with this stage. In the current work this phase is characterised by a sudden decrease in rate of pressure rise (shown in Figure 4-6), and lasts up until the burning regains its momentum with the onset of higher amplitude oscillatory burning. As discussed in Section 2.3.2, the oscillations superimposed on the pressure trace following interaction of the flame with the vessel walls have been linked to Rayleigh-Taylor instabilities.

Phase 4: The final phase of combustion is an amplification of the oscillatory combustion triggered by the sudden cooling of Phase 3 and can be linked to the onset of Taylor instabilities triggered by reflected pressure waves reflected by the confining geometry and causing acceleration of the flame front in the unstable direction as discussed in Section 2.3.2. This phase can involve high frequency high amplitude oscillations as in the case of faster burning more reactive fuels, or may be absent completely in the case of slower burning, less reactive fuels. In the current work this phase was only observed for the higher concentration tests. The increase in amplitude of the oscillations is visible on Figure 4-6, and will be discussed in greater detail in Section 4.3.

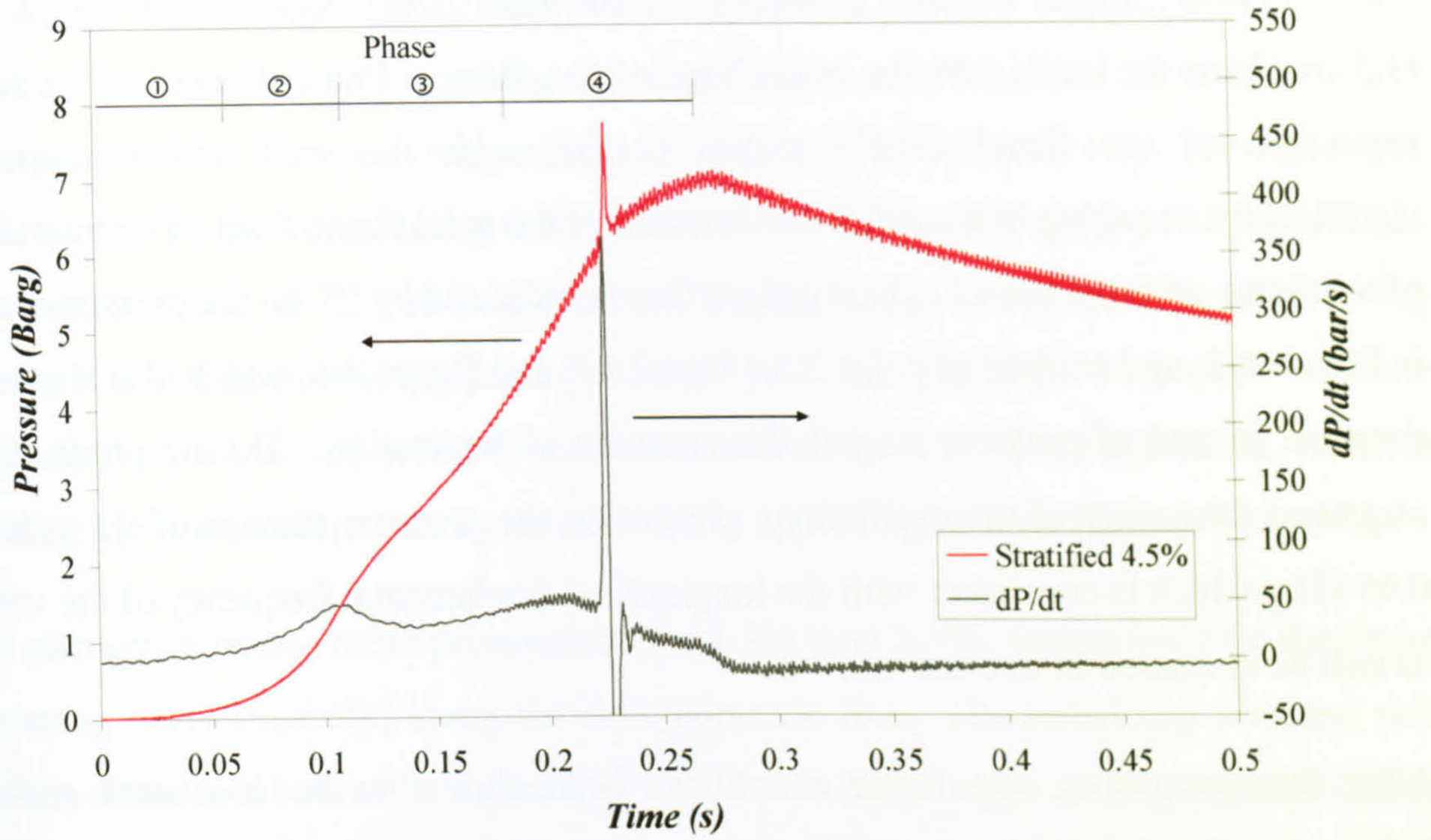

Figure 4-6: Comparison between pressure-time and rate of pressure rise for 4.5% homogeneous mixture, end ignition

Where only a two phase combustion regime is described [30, 40, 90, 91], the phases are separated by the interaction of the flame front with the cylindrical inner surface, and a similar progression is described. Phase 1 begins immediately after ignition, where the flame briefly grows as a hemisphere from the ignition point and then becomes elongated, with sections becoming parallel with the cylindrical surface of the vessel. The transition to the second phase of combustion occurs as these parallel sections make contact with the vessel's surface, and the flame front becomes drastically reduced in area, which also reduces flame speed and rate of pressure rise. Slide 1 on Figure 4-5 corresponds to the flame shape during this phase, and the section of increasing pressure rise on the pressure trace (and the corresponding section of the flame for the current work has been marked on Figure 4-6). It can be seen from this figure that the overall trend of the pressure trace is very similar with respect to shape as to that reported in literature. The oscillations are not present on the traces in Figure 4-3a and Figure 4-3b as the curves presented were smoothed for clarity of presentation. However, a similar oscillatory pattern is shown on the raw trace presented in Figure 4-6.

The flame up until contact with the wall has a relatively smooth surface, elongated in shape due to faster axial burning and slower radial burning as the flame approaches the

walls. Slower radial burning accounts for the time delay between arriving at Tc_6 (1.5 cm from the wall) and the quenching of the flame. Phase 1 ends as the radial expansion of the flame finally makes contact with the wall and is quenched significantly; resulting in a sudden deceleration of the axial flame front. The interaction of the flame with the vessel cylindrical surface is indicated by '*' on the pressure curves in Figure 4-3, and marked as point 2 on Figure 4-5 and Figure 4-6, which also shows the decrease in rate of pressure rise at this moment of interaction. During phase 3, the measured frequency of the oscillations present on the pressure trace is of the order of 0.45 kHz, which is consistent with the longitudinal fundamental frequency of the vessel, as will be discussed in Section 4.3.

After this quenching, the flame shape has been shown to be consistent with an indentation forming in the centre, in the direction of the ignition, to produce a 'tulip' shaped flame [25, 40, 90, 91]. This has been attributed to the sudden slowing of the flame front, and interaction with the returning shock wave produced as the flame made contact with the vessel's surface. This phase of the explosion is greatly associated with oscillatory burning. Although it was not observed directly in this vessel, comparison of the data recorded with previous literature is consistent with the formation of a 'tulip' shaped flame within the vessel. That is where the flame growth is not completely hemispherical from the point of ignition, but rather elongated until the point where the flame touches the cylindrical vessel surface, thus slowing the flame, and then inverting it back in the direction of the ignition to create a 'tulip' shaped flame.

This phenomenon has been reported for both long closed cylinders, and for cylinders which are open at the ignition end only [40]. In early research [91], it was observed that in relatively short cylinders (L/D = 2) the indentation of the flame into a 'tulip' shape was not present, and the development merely slowed to an almost flat flame front towards the end of the vessel. However, later research using different gases (Leyer & Manson [40] using $C_3H_8/O_2/N_2$ mixtures, and Starke & Roth [90] using C_2H_2/air mixtures) observed that while the 'tulip' flame would not develop fully in vessel with an L/D ratio of 1, with an L/D ratio of 2 the flame was showing a distinct indentation in the centre which was actively starting to move backwards - although not as significantly as in longer vessels. This stalling of the flame front towards the end of the vessel is consistent with the thermocouple arrival times in the current work, shown in Figure 4-4

(a & b). In these graphs, the flame is seen to speed up between Tc_3 and Tc_4, then slow between Tc_4 and Tc_5, before taking a further 130 ms until the end of burning which corresponds to the flame reaching and interacting with the end wall away from the spark (with the end of the vessel being 0.16 m away from Tc_5). This gives an average flame propagation speed of 1.23 m/s in the final stages, which is approaching the burning velocity for stoichiometric propane (0.46 m/s [6]), and therefore there must be some mechanism of interaction on the flame front, such as the inversion mechanism, which is allowing the continued pressure evolution while appearing to slow flame progression.

This phenomenon was more pronounced for 4.5% than 5.5%, suggesting that the flame is burning faster (initially) along the stoichiometric line. The remaining lean and rich portions above and below the centre line would then have begun mixing together due to turbulent mixing in the wake of the leading edge of the flame front, similarly to that reported in literature [70, 81], and burning as a diffusion flame, through a mixture closer to that of the global concentration injected. The frequency of the oscillations superimposed over the pressure trace in phase 4 (Figure 4-6) is of the order of 1.2 kHz, which is close to the sideways harmonic frequency of the vessel, approximated to be of the order of 1.0 kHz.

What is not mentioned in the previous literature is the occurrence of the small spike on the pressure trace which corresponds to a very fast rate of pressure rise (close to 375 bar/s). The potential mechanisms giving rise to this phenomenon will be discussed in Section 4.2.6.

4.2.4. Maximum Recorded Pressures

Figure 4-7 displays the maximum pressures recorded in the test vessel under standard ambient initial conditions for both homogeneous and stratified tests using propane-air mixtures between 2.9 and 5.5% (Φ = 0.71-1.35). Values have been normalised against initial pressure, P_i, to enable meaningful comparison to the vented tests in the following chapters. Figure 4-7 shows that the maximum pressures recorded for homogeneous and stratified gas compositions are similar in magnitude to each other, as noted in the previous section, but well below the calculated adiabatic temperature (shown by the

dotted curve in Figure 4-7) due to the cooling and quenching effects of the flame interaction with the vessel walls.

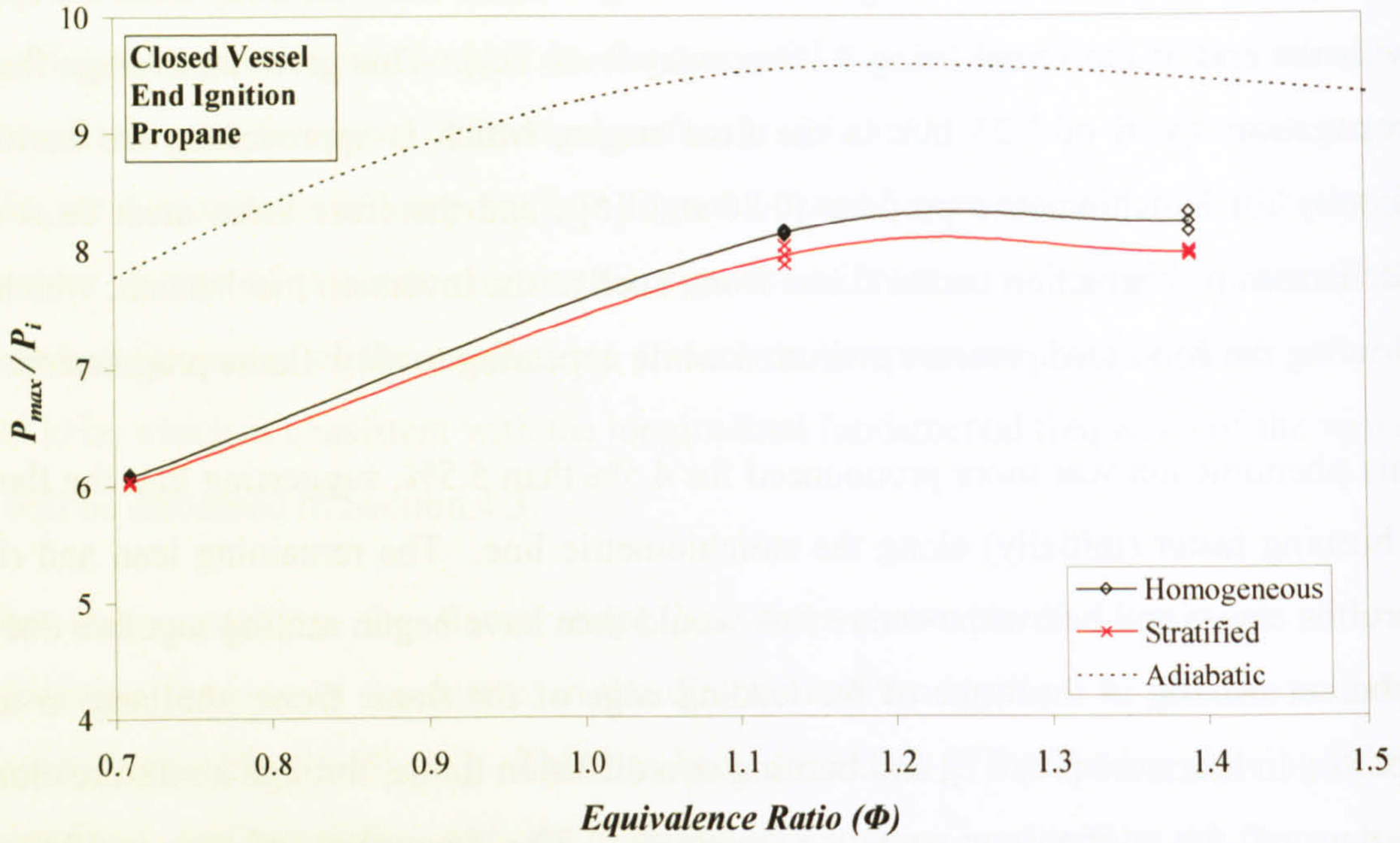

Figure 4-7: Comparison between maximum pressures (P_{max}) observed for homogeneous and stratified propane-air mixtures in a closed vessel.

The maximum pressure to the rich side of stoichiometric (5.5%) is slightly higher than would be expected, and this is more pronounced when looking at the rate of pressure rise, $(dP/dt)_{max}$, for both homogeneous and stratified mixture compositions. Figure 4-8 displays the maximum recorded rate of pressure rise in the vessel for the main peak. The rate of pressure rise attained at the spike was deemed to be of little importance structurally and is therefore omitted from the curves at this point. At very lean concentration, stratified mixtures show a slightly higher rate of pressure rise than homogeneous, but this difference is not significant in the current vessel. Homogenous mixtures exhibit slightly faster rates of pressure rise at 4.5%, which is increased further by 5.5% where the difference is significant.

The unusual dP/dt_{max} behaviour displayed on Figure 4-8 corresponds to the increased oscillatory combustion which has been observed on the pressure time traces in this vessel, increasing to the rich side of stoichiometric.

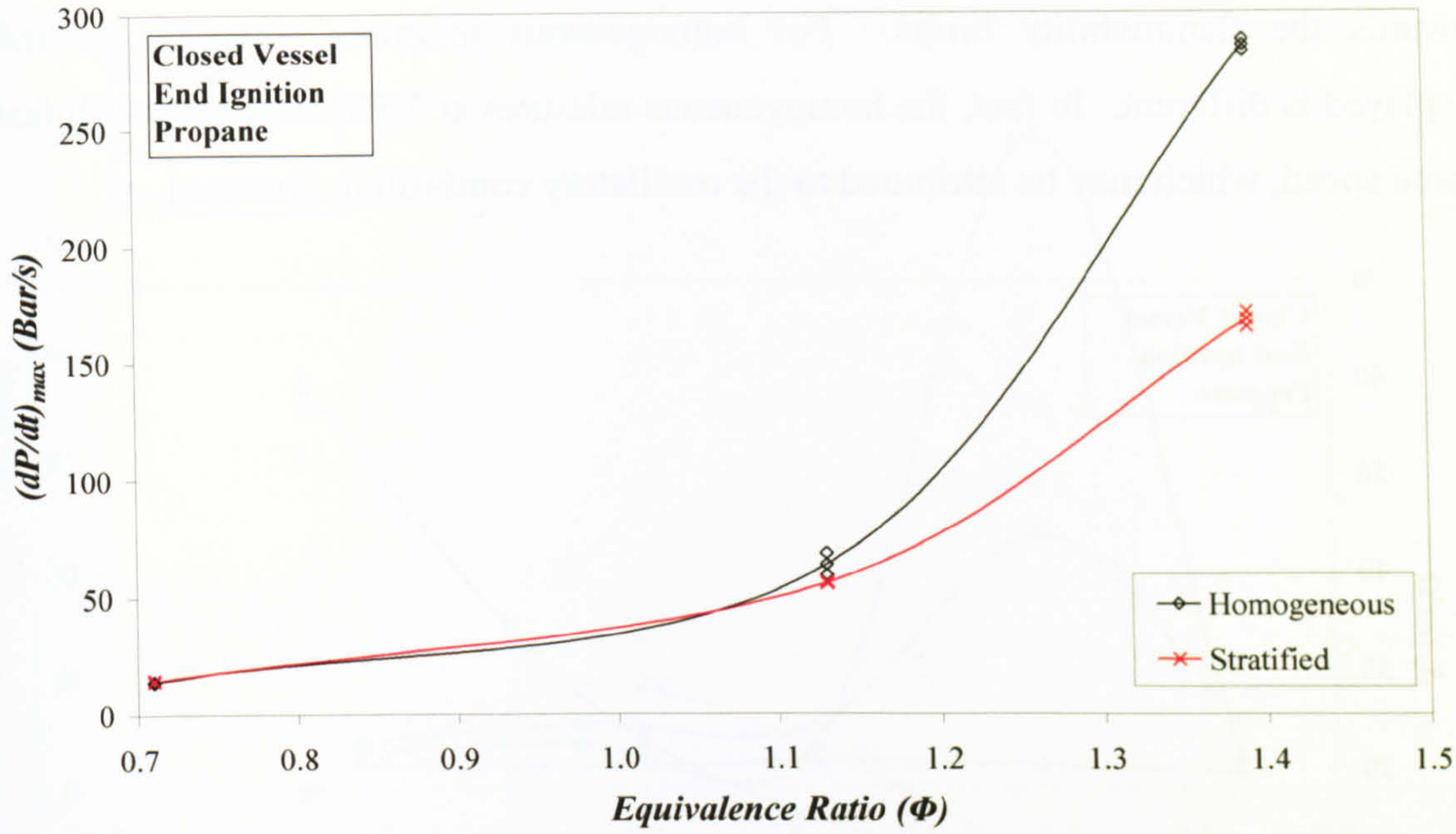

Figure 4-8: Comparison between maximum rates of pressure rise, $(dP/dt)_{max}$, observed for homogeneous and stratified propane-air mixtures.

Bartknecht [11] attributes similar irregular behaviour of propane at rich concentration to the fact that at slightly above stoichiometric, the heat of the combustion is sufficient to increase the velocity of the explosion reaction after an acceleration path to a velocity close to the speed of sound, thereby creating a noticeable velocity (or ramming pressure). This is reported to cause additional heating of the mixture and increases the combustion process accordingly, therefore resulting in unusually high P_{max} and $(dP/dt)_{max}$. Bartknecht [11] goes on to describe that this behaviour can lead to the transition to detonation, over a sufficient run-up distance. However in the current geometry of L/D = 2, such onset of detonation cannot occur.

4.2.5. Maximum Recorded Flame Speeds

Figure 4-9 shows the maximum flame speed recorded between any two consecutive thermocouples. In most cases, this maximum occurred between the Tc_3 and Tc_4, i.e. in the latter half of the vessel. In theory, the most reactive mixture should have the highest flame speed, and for propane that is slightly to the rich side of stoichiometric. In Figure 4-9, the stratified curve demonstrates what would be typically expected, with higher flame speeds close to stoichiometric, and lower flame speeds as the concentration tends

towards the flammability limits. For homogeneous mixtures however, the trend displayed is different. In fact, the homogeneous mixtures at 5.5% display a much faster flame speed, which may be attributed to the oscillatory combustion observed.

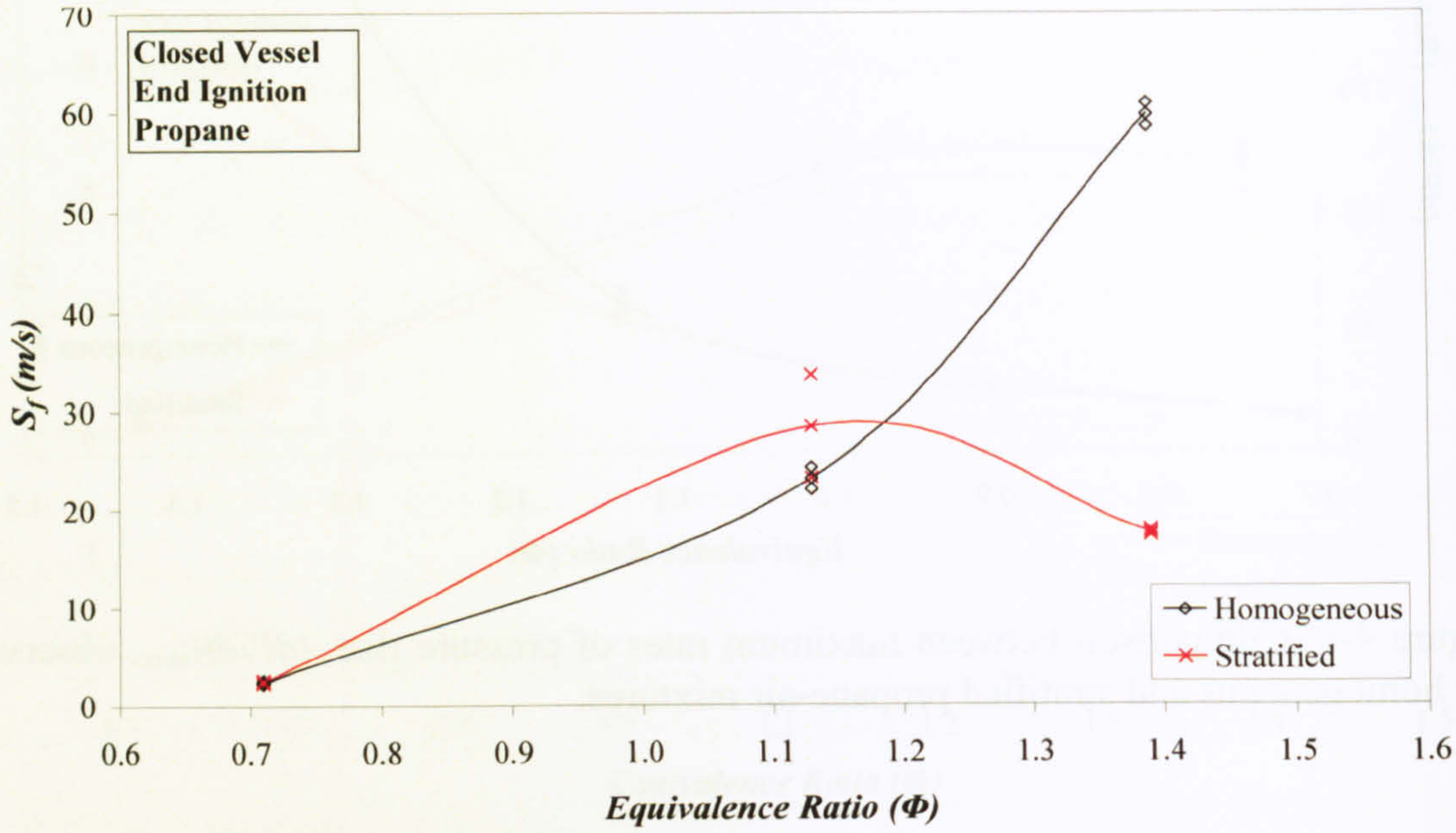

Figure 4-9: Comparison between maximum flame speeds (S_f) observed for homogeneous and stratified propane-air mixtures.

Figure 4-10 shows the flame speed measurements calculated from the arrival times between two consecutive thermocouples. The flame speeds recorded for 2.9% and 4.5% are comparable between the stratified and homogeneous mixtures, however, as shown in Figure 4-9, the maximum flame speeds recorded for 5.5% far exceed any other measurement taken.

The decrease in flame speed observed between the last two thermocouples (Tc_4 and Tc_5), compared to the sudden increase between the previous two thermocouples (Tc_3 and Tc_4) shown for all concentrations and for stratified and homogeneous mixtures in Figure 4-10, can be attributed to the time of flame quenching of the radially growing portions of the flame front, which will have initially encouraged faster growth in the axial direction before the flame became inverted and started to retreat slightly as discussed above. Similar phenomena have been observed previously in the work of Starke and Roth [90], which they also link to the onset of strong vibrations on the pressure signals.

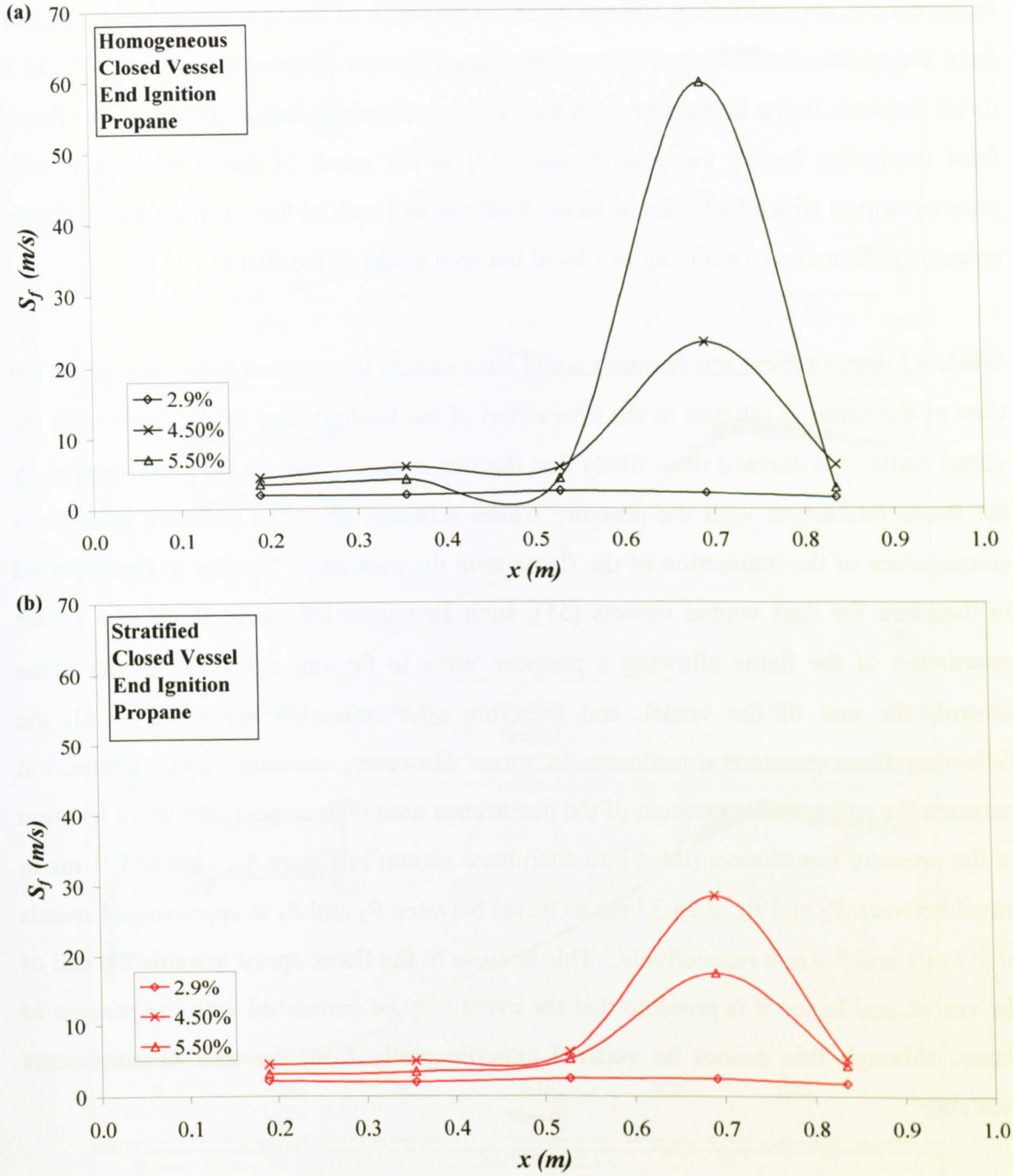

Figure 4-10: Flame speed measurements taken between consecutive thermocouples for (a) homogeneous and (b) stratified mixtures

4.2.6. Spike Phenomenon

Figure 4-11 shows the individual pressure-time curves for a 4.5% homogeneous propane mixture, recorded at all four pressure transducers in the vessel, for a single test. The spike appears on three of the four traces recorded in the vessel, with the earliest

occurrence at approximately 107 ms on P_2. The origin of the spike initiation is unclear from the results available, but is possibly caused by one of three mechanisms; (1) as a direct response to the interaction with the vessel walls which begins to perturb the flame front increasing locally the reaction rate; (2) as the result of flame interaction with pressure waves which had been reflected from the end wall of the chamber, or (3) due to an auto ignition event occurring in a local hot spot ahead of the flame.

While all three of these mechanisms could have caused the unusual behaviour, given the time of the spike in relation to the interaction of the leading edge of the flame with the vessel walls, it is deemed most likely that the first event, shown on P_2, was triggered by the flame interaction with the pressure waves reflected from the end wall as a direct consequence of the interaction of the flame with the geometry. Similar to that reported in literature for duct vented vessels [51], such an interaction could result in a severe retardation of the flame allowing a pressure wave to be sent out ahead of the flame towards the end of the vessel, and therefore after reflection appearing on all the following three pressure transducers in turn. However, assuming some connection between the spikes, measurement of the occurrence time with respect to relative location of the pressure transducers (inset into each trace shown in Figure 4-11 gives 101 ms to travel between P_2 and P_3, then 33 ms to travel between P_3 and P_4 at approximate speeds of 4.7 m/s and 5.0 m/s respectively. This is close to the flame speed towards the end of the vessel, and hence it is possible that the event may be connected with the passage of flame, although this cannot be verified experimentally from the data measurements available

The 'spike' that occurred on P_3 (at ~ 209 ms) appeared to coincide with the onset of a higher frequency, higher amplitude oscillatory behaviour in the vessel, although it is not proven that one is caused by the other. The final and much smaller spike appears on P_4 some 33 ms later and in this case does not coincide with the further onset of oscillations, but merely signifies the start of the decay of the disturbance. It is possible given the time that the spike on P_4 occurred (at ~ 242 ms) that the spike shown in P_3 and P_4 are connected, but independent of that displayed on P_2in this vessel.

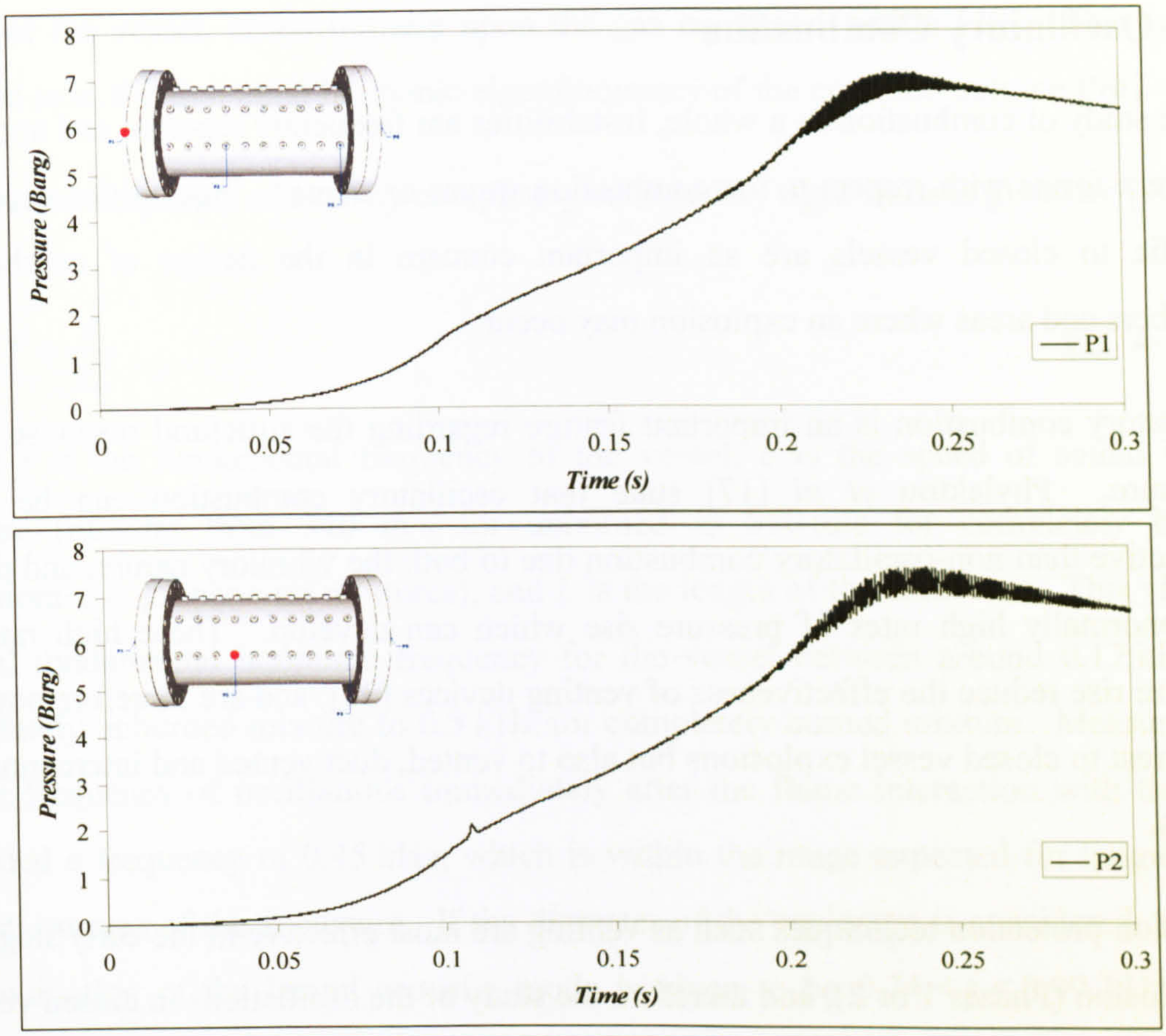

Figure 4-11: Pressure-Time curve for homogeneous propane showing a 'spike' at different times on pressure transducers P_2, P_3 and P_4.

4.3. Oscillatory Combustion

In the study of combustion as a whole, instabilities are frequently reported and appear in different forms with respect to the combustion waves or flames. Instabilities which are specific to closed vessels are an important concern in the design of combustion chambers and areas where an explosion may occur.

Oscillatory combustion is an important feature regarding the structural response of an enclosure. Phylaktou *et al* [17] state that oscillatory combustion can be more destructive than non-oscillatory combustion due to both the vibratory nature, and due to the abnormally high rates of pressure rise which can develop. These high rates of pressure rise reduce the effectiveness of venting devices [30], and are therefore not only of interest to closed vessel explosions but also to vented, duct vented and interconnected vessels.

Explosion protection techniques such as venting are most effective in the early stages of an explosion (Phases 1 or 2), and therefore the study of the oscillations in closed vessels is of secondary concern to this research. However, the phenomenon is noteworthy as a point of interest and applicability between the homogeneous and stratified experimental data provided in this chapter. A short discussion of the oscillatory combustion modes present in this section will be provided, although this is not intended to be a comprehensive study of the subject. More comprehensive details and descriptions are available from the associated literature [27, 29, 30, 40, 90].

In closed cylindrical vessel explosions, the progression of a smooth flame front up to the point at which the flame touches the cold inner surfaces of the cylinder has been discussed. The absence of oscillations on the pressure trace during this period indicates that the perturbation of the flame front is too weak to initiate vibratory motion [40], and therefore the curve at this point is consistently recorded as smooth.

Following the flame interaction with the walls of the chamber, the sudden deceleration of the flame and quenching effects give rise to new perturbations in the flame front which manifested as oscillations on the pressure traces [90]. These oscillations have been recorded to be close to the fundamental frequency of the longitudinal acoustic

mode of the vessel, based initially upon the gas contained within [40]. This is also referred to as the first axial harmonic eigenfrequency of the enclosed column [90].

The natural frequency of a cavity completely enclosed by rigid walls is given by [92]:

$$f = \frac{c}{2L} \qquad \text{Eq. 4-1}$$

where f is the fundamental frequency of the vessel, c is the speed of sound in the mixture (ranging from 340 m/s for unburned to 990 m/s for completely burned stoichiometric propane-air mixtures), and L is the length of the enclosure. This yields a typical fundamental harmonic frequency for the vessel between around 0.17 kHz for completely unburned mixture to 0.5 kHz for completely burned mixture. Measurement of the frequency of oscillations immediately after the flame interaction with the wall provided a frequency of 0.45 kHz, which is within the range expected for longitudinal acoustic waves of the enclosure. If the diameter of the enclosure is considered, a crude approximation of the lateral acoustic mode is given to be $0.34 < f < 0.99$ kHz. The frequency of oscillations observed later in the explosion then is in excess of both the longitudinal and lateral acoustic modes of the vessel, indicative of some other influencing factor causing the disturbance.

Another well documented phenomena relating to oscillatory combustion is the cellular structure of the flame. Such structures have been photographed as occurring immediately after the interaction with the wall as a result of the velocity fluctuation which trigger the hydrodynamic instability of the flame front. However, it is reported that the appearance of the cellular structure is not sufficient alone to increase the amplitude of the oscillations above that initially caused by the interaction [40]. Therefore there must be some other interaction which increases these oscillations. The expansion waves generated at the moment of initial contact with the walls can trigger the hydrodynamic instability of the flame front, which in turn can have the effect of amplifying the initial oscillatory burning, but only where the initial amplitude of the oscillations is above a critical value (approximately 50 mbar). Below 50 mbar, the oscillations either remain constant (neutral behaviour) or dampen and disappear without any amplification [40].

In the previous sections, the inversion and reversal of the flame has been discussed as the flame progresses along the cylinder after initial interaction. Where the acceleration is in the direction of the heavy fluid, or unburned gas, the surface remained stable. However, when the flow is reversed, as observed in the case of cylindrical closed vessels, this inversion will force the flow in the opposite direction, facilitating the onset of Taylor instabilities in the system. Taylor instabilities occur where a contact surface separating a light and a heavy fluid (i.e. burnt and unburnt gases) is accelerated in the unstable direction towards the less dense fluid, in this case, the burned gas. This additional force can be a factor in increasing the oscillations on the pressure traces.

There are several theories of what can cause the inversion or 'tulip' shape of the flame. Markstein [30] applied the Taylor Stability Theory to the propagation of the flame front, explaining the indentation of the tulip flame as being caused by the passage of a shock wave in the unstable direction, and explained the phenomenon as due to the flow behind a shock wave, with reference to Taylor instabilities.

Starke and Roth [90] theorise that the appearance of the tulip flame was simply caused by the quenching effects of the walls, forcing the flame to act as a weaker velocity source and causing less motion in the unburned gas. Similarly, Strehlow [28] also attributes the tulip flame to the interaction with the walls, causing deceleration of the flame front, which they refer to as a 'Taylor-Markstein' instability. Dunn-Rankine (quoted in [93]) consider the appearance of the tulip flame to be due to a vortex structure in the flame prior to flame quenching, and finally Rotman and Oppenheim (quoted in [93]) explain the tulip flame occurrence as a result of Tollmein-Schlichting waves set up by the wall following the break down of laminar flow in the tube.

It is not the intention here to comment on the validity of the above theories on oscillatory combustion and tulip flame formation in closed cylindrical vessel explosions, merely to point out the presence of such theories and acknowledge them as possible causes of the phenomena observed in the current work. However, it certainly seems to be the case for the phenomena recorded in the present work that the oscillatory combustion and subsequent formation of the tulip flame were linked to the attachment of the flame with the wall, and the interaction of the flame with the reflected pressure

wave occurring as the result. This is not to say that other theories are not valid, but may not relate well to the geometry discussed in this chapter.

4.4. Summary of Closed Vessel Experimental Data

The results presented in this chapter have provided a useful comparison between the relative severities of explosions under the regimes of the well researched homogeneous mixtures, and the less well researched stratified mixtures, to the conclusion that in a vessel of L/D = 2, the difference in the maximum pressures of the two compositions is surprisingly small. The behaviour of stratified mixtures being similar in nature to that of homogeneous has been attributed to the mixing of the fuel-rich and air-rich portions of the unburned gas as the combustion progressed.

Further comparisons were made between previous literature on short and long cylindrical vessels, and it was found that the behaviour of the flame in the current geometry exhibited a flame structure more akin to the longer vessels reported in recent works [40, 90]. In fact, in the current work it seems that the tulip flame structure developed for both homogeneous and stratified mixtures, which is again likely to be a factor related to the mixing in the vessel quickly after ignition, and before the flame attachment to the walls where the oscillatory combustion was initiated.

Several theories are prominent for the explanation of oscillatory combustion observed on pressure traces in closed vessels. The most likely explanation for the current work is that the oscillations were triggered by the event of flame interaction with the vessel walls. In longer tubes this interaction can reduce the flame surface area by up to 80% [90], in the current vessel this figure will be lower due to the reduced distance available for the flame to expand before the interaction. The contact between the flame and the cylindrical walls of the vessel was, therefore, the likely cause of the onset of oscillatory combustion, which was then amplified by growing perturbations of the flame front caused by other interactions such as returning shock waves causing inversion of the flame front in the unstable direction. Whatever the causes of these instabilities, the resulting curve is increased slightly in magnitude, and the individual peaks will have a structural response implication which must be taken into account when designing vessels that must completely contain any explosion which may occur.

This chapter has demonstrated the powerful nature of stratified propane explosions, which has indeed proven quite useful in the development of the lean stratified internal combustion engine. The results presented do give weight to the design of industrial installations which use containment as a protection technique, where the vessel is designed to withstand the greatest homogeneous explosion which may occur. However, as will be shown in the following chapters, it is not necessarily always the case that homogeneous mixtures will provide the worst case for all conditions.

CHAPTER 5:

SIMPLY VENTED: HOMOGENEOUS AND STRATIFIED EXPLOSIONS

5.1. Introduction

Venting to induce pressure reduction within an enclosure likely to contain an explosive mixture is a commonly used protection technique. The presence of the vent reduces confinement and allows a relief mechanism to prevent explosion pressures exceeding the design pressure of the confining vessel. This effectively reduces the required vessel strength, and thereby the cost of production. The relative success of such mitigation techniques depends largely upon the specific conditions within the vessel, including mixture reactivity, concentration and composition.

The importance of venting has been well documented in previous years. However, despite this large body of research, the majority of literature presented addresses only homogeneous gas explosions [39, 42, 43, 46, 49, 94-116]. Whilst there exists a significant number of works which deal with a stratified gas-air explosions [55, 70, 71, 77, 117-123], relatively few of these deal specifically with the issue of *venting* of a stratified gas-air mixture and even fewer deal with the venting of propane-air explosions. The most recent works into propane-air vented explosions have been dominated by the works of Tamanini [67, 68, 79, 80, 82, 124], whose research has principally focussed upon a single large scale vented enclosure. In his works, Tamanini has pointed out the importance of the rich fraction of the mixture which he regards as the portion which is above the upper flammability limit. However, because the works have focussed largely upon a single large geometry, where the lean fraction, and therefore the available air within the enclosure was also large, the applicability of this emphasis on the rich fraction is unknown on smaller scale vessels. An understanding of the explosion development within smaller scale vented stratified gas-air explosions may be used to develop and validate prediction techniques and modelling programs. Therefore the need exists for new experimental data in the field of stratified gas-air explosions on small and medium scale geometries.

The test programme presented in this chapter involved collection of experimental data from test-vessel 2, which comprised a compact cylindrical vessel (L/D = 2), with a vent hole at one end, with a vent coefficient, K_v (= $V^{2/3}/A_v$) = 16.4. The

pressure generation and flame passage were monitored throughout the vessel, as shown in Figure 5-1. More detailed technical specifications of test-vessel 2 are provided in Section 3.5.

The range of variables considered in this test programme included concentration, composition (homogeneous or stratified), and ignition position. The main focus of the study was on propane-air mixtures, although a small study involving homogeneous methane-air mixtures was also undertaken. It was the original intention to investigate stratified methane-air mixtures in this configuration, however, a reliable technique for stratification of methane was not developed until later in the research. For each condition, at least three tests were performed to ensure repeatability. Additional tests were performed for conditions where more variation was exhibited.

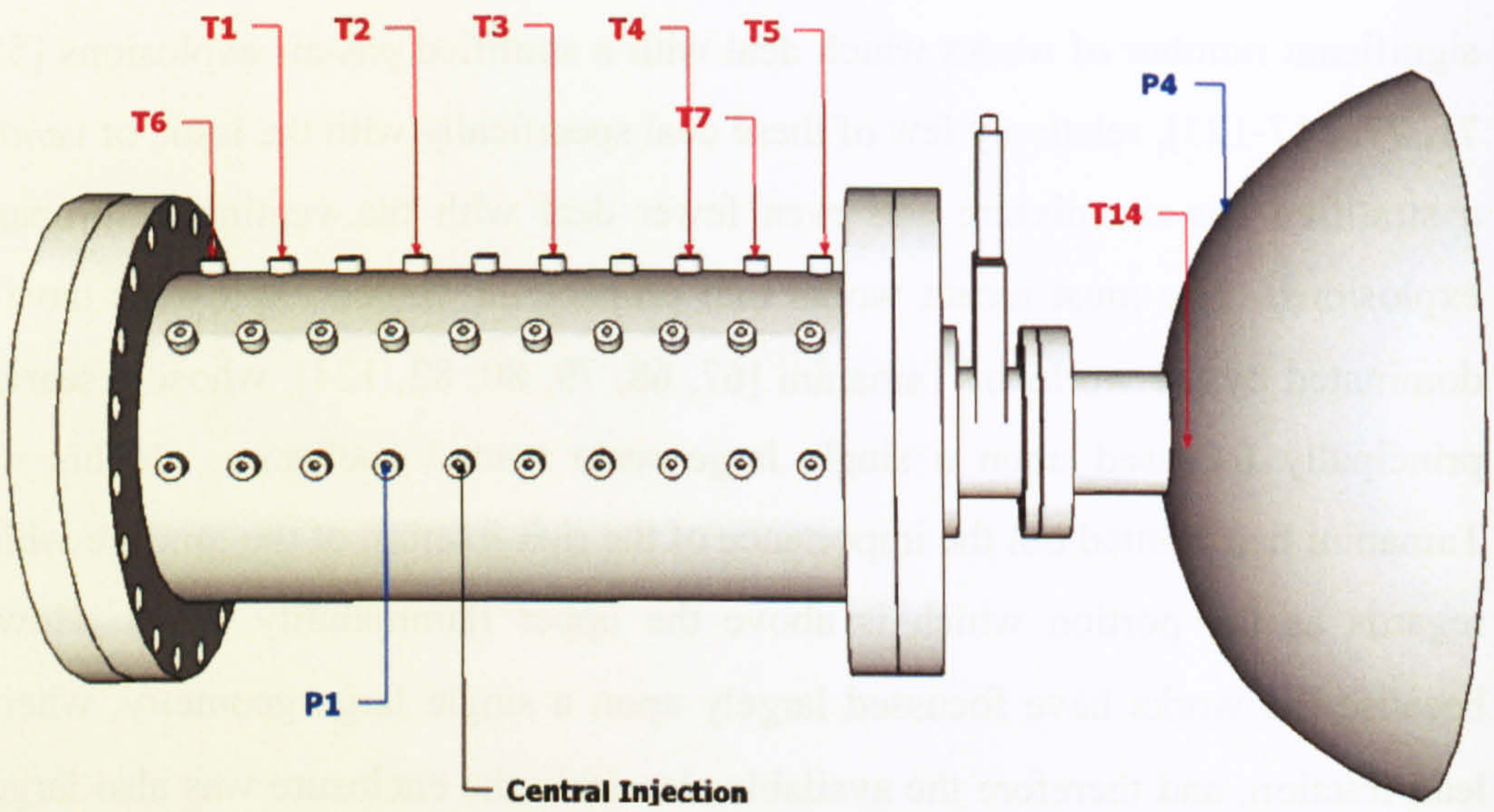

Figure 5-1: Rig 2 - Simply vented test geometry, including details of instrumentation. Items labelled P & T denote the location of the pressure transducers and thermocouples respectively.

5.2. Experimental Data (Propane)

In this section new experimental data are presented, obtained using propane-air mixtures with homogeneous and stratified composition in the range 2.9-5.5% (Φ = 0.72-1.37), in test-vessel 2. Results are presented in terms of maximum

(reduced) pressure, P_{red}, maximum rates of pressure rise, $(dP/dt)_{max}$, and flame speeds, S_f, followed by any comments on observations of unusual behaviour. For all tests in this section, starting pressure and temperature was local day ambient conditions. Therefore, where maximum pressures are presented, they have been normalised to take this into account. In order to best present the stratified data collected in terms of that already researched, for each test conducted using a stratified mixture composition, a comparable test was performed under homogeneous mixture composition.

5.2.1. Stratified Mixture Composition

Figure 5-2 illustrates the average concentration gradient for the concentrations of stratified propane-air mixtures presented in this test series, as a function of the non-dimensional parameter h/D, where h is the height in the vessel at which the sample was taken, and D is the diameter of the primary vessel. The line marked '*Ignition*' relates to the height in the vessel at which the end and central ignitions were positioned, along the central axis at $h/D = 0.5$. The shaded portions indicate the positions at which the mixture is not flammable. Figure 5-2 shows that the end and central ignitions were within the flammable range for all concentrations investigated in this programme, but that ignition at the very top of the vessel would have fallen outside the flammable range, despite the overall global concentration being within the flammable range. The effect of a stratified mixture with an overall concentration outside the flammable range is not addressed here, but will be afforded some attention in Chapter 6.

Figure 5-2 is intended to give an estimation only of the concentration profiles. Further clarification may have been obtained by withdrawal of additional samples from the vessel prior to ignition. However it was deemed that three samples was sufficient to confirm a concentration gradient without appreciably altering the integrity of the mixture or reducing the global concentration, in order to maintain the validity of direct comparison with homogeneous mixtures at the same global concentration.

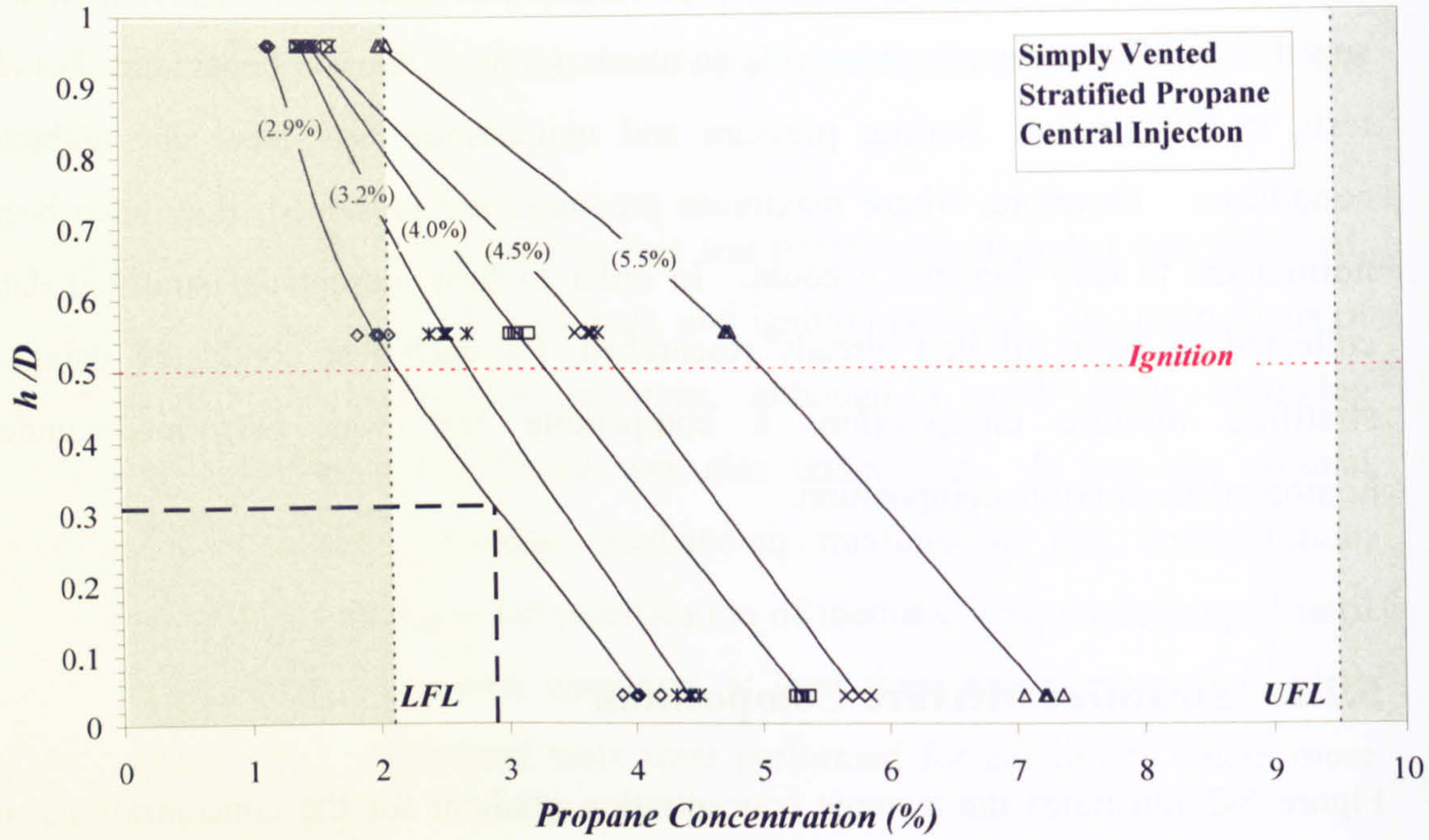

Figure 5-2: Propane-air concentration gradients measured by gas chromatography. The dashed lines shows how the graph can be used to provide an estimate of the propane concentration at a given height within the vessel for a known global concentration injected.

5.2.2. General Observations on Explosion Development -End Ignition

The explosion was initiated by means of an electric spark positioned either flush with the end flange (end ignition) or at the centre of the vessel (centre ignition). The direction of unburned gas flow was therefore to a large extent governed by the ignition position. Figure 5-3 shows representative pressure-time curves for 4.5% propane-air with (a) homogeneous and (b) stratified mixture composition with end ignition. The vertical line marked t_{in} indicates the time at which the flame reached the vent opening (as recorded by the last thermocouple in the vessel, Tc_5 in Figure 5-1).

In both homogeneous and stratified tests, an initial slow pressure increase was observed, up to around 0.02 bar. Pressure was maintained at this level until the flame reached approximately half way along the vessel (x = 0.5m), at which point

the pressure increased much more rapidly, corresponding to the maximum recorded rate of pressure rise of 24.1 bar/s and 6.75 bar/s for homogeneous and stratified conditions respectively. This yielded a ratio of close to 4:1 homogeneous to stratified. The peak pressure recorded was reached after 108 ms for homogeneous and 119 ms for stratified, in both cases this occurred some time after the leading flame front had exited the vessel, as indicated by the line marked t_{in}. There was also a marked difference in maximum pressure between the two conditions (0.666 barg to 0.1566 barg for homogeneous and stratified mixtures respectively).

Using the same criterion as that discussed for closed vessels, the explosion development within the vented vessel follows 4 phases, which have been shown diagrammatically in Figure 5-4, along with the corresponding phase for central ignition.

Phase 1 was a very short phase describing the explosion from ignition to the point at which the radial flame has grown to approximately half the diameter of the cylinder. Very low pressure and rates of pressure rise are associated with this phase.

Phase 2 began as the flame started to elongate in the direction of the vent as the unburned gas flow-field was set up. This skewing of the flame promoted by the unburned gas venting through the open vent is consistent with literature on vented vessel explosions [125]. During this phase, a significant amount of unburned gas was vented out into the dump volume. Figure 5-3 shows that the flame took 87 ms and 105 ms from ignition to reach the vent opening for homogeneous and stratified mixtures respectively. This equated to an average speed through the vessel of 9.6 m/s and 7.9 m/s, which was considerably faster than the flame speed recorded in the closed vessel explosions for the same equivalent global concentration.

During Phases 1 & 2, the pressure within the primary vessel was always significantly greater than that within the dump volume, signifying that gas flow was always in the positive direction, i.e. from the primary vessel into the dump volume. As the flame surface area increased, the unburned gas within the vessel was pushed much more quickly through the vent, which caused further stretching and elongation of the flame in the axial direction [9, 15, 23, 39, 42, 43]. This effect, in addition to the natural elongation of the flame along the vessel, as described above for isolated

cylindrical vessels, created a more rapid acceleration of the leading edge of the flame front towards the vent, thereby promoting slower radial burning. Phase 2 ended as the flame reached the vent.

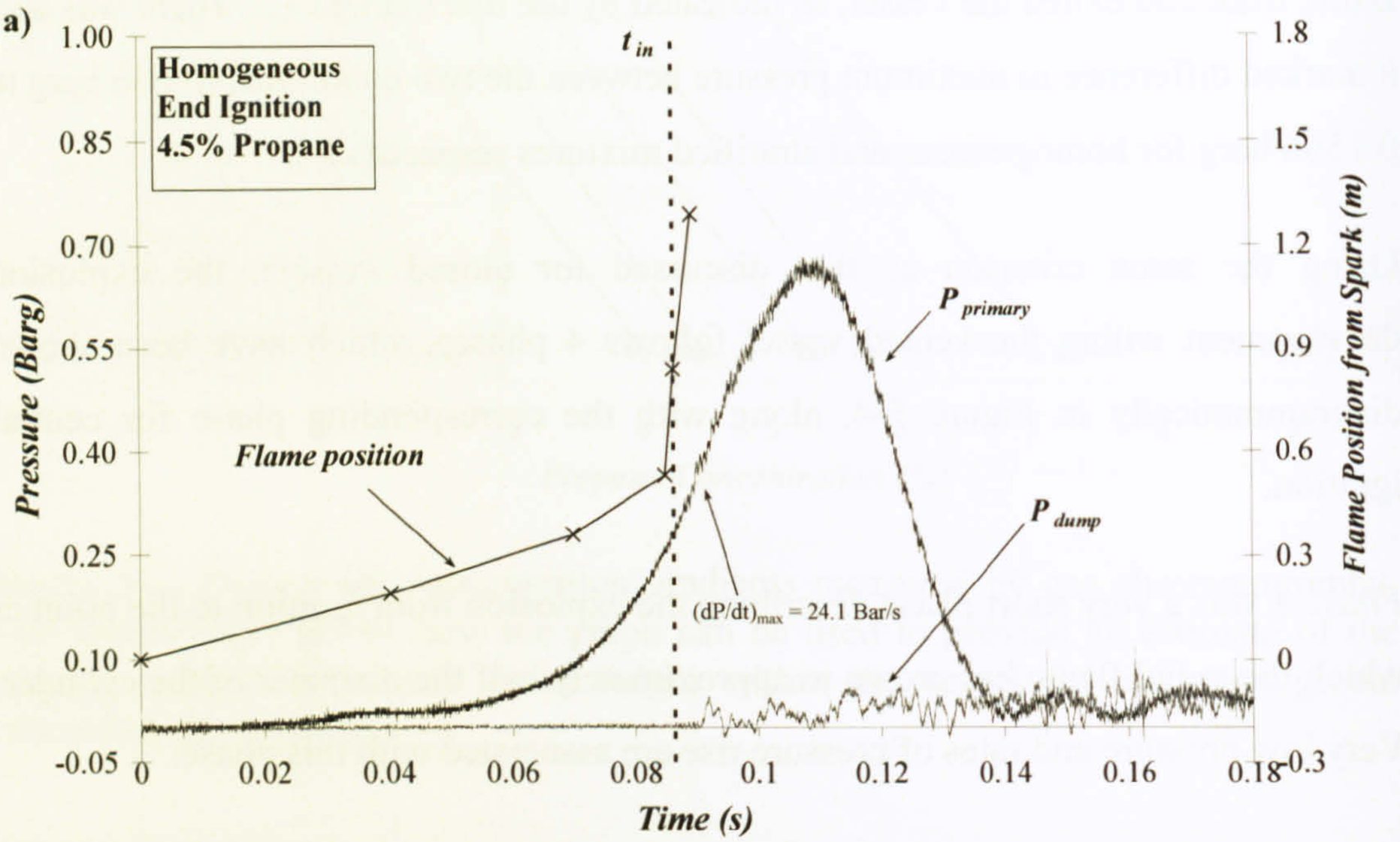

Figure 5-3: Pressure-time curves in the primary vessel and dump volume for (a) homogeneous and (b) stratified propane-air mixtures at 4.5% global concentration with end ignition (relating to conditions 4 and 17 from Table 5-1 respectively).

Phase 3 was characterised by the rapid burning of the flame through the turbulent unburned gases pushed ahead of the flame and out into the dump volume. The relative flame speed as the flame passed through the vent (measured between Tc_5 and Tc_{12}) was ~106 m/s and ~154 m/s for homogeneous and stratified mixtures respectively. During Phase 3, the unburned gases that had been pushed ahead of the flame in Phases 1 & 2 were ignited by this fast jet of flame exiting the primary vessel, creating an 'external' explosion. The sudden expansion of the gases in the dump volume caused by this external explosion corresponded to the sudden rise shown on the dump volume pressure trace in Figure 5-3. This created a momentary decrease in the rate of pressure evolution from the vessel, and in some cases a flow reversal from the dump volume back into the primary vessel, before the strong venting from the primary vessel was re-established. The high jet velocities produced a very turbulent jet in the dump volume, which gave rise to Phase 4 of the explosion.

Phase 4 was associated with the burning of the remaining fuel within the primary vessel, which had been compressed by the expanding radial flame, creating elevated temperatures and pressures prior to burning. Consequently the flow rate through the vent increased further, exceeding the volume flow through the vent and creating the maximum burning peak.

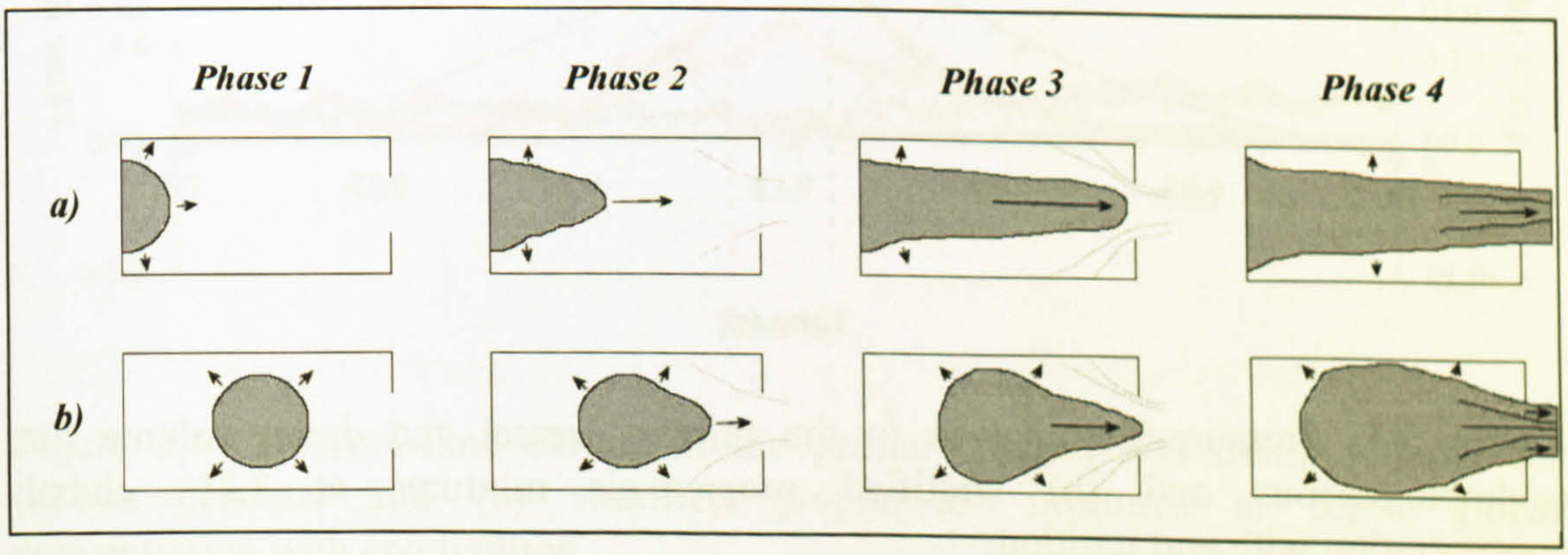

Figure 5-4: Flame development in a vented vessel for (a) end and (b) central ignition.

Similar phases were observed in lean and rich mixtures, shown in Figure 5-5 and Figure 5-6 respectively, albeit with reduced overall severity. It is interesting to note that at lean concentration, the explosion pressure produced for the stratified explosion was slightly higher than the equivalent homogeneous test. This phenomenon is discussed in more detail in Chapter 6, duct vented vessels.

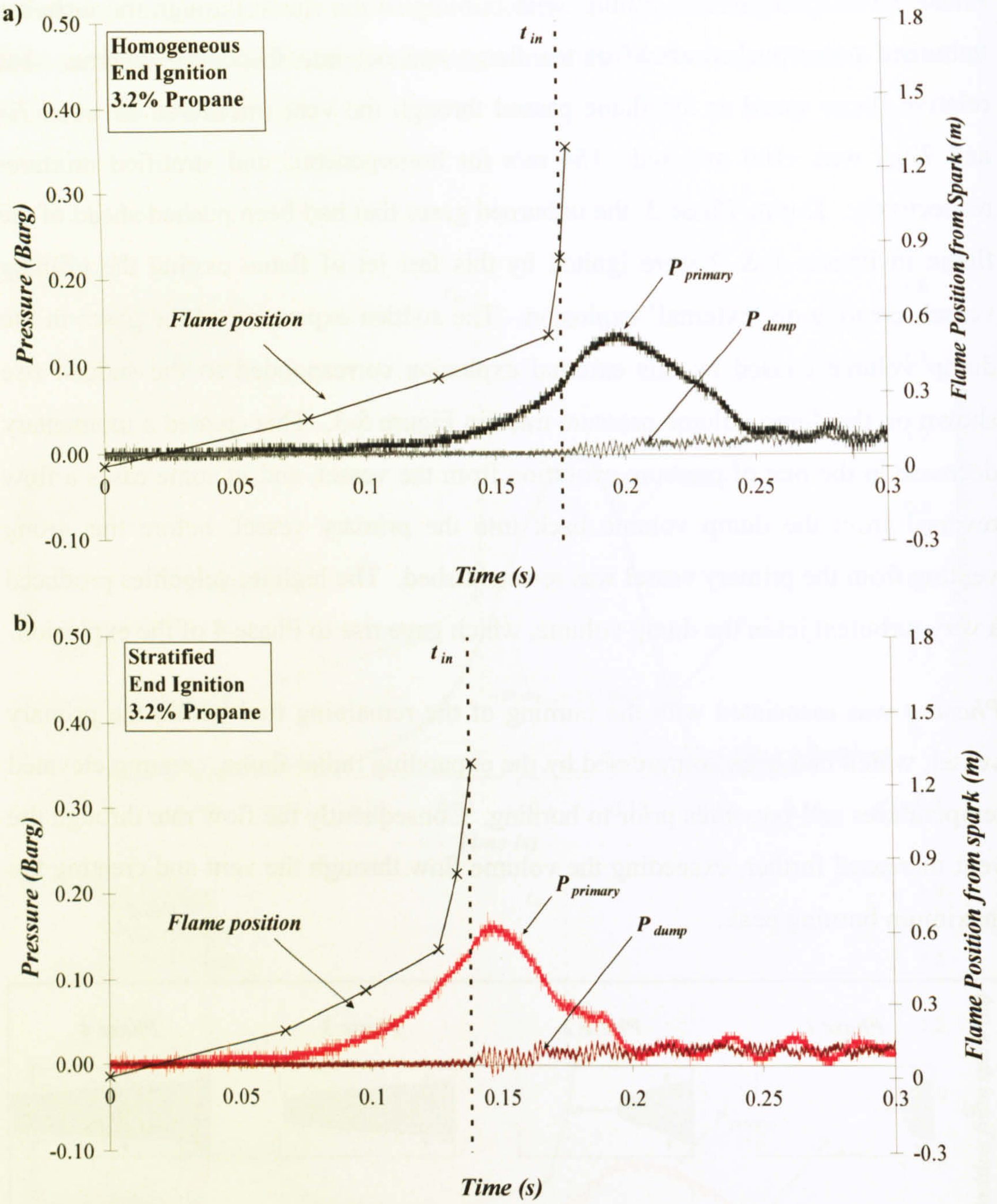

Figure 5-5: Pressure-time curves in the primary vessel and dump volume for (a) homogeneous and (b) stratified propane-air mixtures at 3.2% global concentration with end ignition.

In all cases, as the flame reaches the vent opening and begins to burn through the unburned mixture forced out of the vent. The rapid burning of this unburned mixture causes an external explosion outside the vent opening, which triggers the onset of Helmholtz oscillations. This oscillatory motion causes the flame front within the vessel to be driven in the unstable direction, thus satisfying the Taylor

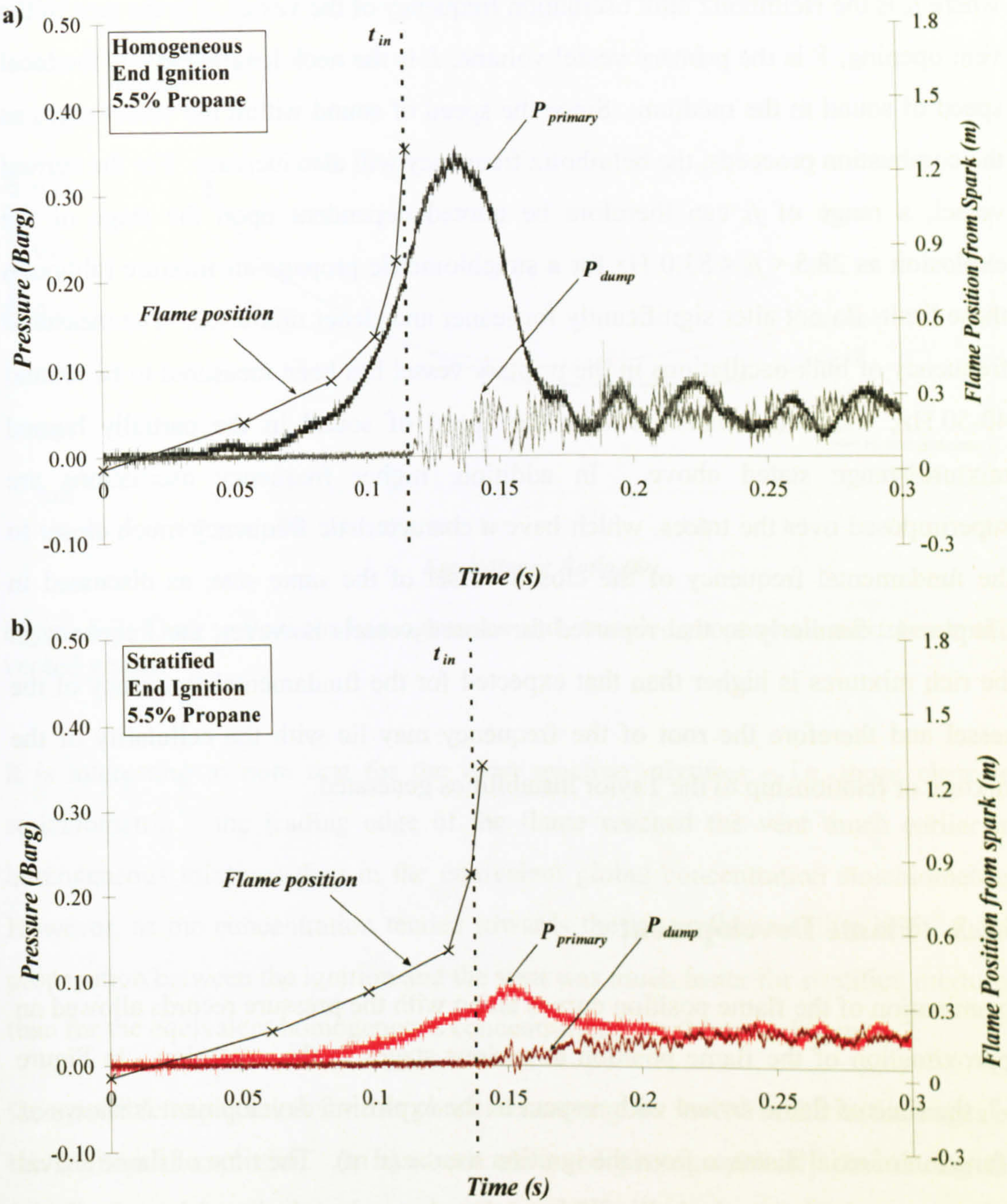

Figure 5-6: Pressure-time curves in the primary vessel and dump volume for (a) homogeneous and (b) stratified propane-air mixtures at 5.5% global concentration with end ignition.

criterion. For a single vessel, fitted with a vent opening, the frequency of Helmholtz bulk oscillations within the vessel can be approximated by [92]:

$$f_h = \frac{c}{2\pi}\left(\frac{A}{VL}\right)^{1/2} \qquad \text{Eq. 5-1}$$

where f_h is the Helmholtz bulk oscillation frequency of the vessel, A is the area of the vent opening, V is the primary vessel volume, L is the neck length and c is the local speed of sound in the medium. Since the speed of sound within the vessel alters as the combustion proceeds, the helmholtz frequency will also increase. For the current vessel, a range of f_h can therefore be quoted dependent upon the stage of the explosion as $28.5 < f_h < 83.0$ Hz for a stoichiometric propane-air mixture (although these limits do not alter significantly for leaner and richer mixtures). The measured frequency of bulk oscillations in the primary vessel has been measured to be around 40-50 Hz, which is consistent with the speed of sound in the partially burned mixture range stated above. In addition, higher frequency oscillations are superimposed over the traces, which have a characteristic frequency much closer to the fundamental frequency of the closed vessel of the same size, as discussed in Chapter 4. Similarly to that reported for closed vessels however, the frequency in the rich mixtures is higher than that expected for the fundamental frequency of the vessel and therefore the root of the frequency may lie with the cellularity of the mixture or relationship to the Taylor instabilities generated.

5.2.3. Flame Development

Examination of the flame position curves along with the pressure records allowed an approximation of the flame position at various stages in the explosion. In Figure 5-3, the time of flame arrival with respect to the explosion development is shown as a function of axial distance from the ignition source (x m). The time of flame arrival at the vent, t_{in} is also marked. Similarly to closed vessel explosions where the flame initially elongates along a cylindrical vessel from the ignition at the end wall, in vented explosions the direction of flame growth was also preferentially in the axial direction, as the unburned gas flow behind the flame front was effectively skewed towards the vent opening by the entrainment of the unburned gas flow field. The more reactive the mixture, the faster this elongation mechanism occurred in the current work, with a maximum observed at around 4.5%. Indeed, this flame elongation towards the vent after the initial phase of the explosion is a well known phenomenon which has been observed by several authors for homogeneous explosions in vented enclosures [8, 42, 43, 126].

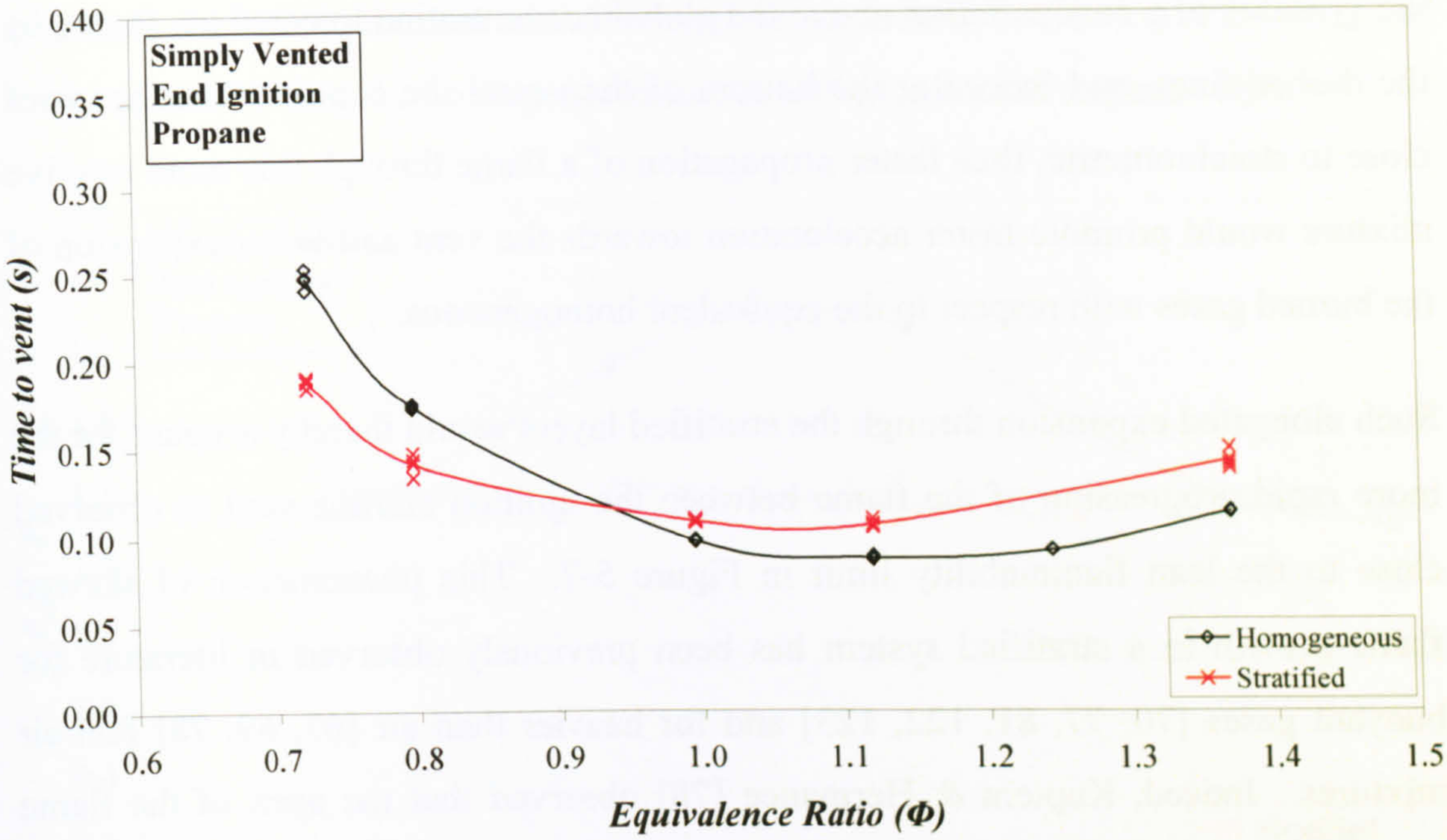

Figure 5-7: Time to vent for homogeneous and stratified propane-air mixtures in the vented vessel.

It is interesting to note that for the most reactive mixtures – i.e. those close to stoichiometric – the leading edge of the flame reached the vent much earlier in homogeneous mixtures than in the equivalent global concentration stoichiometric. However, as the concentration tended towards the lower flammability limit, flame propagation between the ignition and the vent was much faster for stratified mixtures than for the equivalent homogeneous concentrations, as shown in Figure 5-7.

One possible explanation for this phenomenon may be rooted in the initial stages of the individual explosion. It has been observed photographically that during the initial stages of a homogeneous explosion, flame propagation is approximately spherical – or hemispherical in the case of ignition against the surface of a vessel – prior to the unburned gas flow-field taking effect on the leading edge of the flame and skewing growth in the direction of the vent [43]. In less reactive mixtures – i.e. those approaching the flammability limits – this initial spherical growth phase will be longer due to the slower expansion of gases and expulsion of the unburned gases through the vent. Conversely, in stratified mixtures, the inherently layered nature of the mixture may well facilitate earlier elongation of the flame front along a more reactive path. For example, based on the average concentration gradients provided in Figure 5-2, for a 2.9% global concentration, below $h/D = 0.31$ all of the mixture in

the vessel is of a concentration above the global concentration injected (as shown by the dashed line), and indeed at the bottom of the vessel the concentration becomes close to stoichiometric, thus faster propagation of a flame through this more reactive mixture would promote faster acceleration towards the vent and faster expansion of the burned gases with respect to the equivalent homogeneous.

Such elongated expansion through the stratified layers would thereby account for the more rapid progression of the flame between the ignition and the vent as observed close to the lean flammability limit in Figure 5-7. This phenomenon of skewed flame growth in a stratified system has been previously observed in literature for buoyant gases [70, 77, 81, 122, 123] and for heavier than air [67, 69, 78] fuel-air mixtures. Indeed, Kaptein & Hermance [78] observed that the apex of the flame through a stratified mixture was coincident with the Φ=1.08 concentration line for n-hexane, n-heptane and benzene.

Whilst concentrations towards the UFL were not included in the current test-programme, based on Figure 5-7, it is likely that a similar trend will be repeated for rich mixtures.

5.2.4. Maximum Recorded Pressure and Rates of Pressure Rise

Figure 5-8 illustrates the maximum reduced pressure, P_{red}, recorded in the primary vessel under ambient initial conditions for both homogeneous and stratified tests, in the range 2.9-6.5% (Φ = 0.71-1.655) and 2.9-5.5% (Φ = 0.71-1.35) for homogeneous and stratified tests respectively. Values have been normalised against ambient pressure, P_i, to enable meaningful comparison with other test series.

It is clear from Figure 5-8 that homogeneous constituted the most severe explosion hazard. The maximum occurred to the rich side of stoichiometric, with an average maximum P_{red} of 1.7 barg. Conversely, the maximum average P_{red} for stratified mixtures was below 1.2 barg, occurring just below stoichiometric. In both cases, the pressures recorded were well below the adiabatic pressures expected for propane-air mixtures in a closed volume of the same geometry, and also below actual pressures

measured for the equivalent closed vessel as described in Section 4.2.4 (P_{max} of 7.4 barg and 7.1 barg for homogeneous and stratified mixtures respectively).

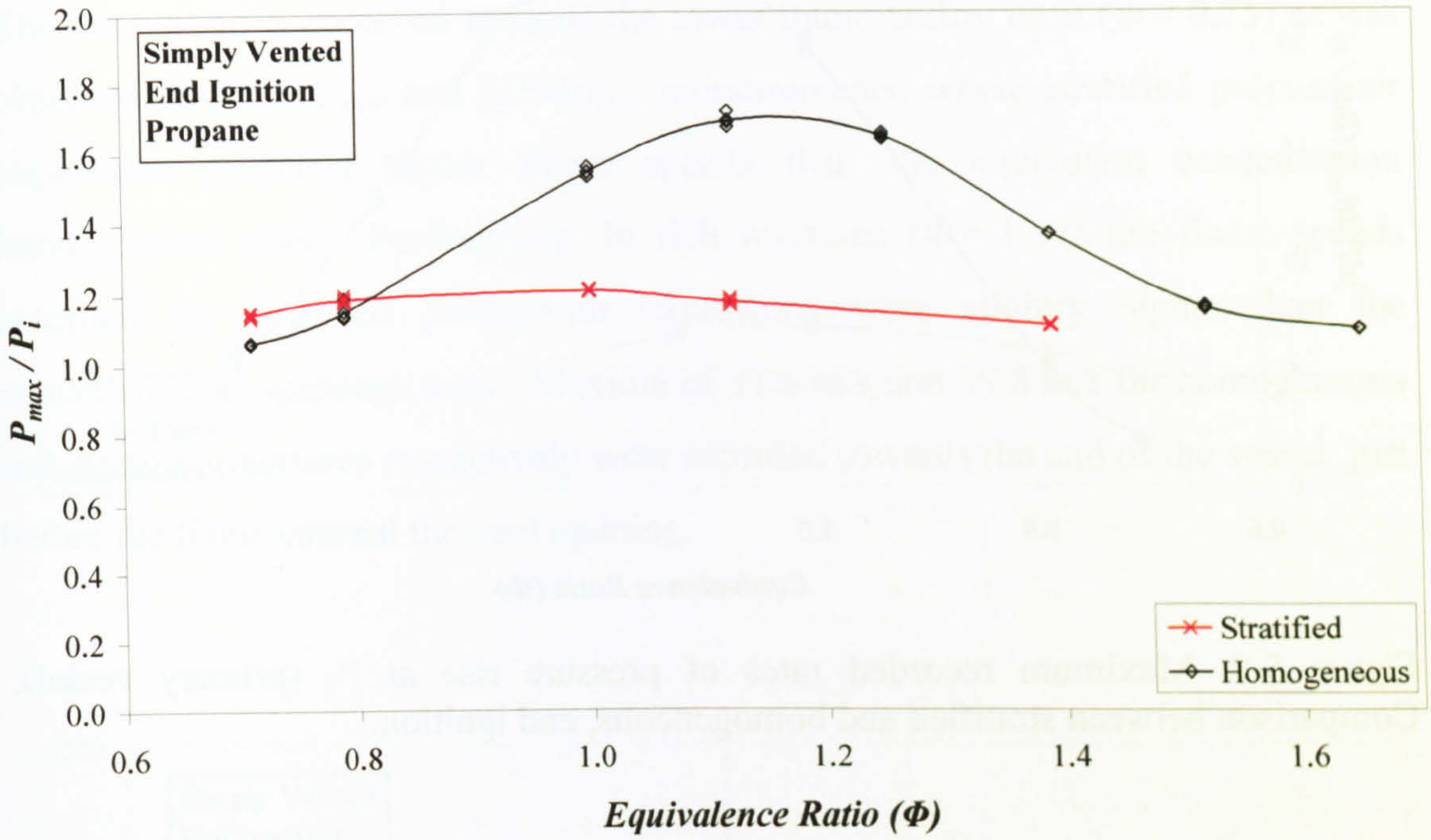

Figure 5-8: Normalised maximum reduced pressure, comparison between stratified and homogeneous test results, end ignition.

It is important to note from Figure 5-8 that at lean concentrations – in the current work 2.9-3.2% ($\Phi = 0.71$-0.79) – stratified mixtures once again proved to be the more severe condition in terms of P_{red}. The trend is echoed in the measurements of maximum reduced rates of pressure rise, $(dP/dt)_{max}$.

Figure 5-9 displays the maximum recorded rate of pressure rise in the primary vessel relating to the main burning peak. At lean concentration, once again, stratified mixtures exhibit a more severe explosion than the equivalent global homogeneous concentration. Above 3.2% ($\Phi = 0.79$), homogeneous mixtures quickly become the more severe condition, consistent with the maximum pressures recorded. Maximum average $(dP/dt)_{max}$ was 24.9 bar/s for homogeneous, occurring at around 4.5%, and 7.2 bar/s for stratified, occurring at around 4.0%. In all cases, end ignition tests exhibited relatively low oscillatory combustion; therefore there was good agreement in maxima between tests.

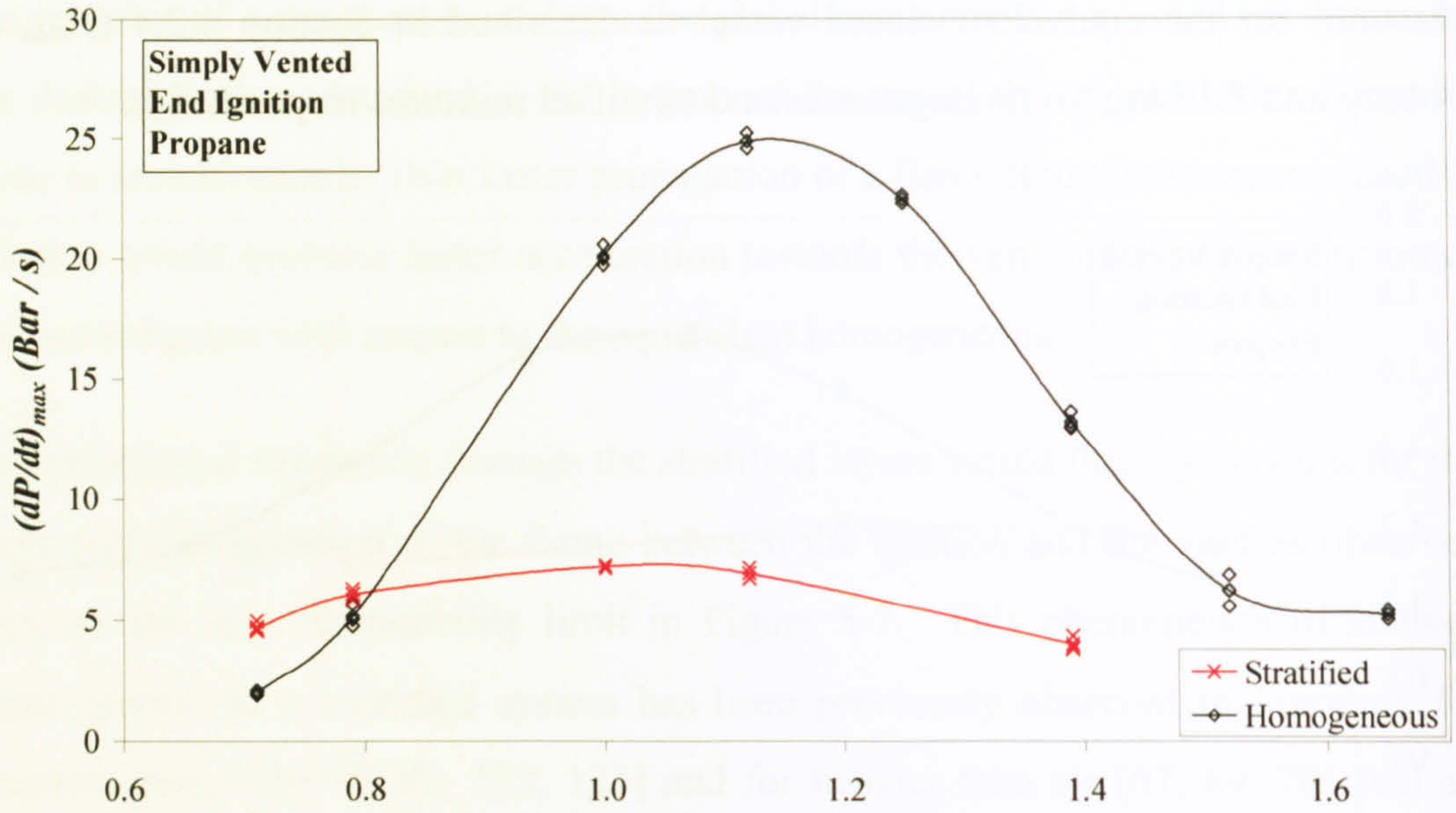

Figure 5-9: Maximum recorded rates of pressure rise at P_1 (primary vessel). Comparison between stratified and homogeneous, end ignition.

The unusual behaviour of stratified tests posing the worst case scenario for both P_{red} and $(dP/dt)_{max}$ is significant in terms of explosion calculation, where existing methods of prediction, based on homogeneous models, are used post-event to calculate the amount of fuel released; i.e. where a certain level of damage is equated to a specific overpressure and fuel volume. If a stratified mixture can produce an explosion severity greater that expected for homogeneous mixtures, then such prediction models may overestimate the amount of fuel in relation to the damage observed.

5.2.5. Maximum Recorded Flame Speeds

Flame speeds were recorded using the fixed position thermocouples located along the centre line of the primary vessel, including in some tests a thermocouple placed at the vent exit, marked as Tc_{12} in Figure 5-1. Figure 5-10 shows the maximum flame speed recorded between the last two thermocouples in the primary vessel (solid lines) and the average flame speed observed as the flame passed through the vent (dashed lines). In each case, the maximum was recorded to the rich side of

stoichiometric. This corresponds with the concentration at which the maximum pressure and rate of pressure rise were recorded, at $\Phi = 1.12$.

The same trend is observed towards the lower flammability limit ($\Phi < 0.75$) as was observed with the P_{max} and $(dP/dt)_{max}$ measurements, where stratified propane-air explosions produced higher flame speeds than the equivalent concentration homogeneous tests. Furthermore, in rich mixtures ($\Phi = 1.37$) the flame speeds recorded for stratified propane-air explosions were slightly higher than the equivalent homogeneous tests. Maxima of 31.8 m/s and 39.8 m/s for homogeneous and stratified mixtures respectively were recorded towards the end of the vessel, just before the flame entered the vent opening.

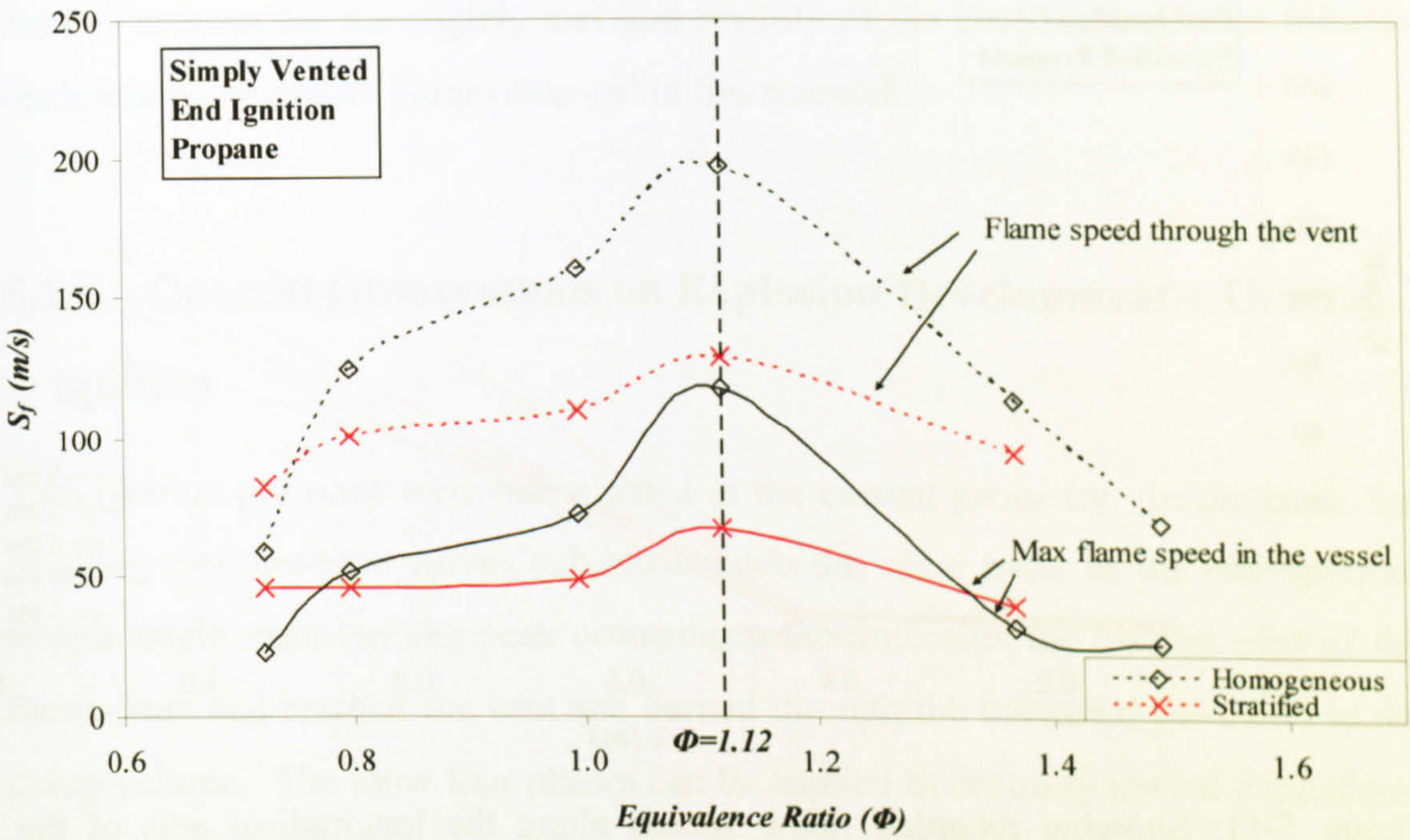

Figure 5-10: Maximum recorded flame speeds observed at the end of the primary vessel (solid lines) and through the vent (dashed lines) for homogeneous and stratified propane-air mixtures, end ignition.

Figure 5-11 illustrates the average flame speeds recorded between consecutive thermocouples through the primary vessel and into the vent for (a) homogeneous and (b) stratified propane-air mixtures. The line marked x_{in} in each figure denotes the position of the vent opening.

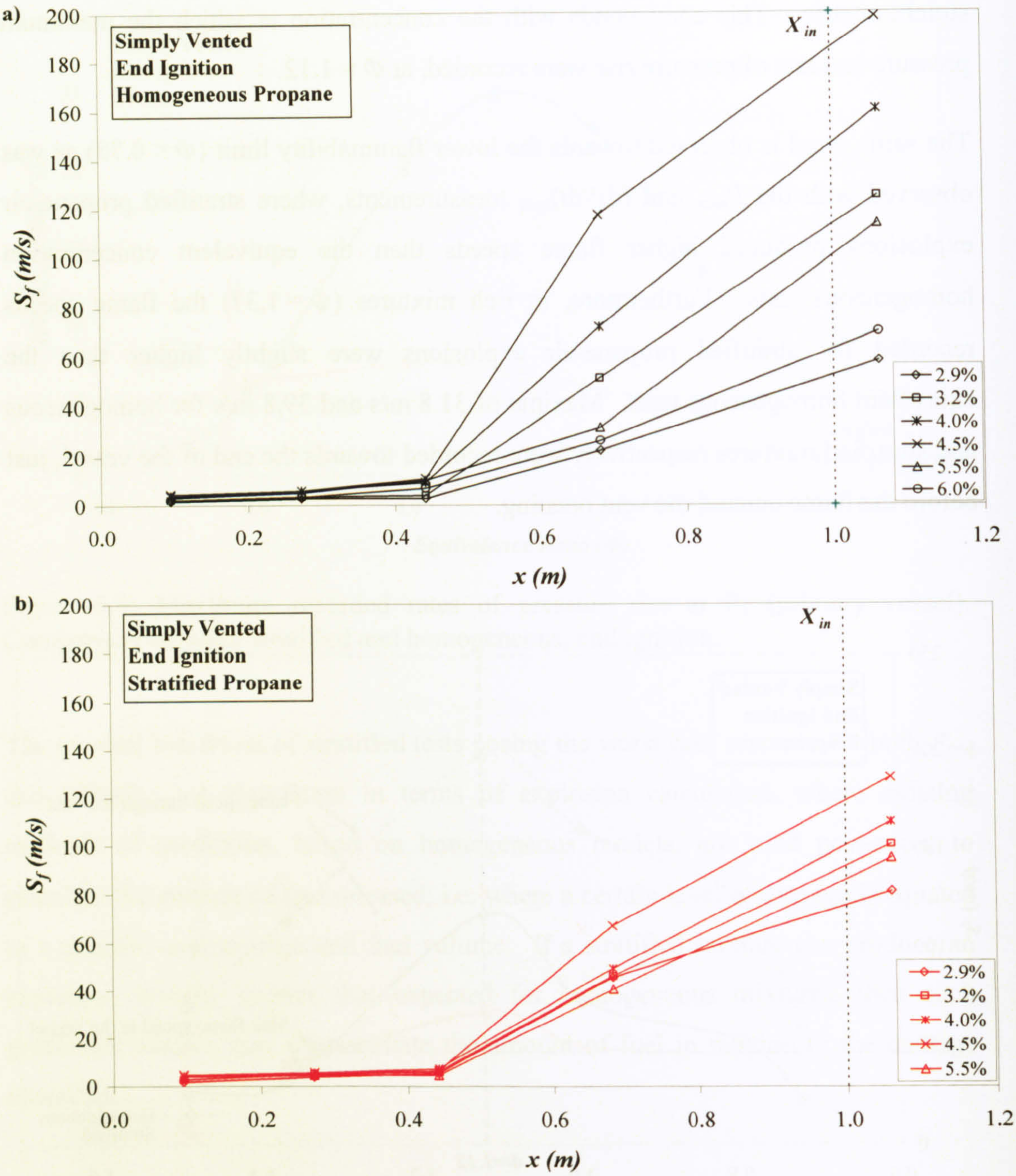

Figure 5-11: Showing recorded flame speeds along the longitudinal axis of the vessel and into the vent for (a) 2.9-6.0% homogeneous and (b) 2.9-5.5% stratified, end ignition.

In the early stages of the explosion the flame speed was low. This corresponded to Phase 1 of the explosion, where the flame growth was roughly spherical away from the ignition position. As the flow mechanism towards the vent begins to take effect in Phase 2, the flame speeds showed a slight increase, which lasted up until the point at which the flame reached roughly half way along the vessel. For all concentrations, as the flame passed into the second half of the vessel the flow began

to accelerate rapidly due to the flow of unburned gases out through the vent opening, which served to draw the flame front in the axial direction towards the vent. As the flame approached and passed through the vent, the flame speed increased further to produce the high maxima shown in Figure 5-10 and Figure 5-11.

As the flame was drawn more quickly towards the vent in more reactive mixtures, there was an increased amount of fuel that would have remained within the vessel, compressed towards the cylindrical vessel walls, which would have contributed to the main peak pressure once the flame had left the vessel. While this mechanism is also true to a certain extent in stratified mixtures, if the air lean and air rich portions of the unburned mixture were pushed/pulled through the vent differentially, the resulting mixture inside the vessel that would contribute to the main pressure peak could then be more reactive than the global concentration would suggest, and thereby account for the slightly elevated severity of the stratified mixtures towards the lower flammability limits observed in this research.

5.2.6. General Observations on Explosion Development – Central Ignition

Two ignition positions were investigated in the current geometry. In the main, the resulting pressure-time curves exhibited much the same trend as the end ignition, with a single main burning peak occurring some time after the leading edge of the flame front had reached the vent and burned through the unburned gas cloud in the dump volume. The same four phases can be applied to centrally ignited explosions. However, for rich mixtures, the pressure trace exhibited a slightly different behaviour.

In the work of Cooper *et al* [43] there was a total of 4 pressure peaks for ignition at the centre of a near cubic enclosure with low venting pressure. The peaks related to vent displacement, external combustion of the unburned mixture, flame interaction with the vessel geometry and interaction with pressure oscillations. The peaks described corresponded closely to the four explosion phases set out in Section 5.2.2 above, and have been marked where applicable on the graphs presented in this

section. It was argued that the presence of each individual peak was largely dependent upon the initial conditions within the vessel. *Peak 1*, which was related to the displacement of the vent cover, they argue could also be present to some degree, even where the vent was initially open, i.e. $P_{stat} = 0$.

Peak 2 was formed during Phase 2, as the flame surface area continued to grow until the net rate of volume production exceeded the rate at which the unburned gas could be vented out, thereby increasing the overall pressure in the vessel. The flame surface was also taking on an irregular small scale cellular structure, which is attributed to selective diffusion and hydrodynamic instability mechanisms [43]. As the flame reached the vent and ignited the external unburned gas, this caused a sharp increase in vessel internal pressure as the external explosion prevented effective volumetric flow out through the vent. Peak 2 was therefore governed by one of two mechanisms; either the vent size, or the stage of combustion when the flame reaches the vent. If the combustion within the vessel was at an early stage, this gave rise to a low burning rate in the vessel, and higher rates of pressure rise outside the vent, therefore the pressure wave generated externally would be able to propagate back into the vessel, halting or hindering volume outflow from the vessel. This peak is reportedly the most important in explosions involving low vent failure pressures or mixtures with high burning velocities. As the external explosion subsides and the venting process allows outflow from the vessel to be dominant once more, the pressure within the vessel begins to drop, forming the peak. The magnitude of this peak has been found to increase with the burning velocity of the unburned mixture within the vessel [43].

Peak 3 corresponded to Phase 3, where the onset of the burned gas venting from the vessel coincides with the onset of Helmholtz oscillations, which is where the pocket of burned gas within the vessel undergoes bulk motion towards and away from the vent opening. The third peak was therefore a predominantly oscillatory peak which was eventually dampened down as the flame expanded and reached the vessel walls. The interaction of the flame surface with the geometry decreases the rate of production of burned gases due to a sudden reduction in flame surface area. The burning rates during this phase are enhanced by the turbulence generated between the burned gases flowing out through the vent, and the unburned gases remaining in

the vessel. Taylor instabilities are believed to be triggered by Helmholtz oscillations, as the density interface between the gases is accelerated in the direction of the higher density medium. In which case, this peak would be expected to occur preferentially in central ignition over end ignition.

Finally, *Peak 4*, was a high frequency oscillation pressure peak. Sustained pressure oscillations are set up by the interaction between the pressure waves generated by the combustion processes and the acoustic properties of the vessel (thereby satisfying the Rayleigh criterion). Cooper *et al* [43] suggest that this oscillatory fourth peak is associated with burning into isolated pockets of gas, located in the corners of the vessel. They further argue that this final peak most readily occurs in fuel rich mixtures for methane, propane and ethylene, with the maxima recorded well to the rich side of stoichiometric. This is consistent with the findings of other authors [46, 49]. The presence of such high frequency oscillations towards the end of the venting process has been observed by several research works [39, 42, 44], which state that such oscillatory behaviour was the result of the coupling of the combustion instabilities with the resonant acoustic modes of the vessel, which tended to be superimposed over the main pressure peaks. Similarly, it has been suggested that the presence of additional explosion peaks which occurred at a time long after the main burning peak, occurs as the result of the interaction between the combustion of the remaining unburned mixture within the vessel, and the acoustic pressure waves generated by fluctuations in the heat release rate [23].

According to the criteria set out above, the current work should display no significant pressure peak associated with Phase 1, since no vent burst pressure is involved. Instead, the most important peak was Peak 2, with the possibility of Peaks 3 and 4 occurring dependent upon the initial conditions.

Figure 5-12 shows a typical pressure-time curve for centrally ignited, homogeneous, propane-air mixtures at 4.5%. Two distinct peaks of similar magnitude were apparent on the pressure trace, corresponding to Peaks 2 and 4 as described above, with the second exhibiting much a more oscillatory combustion mode than the first. Such a double peak phenomenon was not observed in the same vessel with end

ignition, but has been noted by previous works dealing with vented centrally ignited explosions [39, 43].

The flame position curve marked in Figure 5-12 gives an indication of the position of the expanding flame front with respect to the pressure evolution within the vessel. From the central ignition (at $x = 0.5$ m), the flame initially developed spherically, unimpeded by the specifics of the geometry. However, the flame was quickly drawn towards the vent by the flow field created by the venting of unburned gases through the vent. This, as expected, occurred marginally more quickly than in the equivalent end ignition tests, as a simple result of the ignition position being closer to the vent. As the unburned gas flow field initiated, the flame then travelled more rapidly towards the vent (towards $x = 1$ in Figure 5-12) and much more slowly towards the closed end of the vessel (towards $x = 0$ in Figure 5-12). The flame was recorded as reaching the vent (t_{in}) at 57.7 ms, some 40.6 ms prior to the flame being recorded as approaching the closed end of the vessel, at Tc_1. This is consistent with previous research on vented geometries which discuss this flame skewing phenomenon.

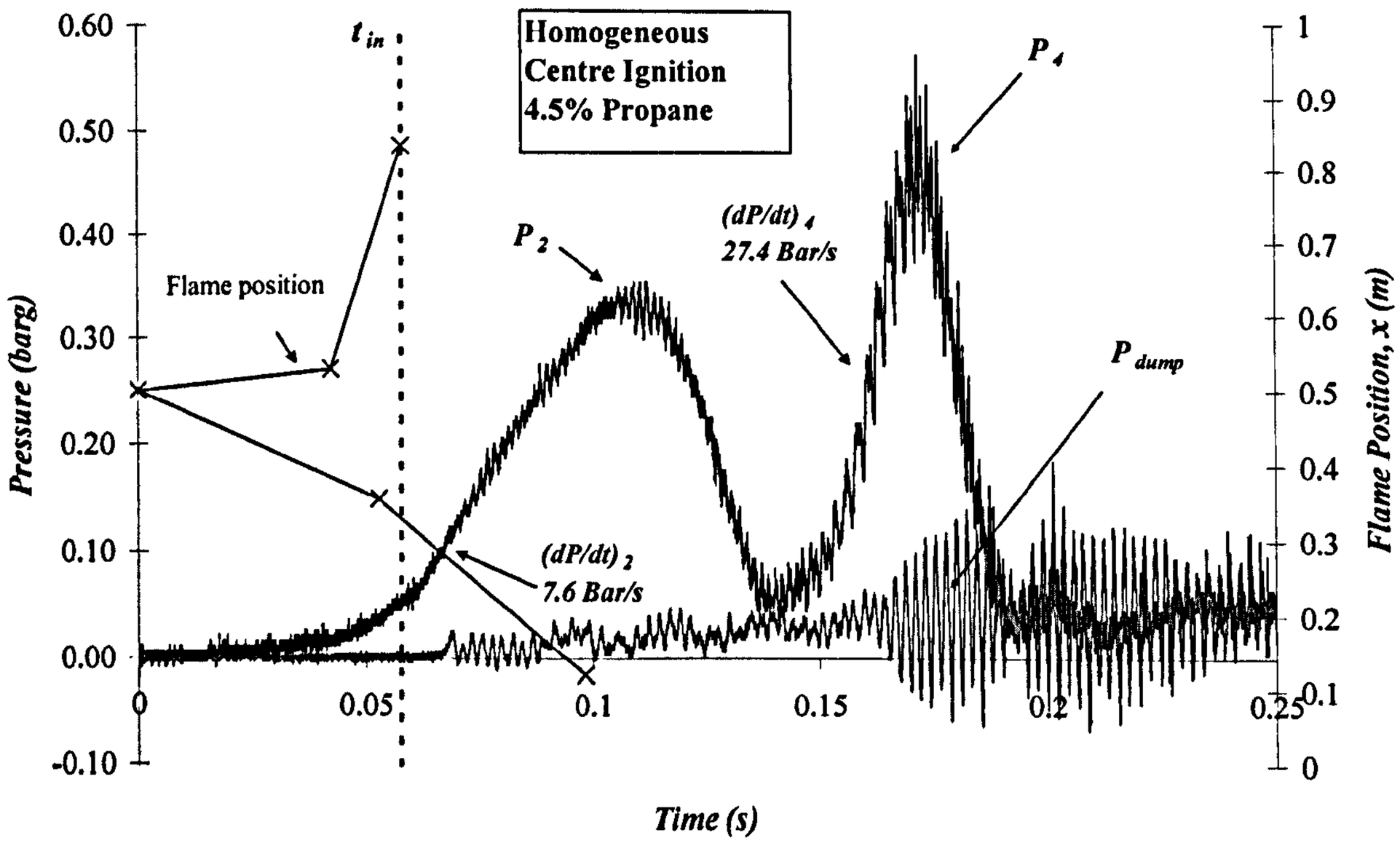

Figure 5-12: Pressure-time curve for 4.5% Propane-air mixtures, central ignition.

The first peak, marked P_2 in Figure 5-12, was reached after the flame had already exited the vent at a time, $t_2 = 107.5$ ms, which was slightly faster than that recorded

for the main pressure peak at the same concentration with end ignition, $t = 111$ ms. In several rich propane-air mixtures with central ignition, a second peak P_4, then occurred. In Figure 5-12, this second peak occurred at a time, $t_4 = 171.8$ ms. There appeared to be no correlation between the time interval between the two peaks and the global concentration injected. In all cases, the second peak occurred at a much later stage in the explosion than the first peak, and in any case a considerable time after the flame had left the vent and the main pressure peak had occurred. Furthermore, this second peak generally exhibited a more oscillatory pattern than the first peak. It is accepted that a propagating flame will rarely form a perfect uniform advancing flame, due to the wrinkled cellular structure of the flame which initiates very soon after ignition, and therefore some oscillations are always present superimposed over the pressure signal. However, the oscillations present on the second peak exhibited a much higher frequency oscillation, and a much higher frequency than is expected of any Helmholtz bulk oscillations. In physical terms, where present, this second peak manifested as a high pitch 'screech' after the main explosion event, which is consistent with some previous research denoting the same phenomenon [39].

It appears, therefore, that the two peaks were most akin to Peaks 2 and 4 as described above, with Peaks 1 & 3 being absent or barely detectable. Indeed, several authors make reference to the presence of multiple pressure peaks on centrally ignited, vented explosions, where a main burning peak followed by a subsequent acoustic peak has been observed [23, 39, 42-44].

Whilst it was the case that for most tests throughout this test series, either Peak 2 alone or Peaks 2 & 4 were observed, in a small number of tests, an oscillatory peak, similar to that described as Peak 3 was obtained. Figure 5-13 illustrates one such occurrence, where a small peak, P_1, possibly similar to that discussed by Cooper *et al* [43], at $P_{stat} = 0$, Peak 1 could be seen, in addition to Peaks 2 & 3 for stoichiometric propane-air. Peak 3 was then quickly dampened by the interaction of the flame with the confining geometry, and did not lead to a subsequent high frequency oscillatory peak corresponding to Peak 4. In general, the double peak phenomenon observed throughout this test-programme for central ignition either incorporated Peaks 2 & 3 or Peaks 2 & 4, but not both Peaks 3 & 4 together.

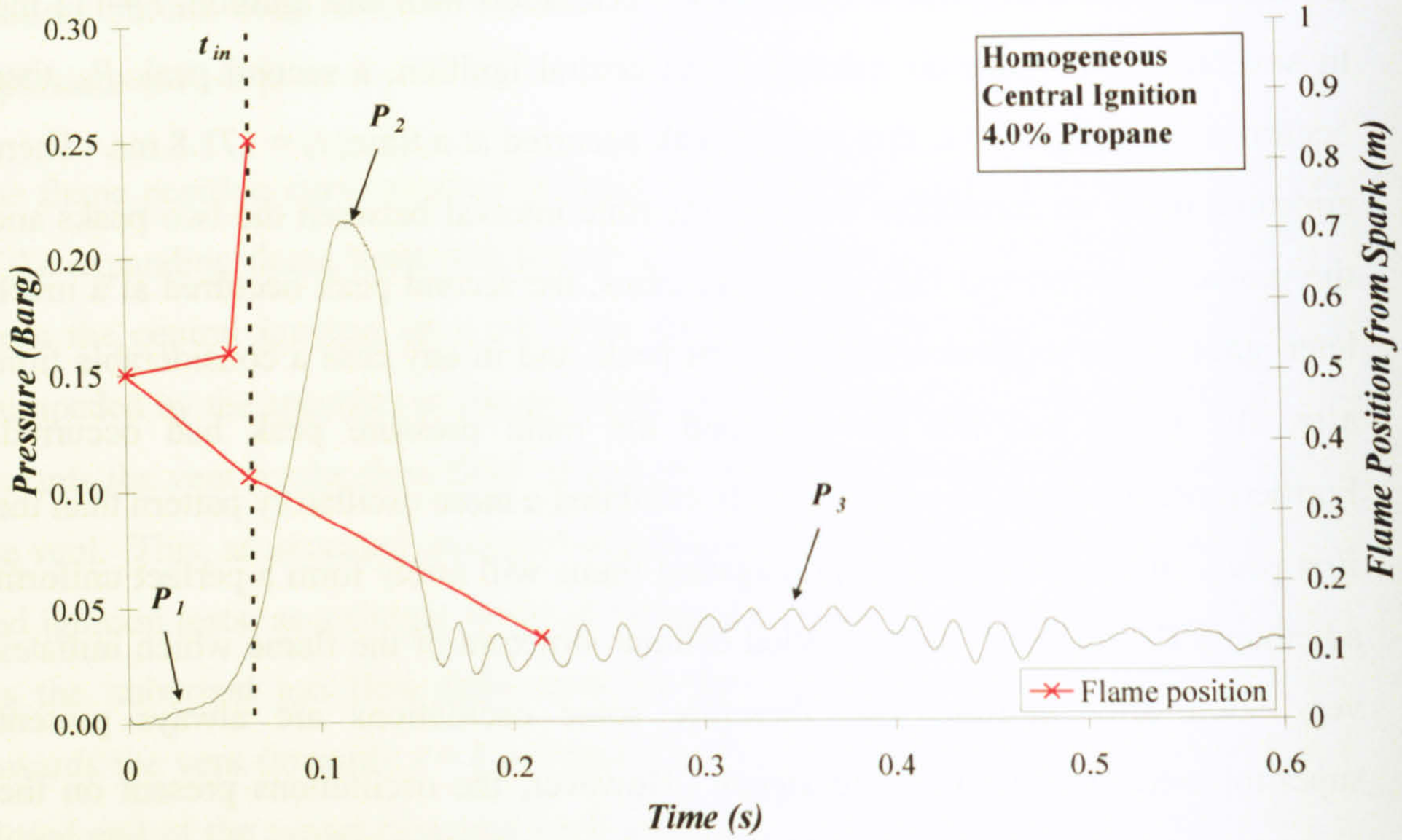

Figure 5-13: Pressure-time curve for 4.0% propane-air mixture, central ignition.

5.2.7. Influence of Ignition Position on Maximum Recorded Pressure and Rates of Pressure Rise

As previously discussed, ignition position has some influence on the explosion development within the given geometry, and as a consequence effects the overall severity of the explosion. In this section, a comparison is made between maximum pressures and rates of pressure rise obtained for the same conditions using end and central ignition, along with a brief discussion of the results obtained.

Figure 5-14 shows the maximum recorded values of P_{red} for homogeneous propane-air mixtures in the range 2.9-6.5% (Φ = 0.71-1.65) for end and central ignition. It is clear from Figure 5-14 that at stoichiometric concentrations, end ignition provided the most severe explosion pressures, with an average maximum P_{red} of around 1.7 barg as opposed to an average of around 1.35 barg for central ignition. However, at richer concentrations, the presence of the second (acoustic) peak on centrally ignited tests, resulted in higher pressures being recorded than for the equivalent end ignition tests. The greatest degree of scatter was observed for 6.0% (Φ = 1.49),

where maximum pressures between 1.04 barg and 2.14 barg were recorded, although some degree of scatter was observed at all concentrations above stoichiometric, corresponding to the measurement of pressure at this oscillatory peak.

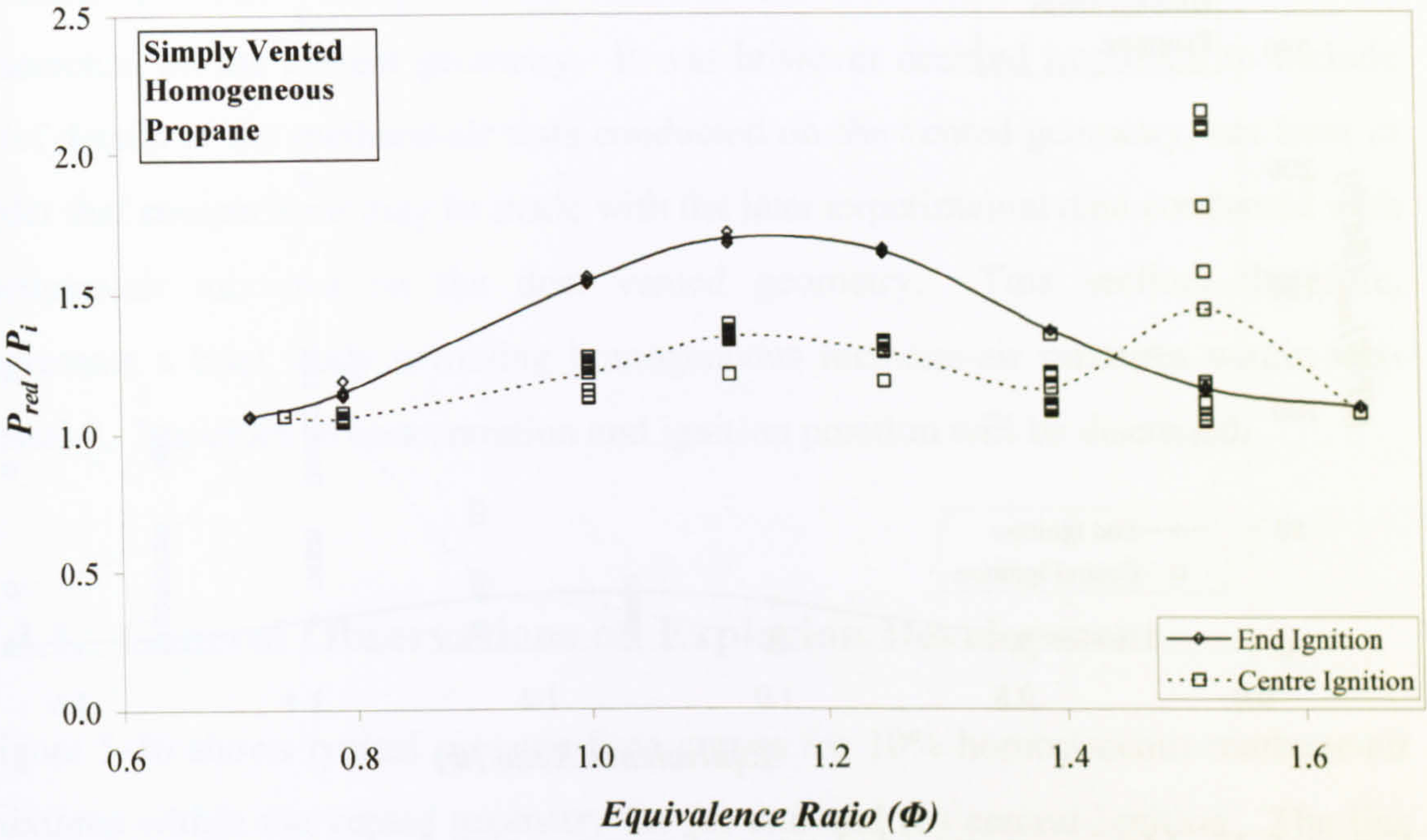

Figure 5-14: Maximum reduced pressure, for simply vented homogeneous propane-air mixtures, comparison between end and central ignition.

Figure 5-15 displays the maximum recorded rates of pressure rise obtained in the primary vessel. The degree of scatter observed on the pressure traces for central ignition was even greater in measurements taken of rates of pressure rise, as shown in Figure 5-15, with a maximum average of around 100 bar/s being observed for 5.5% ($\Phi = 1.37$), with actual readings between 30 and 270 bar/s being recorded. The $(dP/dt)_{max}$ values recorded were those of the smoothed pressure curve and not the individual oscillations, which in fact would be higher. The uncharacteristically high values of $(dP/dt)_{max}$ at rich concentrations can be attributed to the flame instabilities and oscillatory combustion occurring on the rich side of stoichiometric for propane-air mixtures. This effect may well be exacerbated or linked to the spontaneous cellularity of rich propane-air mixtures. However, in all cases, end ignition tests exhibited relatively low oscillatory combustion modes; even at rich concentration, resulting in a much better agreement between recorded maxima. This suggests that the acoustic interactions which cause such high oscillations on the centrally ignited

tests are not as readily imposed upon the end ignition tests, which provides a more stable combustion mode.

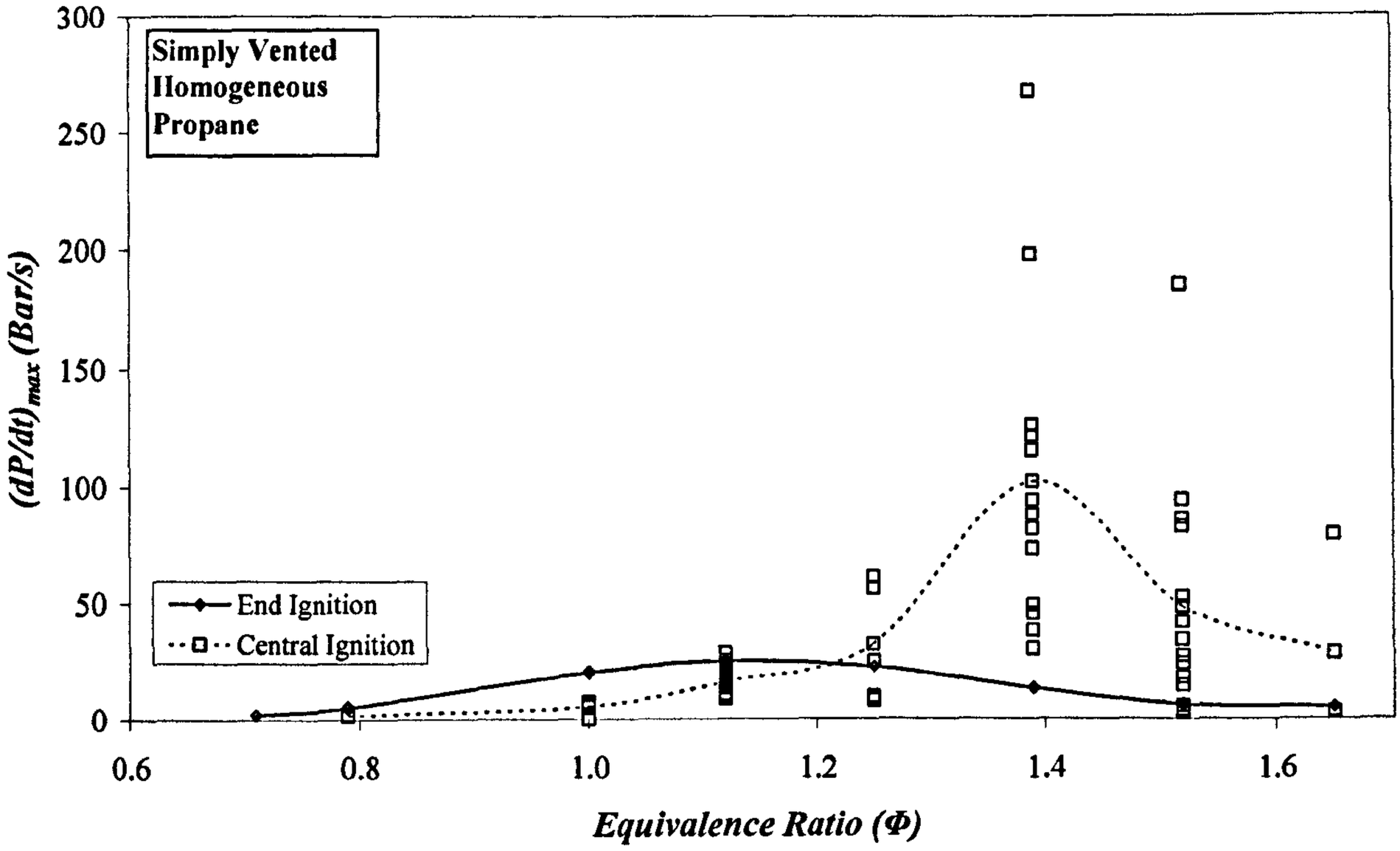

Figure 5-15: Maximum recorded rates of pressure rise for homogeneous propane, simply vented, comparison between end and central ignition.

As discussed in Chapter 4, the presence of oscillatory combustion on the pressure waves, particularly prevalent in the centrally ignited tests, is important where structural response is concerned. Indeed, as discussed in Chapter 2, when a vent is added to a chamber, there is always a finite distance between the vent and, in this case, the dump volume, which could affect the significance of any external explosion in the internal pressure, especially at low venting pressures, such as stratified mixtures or homogeneous mixtures approaching the flammability limits. Such oscillatory combustion can result in a reduction in the effectiveness of the venting [30], and therefore cause higher peak pressures and rates of pressure rise which may not have been fully accounted for in vessel design calculations.

5.3. Experimental Results (Methane)

In this section, tests are presented using homogeneous methane-air mixtures with central ignition, and using the homogeneous propane-air end ignited tests discussed

above for comparison. As previously noted, it was the intention to present both homogeneous and stratified methane-air test results in this section. However, due to time constraints and the fact that a reliable stratification technique for methane-air mixtures had not been perfected, stratified mixtures have regrettably not been researched on the current geometry. It was however deemed important to include brief details of the methane-air tests conducted on the vented geometry, not least in order that comparisons may be made with the later experimental data conducted with methane-air mixtures on the duct vented geometry. This section, therefore, represents a brief study involving homogeneous methane-air mixtures within test-vessel 2. Variables of concentration and ignition position will be discussed.

5.3.1. General Observations on Explosion Development

Figure 5-16 shows typical pressure-time curves for 10% homogeneous methane-air mixtures within the vented geometry for (a) end and (b) central ignition. The line marked t_{in} denotes the time from ignition at which the flame entered the vent, approximated from the time at which the flame passed the last thermocouple in the vessel. In the methane test series, the results gained from the thermocouple at the vent exit (Tc_{12}), were not reliable and therefore have been omitted.

For both end and central ignition, a single main burning peak was evident. The test series comprised a total of 37 tests, in which only 2 tests exhibited a second peak. Both occurrences manifested at 10% methane-air, with central ignition, which is to the rich side of stoichiometric, contrary to that reported in literature [30, 43].

For end ignition, at 10% methane-air, the flame took approximately 107 ms to reach the vent, at an average speed of 9.35 m/s and approximately 70 ms to reach the vent from the central ignition, at an average speed of 7.14 m/s. The faster flame speeds recorded in the end ignited tests is a direct result of the increased distance between the ignition position and the vent, which gave a longer distance for the flame to accelerate, facilitated by the expanding region of burned gas behind it and the unburned gas flow through the vent skewing the flame in the axial direction towards the vent.

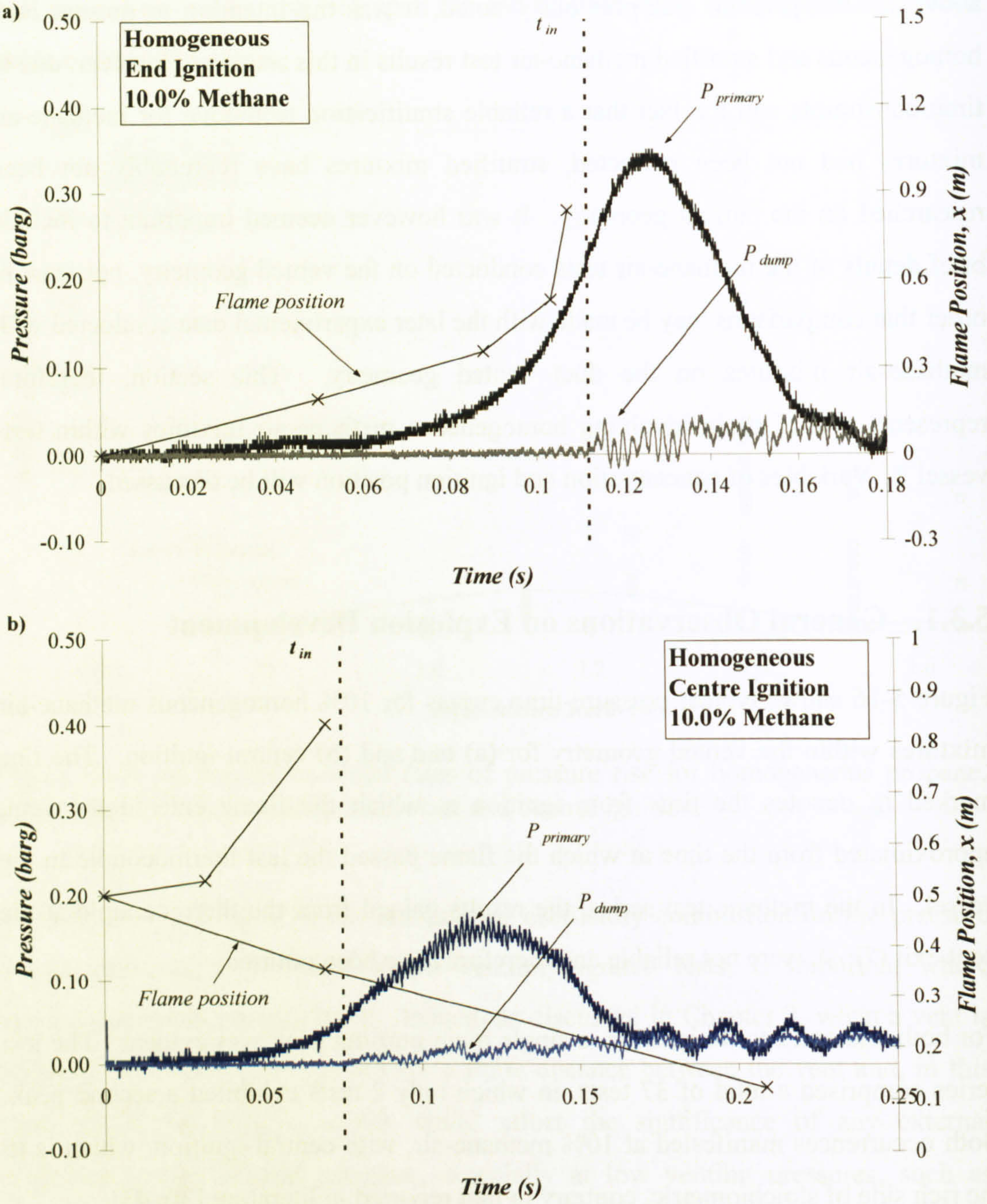

Figure 5-16: - Pressure-time curves in the primary vessel and dump volume for (a) end and (b) central ignition, 10% methane-air mixtures for simply vented vessel.

The additional distance in the end ignition tests allows a longer time between ignition and flame exit through the vent, during which unburned gases are being vented into the dump volume. The greater volume of unburned gases in the dump volume would then lead to a more powerful external explosion which would impede the volume outflow of burned gas from the vessel, thereby generating large pressure rises in the primary vessel.

The development of a methane-air explosion is similar to that presented in the previous section for propane-air mixtures, albeit with less severity and less susceptibility to acoustic interaction. The lower reactivity of methane-air mixtures with respect to propane-air mixtures will account for this reduction.

5.3.2. Maximum Recorded Pressure and Rates of Pressure Rise

Figure 5-17 displays the maximum pressure and rates of pressure rise recorded in the primary vessel for methane-air explosions with end and central ignition. The results indicate that while there is only a small difference between average maximum pressures attained using end and central ignition, 1.32 barg to 1.17 barg for end and central ignition respectively, there is a much more pronounced difference in rates of pressure rise. Values of 13.8 bar/s and 5.4 bar/s for end and central ignition respectively were recorded for maximum rate of pressure rise. It should be noted, however, that while this appears to constitute a large difference, in fact in comparison to the results obtained in the previous test series for propane-air explosions, both maximum pressures and rates of pressure rise are significantly reduced.

The trend shows that end ignition consistently produces the worst overall explosion in terms of both dP/dt and P_{red}, with the exception of 13.6% ($\Phi = 1.44$) where the pressure recorded for central ignition is slightly higher. It has been stated in literature that rich mixtures of methane-air mixtures are susceptible to the coupling of the combustion instabilities with the resonant acoustic mode of the vessel, despite not being susceptible to spontaneous cellularity at rich concentrations. In this regard, despite the lack of a second acoustic peak, the amplitude of the oscillations superimposed over the pressure trace in rich central ignition, methane-air mixtures was greater than that for lean mixtures, thereby supporting this conclusion.

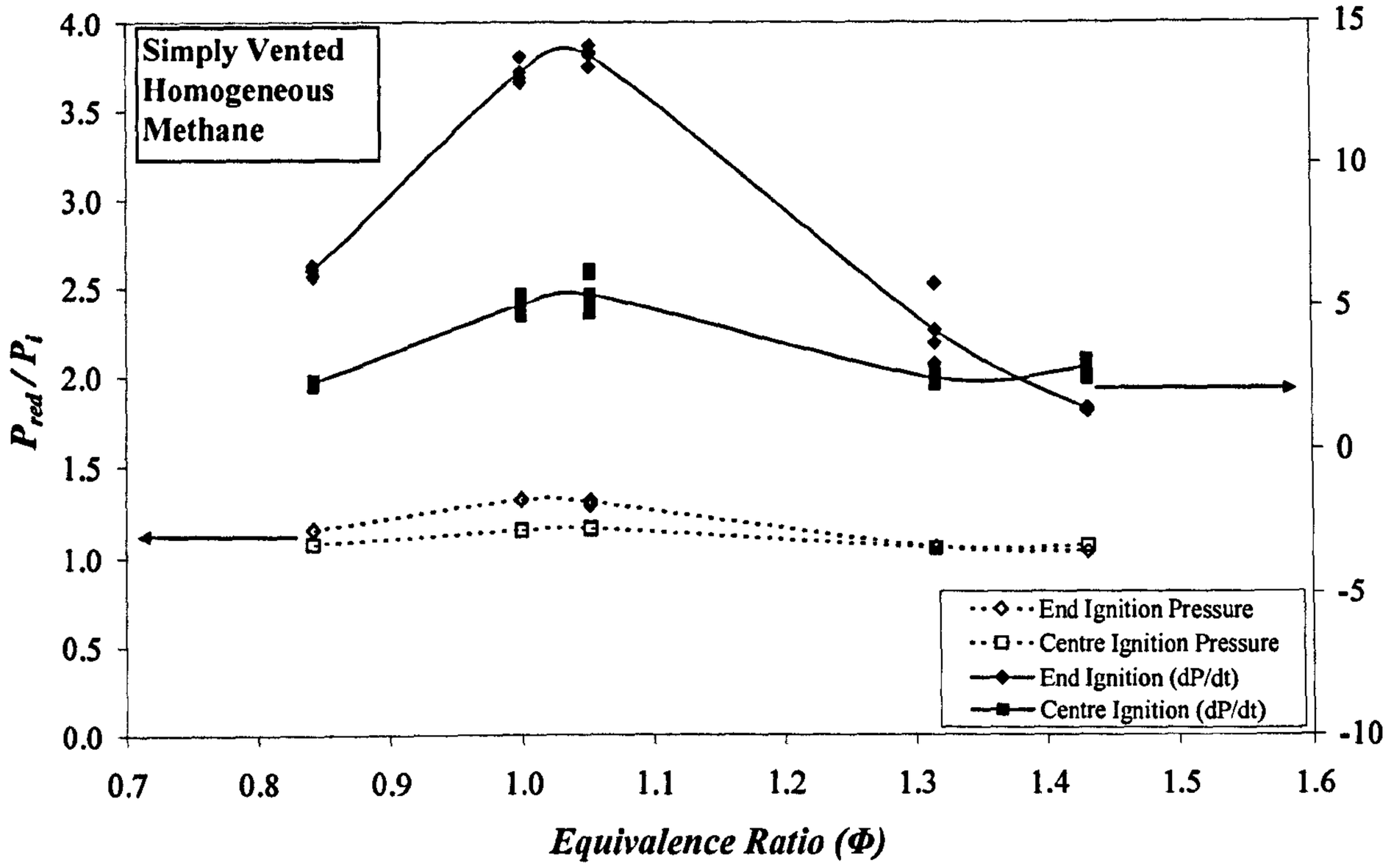

Figure 5-17: - Comparison between end and central ignition, methane-air mixtures for maximum recorded pressure and maximum recorded rates of pressure rise in the primary vessel.

5.4. Summary of Vented Vessel Experimental Data

The results presented in this chapter included small studies into homogeneous and stratified propane-air mixtures and homogeneous methane-air mixtures, in a vented vessel connected to a dump volume, which was sufficiently large as to allow an approximation to an explosion vented into the atmosphere. The work was intended as an intermediary study to provide a link between closed vessel and duct vented vessel explosion data. Whilst it was not possible to investigate all conditions which will be presented in Chapter 6 for duct vented vessels, the data presented in the simply vented vessel regime will enable meaningful comparisons between the closed vessel and duct vented systems.

The results presented indicate that within this vented geometry, the combustion development followed closely the 4-phase regimes set out previously in literature, where an initially spherically expanding flame was drawn towards the vent as the result of an unburned gas flow field entraining the reaction zone in this direction. This was closely followed by a reduction in venting effectiveness as the flame

reached the vent and ignited the unburned gas cloud formed directly outside the vent, which was then followed by the onset of venting once more as the flame continued to burn into the remaining unburned mixture within the vessel. It is interesting to note that both homogeneous and stratified propane-air mixtures closely followed the first three stages. In some tests, mainly rich concentration propane, the onset of flame instabilities also triggered an oscillatory peak, which exhibited a much higher oscillatory frequency than expected for the fundamental harmonic frequency of the vessel. In such cases, the peak has been attributed to the interaction between the combustion of the remaining unburned mixture within the vessel, and the acoustic pressure waves generated by fluctuations in the heat release rate.

The results also indicate that while the near stoichiometric homogeneous concentrations generally represent the most severe overall explosion severity in each case, in propane-air mixtures towards the lower flammability limit, the stratified mixtures actually posed a more severe condition than the equivalent homogeneous. It is likely that the main reason for the increased severity in stratified tests towards the lean limit is due to the concentration gradient in the vessel and the increased mixture reactivity at the ignition site, which would allow the explosion to initiate more quickly. In stratified mixtures, if the air lean and air rich portions of the unburned mixture were pushed through the vent differentially, the resulting mixture inside the vessel to contribute to the main pressure peak could then be more reactive than the global concentration would suggest, and thereby account for the slightly elevated severity of the stratified mixtures towards the lower flammability limits. Further investigation into this matter is clearly required. It is the prediction of this work that a similar trend would occur close to the upper flammability limit.

While it is an important conclusion from the work presented in this chapter that close to the lean limit the stratified explosion severity is greater than its global concentration would normally indicate, it should be stressed that homogeneous stoichiometric tests still constitute the worst case scenarios. Therefore, it is not the suggestion of this work that the design of vented vessels should be modified to represent the maxima obtained in stratified work. However, there is certainly a value associated with this research in the field of post-explosion investigation.

CHAPTER 6:

DUCT VENTED: HOMOGENEOUS AND STRATIFIED EXPLOSIONS

6.1. Introduction

As already discussed in the previous chapter, the presence of a vent on an enclosure likely to contain an explosive mixture is a commonly implemented design feature, as indeed are duct vented vessels. The addition of a duct onto the outside of a vent opening is a common feature in modern industrial installations where a vessel is required to be protected from internal explosion pressures, and where the explosion products need to be directed away from sensitive areas. Whilst it has already been shown in test-vessels 1 & 2 that the presence of a vent will reduce the overall explosion pressure, it is a well known fact that the effect that the addition of a duct to the exterior of the vent will subsequently increase the overall maximum pressure obtained from within the vessel by a factor of 10 or more with respect to simply vented vessels [8].

While there is a large body of work which details the issue of homogeneous explosions within a wide variety of duct vented vessels, to the authors knowledge no comprehensive study of stratified gas-air mixtures in a duct vented environment exists.

In this chapter, homogeneous and stratified propane-air explosions are investigated in a vented vessel connected to a vent pipe of the same diameter as the vent. Concentration, injection position and ignition position were varied, and, where possible, comparisons were made with homogeneous tests at the same global concentration for each condition. It was the original intention to present the results in relation to methane and hydrogen experimental data obtained using the same test-vessel. However, time constraints prevented this data being analysed effectively, and this will form the basis for continuing work. An understanding of the explosion development for homogeneous and stratified propane-air mixtures within a duct vented vessel is important in terms of explosion protection, and such results may be used in validation of prediction techniques and CFD modelling programs, without which the results obtained from such models would be meaningless.

The test programme presented in this chapter was conducted in test-vessel 3, shown in Figure 6-1, which comprised a compact cylindrical vessel ($L/D = 2$) with a vent

hole at one end, having a vent coefficient of K_v = 16.4 with respect to the primary vessel. More detailed technical specifications associated with test-vessel 3 are presented in Chapter 3.

The data presented in this chapter has previously been published [41, 86, 127-129].

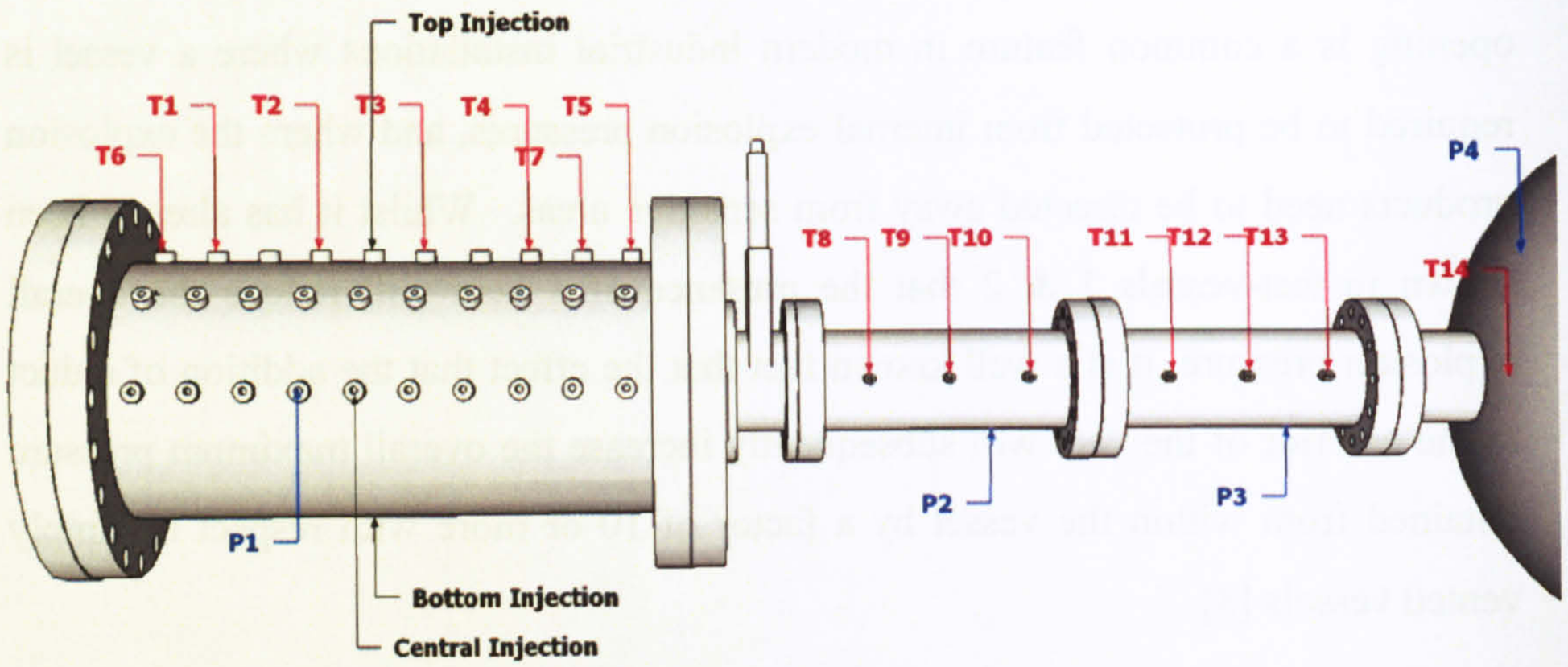

Figure 6-1: Duct vessel test geometry, including details of instrumentation and evacuation positioning.

6.2. Experimental Data

In this section new experimental data are presented, obtained using propane-air mixtures with homogeneous and stratified composition within test-vessel 3. The concentrations investigated in this test programme include 2.5-9.0% (Φ = 0.62-2.24) homogeneous and 1.5-15.0% (Φ = 0.37-3.73) stratified. In addition, variables of ignition position, injection position and concentration gradient are addressed.

Results are presented in terms of P_{red}, $(dP/dt)_{max}$ and S_f, followed by comments on any observations of unusual behaviour. Similarly to the explosions conducted in test-vessel 2, initial pressures and temperatures were local day ambient conditions. Where presented, maximum pressures are normalised against ambient day pressure. In order to best present the severity of stratified mixtures, for each test conducted using a stratified mixture composition where possible a comparable test was performed under homogeneous mixture composition. Although for global concentrations outside the flammability limits, this was not possible.

6.2.1. Stratified Mixture Composition

The concentration gradient measured by gas chromatography has been plotted graphically in Figure 6-2, giving an indication of the concentration gradient through the vessel for each global concentration. From Figure 6-2 it is possible to obtain a rough estimation for the amount of propane available for combustion in the premixed flame (i.e. that within the flammability limits) and also the amount of propane with a concentration above the UFL, which will contribute as part of the diffusion flame burning.

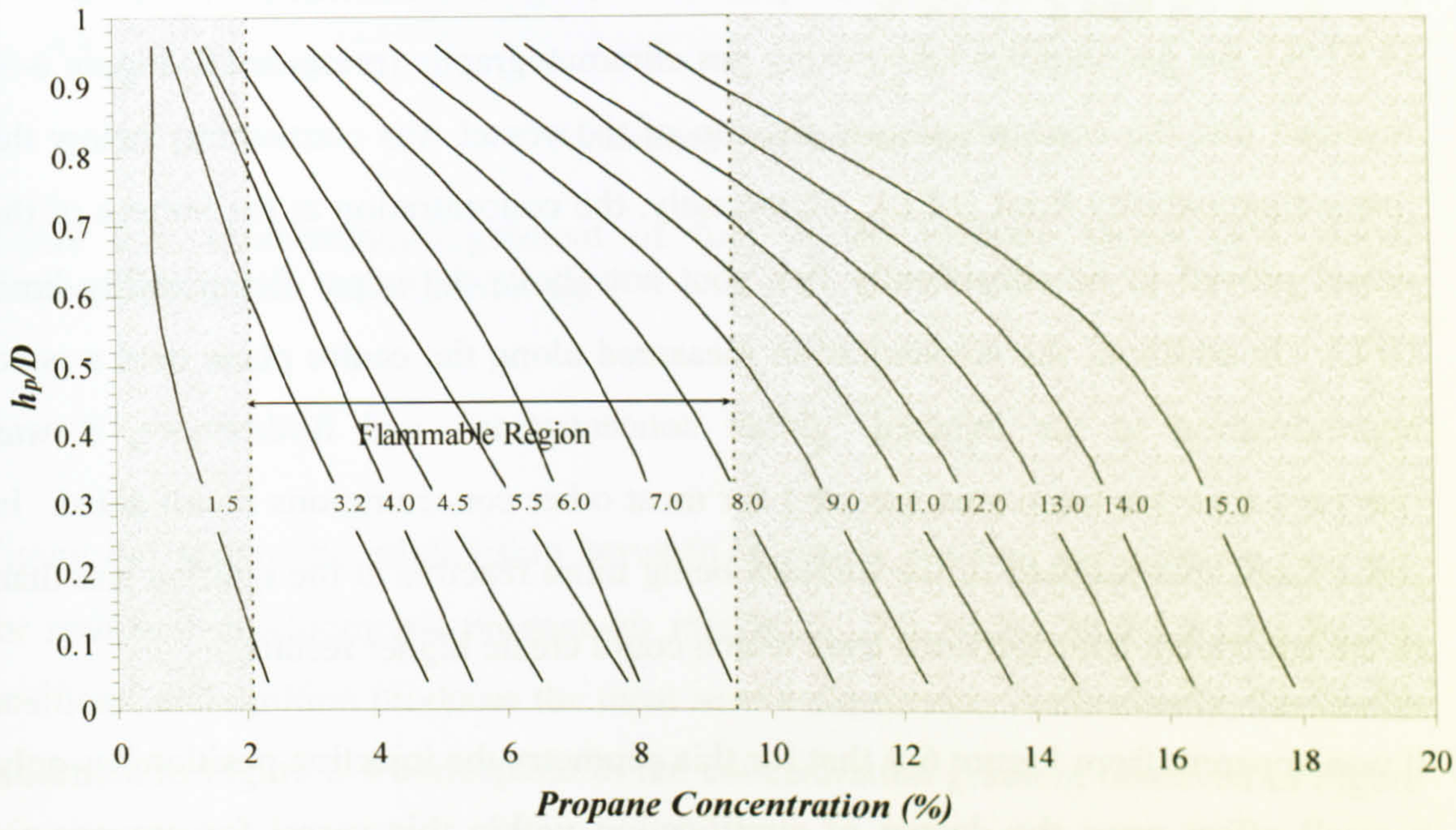

Figure 6-2: Propane-air concentration gradients measured by gas chromatography with global concentration injected inset for each curve.

The highest concentration successfully ignited in this research was 15% ($\Phi = 3.73$). However it may be possible to ignite at a higher concentration if time dependent stratification were taken into consideration. Indeed, concentrations as high as 29% global concentration have been ignited successfully in previous research in a much larger scale vessel [67, 79, 82].

Figure 6-2 also allows an approximation of the concentration along the plane of the ignition. The actual concentration at the ignition site has some bearing on the

explosion development in the early stages of combustion, as will be discussed in the following sections.

6.2.2. Effect of Injection Position

In this section the three injection positions will be considered. In order to gain a clear picture of the concentration gradients produced, initially only stoichiometric global concentration and central ignition were considered. Results indicated that for this vessel there was an adequate concentration gradient formed using the partial pressure method described in Chapter 3. For global concentrations of $\Phi = 1$ (4.02 %), the gas samples taken using gas chromatography (presented in Figure 6-3) revealed that the concentration at the top of the vessel was consistently below the lower flammability limit (LFL). Conversely, the concentration at the bottom of the vessel proved to be consistently rich (but not above the upper flammability limit UFL). In addition, the concentration measured along the centre plane held a good approximation to the injected 'global concentration', and furthermore, it was observed that this trend was repeated for most other concentrations investigated. In some cases this resulted in the mixture being more reactive at the ignition site than in the equivalent homogeneous tests which could create higher results.

It was apparent from Figure 6-3 that for this geometry the injection position has only a small effect upon the degree of stratification within this vessel for propane-air mixtures. Exactly repeatable concentration profiles in the vessel were difficult to achieve, however with an error of 0.5% inherent in the gas chromatograph, the scatter recorded in Figure 6-3 may be somewhat artificial. Comparison of the tests conducted at central ignition, central injection, Φ=1.0 indicate that the small fluctuations in pressure serve to alter slightly the shape of the curve, but not the P_{max}, flame-speed or $(dP/dt)_{max}$ obtained.

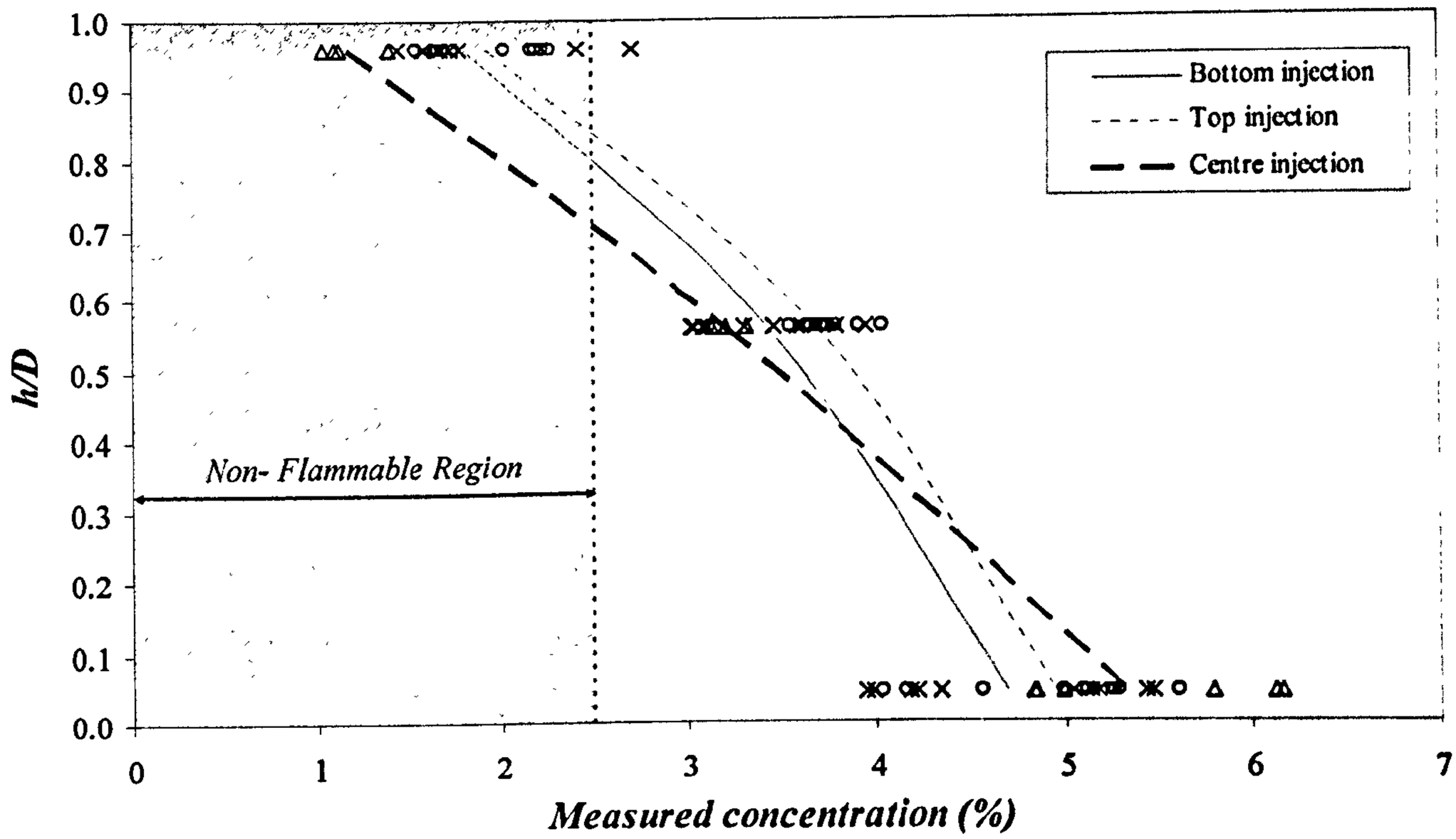

Figure 6-3: Concentration gradient of fuel in the primary vessel (4% global concentration) with normalised height

Figure 6-4 shows the relationship between injection position and ignition position for stratified stoichiometric propane-air mixtures. It is shown that for all injection positions, end ignition produces the most severe explosion. Additionally, the results presented in Figure 6-4 correspond to the concentration gradient observed in Figure 6-3, with the greatest concentration gradient (produced by central injection) exhibiting the least severe result, and for the other two injection positions as the gradient approaches 1 (i.e. fully homogeneous) the severity increased.

There was little overall difference between the pressures produced from the gradients formed through top and bottom injection over the full range of ignition positions, with a maximum difference of just 50 mbar for end ignition. For centre and bottom injection, end ignition produced the most severe explosion, however for top injection there was a dependency upon the acoustic interaction. For those tests where acoustics were apparent central ignition posed the worst case, whereas where little or no acoustics were apparent end ignition was more severe. A similar pattern

was observed for $(dP/dt)_{max}$ values. The acoustic interaction is beyond the scope of this work, and so will not be discussed further here.

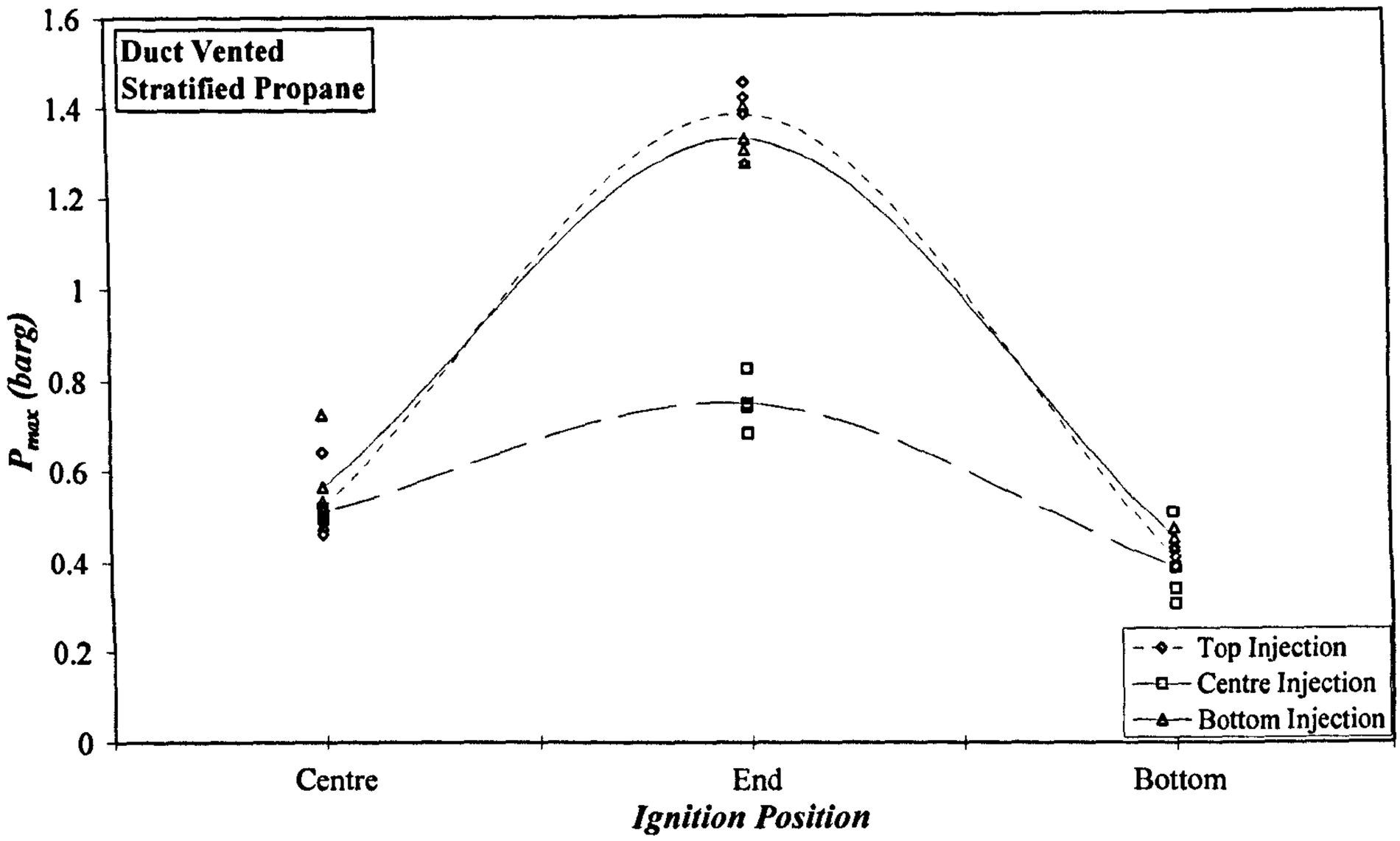

Figure 6-4: P_{max} recorded for stratified mixtures, comparison of ignition position and injection position ($\Phi = 1$).

Overall, the suggestion of Figure 6-3 and Figure 6-4 is that central injection produced the greatest concentration gradient through the vessel, and also the most repeatable results in terms of P_{max} and curve shape in the primary vessel, but produced the least severe explosions.

Injection position for this configuration had only a small effect upon the concentration gradient present within the vessel before ignition, but evidence suggests that injection position will be a greater factor in vessels with a larger capacity, where some areas may be completely uncontaminated by the flammable mixture [79]. More research in this area is certainly needed.

6.2.3. General Observations on Explosion Development

The explosion traces presented in Figure 6-5 and Figure 6-6 show the explosion development for a globally stoichiometric propane-air mixture, with central ignition,

central injection and $\Phi = 1$, under (a) homogeneous and (b) stratified conditions, Figure 6-5 having been ignited centrally to the vessel, and Figure 6-6 at the end of the vessel directly opposite the entrance to the duct. The lines marked t_{in} and t_{out} signify the time of flame passage into and out of the duct from t_{ign}, recorded by the first and last thermocouples in the duct.

For both central and end ignition, a two stage flow was evident in all tests. During the first stage a slow laminar flow was observed, characterised by low pressures and slow flame propagation. Towards the end of this stage, the flame position indicated much faster propagation towards the duct from the vessel centre. This phenomenon is consistent with literature for vented vessels [43, 125], and was due to the elongation of the flame from the ignition point towards the vent opening. This flame elongation is caused by the expansion of the flame forcing unburned gas out of the vent, creating a flow field towards the vent which skewed the flame, and is comparable to phases 1 & 2 described for vented vessels. The second phase, corresponding to phases 3 & 4 described for vented vessels, began as the flame accelerated through the duct. This phase was characterised by much faster flame-speeds, higher rates of pressure rise and increased maximum pressures. At the time when the flame exited the duct, there was still fuel present in the vessel which had become compressed by the expanding flame; the subsequent burning of this remaining fuel was the main contributor to the maximum pressure, which was observed in the vessel after the initial flame passage. A corresponding peak was observed slightly later in the duct, caused by the venting of the products of the main explosion event.

The main difference between end and central ignition is the length of the slow burning laminar phase, i.e. the time between ignition and the flame accelerating through the duct. The difference in the length of this phase was also evident between homogeneous and stratified for end ignition, much more so than for central ignition as will be discussed later.

The severity of the explosion was also slightly higher for end ignition than for central ignition. This is further evident when comparing maximum pressures obtained, as will be discussed in Section 6.2.4.

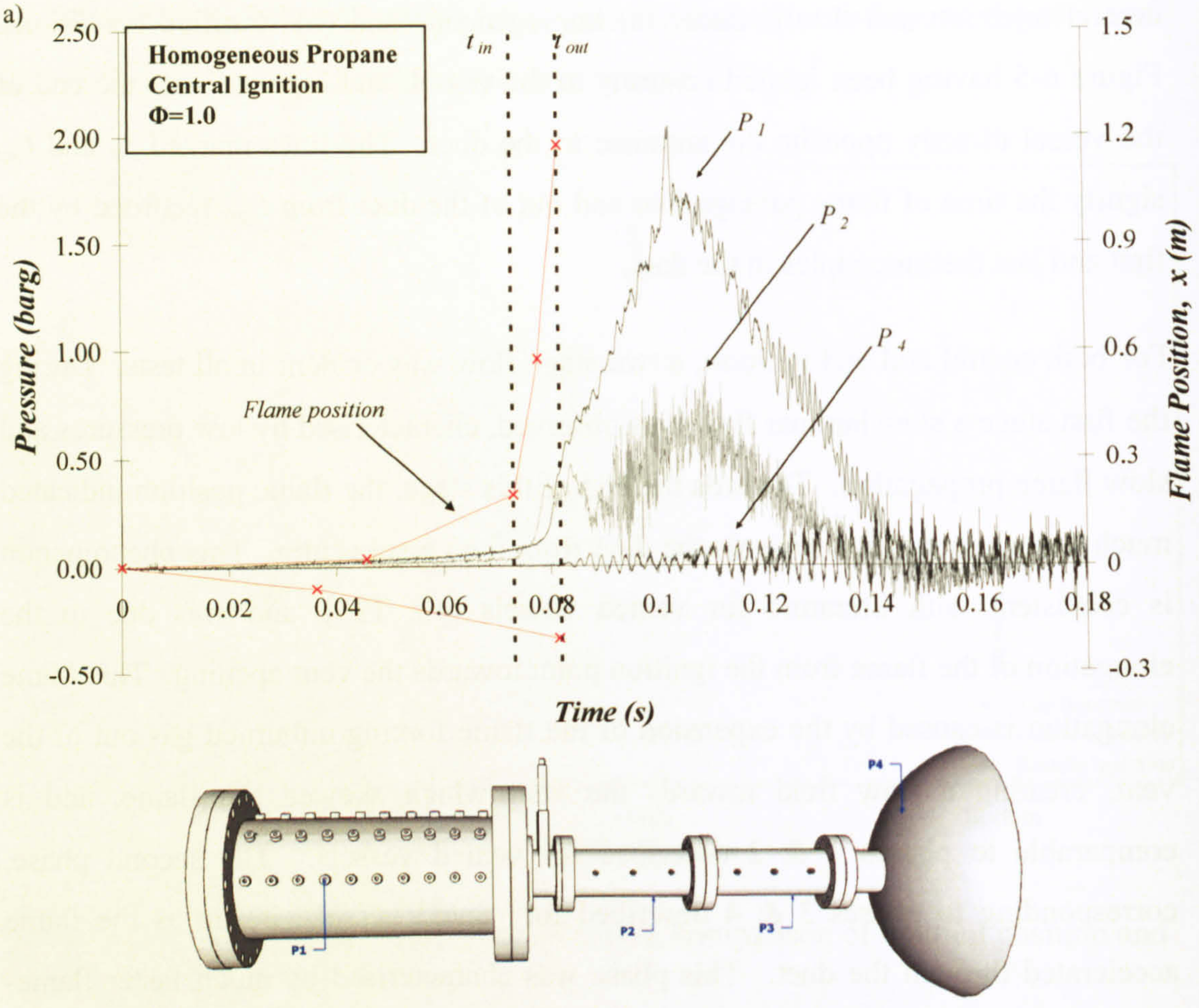

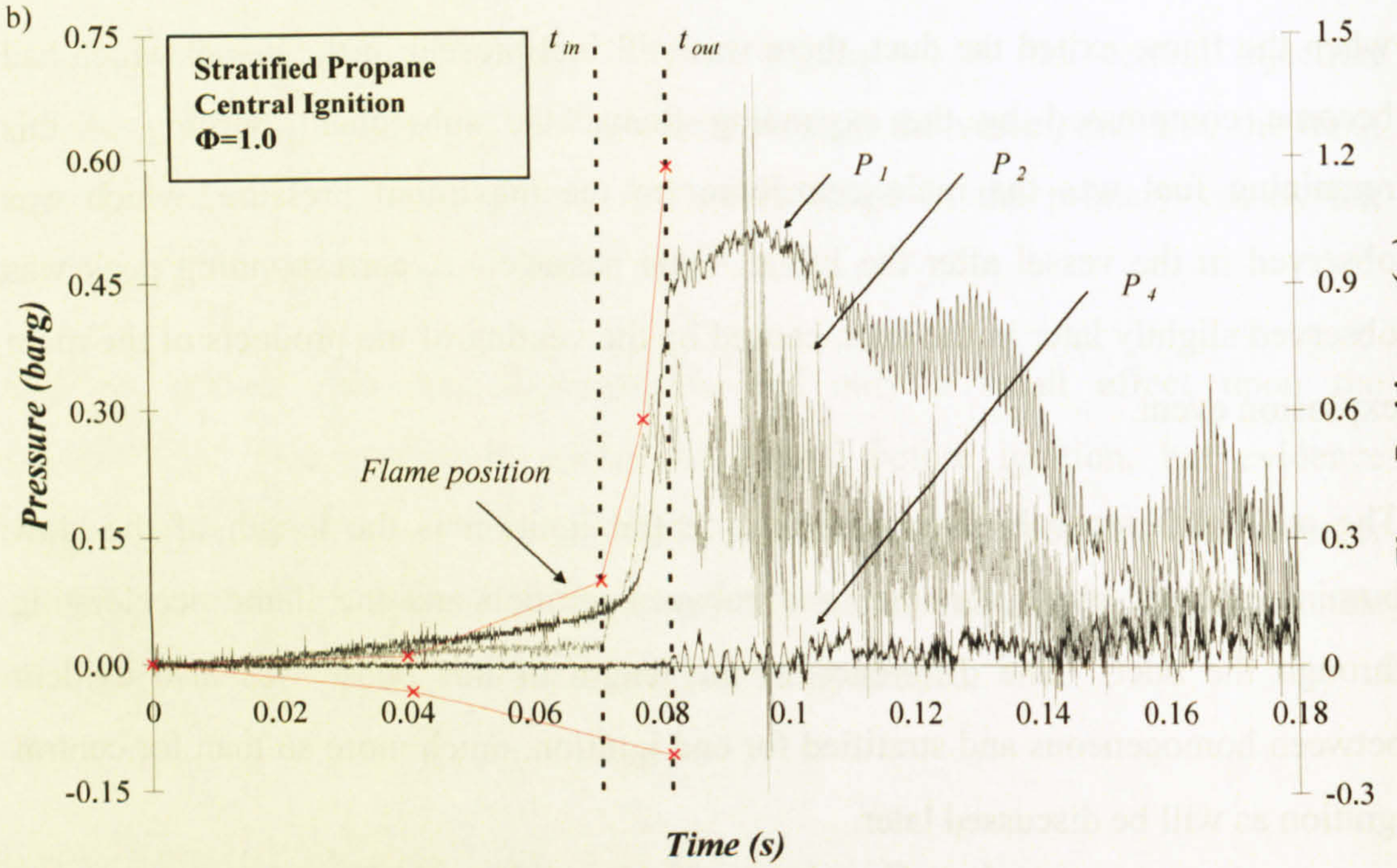

Figure 6-5: Pressure-time curves for (a) homogeneous and (b) stratified mixtures with $\Phi = 1$, centre ignition and central injection.

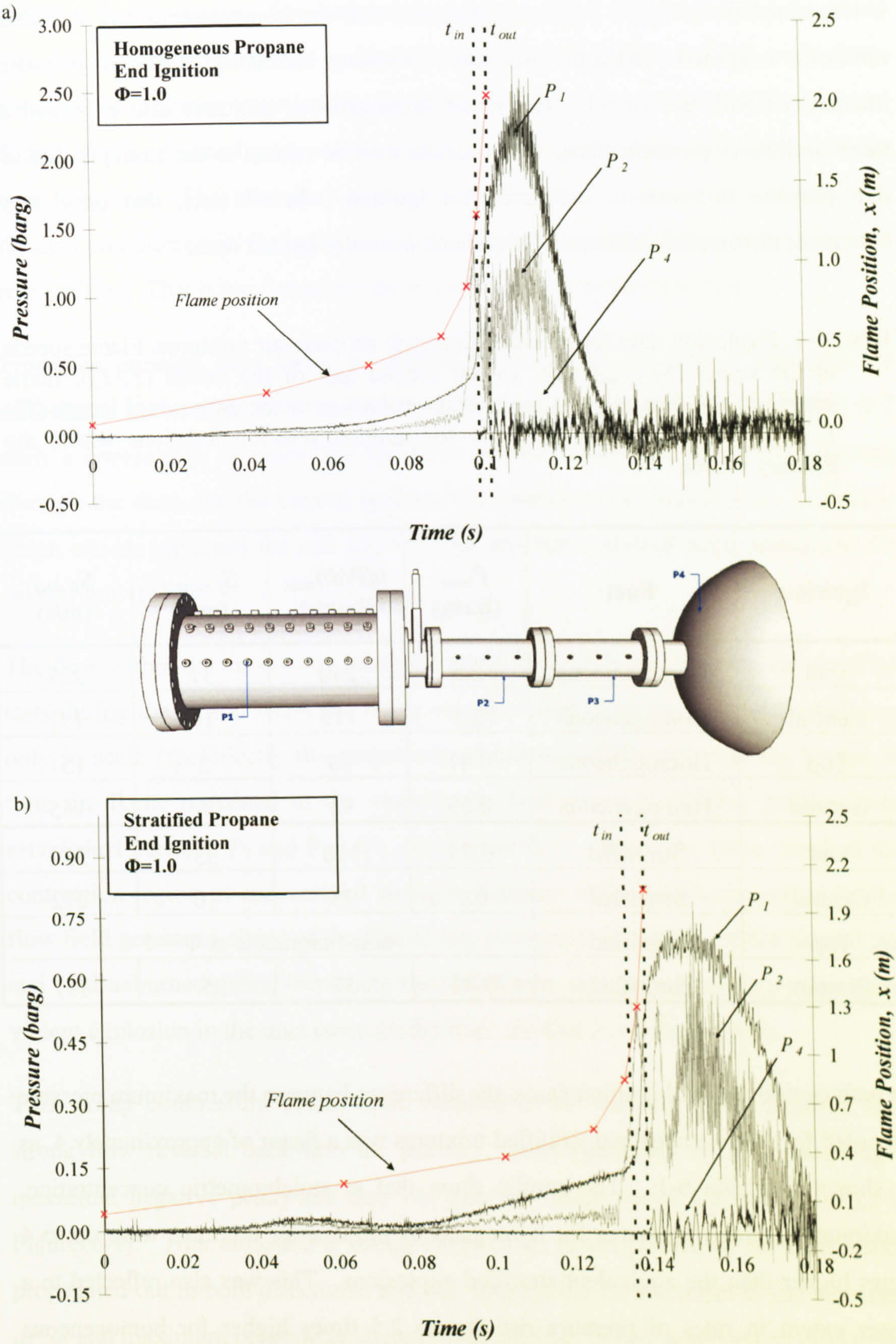

Figure 6-6: Pressure-time curves for (a) homogeneous and (b) stratified mixtures with $\Phi = 1.0$, end ignition and central injection.

It was noted from Figure 6-5 and Figure 6-6 that the homogeneous and stratified mixtures exhibited different oscillatory modes, indicating different acoustic interactions with the vessel. The richer homogeneous mixtures also exhibited a more oscillatory pressure trace. Such results may be related to the susceptibility of rich propane mixtures to cellularity on ignition. In all tests, this oscillatory behaviour manifested differently for end and centrally ignited tests.

Table 6-1: Explosion data for the stoichiometric propane-air mixtures. Flame speeds in the vessel ($S_{f,\ vessel}$) refer to the second half of the vessel (T_4-T_5); flame speeds in the duct ($S_{f,\ duct}$) are average values over the entire duct length (T_8-T_{13}) for $\Phi = 1$. See Figure 6-1 for ignition position locations within the primary vessel.

Ignition	Fuel	P_{max} (barg)	$(dP/dt)_{max}$ (bar/s)	$S_{f,vessel}$ (m/s)	$S_{f,\ duct}$ (m/s)
End	Homogeneous	2.5	240	37	227
Central	Homogeneous	2.1	115	10	171
Top	Homogeneous	0.41	49	5	151
Bottom	Homogeneous	0.69	95	4	155
End	Stratified	0.75	110	33	332
Central	Stratified	0.5	75	10	212
Top	Stratified	non-flammable at $\Phi = 1$			
Bottom	Stratified	0.32	37	5	197

In both central and end ignition cases, the difference between the maximum pressure recorded for homogenous and stratified mixtures was a factor of approximately 4, as is shown in Table 6-1. The results show that at stoichiometric concentration, maximum recorded pressures for homogeneous propane-air mixtures were up to 4 times higher than the equivalent stratified explosions. This was also reflected to a lesser extent in rates of pressure rise (up to 2.5 times higher for homogeneous mixtures). However, when considering flame-speed measurements, there was little difference between the two conditions in the laminar phase, and the flame actually travelled more quickly along the duct in stratified explosions than for the equivalent

condition homogeneous. For both homogeneous and stratified mixtures, the flame recorded for end ignition was greater than all other ignition positions, as a direct result of the distance travelled by the flame at this point, and the additional time during which unburned gases were venting, increasing the flame entrainment in the axial direction. The secondary explosion in the duct, which in turn affected the residual combustion in the main vessel, is therefore expected to be more severe for rear ignition. This is confirmed by the results obtained in this test-vessel.

From the pressure data taken at various points along the vessel, the pressure differences between sections can be derived as a function of time. In Figure 6-7 such a comparison is made for the time interval where the flame was passing through the duct, for the central ignition tests presented in Figure 6-5. A similar graph can be produced for end ignition, but has been omitted from discussion for sake of brevity.

The flow within the vessel was much the same for both homogeneous and stratified tests during the period when the flame was travelling through the vessel, differing only in scale (specifically the magnitude of pressure difference and the length of time the flame remained in the vessel). In both cases, a positive gradient was established between P_1 and P_2 ($\Delta P_{1\text{-}2}$ on Figure 6-7). When the flame reached the contraction region, it encountered strong turbulence which had been created by the flow field generated ahead of the flame; this promoted the mixing of hot burned gas and cold unburned gases, increasing the turbulence, and giving rise to a subsequent violent explosion in the duct (seen on the trace marked P_2 on Figure 6-5).

This strong combustion event, often referred to as '*burn-up*', then resulted in a strong flow reversal back into the primary vessel (indicated by $\Delta P_{1\text{-}2}$ reaching a maximum negative peak) and also out into the dump vessel (shown by $\Delta P_{3\text{-}4}$ in Figure 6-7). This indicated a strong event close to the middle of the duct which propagated out in both directions, and was responsible for the onset of the increased *dP/dt* and maximum pressure upstream in the primary vessel, achieved by effectively stopping and reversing the flow being vented out into the duct at this instant. This induced greater turbulence, increased the burning of the fuel remaining in the primary vessel, and contributed to the final maximum pressure shown in Figure 6-5.

The pressure drop across the duct entrance as a function of time can be approximated by the value of $\Delta P_{1\text{-}2}$ immediately prior to the flame entering the duct.

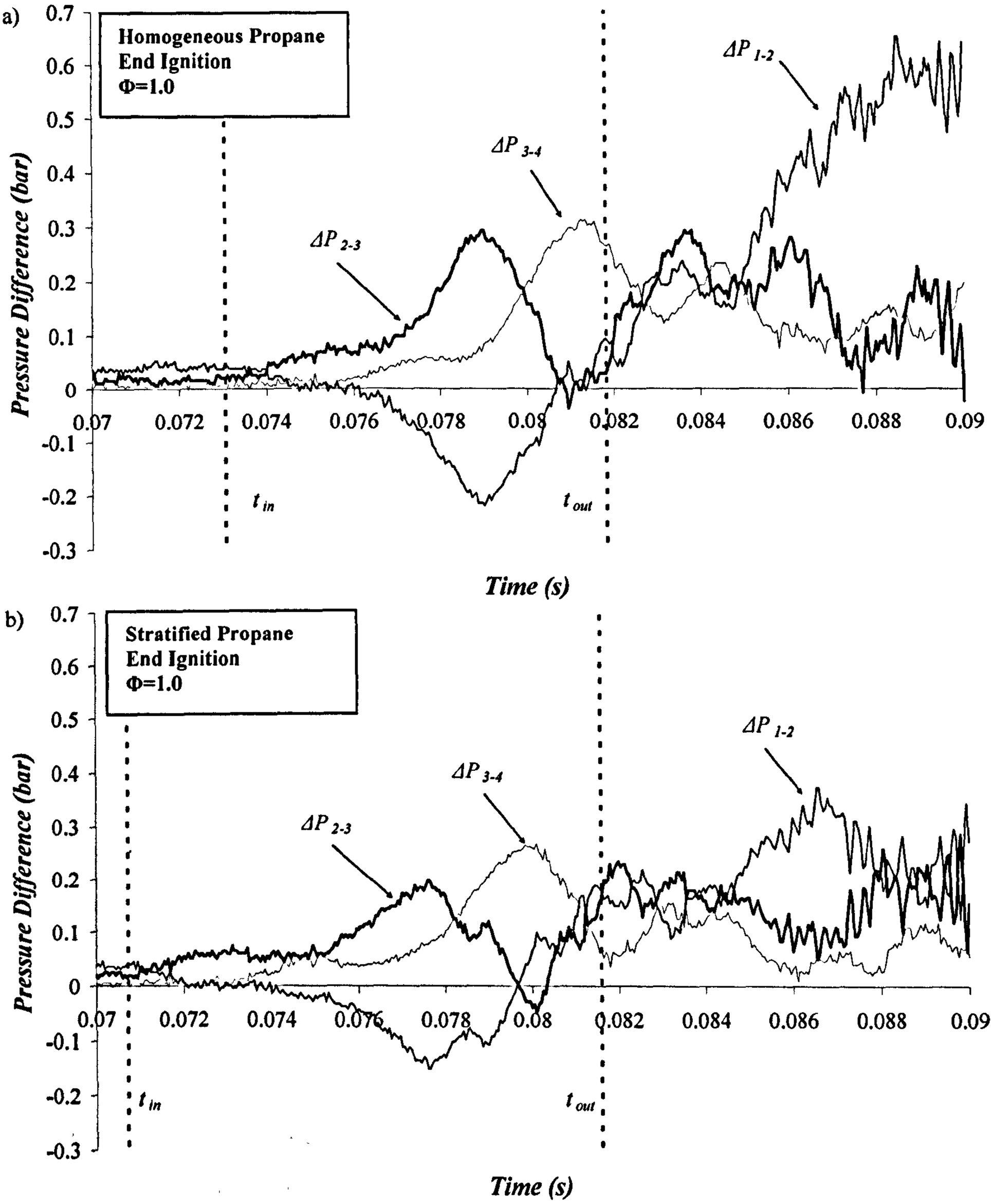

Figure 6-7: Pressure differences at selected positions along the test geometry ($\Phi = 1$, centre ignition, centre injection) for (a) homogeneous and (b) stratified mixtures.

The pressure in the dump vessel (external pressure) was recorded by transducer P_4 and the trace from this is shown in Figure 6-5. It is considered that its influence on

the vessel overpressure observed was insignificant compared to the other parameters reported in this study.

It is apparent from Figure 6-7 that there is a difference in duct entry time between the homogeneous and stratified tests (which was greater in the end ignition tests). An explanation for this can be offered by determining the concentration gradient at this point. It was apparent in Figure 6-2 that in stratified tests, a near stoichiometric layer of propane was formed along the centre plane of the vessel (encompassing the ignition site) with lean and rich concentrations above and below respectively. Since a flame will always follow the easiest burning route, one explanation for the earlier arrival of the flame at the vent in stratified tests could be that the flame spread in the stratified case may have had an initially elliptical growth along the centre plane rather than spherical as in the homogeneous tests. Thereby encouraging the flame to grow more quickly along the horizontal plane and therefore enter the duct earlier than the more spherically growing homogeneous flame, assuming that both are still influenced by the skewing towards the vent as described in literature [43]. Other explanations for this phenomena include variations in the initial growth of the flame or slightly faster flame propagation where the flame burned through the $\Phi = 1.1$ part of the mixture. It was not possible to determine which was the more likely from the measurements taken.

Where the maximum explosion pressure was high, the shapes of the pressure-time curves for stratified tests were also different to homogeneous, often with an elongated double peak (illustrated in Figure 6-8 for top ignition), and often with an acoustically-enhanced second peak generating the highest peak pressure. As previously discussed, this is likely to be associated with the interaction of the flame front with the geometry, having an effect on the combustion of isolated residual fuel and/or unburned gas pockets in the corners of the primary chamber.

The effects of scale up are not known and there has been little work on large scale with stratified mixtures. The works of Tamanini [67, 68, 80] mentioned earlier showed a relationship between the rich mixture layer height and the overpressure within large scale vessels and this has been shown to apply to the medium scale

experiments conducted with the addition of a duct in this laboratory, as discussed in Willacy *et al* [127].

In both end and centrally ignited tests, a strong pressure pulse is clearly detectable on P_2 positioned within the duct. This strong pulse is linked to the violent combustion promoted by the very fast mixing of the burned and unburned gases, corresponding to the event of the flame entrance into the duct. Indeed, this phenomenon has been observed in smaller scales geometries [8].

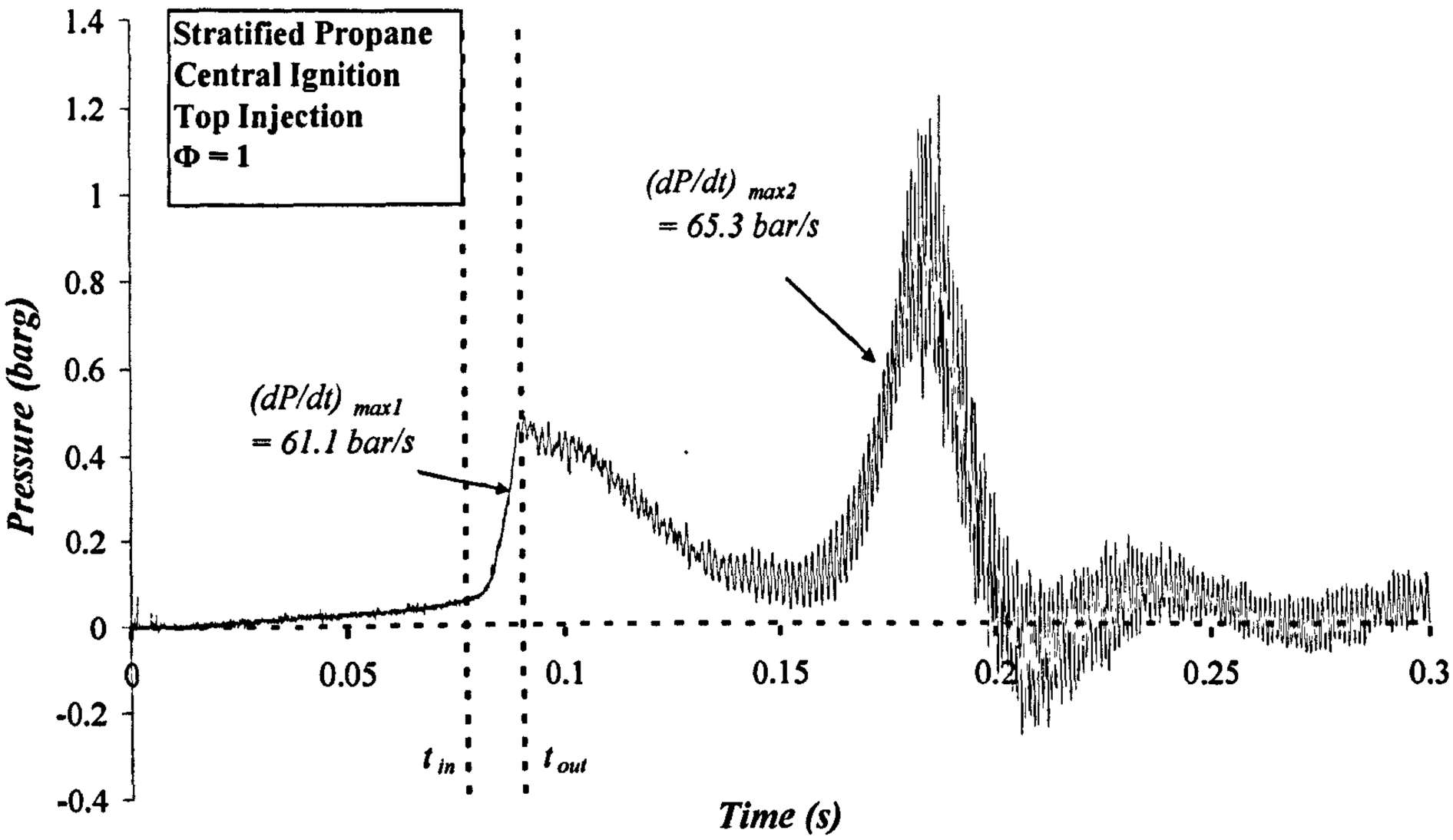

Figure 6-8: Pressure-Time history at transducer P_1 for stratified propane-air ($\Phi = 1$, central ignition, top injection), with (inset) values of rate of pressure rise for each peak.

6.2.4. Effect of Ignition Position

It was shown in Section 6.2.2 that central injection produced the greatest concentration gradient of propane in the vessel (Figure 6-3). Therefore, using predominantly Φ=1 propane-air with central injection, the influence of ignition position will be assessed in this section. Figure 6-9 shows typical pressure-time traces for the four ignition positions investigated in this test series. From Figure 6-2 and Figure 6-3 it is apparent that the resulting concentration gradient was non-

flammable at top ignition, therefore, no top ignition curve exists for stoichiometric stratified tests.

From literature, it is expected that an ignition position central to the vessel should produce the most severe explosion [8, 50]. However, it has already been discussed that for this venting configuration end ignition produces the worst case in stratified tests and this is similar, if less pronounced, for homogeneous mixtures. Maximum pressures in the primary vessel (at P_1) showed a greater scatter in the homogeneous tests than in the stratified (shown in Figure 6-10) particularly for rich mixtures, however the general trend of end ignition posing worst case as stated above was still present. The flame-speeds and $(dP/dt)_{max}$ measurements were recorded from the primary vessel.

From Figure 6-10 the influence of ignition position and Φ on the maximum recorded pressure and rate of pressure rise for homogeneous and stratified propane-air explosions is apparent. It is clear, despite the scatter, that end ignition provides the worst case in terms of rates of pressure rise, a finding echoed though the data of flame speed in the primary vessel and duct. From these results, the relationship between overall explosion severity and ignition position for both homogeneous and stratified explosions therefore becomes: *end* > *central* > *bottom* > *top*. This conclusion is in agreement with recent experimental work based upon homogeneous duct vented explosions [41], and highlights an inadequacy in published venting correlation standards which assume that central ignition poses the worst-case explosion risk.

Furthermore, for central ignition in the homogeneous tests, the primary vessel flame-speeds (measured at the end of the vessel, between T_3 and T_4) ranged from 5 to 10 m/s, with the maximum to the rich side of stoichiometric ($\Phi = 1.125$). However, for end ignition the recorded flame-speeds were up to 5 times higher than this, ranging from 15-20 m/s in the lean mixtures and up to 50 m/s at $\Phi = 1.125$.

The higher flame-speeds exhibited by end ignition were due to the unidirectional expansion of the flame from the end wall. Expansion predominantly in one direction only causes elongation of the flame and hence greater surface area leading to faster

burning, in addition to the extra distance available for acceleration, in the same way as described for vented explosions in Chapter 5.

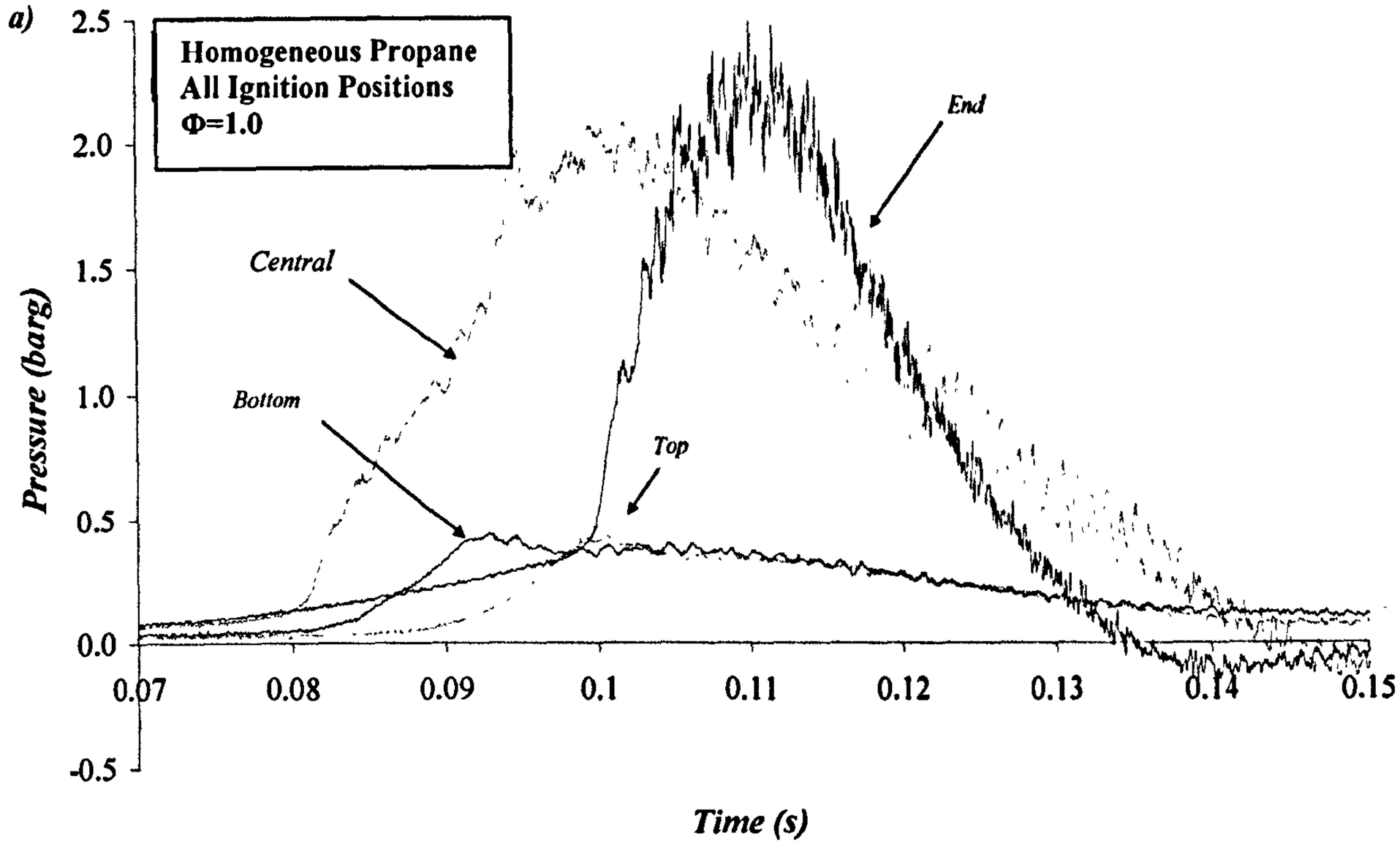

Figure 6-9: Pressure-Time curves for all ignition positions at Φ = 1.0, for (a) homogeneous and (b) stratified propane-air mixtures in test-vessel 3. All pressure traces were recorded at P_1.

For stratified mixtures, the overall maximum pressures were much lower than the equivalent global concentration homogeneous, but the same general trend was apparent. In the stratified tests, bottom ignition was much stronger for lean

mixtures, compared to homogeneous. This could be due to the increased propane concentration at the ignition site (still within the flammability limits) hastening the initial stages of the explosion. Additionally, as the global concentration tended towards the lean, the concentrations measured at the bottom of the vessel were close to stoichiometric, which served to increase the severity of the stratified explosion above the homogeneous.

Overall, it is clear that despite there being little conclusive difference in the maximum pressure observed for end and central ignition positions, measurements of rate of pressure rise and flame speed, which are often more important with respect to structural response, show that in fact, where free venting is allowed through a duct, end ignition is the most severe ignition position.

6.2.5. Maximum Recorded Pressures and Rates of Pressure Rise

In order to best present the data, Figure 6-10 displays the maximum explosion pressure recorded for all tests performed on this vessel, using central fuel injection as a function of equivalence ratio for (a) top ignition, (b) centre ignition, (c) bottom ignition and (d) end ignition. In addition, explosion tests were performed outside the range presented, but no detectable pressure rise was recorded. As presented in Table 6-1, the most severe explosions recorded in each case were that of end ignition, followed by central. However, ignition at the top or bottom of the vessel also produces maximum overpressures which are significant in terms of structural response.

For all ignition positions, as the global concentration approached the flammability limits, explosion severity was consistently higher for stratified mixtures than the equivalent global homogeneous by up to an order of magnitude, which illustrates the potential severity of the stratified mixtures when compared to homogeneous.

As the concentration increases, the premixed layer became more shallow at the top of the vessel (see Figure 6-2), ranging from ~35cm at 10% to ~5cm at 15%. This is reflected in the decaying pressure traces seen on Figure 6-10(a) for $\Phi > 2.5$. The variable of time dependence has not been considered here, but it is possible that

layer heights will increase in size from the top of the vessel as the propane is allowed to settle.

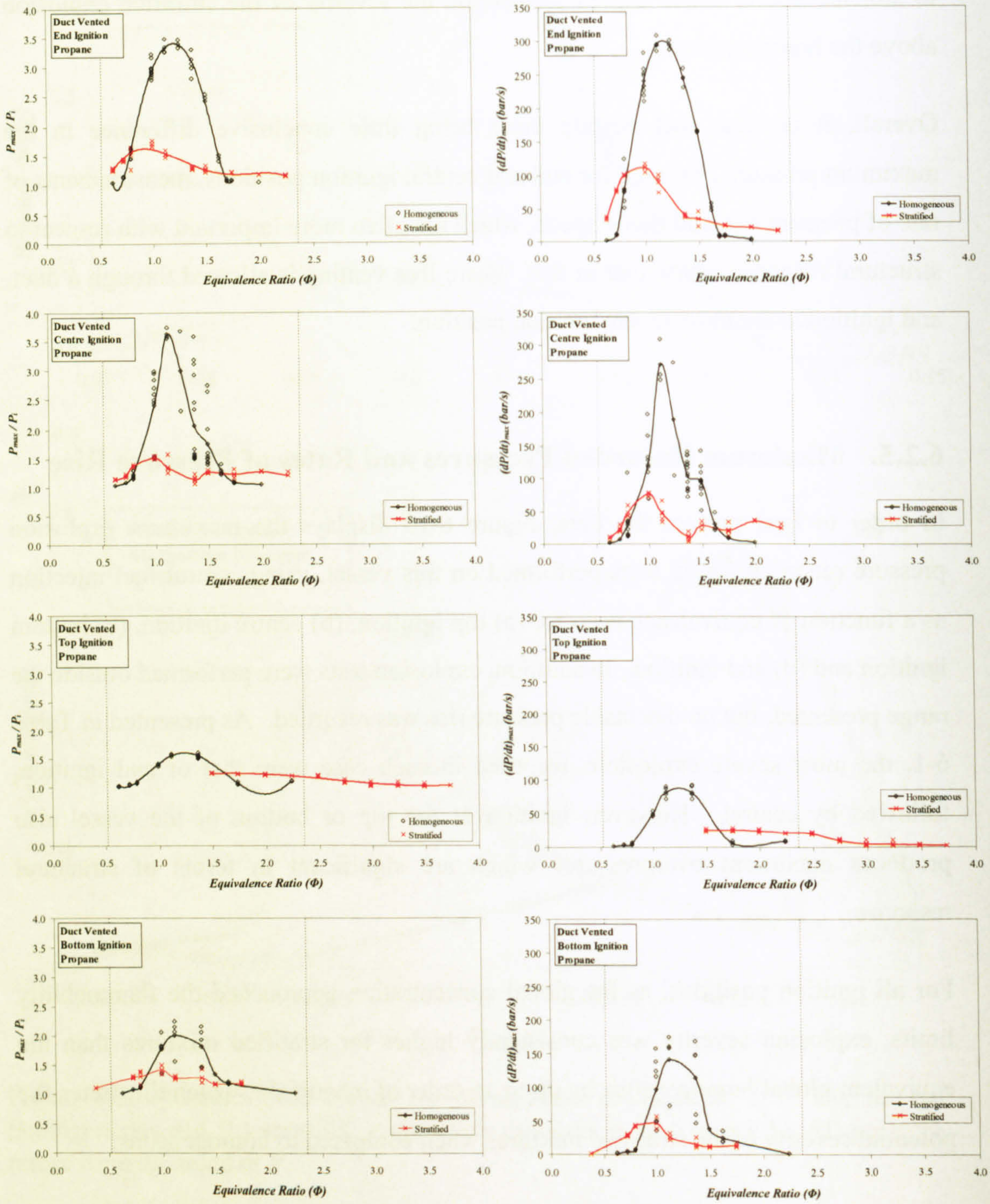

Figure 6-10: Maximum recorded pressures and rates of pressure rise for premixed and stratified propane-air explosions with ignition at a) End, b) Centre, c) Top and d) Bottom. Individual dots represent repeat tests.

Figure 6-10 shows that stratified mixtures with global equivalence ratio around stoichiometric produce significantly lower pressures than their homogeneous equivalents. However, stratified (globally) near-limit mixtures produced overpressures that were several hundred mbar higher than those of the equivalent homogeneous mixtures. Even beyond the flammable range (globally), the stratified mixtures produced significant overpressures.

The maximum rates of pressure rise $(dP/dt)_{max}$ recorded for all tests performed for end and centre ignition occurred at a time approximating to the burn-up in the duct. The burn-up event contributed to a faster burning rate and hence produced increased pressures at this time.

Flame speed data recorded indicate a similar pattern to P_{max} and $(dP/dt)_{max}$. For homogeneous concentrations, the maximum flame-speed was recorded at Φ=1.125, slightly to the rich side of stoichiometric; for stratified tests, maximum flame speeds were observed at lean concentrations.

For all of the results obtained from this duct vented geometry, (P_{max}, dP/dt_{max} and S_f), a definite pattern was evident. For explosion tests conducted close to the flammability limits, the stratified mixtures created a more severe explosion, with the greatest difference observed between the flame speed measurements in the duct.

6.3. Stratified Layer Fractions

In the work by Tamanini, it was proposed that the volume can be treated as three separate fractions, (1) oxygen-rich, (2) flammable (which Tamanini refers to as the premixed fraction) and (3) fuel-rich (non-flammable). It is reported that only the flammable and rich fractions play a significant part in the evolution of pressure in the vessel. From his results, Tamanini proposed a simple equation to account for the relative contribution of these two layers. Whilst the work of Tamanini was conducted in a large rectangular vessel, by modifying the fraction calculations to account for a cylindrical vessel it is possible to look at the contribution of such layers in a smaller vessel.

In a similar manner to the gradient graph presented in Figure 6-2, a crude approximation for the layer height of the UFL (h_p) and LFL was obtained for each test individually. From the layer heights, the fill fraction corresponding to the lean, flammable and rich fractions were calculated and employed into Eq. 6-1. For this particular geometry, a maximum of only two layers were present for each test (either lean and flammable or flammable and rich, as shown in Figure 6-2).

$$f_p = X_{fp} / [X_{fp} + X_{fr}] \qquad \text{Eq. 6-1}$$

where X_{fp} is the fraction occupied by flammable gases and X_{fr} is the fraction occupied by the rich mixture, and f_p is a parameter that Tamanini describes as representative of the fraction of a reactive mixture that supports premixed flame propagation, as opposed to diffusive/convective burning

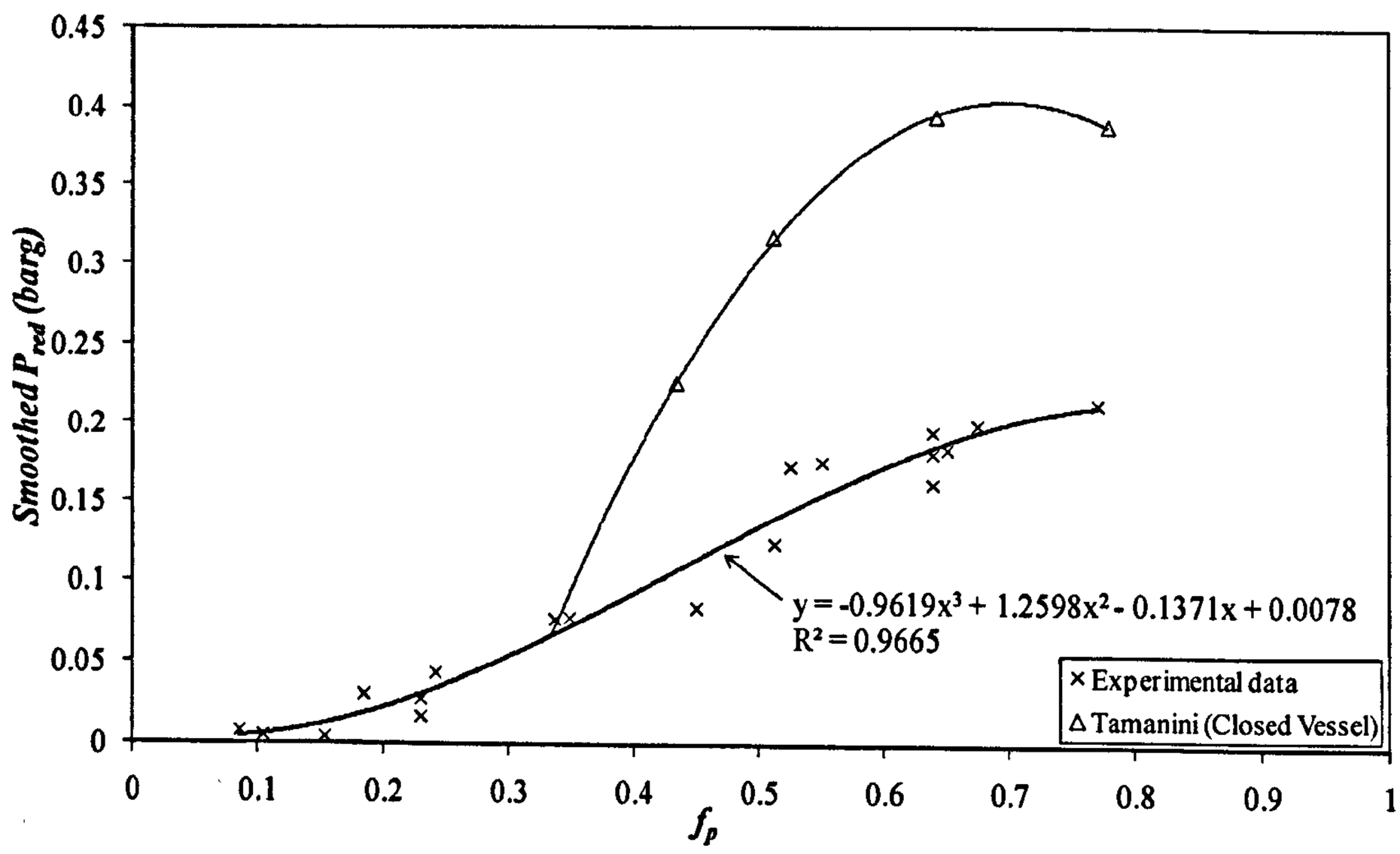

Figure 6-11: (a) global concentration and h_p/D, and (b) Comparison between filled fraction ratio, f_p and measured reduced pressure, P_{red}.

Using an approximation for the layer heights based on the crude gradient obtained in Figure 6-2, a value for the filled fraction ratio was obtained from Eq. 6-1. The relationship between the maximum reduced pressure observed in the primary vessel for each test (P_{red}) is shown in Figure 6-11. Data from Tamanini [67] is also presented. It should be noted that the data presented for Tamanini's work are

obtained using a closed vessel and therefore not directly comparable. Nevertheless the results shown in Figure 6-11 show a significant correlation (95%) between the calculated filled fraction parameter f_p and the measured reduced pressure. Clearly further research into the applicability of this factor would be of benefit to modelling and prediction works for partially filled or stratified mixtures. It is worth noting however, that even where a concentration gradient is present, if there is no rich fraction is present, i.e. where the gradient lies wholly within the flammable region, or where only flammable and lean regions are present, the correlation will not work.

6.4. Comparison of the Results with Closed Vessel and Vented Vessel Results

Figure 6-12 and Figure 6-13 show the maximum recorded pressures and rates of pressure rise respectively for all propane-air explosions conducted on the closed vessel, vented vessel and duct vented vessel. The results show that for both homogeneous and stratified mixtures, the closed vessel explosions were by far the most severe, in each case reaching levels of around 7 bar for both homogeneous and stratified results. As discussed in Chapter 4, the difference between the maximum recorded pressures for homogeneous and stratified mixtures in a closed vessel was relatively low, owing to the turbulent mixing of the fuel rich and fuel lean portions of the mixture in the wake of the premixed flame.

In all tests, it is apparent that the addition of a vent to the system reduces the explosion severity by up to a factor of 7 with respect to the closed vessel experimental data. However, comparison of the duct vented vessel data shows that the explosion severity

is once again increased for all concentrations when a duct is added to the vented system. This is consistent with that observed in literature for homogeneous mixtures. It is of course interesting to note that the addition of such a vent duct in stratified mixtures has the same effect as that observed for homogeneous mixtures, showing that while the overall explosion severity is reduced, similar governing mechanisms apply. Therefore, as an extension to this work, it would be interesting

to compare the results to the correlations and explosion prediction correlations which were originally developed for homogeneous mixtures, and it is hoped that such comparisons may be made in the future.

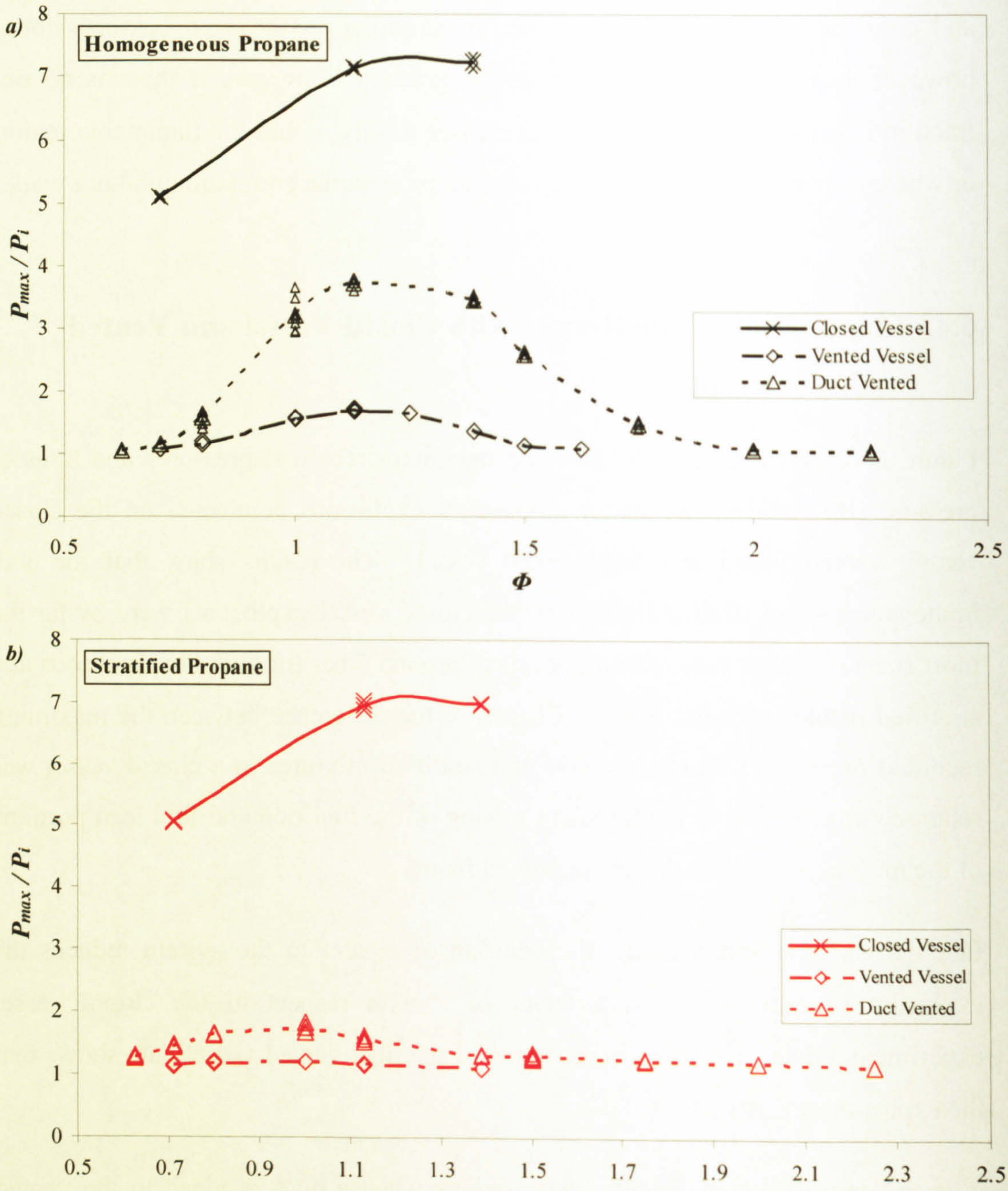

Figure 6-12: Maximum pressure recorded in the primary vessel for closed vessel, vented vessel and duct vented vessel explosions for (a) homogeneous and (b) stratified propane-air explosions.

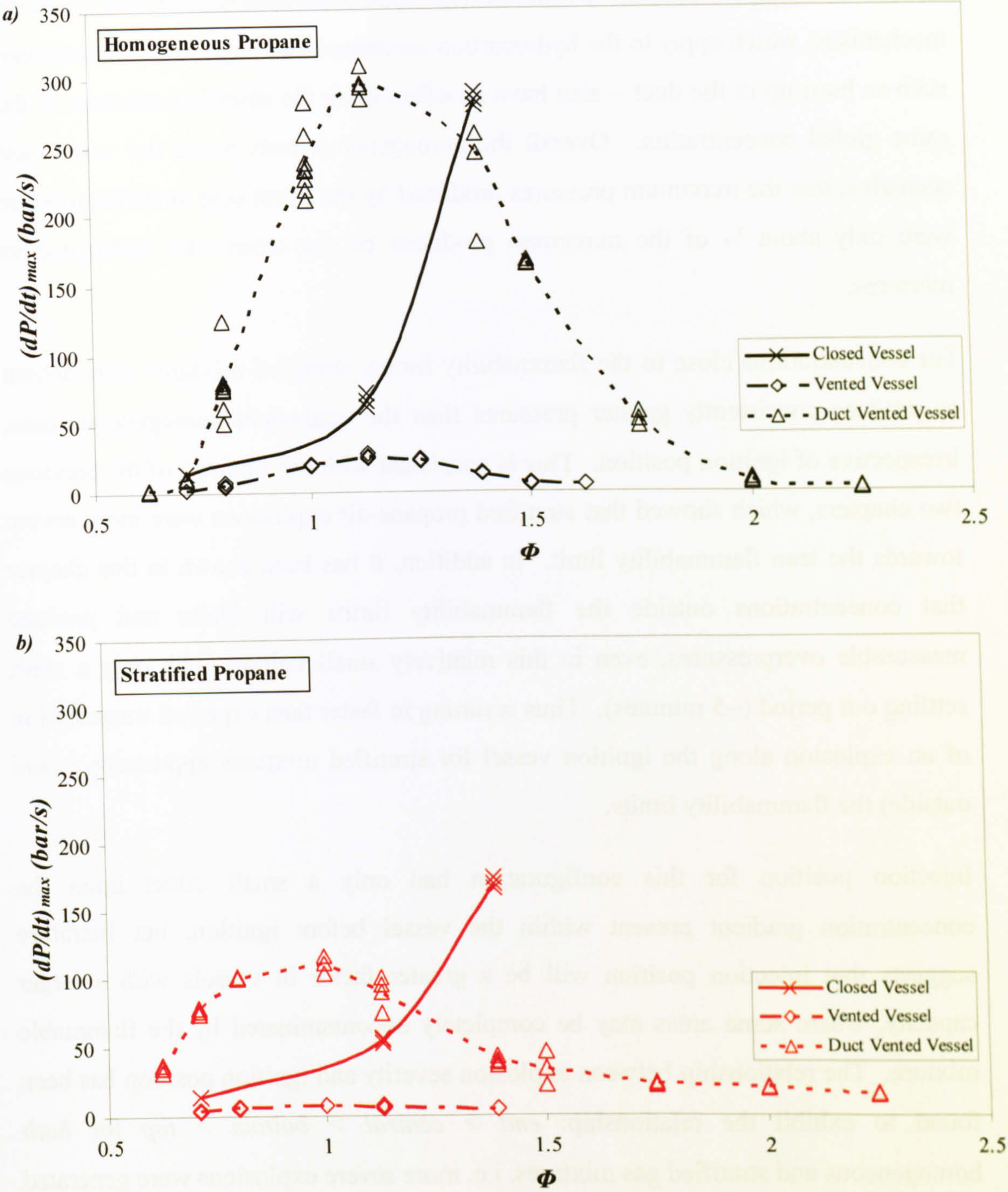

Figure 6-13: Maximum rates of pressure rise recorded in the primary vessel for closed vessel, vented vessel and duct vented vessel explosions for (a) homogeneous and (b) stratified propane-air explosions.

6.5. Summary

In this chapter, new experimental data has been presented which has shown the severity of explosions in the duct vented geometry, and in comparison to vented and

closed vessel explosions in the same scale vessel. The results show that the same mechanisms which apply to the hydrocarbon mixtures in homogeneous explosions – such as burn-up in the duct – also have an effect upon the stratified mixtures of the same global concentration. Overall the homogeneous tests posed the worst case scenarios, and the maximum pressures produced by the worst case stratified mixture were only about ¼ of the maximum produced by the worst case homogeneous mixtures.

For concentrations close to the flammability limits, stratified mixtures were shown to produce consistently greater pressures than the equivalent homogeneous case, irrespective of ignition position. This is consistent with the findings of the previous two chapters, which showed that stratified propane-air explosions were more severe towards the lean flammability limit. In addition, it has been shown in this chapter that concentrations outside the flammability limits will ignite and produce measurable overpressures, even in this relatively small volume with only a short settling out period (~5 minutes). Thus resulting in faster than expected transmission of an explosion along the ignition vessel for stratified mixtures approaching (and outside) the flammability limits.

Injection position for this configuration had only a small effect upon the concentration gradient present within the vessel before ignition, but literature suggests that injection position will be a greater factor in vessels with a larger capacity, where some areas may be completely uncontaminated by the flammable mixture. The relationship between explosion severity and ignition position has been found to exhibit the relationship: *end* > *central* > *bottom* > *top* for ***both*** homogeneous and stratified gas mixtures, i.e. more severe explosions were generated from an end ignition position rather than from central ignition cases as reported in literature [8, 50]. However, it is noted that those reported in literature are for different scale vessels and therefore the same may not strictly apply here.

Pressures measured from the experimental data were compared with the simple layer fractions proposed by Tamanini in a large scale volume and were found to provide a significant correlation between the layer fraction ratio and the maximum recorded reduced pressure after venting (for central injection). Additional research in this

area would determine the extent of the applicability of Tamanini's equation with the results obtained in this scale vessel.

CHAPTER 7:

INTERCONNECTED VESSELS:

GAS POCKETS AND PARTIALLY FILLED SYSTEMS

7.1. Introduction

The importance of research into explosions within interconnected vessels has long been appreciated, with particular relevance to process plants, where the prevention of explosion transmission to a connected vessel is clear. Indeed, several authors have published research focussing on the combustion of a flammable gas-air [3-5, 130] or dust-air [131, 132] mixture completely filling a two or more vessel interconnected system. More recently, the importance of research into partially filled interconnected vessel explosions has been noted for both gas-air and dust-air explosions [62, 133]. Alexiou *et al* [62] discussed the importance of research into gas-air explosions in partially filled interconnected systems. Their work outlined the various combustion stages resulting from a methane-air mixture being formed in the primary chamber and first connecting pipe of a three chamber system, incorporating a 180° bend between the secondary and tertiary vessels. They concluded that the explosion severity in such an enclosure can be much more severe than the fuel to total chamber volume ratio would suggest.

The test programme presented in this chapter involved the collection of new experimental data using test-vessel 4, shown in Figure 7-1. The rig comprised two unequal cylindrical vessels with a secondary to primary volume ratio of 4:1. The vessels were linked via a duct, with a duct area equivalent to an explosion vent coefficient, K_v ($=V^{2/3}/A_v$), of 10.3 with relation to the primary vessel. The connecting duct represented a vent duct for the explosion in the primary vessel, with the secondary vessel representing a capture vessel for the vented gases, hence this work also has applications to safe vent design for toxic substances. In addition, the work presented can serve not only as an extension of current knowledge into the phenomenon, but also as primary experimental data which can later be used to validate CFD software capable of modelling such a situation. The explosion pressures were measured at the axial wall positions shown in Figure 7-1, using four piezoresistive pressure transducers. Each explosion was repeated a minimum of three times, as the connected duct flow expansion created high turbulence in the secondary vessel resulting in some variability in the results. More detailed technical specifications of the geometry can be found in Chapter 3.

Explosion tests were performed using propane and methane-air mixtures at regular intervals over their entire flammable range, but were limited a maximum of 22% for hydrogen-air mixtures as a result of some unexpected behaviour in these tests which increased the overall explosion pressure above the design pressure of the weakest portion of the test vessel, which was the gate valve.

Apart from a small number of tests using methane-air, the fuel-air mixtures were prepared using the partial pressure method in the smaller chamber only, with the connecting pipe and secondary vessel containing only air. During mixing the primary vessel was partitioned from the remainder of the vessel using the 0.162m diameter gate valve. In all cases, the starting pressures were close to standard ambient pressure (~1.0132 bar).

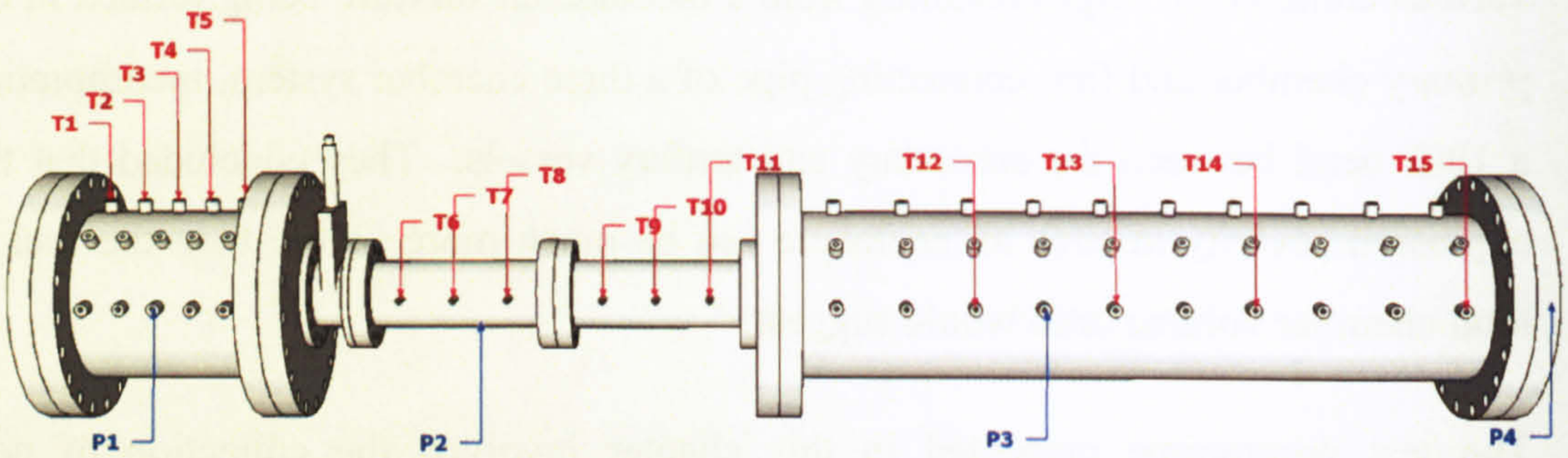

Figure 7-1: Detailed schematic of Rig 4 including instrumentation

The work presented in this chapter has previously been published [37, 134-136].

7.2. Experimental Results (Propane)

This section will discuss the experimental results obtained from this closed interconnected vessel system test series using propane-air mixtures in the range 3.0% to 8.0% (Φ=0.79 to 1.99). In all cases, the initial starting mixture was of homogeneous composition within the primary chamber, under standard atmospheric conditions (~1.0132 bar). This section will provide details of the general explosion development of a propane-air mixture, flame development, maximum pressures attained, rates of pressure rise, and flame speed, followed by possible explanations

for the phenomena observed. The results in this section have previously been accepted for publication [136].

7.2.1. General Explosion Development

In order to give a general overview of the typical explosion development of propane-air mixtures within this configuration, two representative pressure and flame position records from the vessel are shown in Figure 7-2 and Figure 7-4 for 3.5% and 4.5% propane-air mixtures respectively (which equate to global concentrations of <1% if the volume of fuel present had been spread over the entire two-chamber test-vessel - by way of illustration, the equivalent global concentration of all concentrations considered in this research are shown in Table 7-1). The vertical dashed lines indicate the time at which the flame entered and exited the connecting pipe (marked t_{in} and t_{out} respectively), approximated by the arrival time of the thermocouples positioned closest to these areas (marked T_6 and T_{11} respectively in Figure 7-1). Finally, the line marked 'adiabatic' represents the expected adiabatic constant volume maximum pressure. The calculation of the expected adiabatic pressure used the initial mixture concentration, and the gas reaction thermodynamic equilibrium package GASEQ [137] was run to calculate the maximum constant volume pressure. This was assumed to occur in the primary vessel (the volume of the initial flammable mixture) and then distributed the whole system volume using:

$$P_3 = \left(P_1 V_1 + P_2 V_2\right)/V_3 \qquad \text{Eq. 7-1}$$

where P and V relate to the pressure and volume respectively, with the subscripts denoting (1) the primary vessel only, (2) the secondary vessel, including duct and (3) the entire system.

Similarly to the explosion phases discussed above for test-vessels 1-3, the explosion development can be broken down into a series of phases, which roughly coincide with the times at which the flame enters and exits the duct. The explosion development may be summarised in three broad phases – *Phase 1*: initial slow development; *Phase 2*: fast flame propagation through the connecting pipe; and finally *Phase 3*: fast burning of the flammable mixture displaced into the secondary

vessel from the flame expansion in the primary vessel. These explosion phases are discussed in detail below, with specific reference to Figure 7-2.

It is noteworthy that the events in this vessel occurred so quickly that there was insufficient time for the flammable mixture displaced from the primary vessel to mix with the air in the secondary vessel. Hence, the explosion in the secondary vessel was effectively that in a displaced stratified mixture. In theory, if combustion in the primary vessel was completed prior to the flame entering the duct, then the primary vessel volume would be filled with burned gases. Based on an expansion ratio of $E = 7.4$, this would consume less than 15% of the available fuel, and consequently approximately 85% of the initial unburned mixture would have been displaced into the connecting pipe and secondary vessel, through expansion of the burned gases.

Table 7-1: Equivalent global concentration for all propane-air concentrations considered in this research if the volume of propane were homogeneously mixed throughout the entire two vessel interconnected geometry.

Initial Concentration (primary vessel)		**Global Concentration**	
%	**Φ**	**%**	**Φ**
3.0%	0.746	**0.57%**	0.142
3.5%	0.871	**0.67%**	0.166
4.0%	0.995	**0.76%**	0.189
4.5%	1.119	**0.86%**	0.213
5.0%	1.244	**0.952%**	0.237
5.5%	1.368	**1.05%**	0.260
6.0%	1.493	**1.14%**	0.284
7.0%	1.741	**1.33%**	0.332
8.0%	1.990	**1.52%**	0.379

If this were the case, and mixing of the displaced fuel-air mixture with the air within the secondary vessel had then occurred, then flame propagation within the secondary vessel would be impossible in all the tests undertaken in this work, as all the resulting mixtures would have had a concentration well below the lower

flammability limit. However, in actuality the whole volume in the primary vessel was not filled with burned gases when the flame front passed through the unburned gases within the duct and secondary vessel, and indeed considerable unburned gases remained to contribute to the main burning peak in this vessel for this explosion. Eventually the last of these unburned gases trapped in the corner regions were auto-ignited, as will be shown later. The fact, therefore, that a significant explosion did occur within the secondary vessel indicates that significant mixing could not have occurred in that vessel.

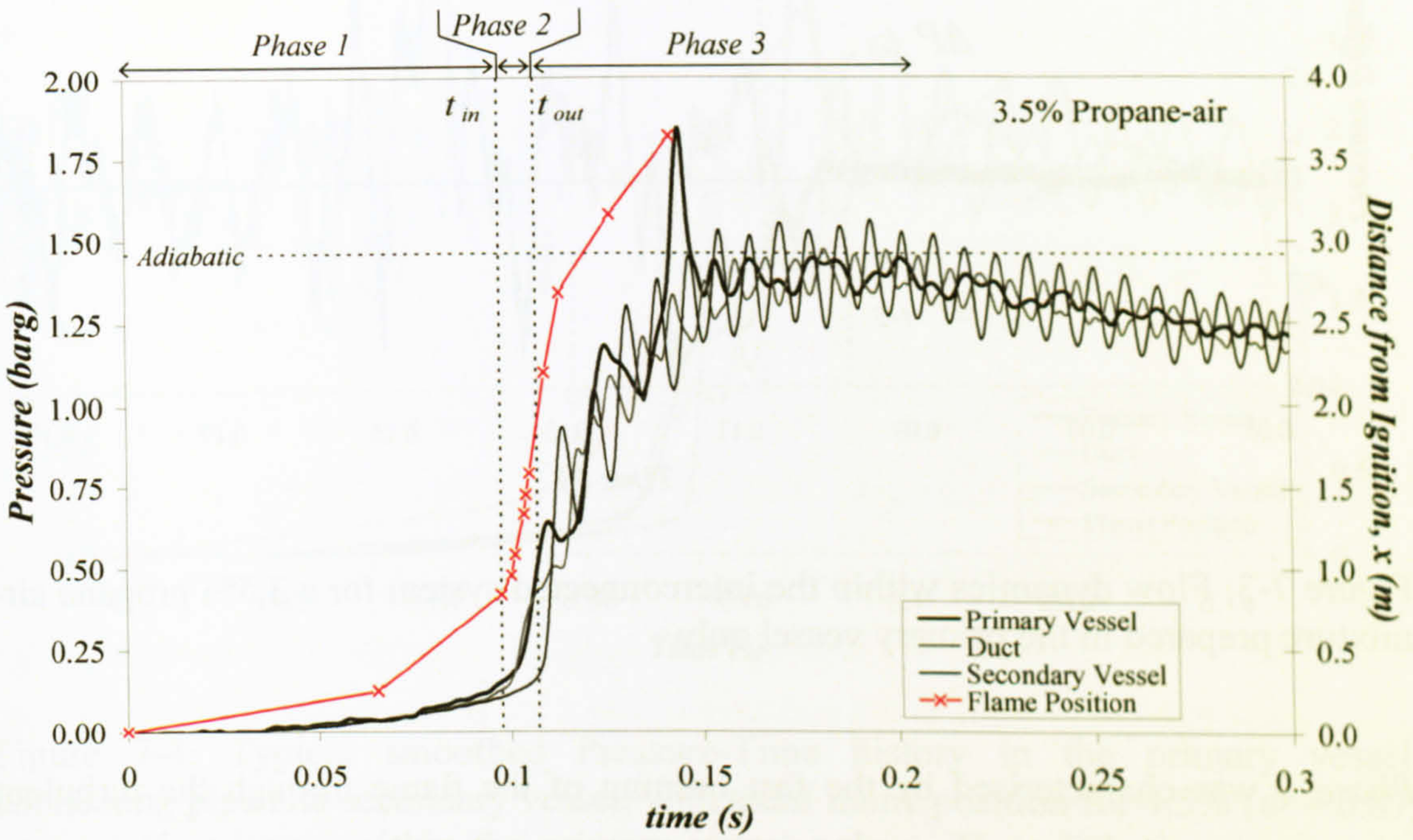

Figure 7-2: Typical smoothed Pressure-Time history in the primary vessel, connecting pipe and secondary vessel, with axial flame position for 3.5% (Φ = 1.12) propane-air present within the primary vessel only. The adiabatic pressure rise expected for this explosion is shown.

Phase 1 in Figure 7-2 is the initial flame propagation in the primary vessel, which took approximately 98 ms to travel from the ignition point to the entrance of the pipe. The average flame speed was 8.5 m/s, which was considerably greater than the laminar flame speed of about 3.5 m/s. As discussed for vented and duct vented vessels, and demonstrated in the records of additional thermocouples positioned in the radial direction of the primary vessel, the flame initially developed hemispherically from the point of ignition at the end wall. Then, as the vented flow field was set up, the flame began to elongate towards the vent (in this case the entrance to the connecting pipe). As the flame accelerated towards the vent,

unburned gases were being vented into the connecting pipe and from there into the secondary vessel. Figure 7-2 shows that during Phase 1 the pressure in the primary vessel was always greater than in the connecting pipe and the secondary vessel.

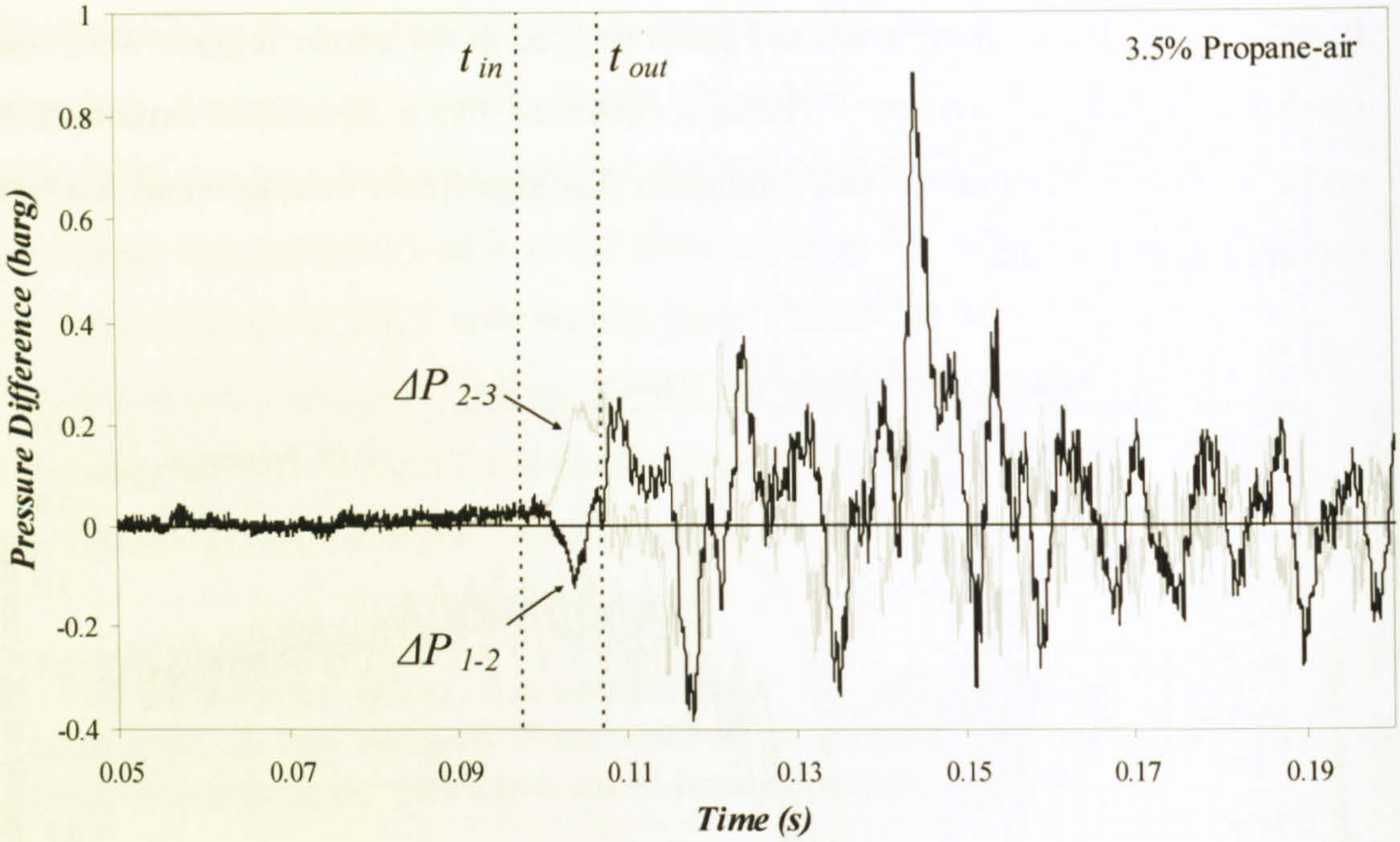

Figure 7-3: Flow dynamics within the interconnected system for a 3.5% propane air-mixture prepared in the primary vessel only.

Phase 2 was characterised by the fast burning of the flame through the turbulent unburned gases pushed ahead of the flame into the duct. It took 7.5 ms to travel through the connecting pipe at an average speed of 100 m/s. For most concentrations, as will be shown later, the flame speed in the connecting pipe reached a peak towards the end of the connecting pipe.

The occurrence of very fast flame speeds in the connecting duct of interconnected vessels was first reported by Phylaktou and Andrews [3] for the same size primary vessel, but with a secondary to primary volume ratio of 1:1, flammable mixture throughout the connected volumes and a smaller (76mm diameter) connecting pipe. Figure 7-2 and Figure 7-4 show that the pressure in the duct was always lower than or equal to that in the primary vessel until the flame discharged from the duct. Just prior to the flame emerging from the duct the pressure difference between the primary and secondary vessels was at least 0.3 bar for 3.5% (as shown in Figure 7-3)

and 0.5 bar for 4.5%, and this would indicate an unburned gas velocity exiting the duct ahead of the flame of about 180 m/s from Figure 7-2 using a 1.5 dynamic head pressure loss in the duct, and 236 m/s from Figure 7-4. These high jet velocities produce a very turbulent jet in the secondary vessel, and this gives rise to Phase 3 of the explosion.

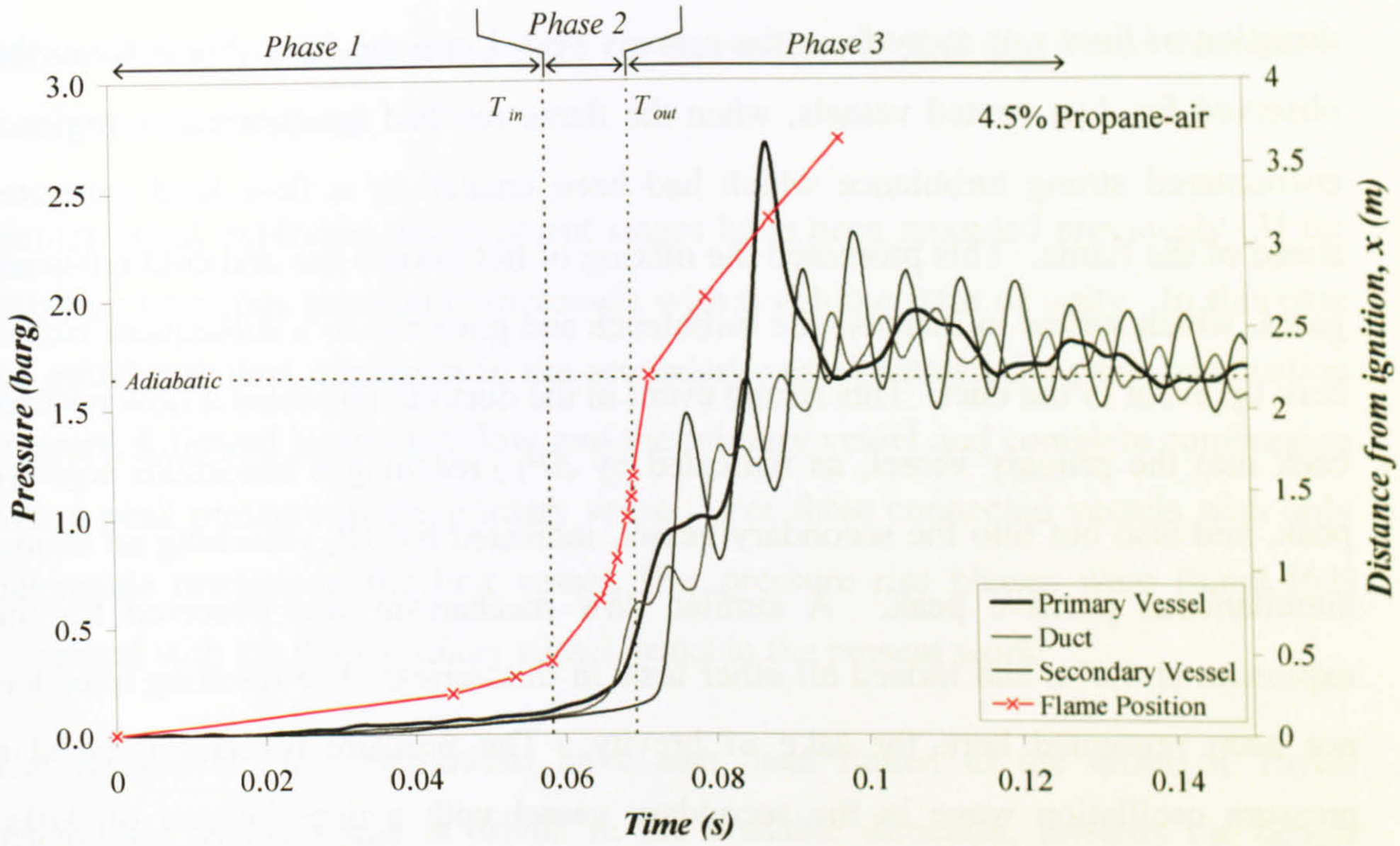

Figure 7-4: Typical smoothed Pressure-Time history in the primary vessel, connecting pipe and secondary vessel, with axial flame position for 4.5% ($\Phi = 0.87$) propane-air mixture within the primary vessel only. The adiabatic pressure rise expected for this explosion is shown.

Phase 3 in Figure 7-2 and Figure 7-4 relate to the events after the flame had left the connecting pipe and entered the second vessel as a fast turbulent flame, and ignited the flammable mixture displaced ahead of the flame from the primary vessel before there was time for the mixture to become diluted significantly by the air in the secondary vessel. This fast event caused a large pressure rise in the secondary vessel from 0.15 bar to 0.9 bar at a rate of pressure rise of around 210 bar/s for 3.5%. This equates to an 'effective' K_G ($=dP/dt_{max}V^{0.33}$) of 260 bar m/s for the secondary volume. Therefore, the turbulent acceleration of combustion in the secondary vessel was at least a factor of 2.5, given that the normal K_G for propane is 100 bar m/s. The peak pressure in the secondary vessel was then higher than in the primary vessel by

0.3 bar, and this caused a flow reversal into the primary vessel and a fall in the pressure in the secondary vessel. The primary vessel pressure then rose to 0.65 bar, due to fast combustion by the reverse jet that created turbulence in a previously laminar situation in the primary vessel. This pressure reversal can be observed in Figure 7-3. Initially, a positive gradient was established between P_1 and P_2 ($\Delta P_{1\text{-}2}$ on Figure 7-3) just prior to the flame entry into the duct, which indicates that the direction of flow was away from the primary vessel into the duct. Similarly to that observed for duct vented vessels, when the flame reached the contraction region it encountered strong turbulence which had been created by a flow field generated ahead of the flame. This promoted the mixing of hot burned gas and cold unburned gases, which served to increase the turbulence and gave rise to a subsequent violent burn up event in the duct. This strong event in the duct then initiated a flow reversal back into the primary vessel, as indicated by $\Delta P_{1\text{-}2}$ reaching a maximum negative peak, and also out into the secondary vessel, indicated by $\Delta P_{2\text{-}3}$ reaching an almost simultaneous positive peak. A similar flow mechanism was observed for the explosion at 4.5%, and indeed all other tests in this series. The resulting trace has not been presented here for sake of brevity. The pressure reversal initiated a pressure oscillation wave in the secondary vessel with a time interval of 0.01s. These pressure oscillations in the secondary vessel had a frequency corresponding to bulk oscillations.

The initial flow reversal into the primary vessel resulted in a sudden increase in the combustion rate of the unburned mixture trapped in the primary vessel, together with a decrease in the pressure in the secondary vessel as noted above. However, a large portion of unburned gas remained in the primary vessel, compressed by the expanding radial flame front, and the burning of this fuel caused the pressure within the primary vessel to continue to rise and generate flow into the secondary vessel – this second peak pressure in the primary vessel was 1.2 bar. Eventually the venting flow caused the primary vessel pressure to reduce. This second venting flow expansion into the secondary vessel caused the primary pressure to fall, until there was a sudden increase in the primary pressure to 1.8 bar, at a recorded rate of pressure rise again of around 210 bar/s. It is considered that this was either caused as a result of pressure wave interaction or the sudden autoignition of the remaining

unburned gas mixture in the corner regions of the primary vessel. Whilst this can only be determined by lining the walls of the vessel with a dampening material, it is considered that the latter was the more likely. In either case, this combustion was so fast that it created pressure piling in the primary vessel, as the maximum adiabatic overpressure for this closed system was 1.5 bar. The effect was more pronounced at 4.5%, as shown in Figure 7-4, where all three pressure traces were above the calculated adiabatic pressure expected for the volume of fuel distributed throughout the entire vessel volume.

Similar initial explosion development stages have been recorded previously [3] for fully homogeneous gases in both vessels with a volume ratio of unity. In this case the initial turbulent explosion in the secondary vessel created the peak combustion pressure, followed by reverse flow into the primary vessel and complete combustion with a peak pressure in the primary vessel. For three connected vessels with only flammable mixture in the first vessel, five pressure rise phases were found [62] compared with the three primary vessel peaks in the present work.

The Helmholtz bulk oscillations have also been linked to the onset of Taylor instabilities as the flame is driven in the unstable direction, towards the denser medium in the vessel [39]. This effectively increases the surface area of the flame by enhancing flame wrinkling, and thereby increases the severity of the explosion. In addition to this, the travelling shock wave ahead of the flame can be reflected by the end wall of the secondary vessel and potentially travel back to the primary vessel. The calculation of the Helmholtz frequency in this vessel will be discussed in more detail later.

7.2.2. Maximum Pressure

Figure 7-5 shows the maximum pressures in the primary and secondary vessels, based on smoothed pressure time records. The pressure in the primary vessel was only greater than that in the secondary vessel when the rapid pressure rise or pressure spike, shown in Figure 7-2 and Figure 7-4, was included. The thin dotted line represents the maximum peak pressure recorded for the pressure spike in the primary vessel. The pressure spike was present for concentrations between 3.2% and 5.5%

(Φ = 0.80 and Φ = 1.37) inclusive, and this was only greater than the peak pressure in the secondary vessel for primary vessel mixtures leaner than Φ=1.3. Figure 7-5 shows that for all concentrations, the main pressure peak, ignoring the pressure 'spike' in the primary vessel, was highest in the secondary vessel. For rich mixtures in the primary vessel the secondary vessel pressure was much greater than any pressure in the primary vessel. This was because the initial rich premixed flame had a slow rate of flame propagation and a low peak pressure, but once this rich mixture vented into the air of the secondary vessel, some of this air mixed in and the mixture burnt locally closer to stoichiometric, and hence all of the energy in the fuel was released instead of only part of the energy due to lack of oxygen in the primary vessel.

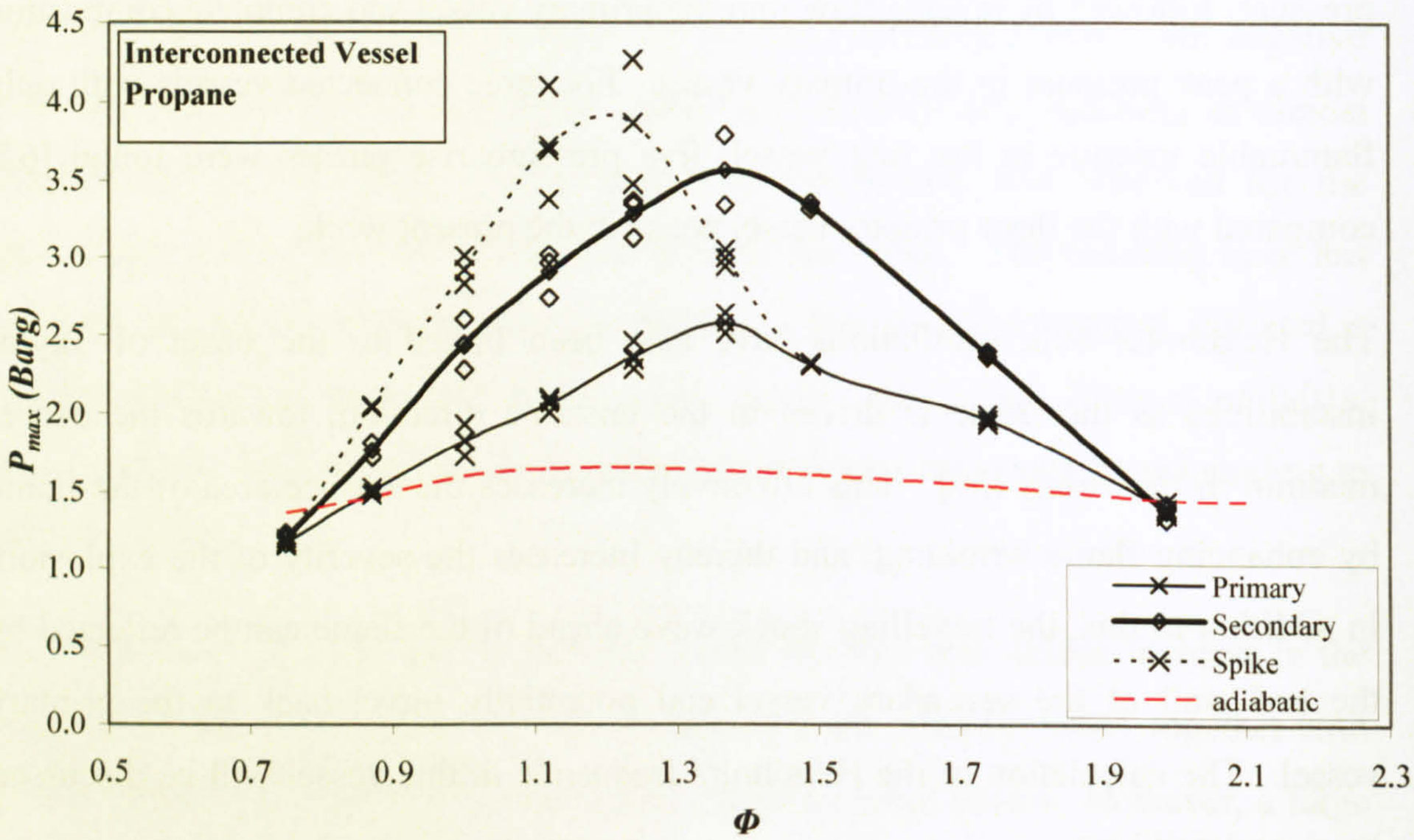

Figure 7-5: Maximum pressures recorded in the primary and secondary vessels with respect to equivalence ratio. Calculated system adiabatic pressures are shown.

7.2.3. Pressure Piling

In order to investigate whether the phenomenon of pressure piling occurred in partially filled systems, the adiabatic constant volume maximum pressure was calculated and is shown in Figure 7-5. The calculation used the initial mixture

concentration and the gas reaction thermodynamic equilibrium package GASEQ [137]. Figure 7-5 shows that, for all concentrations between 3.5% and 7.0% (Φ = 0.87 - 1.74), there was evidence of the pressure piling phenomenon occurring in the primary *and* secondary vessels. This shows that a pocket of gas-air mixture can lead to a severe explosion that would not occur if the same volume of flammable gas was uniformly mixed throughout the entire test vessel volume.

7.2.3.1. Rates of Pressure Rise

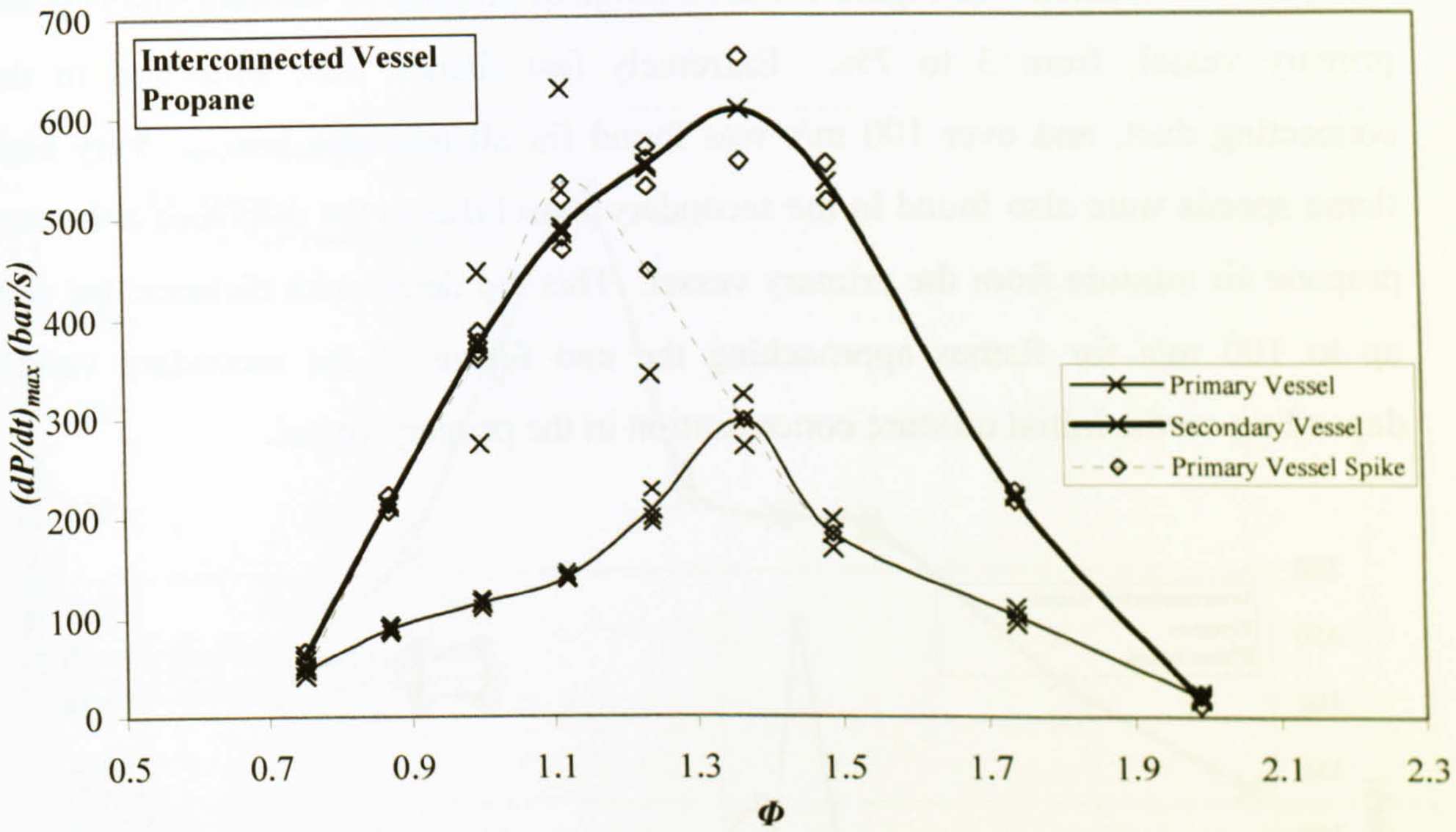

Figure 7-6: Maximum recorded rates of pressure rise in the primary and secondary vessels with respect to equivalence ratio.

Figure 7-6 shows the maximum rate of pressure rise $(dP/dt)_{max}$ recorded in each section of the vessel. The values presented are based upon the differentiation of the smoothed pressure time records. The highest recorded $(dP/dt)_{max}$ were mainly in the secondary vessel, except for those concentrations at which the pressure spike occurred in the primary vessel. These results can be converted to the K_G parameter, and the scale 100-600 in bar/s becomes 73-440 bar m/s for the secondary vessel volume, or 80-480 bar m/s based on the whole volume. These high values of K_G compared with 100 bar m/s for a laminar spherical vessel explosion indicate the high

levels of turbulence that are created by the connecting duct high velocity discharge jet in the secondary vessel. The highest rates of pressure rise, particularly for rich mixtures in the primary vessel, were in the secondary vessel. This was due to the high induced turbulence levels in the secondary vessel caused by the high velocity jet emerging from the connecting duct.

7.2.3.2. Flame Speed

The flame speed is shown – as a function of distance from the end flange in which the spark was located – in Figure 7-7 for a range of propane air concentrations in the primary vessel, from 3 to 7%. Extremely fast flames were measured in the connecting duct, and over 100 m/s was found for all mixtures tested. Very high flame speeds were also found in the secondary vessel due to the displaced unburned propane air mixture from the primary vessel. This did decay with distance, but was up to 100 m/s for flames approaching the end flange of the secondary vessel, depending on the initial mixture concentration in the primary vessel.

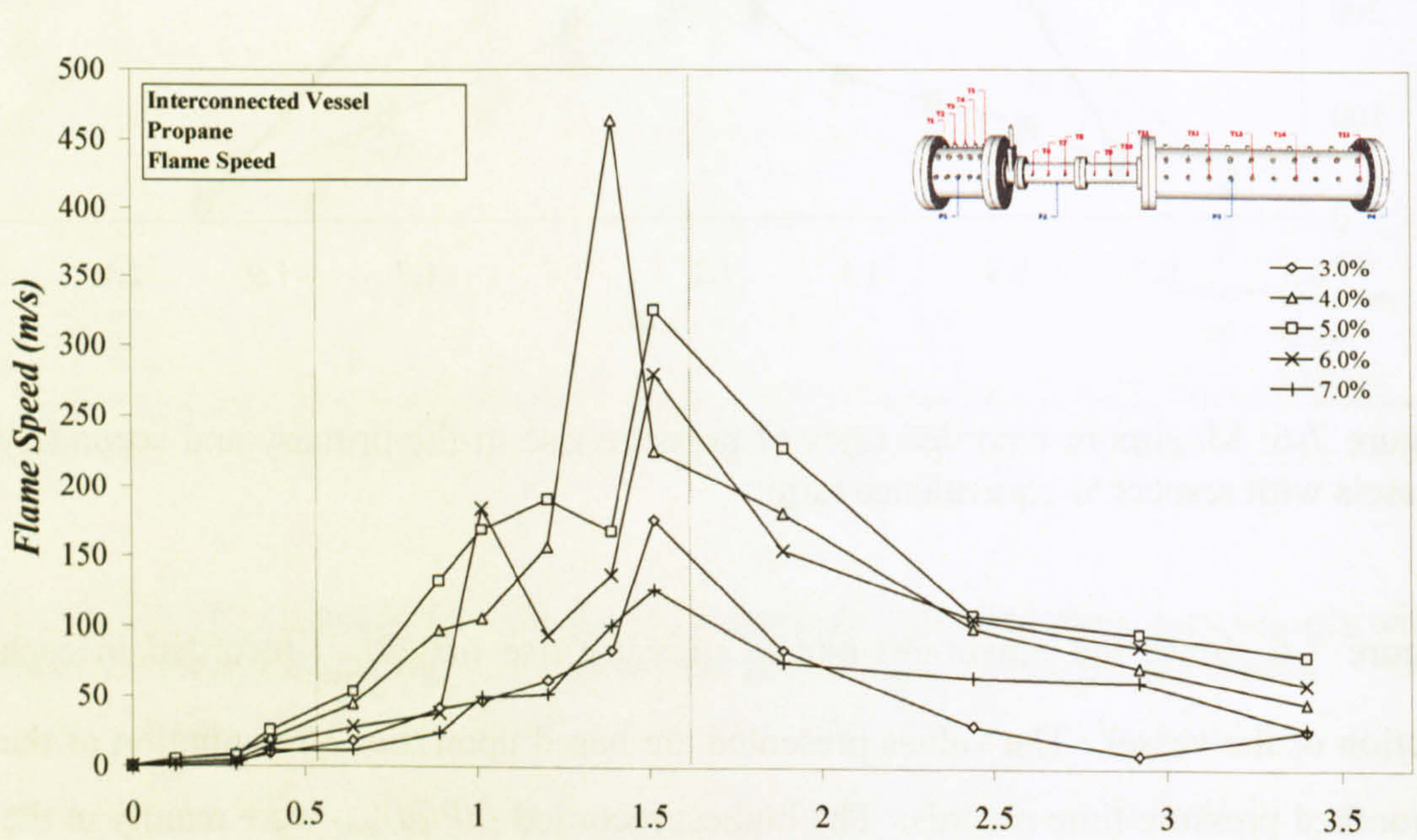

Figure 7-7: Flame speeds recorded along the vessel for initial propane-air concentrations of between 3.0% and 7.0% (Φ = 0.746-1.741).

The maximum recorded flame speed in the connecting duct is shown as a function of propane concentration in the primary vessel in Figure 7-8. This shows a peak flame speed for 4.5 % propane or Φ = 1.119, which is where the maximum flame speed occurs in the primary vessel for premixed mixtures. This flame speed at 600 m/s is extremely high and hence close to the flame speed at which transition to detonation might occur. For lean and rich mixtures the flame speed remained very high at >100 m/s for all but the 8% (Φ=2) mixture. Unburned gas was displaced ahead of these fast flames at 87% [(E-1)/E] of the flame speed if the explosion was adiabatic, and lower if heat losses from the burned gases were significant. It was these very high unburned gas jet velocities that created the turbulence in the secondary vessel.

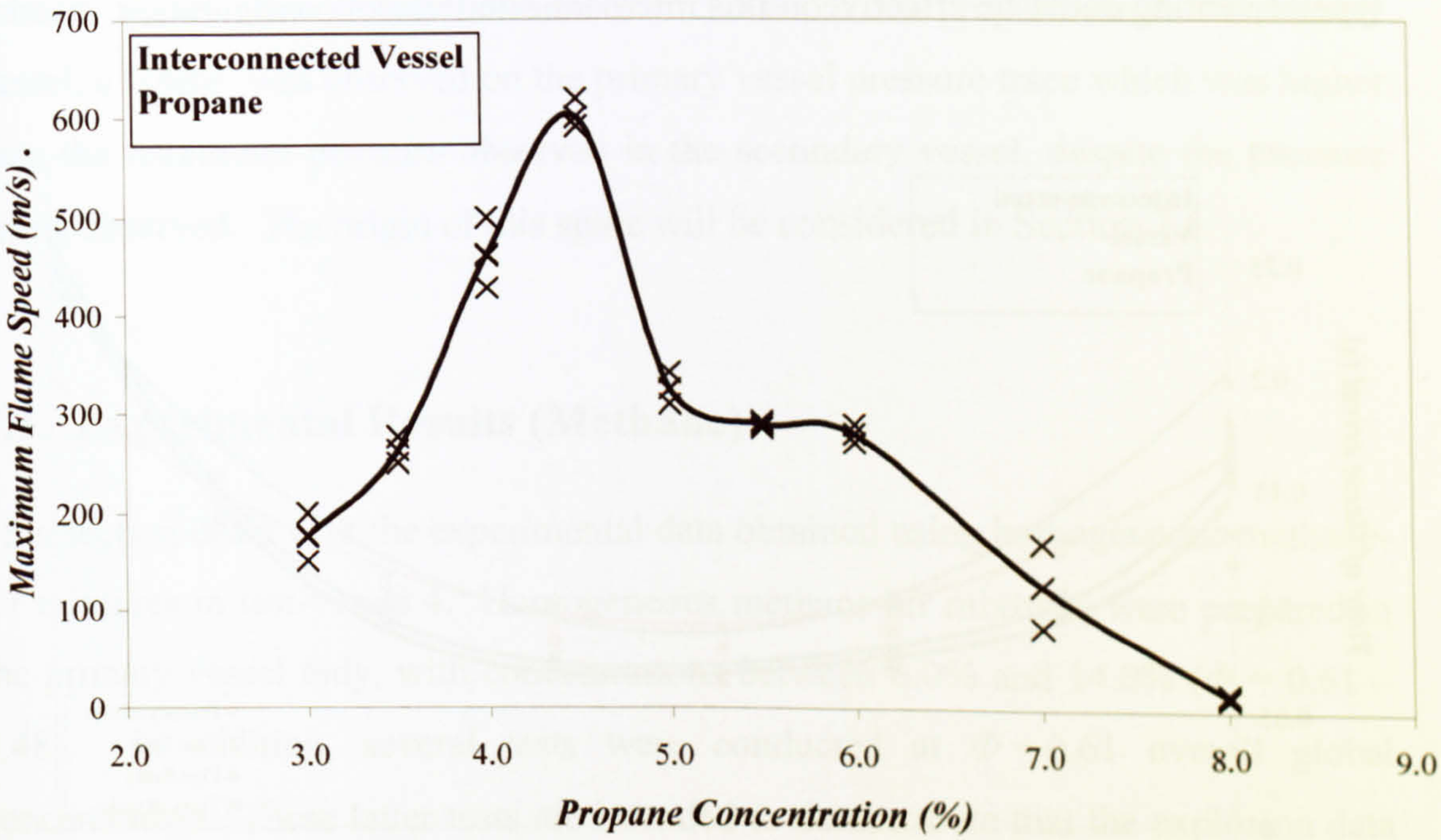

Figure 7-8: Maximum flame speed in the duct as a function of initial propane concentration in the primary vessel.

The fast flame speeds were also reflected in the time of flame arrival data at positions in the two vessels and connecting duct. These are shown in Figure 7-9, which shows that the explosion time was dominated by the slow flame propagation in the primary vessel in Figure 7-7. Once the flame enters the pipe everything else happens very fast. Despite the primary vessel being less than 20% of the total vessel volume, and only 14% of the total vessel axial length, the length of time the flame

took to travel from the end wall ignition to the vent was typically of the order of 80% of the total combustion time.

It is clear that if this type of explosion hazard is to be protected against then the explosion must be detected and extinguished in the primary vessel, preferably using suppression systems. If venting of the primary vessel was used, then the burst pressure must be set to vent prior to the entry of the flame in the connecting duct. Figure 7-2 and Figure 7-4 show that the overpressure was approximately 0.1 bar when the flame entered the vent duct. Thus a vent burst pressure would have to be set at around 50 mbar if it was to be effective in helping to mitigate this type of explosion. However, further research would be necessary to determine whether this type of venting could be effective in this interconnected vessel configuration.

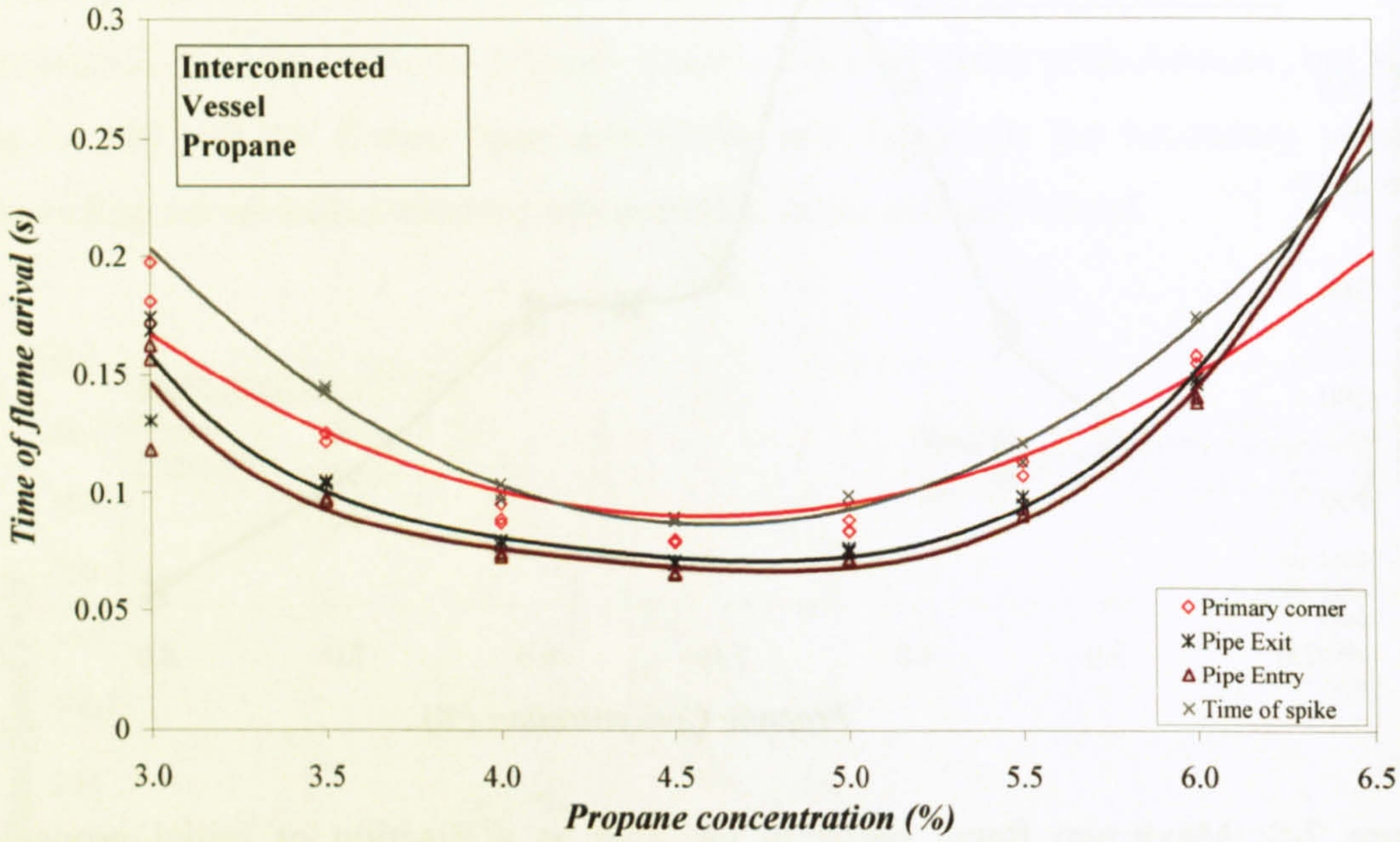

Figure 7-9: Time of flame arrival at various points along the vessel as a function of propane concentration.

7.2.4. Summary (Propane)

The 4:1 volume ratio employed in this section ensured that the simulation of a leak in the primary vessel resulted in mixtures that were not flammable if the air in the secondary vessel mixed with the displaced unburned gases from the first vessel. The

results showed that very severe explosions in the secondary vessel occurred due to the displaced unburned gases from the primary vessel, and therefore this indicated that the fast turbulence combustion of the displaced flammable gases occurred before the displaced gases could mix with the secondary vessel air, despite the overall concentration being less than 1.5% propane-air in all concentrations investigated.

There was evidence of reverse flow from the secondary vessel explosion back into the primary vessel, and subsequent turbulence generation and fast flame development in the primary vessel. Further expansion of these fast primary flame gases into the secondary vessel eventually resulted in a further reverse flow into the primary vessel. In concentrations between 3.5 and 5.5% propane-air in the primary vessel, a 'spike' was observed on the primary vessel pressure trace which was higher than the maximum pressure observed in the secondary vessel, despite the pressure piling observed. The origin of this spike will be considered in Section 7.6.

7.3. Experimental Results (Methane)

This section deals with the experimental data obtained using homogeneous methane-air mixtures in test-vessel 4. Homogeneous methane-air mixtures were prepared in the primary vessel only, with concentrations between 6.0% and 14.0% (Φ = 0.61 – 3.48). In addition, several tests were conducted at $\Phi = 0.61$ overall global concentration. These latter tests are intended to demonstrate that the explosion data presented here may be compared against the explosion severities for methane-air mixtures reported in literature, where the entire vessel is filled with the same flammable mixture. In all cases, the initial starting pressure was approximately 1.013 bar. This section provides details of the general explosion development of a methane-air mixture in the current geometry, flame development, maximum pressures attained, rates of pressure rise and flame speed, followed by possible explanations of the phenomena observed. The results in this Section have previously been published [134, 135].

7.3.1. General Explosion Development

It is worth mentioning at the outset that while individual test results are presented here for clarity, the results explained are indicative of the trends displayed for this vessel. In the main, results for the 10% (Φ = 1.06) methane-air mixture will be presented since this produced the worst case of the concentrations investigated, and also provided the clearest results. Where lower reactivity mixtures differ in ways other than magnitude from the results presented, this will be described. The results in this section will predominantly focus on the results obtained from the partially-filled geometry, with the reference test of 6% (Φ = 0.61) throughout.

Table 7-2: Equivalent global concentration for all methane-air concentrations considered in this research if the volume of methane were homogeneously mixed throughout the entire two vessel interconnected geometry.

Initial Concentration (primary vessel)		**Global Concentration**	
%	**Φ**	**%**	**Φ**
6.0%	0.634	1.142%	0.120
7.0%	0.739	1.333%	0.140
8.0%	0.845	1.523%	0.160
9.0%	0.950	1.714%	0.180
10.0%	1.056	1.904%	0.200
11.0%	1.162	2.094%	0.220
12.0%	1.267	2.285%	0.241
13.0%	1.373	2.475%	0.261
14.0%	1.478	2.761%	0.281

For this geometry, both fully-filled and partially-filled cases produced higher pressures in the secondary vessel. Figure 7-10 shows a comparison between the pressure development for different concentrations in the partially-filled explosion tests as a function of time, while Figure 7-11 shows a comparison of the pressure development for fully- and partially-filled tests at Φ=0.61 only. It is immediately apparent that even at 'worst case' methane (Φ=1.06) the maximum pressure reached in the second vessel was less than that of the fully-filled geometry at Φ=0.61 by a

factor of approximately 2. A comparison of Φ=0.61 partially-filled to Φ=0.61 fully-filled methane-air showed a somewhat more significant increase of approximately 11 times (best illustrated in Figure 7-11). Such large differences can be expected if the overall concentration present in the vessel is considered. For the partially-filled tests, Φ=1.06 methane-air mixture concentrated in the smaller chamber would equate to a 'global' concentration of Φ=0.194 (less than 2%) if an equivalent amount of fuel was mixed into the whole interconnected volume. This would be below the lower flammability limit and therefore pose no risk of explosion as a premixed gas. Therefore, this indicates that where a leak is formed in part of a connected geometry, it can be more dangerous than simple diffusion calculations may indicate. For reference, the concentrations investigated in this section along with the equivalent global concentration and equivalence ratio are shown in

Initial Concentration (primary vessel)		**Global Concentration**	
%	**Φ**	**%**	**Φ**
6.0%	0.634	1.142%	0.120
7.0%	0.739	1.333%	0.140
8.0%	0.845	1.523%	0.160
9.0%	0.950	1.714%	0.180
10.0%	1.056	1.904%	0.200
11.0%	1.162	2.094%	0.220
12.0%	1.267	2.285%	0.241
13.0%	1.373	2.475%	0.261
14.0%	1.478	2.761%	0.281

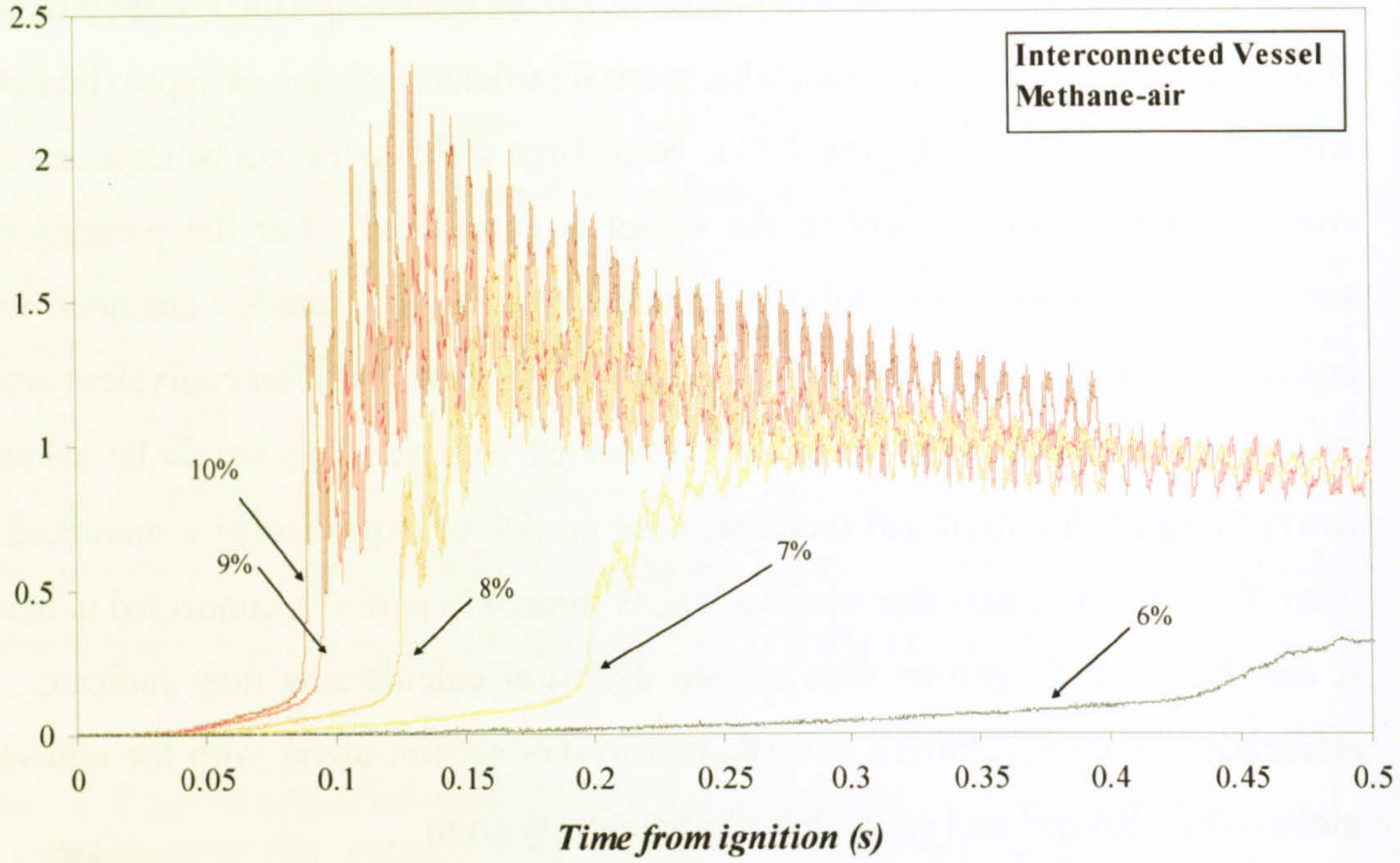

Figure 7-10: Pressure observed (unsmoothed) in the second vessel as a function of time for partially-filled vessels

Maximum pressure differences between fully-filled and partially-filled can be therefore explained relating to the extra fuel available to burn once the flame has entered the second vessel. In this interconnected geometry an increased initial pressure within the second vessel developed as the compressed unburned gases were pushed ahead of the flame. These gases were then ignited as the flame jet exited the pipe (at a time ~T_{out}) into the second vessel and created a greater explosion. As the pressure increased, the flow reversed back into the primary vessel which increased the turbulence levels in the remaining unburned mixture, contributing to the main pressure peak in this vessel. At this point an oscillating flow between the two vessels was established, in a similar manner to that discussed for propane above.

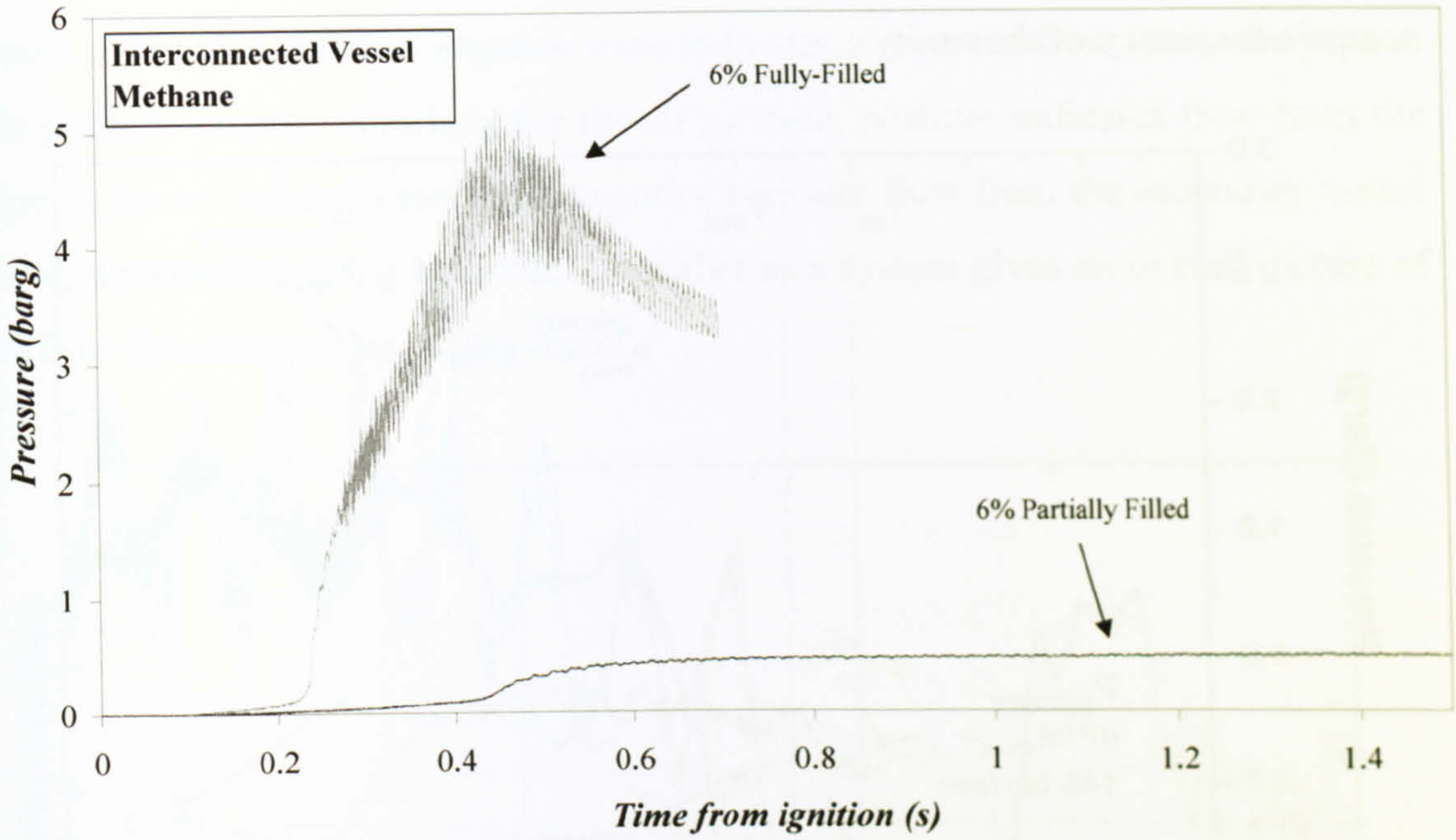

Figure 7-11: Pressure recorded (smoothed) in the second vessel as a function of time for 6% methane

Figure 7-10 and Figure 7-11 also illustrate the time delay between ignition (T_0) and detection of the major pressure increase. This shows the time decreasing with increasing concentration for the partially-filled, also illustrating the fact that 6% fully-filled is approximately 2x faster to react; (roughly equal to that of the 7% partially filled mixture), both having a time delay of ~0.217 seconds, and also beginning with roughly the same initial rate of pressure rise *(dP/dt)*.

In the following figures, the lines marked T_{in} and T_{out} correspond to the measured time at which the flame enters and exits the connecting pipe, measured using the first and last thermocouples in the duct.

The pressure interaction between vessels is a major factor in interconnected vessel geometry (and also in industrial installations where the vessel is entirely enclosed and able to withstand the pressure generated by the explosion). In the current research, an oscillating flow was set up very quickly. The oscillations present here in the second vessel (see Figure 7-12) are a function of the acoustic interaction set up in the vessel [43]. Furthermore, a similar frequency oscillation was observed

between vessels, and both can be attributed to the Helmholtz fundamental system acoustic frequency of the cavity.

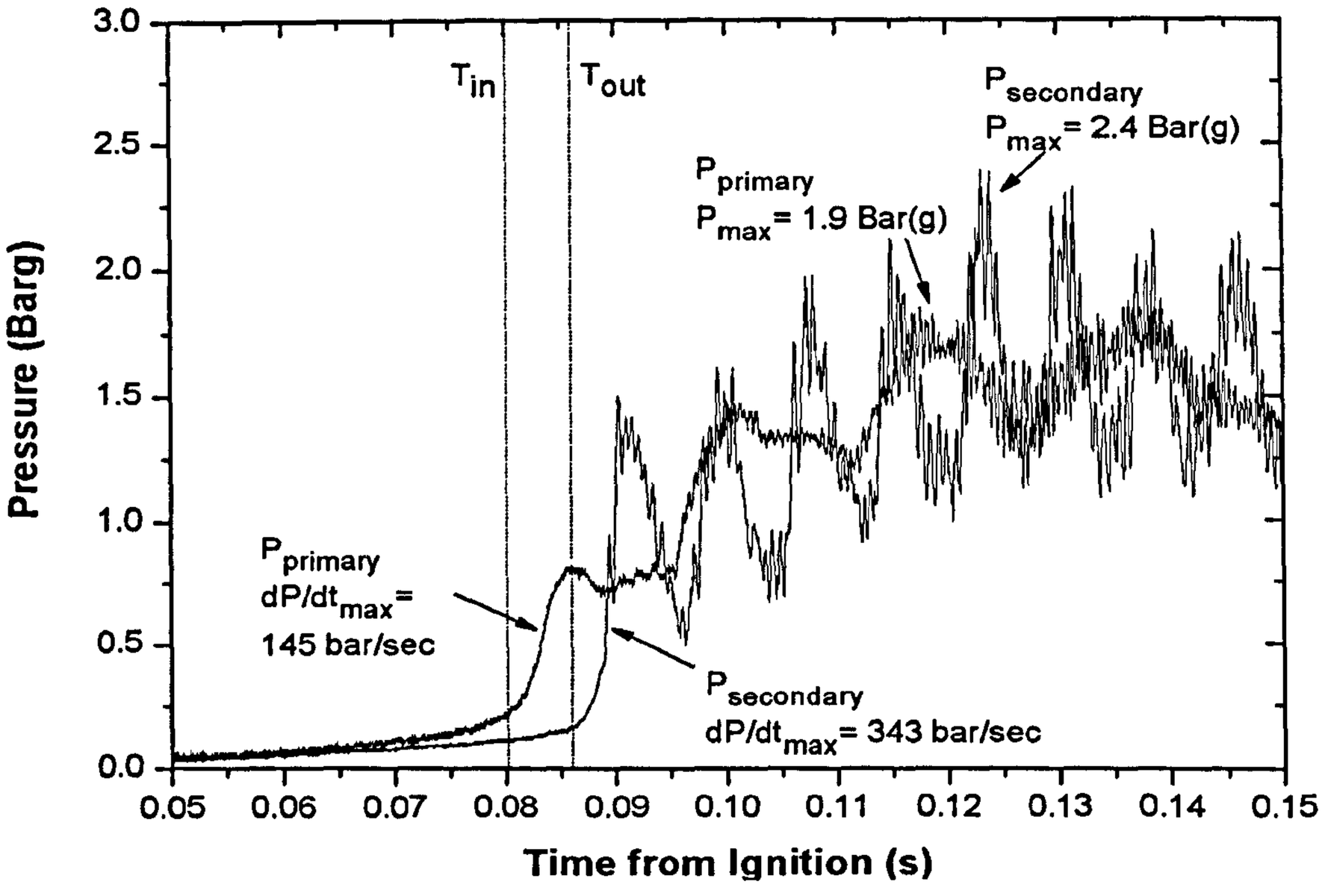

Figure 7-12: Pressure-time signals for primary and secondary vessels at 10% methane-air

Figure 7-12 illustrates a typical pressure scenario where primary and secondary vessels are interacting in a Φ=1.06 methane-air mixture. It is immediately apparent that the explosion is more severe in the secondary vessel than in the primary; *dP/dt* data illustrated here indicate a faster rate in the second vessel of the order of 2.4. This is a similar situation to the fully-filled geometries identified.

Overall, there is only 0.5 bar difference in maximum pressures observed at this concentration. However, the difference in frequency is quite apparent. For this vessel, the flow between vessels has been considered by focussing on pressure histories recorded in the primary vessel (P_1), connecting pipe (P_2) and secondary vessel (P_3). The differences between the recorded pressures allow an indication of flow between the major areas of the vessel; these differences are illustrated in Figure 7-13. The pressure difference between P_1 and P_2 and between P_2 and P_3 are displayed as ΔP_{1-2} and ΔP_{2-3} respectively.

A positive measurement along the $\Delta P_{1\text{-}2}$ trace indicates a flow from the primary vessel to the pipe, while a negative trace indicates a reversed flow (from the pipe to the primary vessel). Similarly for the $\Delta P_{2\text{-}3}$ trace, positive indicates flow from the pipe to the secondary vessel and a negative pressure flow from the secondary vessel to the pipe. Considering both traces together as a system gives an overall picture of the flow dynamics set up in this vessel.

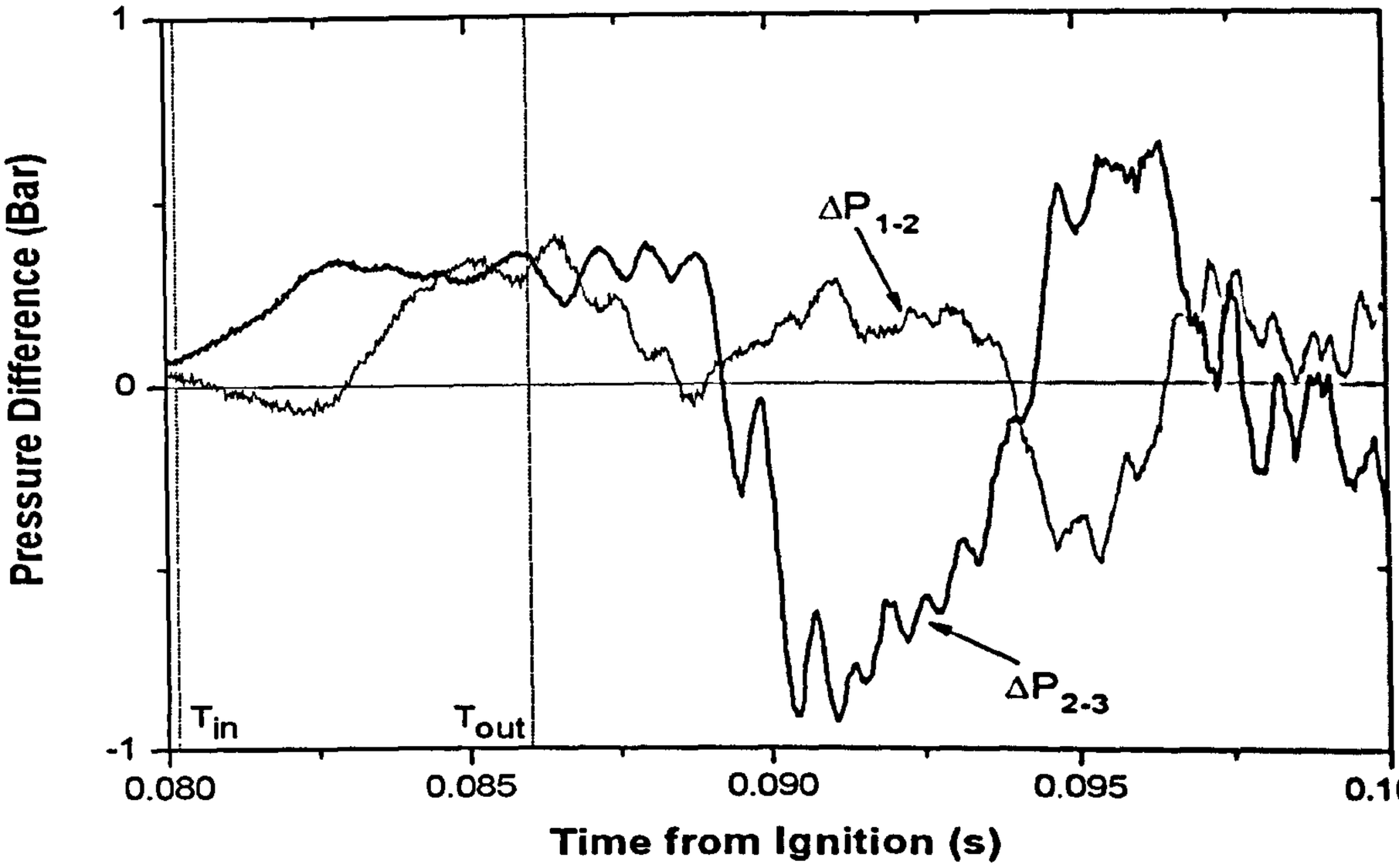

Figure 7-13: Flow interaction for 10% methane partially filled

During the time when the flame was in the connecting pipe, the pressure records for the two vessels indicated that the pressure rose much earlier in the primary vessel, with little going on in the secondary vessel until the flame jet had entered, igniting the unburned material pushed ahead of the flame through the connecting pipe (Figure 7-12). A maximum rate of pressure rise was observed in the primary vessel at a point where the flame was approximately half way through the pipe. This maximum corresponded to a significant increase in flow from the pipe into both the primary and secondary vessels (shown in Figure 7-13). This increased flow was a product of a fast combustion of the highly turbulent mixture in the connecting pipe, which resulted in strong outflows from the pipe in both directions – towards the secondary vessel, and more importantly towards the primary vessel, causing a strong disturbance/mixing in the primary vessel where combustion up to this point had been

slow (laminar or near-laminar), resulting in the fast pressure rise recorded in the primary vessel. Following this, a strong flow was re-established throughout the system in the direction of the secondary vessel, which coincided with the flame exiting the connecting pipe. Beyond this point there was a strong explosion in the secondary vessel, as the flame ignited the turbulent mixture (at $T \sim 0.9$seconds) giving rise to a $(dP/dt)_{max} \sim 344$ Bar/s in the secondary vessel.

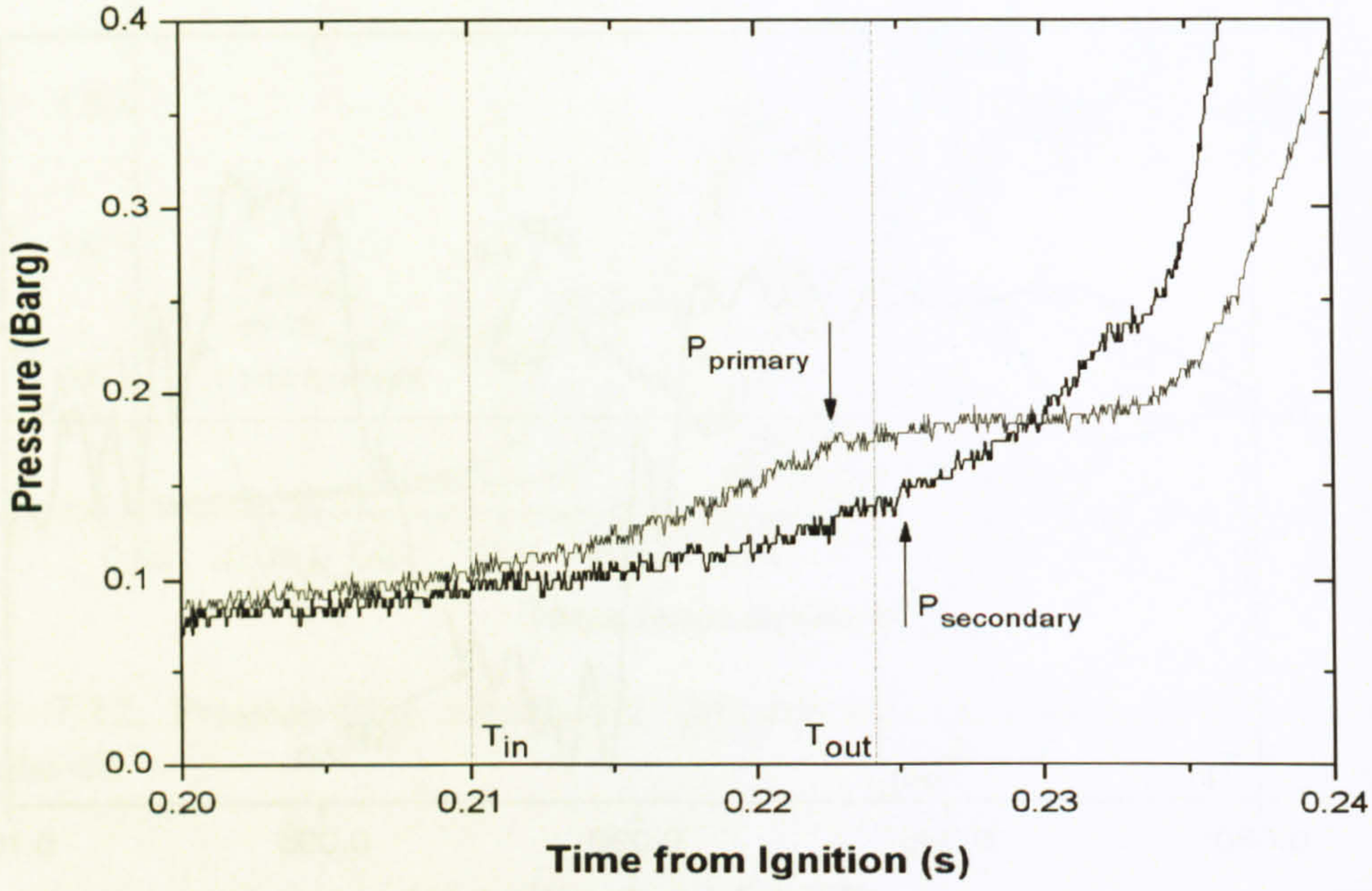

Figure 7-14: Flow interaction for 6% methane fully filled.

From the results presented it is apparent that on the whole there is a major difference in maximum pressures attainable between a partially- and a fully-filled vessel, while more minor differences occurred in total explosion time and order of reactions. The main point is that there is a prominent peak visible in the primary vessel before the first major rise in pressure in the secondary vessel; for fully-filled vessels, this has been shown to be much less pronounced [3] (a trend also illustrated in this work for Φ=0.61 fully-filled scenario – see Figure 7-12 and Figure 7-14). It is also apparent that for closed vessel geometries, an oscillating flow of frequency close to the fundamental Helmholtz bulk frequency of the cavity was generated.

7.3.2. Maximum Pressure

In the partially-filled vessel, a flammable mixture was pushed ahead of the flame into essentially an 'air-space', which introduced oxygen into the system forcing leaner combustion. For the fully-filled vessel, the unburned mixture was forced ahead into a flammable region of the same concentration, allowing more efficient combustion through the pre-compressed and turbulent mixture formed in the secondary vessel, which produced a greatly increased pressure rise. The maximum pressure observed in the second vessel is important as it indicates that the fuel-air mixture that was pushed ahead of the flame into the second vessel was ignited so quickly that there was insufficient time for it to become diluted with the excess oxygen in the secondary vessel, which should have forced such combustion to be lean.

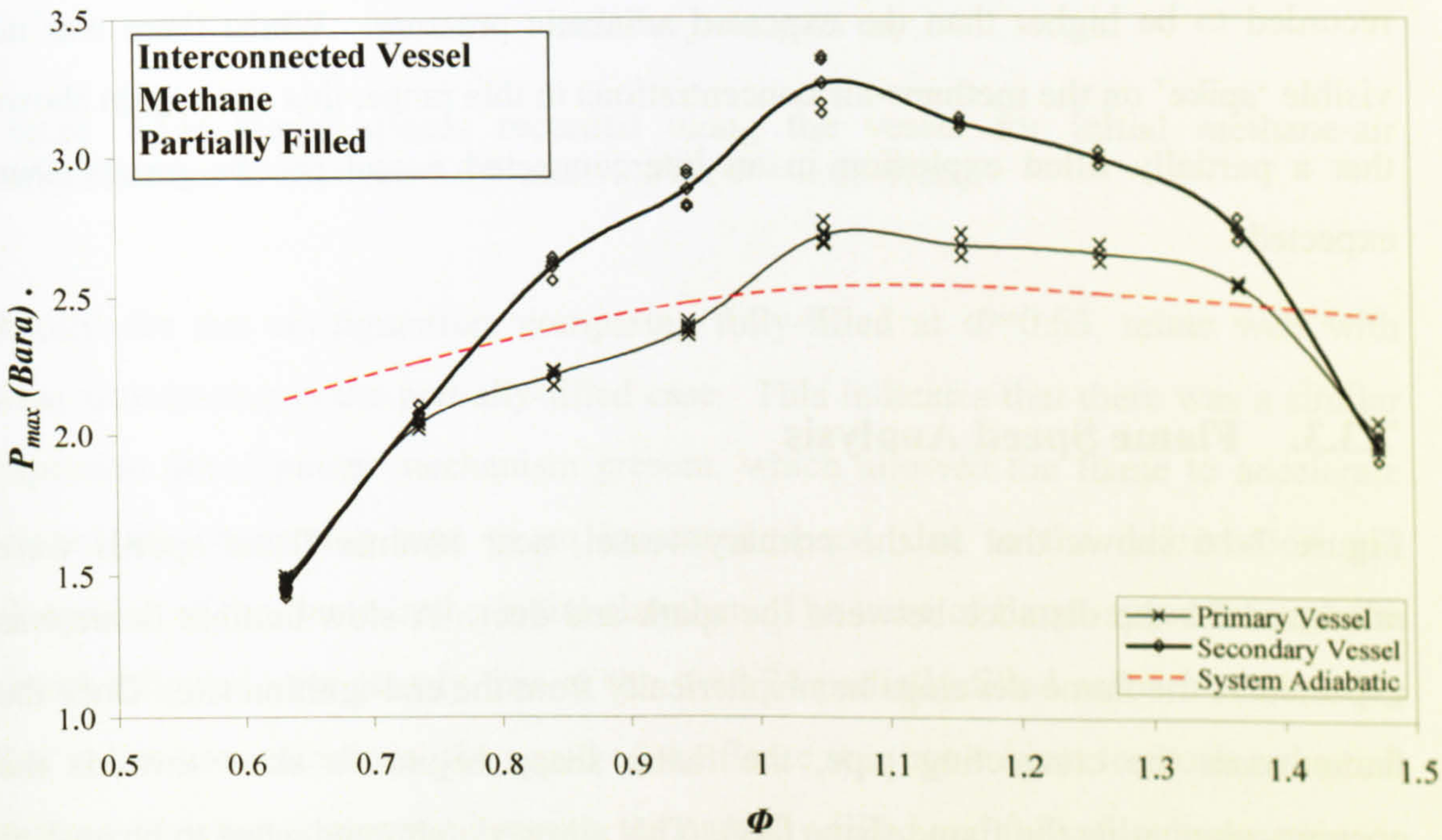

Figure 7-15: Maximum pressure measured in the secondary vessel compared to calculated system adiabatic.

In order to investigate whether the pressure piling phenomenon occurs in methane partially-filled systems as well, the adiabatic constant volume maximum pressure expected in the system was calculated and compared to the maximum measured in Figure 7-15. The calculation method of the expected adiabatic pressure used the

initial mixture concentration, and the gas reaction thermodynamic equilibrium package GASEQ [137] as described previously.

The experimental pressures reported are those of the highest oscillatory peak (as shown in Figure 7-12), and this may be too conservative as such very short transient pulses may not be significant with regard to structural response, however this is counter-balanced by the assumption of adiabaticity in the theoretical pressure calculation. So both lines in Figure 7-15 may be higher than they should be for practical systems. Their relative magnitudes, however, are not expected to change significantly if more realistic values are used. Therefore, Figure 7-15 clearly suggests that pressure piling in the secondary vessel is a feature of partially-filled linked geometries for concentrations between 8% and 13% (Φ=0.85 – 1.37), despite the dilution that the gas mixture may experience as it is pushed/mixed through the system. Furthermore, between 10% and 13%, pressures in the primary vessel were recorded to be higher than the expected adiabatic pressure. Whilst there was no visible 'spike' on the methane-air concentrations in this range, this once again shows that a partially filled explosion in an interconnected vessel can be greater than expected.

7.3.3. Flame Speed Analysis

Figure 7-16 shows that in the primary vessel, near laminar flame speeds were measured for the distance between the spark and duct. A slow laminar flame was expected as the flame develops hemispherically from the end-ignition site. Once the flame nears the connecting pipe, the flame shape begins to skew towards the opening, elongating the flame shape [43]. This allowed unburned gases to be pushed both ahead of the flame through the connecting pipe, and at increased pressure into the corners of the primary chamber to be burned as the major contributor to the bulk of the pressure in this vessel once the flame has passed T_{out}. This could explain how it was possible to get such a large increase in pressure back into the initial chamber once the flame had exited the pipe in the opposite direction. This phenomenon of flame skewing is often reported for both rear and central ignition in vented vessels

[8, 43, 60] which, in initial stages while flow is still laminar, will behave as an interconnected vessel before venting takes effect.

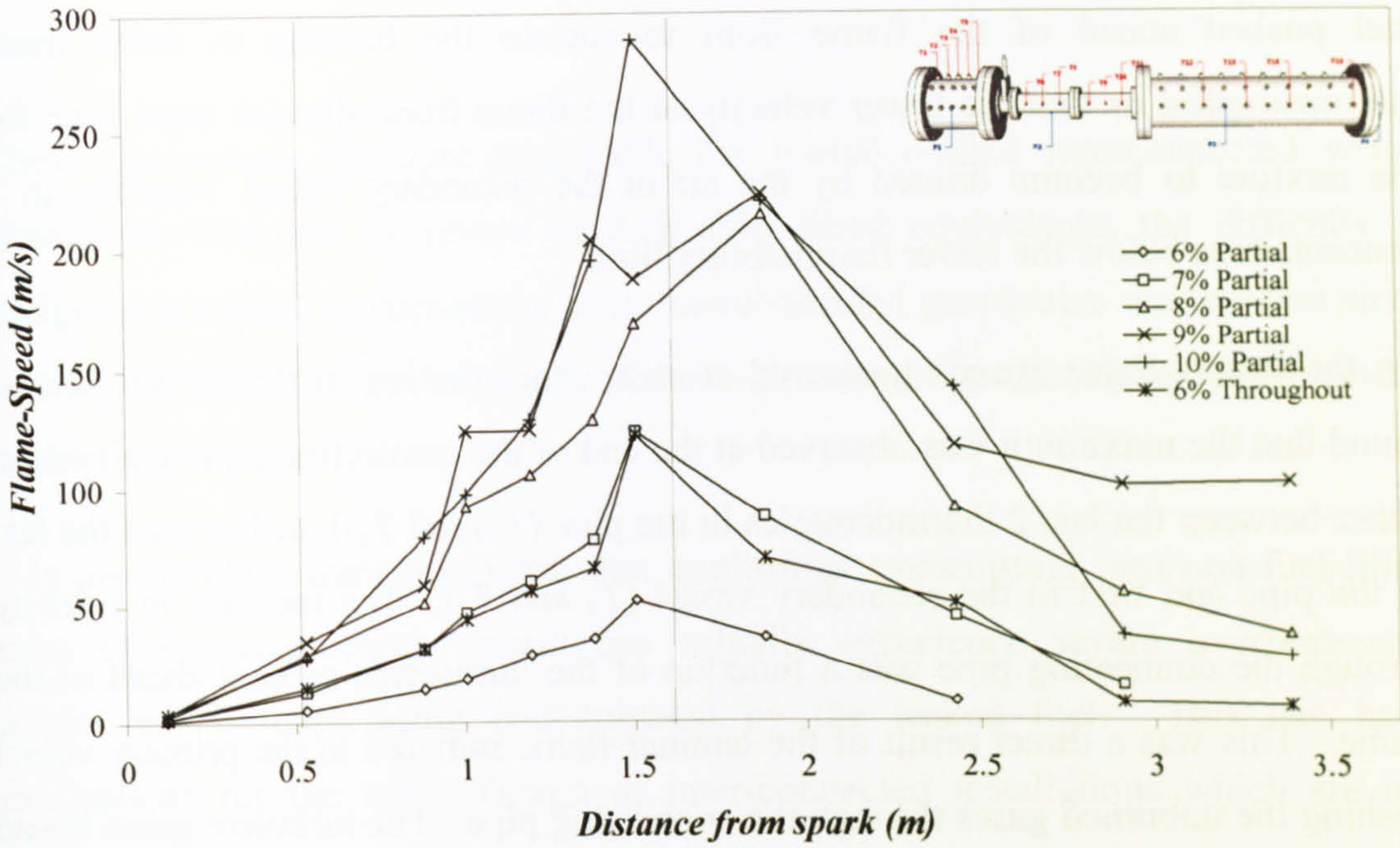

Figure 7-16: Flame speeds recorded along the vessel for initial methane-air concentrations of between 6.0% and 10.0% (Φ = 0.63-1.06).

Results for this configuration, comparing fully-filled at Φ=0.63, relate well with what is occurring in the partially-filled case. This indicates that there was a similar explosion development mechanism present, which allowed the flame to accelerate toward the connecting pipe at an increased speed, due to the deformation and elongation of the flame in the initial chamber. The trace of flame-speed through the vessel followed very closely that of the Φ=0.74 partially-filled scenario, indicating that at low concentrations, the speed of the flame was not subject to much reduction in intensity when comparing between the partially-filled and fully-filled scenarios.

Towards the end of the secondary vessel thermocouple responses were difficult to distinguish for lean concentrations, therefore for $\Phi \leq 0.72$ flame speeds were not shown towards the end of the secondary vessel. It is interesting to note that this is also the concentration at which the pressure piling phenomenon was absent. However, in the fully-filled case the response times were stronger at this point allowing a reading to be ascertained. Possible reasons for this could be that the lean concentrations produce slower flame fronts and so are much more susceptible to

buoyancy effects, which can lift the flame above the line of the exposed junction thermocouples placed along the centre of the secondary vessel. Additionally, it is possible that in the lower concentration partially-filled tests, there was not sufficient fuel pushed ahead of the flame front to sustain the burning to reach these thermocouples, or that the lower velocity of the flame front allowed more time for the mixture to become diluted by the air in the secondary vessel, resulting in a concentration below the lower flammability limit.

On the fastest flame speeds measured at each concentration in this vessel, it was found that the maximum was observed at the end of the connecting pipe in all cases, either between the last 2 thermocouples in the pipe (T_{10} and T_{11}), or between the last in the pipe and first in the secondary vessel (T_4 and T_5). The increase in velocity through the connecting pipe was a function of the turbulence created ahead of the flame. This was a direct result of the laminar flame initiated in the primary vessel pushing the unburned gases through the connecting pipe. The turbulent gases ahead of the flame mixed with the cool air in the secondary vessel, creating a more turbulent mixture, and also having an accelerating effect on the flame front as the flame became further fragmented and torn apart by the turbulence, effectively increasing the surface area of the flame and allowing the speed of the flame to further increase.

Flame-speeds dropped off rapidly in the secondary vessel as the flame entered a region which was less turbulent and had lower fuel concentration (for the partially-filled geometry). Also, the flame was able to propagate more three-dimensionally in this vessel given its extra diameter, allowing buoyancy effects to act on the flame as it continued along the vessel.

7.3.4. Summary (Methane)

In summary, the results presented in this section have shown the potential severity of an interconnected vessel partially-filled with a homogeneous methane-air mixture, and that the mechanisms of flame and pressure development were found to be similar to those reported in the literature for fully-filled systems. In particular, the mechanism of pressure piling was evident for initial starting mixtures of between 8%

and 13% (Φ = 0.85-1.37), which equated to global concentrations of between 1.5% and 2.5% (Φ = 0.16-0.26), when the equivalent volume of fuel was distributed throughout the entire volume, well below the lower flammability limit for methane in air.

These phenomena illustrate that while the partially-filled interconnected vessel explosions were not as severe as their fully-filled equivalents; the difficulty in designing adequate protection for such interconnected geometries was evident since a relatively small pocket of weak methane-air mixture produced relatively severe explosions.

It is also evident from this work that explosions transmitting into non-fuel-filled areas of interconnecting vessels can actually experience severe overpressures, despite not initially being contaminated by the leaked fuel. This can have implications for the safety design of inter-connected installations which are not intended to be subject to flammable mixtures.

7.4. Experimental Results (Hydrogen)

The third and final fuel mixture investigated in this system was hydrogen-air. In this test programme, homogeneous hydrogen-air mixtures between 10% and 22% (Φ=0.34-0.75) were investigated. This equated to global concentrations throughout the entire vessel as shown in Table 7-3. Again, all of the concentrations investigated would be below the flammability limit if the equivalent volume of fuel were mixed throughout the entire volume. It was the original intention to present hydrogen-air mixtures over the entire flammable range, however, as will be seen, this was limited by the unusual behaviour of hydrogen in this vessel, which stopped the test-programme at 22%. Despite this partially complete test-series the results obtained were deemed important to the advancement of knowledge in this area and have therefore been included here. The results presented have been published [37].

In all cases, the initial starting mixtures were of homogeneous composition within the primary chamber at standard atmospheric pressure and local ambient temperature. Similarly to that presented in Sections 7.2 & 7.3 for propane-air and

methane-air explosions under the same conditions, this section will provide details of the explosion behaviour for hydrogen in terms of general explosion development, flame development, maximum pressures attained, rates of pressure rise and discussion of the unusual detonation-like event, the occurrence of which had limited the work. Further reference to this phenomenon and the similar phenomenon occurring in the propane-air test series is then presented in Section 7.6.

Table 7-3: Equivalent global concentration for all hydrogen-air concentrations considered in this research if the volume of hydrogen were homogeneously mixed throughout the entire two vessel geometry.

Initial Concentration (primary vessel)		**Global Concentration**	
%	**Φ**	**%**	**Φ**
10.0%	0.339	1.90%	0.066
12.0%	0.407	2.29%	0.079
14.0%	0.475	2.67%	0.092
16.0%	0.542	3.05%	0.105
18.0%	0.610	3.43%	0.118
20.0%	0.678	3.81%	0.131
22.0%	0.746	4.12%	0.144

7.4.1. General Explosion Development

Figure 7-17 illustrates a typical low concentration (14% in this case) explosion for this configuration. Pressure traces for the primary vessel, connecting pipe and secondary vessel are presented with respect to time. The vertical dashed lines on the graph show the time at which the flame enters (t_{in}) and exits (t_{out}) the connecting pipe, the difference being the flame propagation time between the two vessels. In addition, the horizontal solid line represents the adiabatic pressure expected for this set-up calculated using GASEQ [137] as discussed previously.

In Figure 7-17 three distinct phases of the explosion can be observed in this geometry, as observed for propane and methane. *Phase 1*: Initial slow development;

Phase 2: Fast flame propagation through the connecting pipe, with initiation of fast burning in the primary vessel; and *Phase 3*: Ignition and fast burning of the flammable mixture displaced in the second vessel, and of the remaining mixture in the primary vessel.

In *phase 1*, Figure 7-17 shows that the flame took around 70 ms to travel from the ignition point to the entrance of the pipe at an average flame-speed of 11 m/s. It is assumed that the flame initially develops as a hemisphere from the point of ignition and then, as the vented flow field is set up, the flame elongates towards the vent. This is a phenomenon common in vessels with vents [125]. During this phase, premixed hydrogen air mixture was being pushed out of the primary vessel and into the connecting pipe as the burned gases expanded.

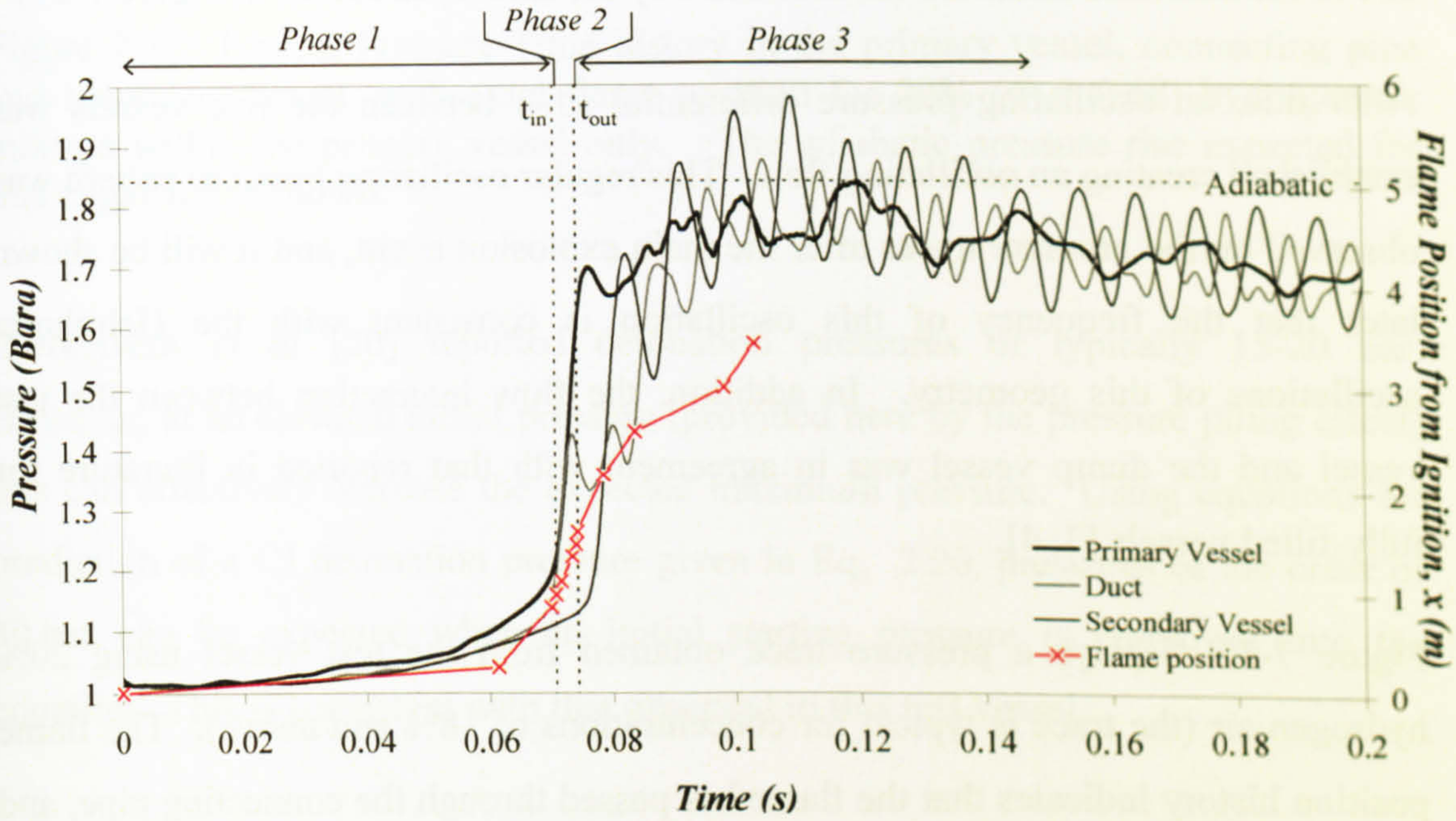

Figure 7-17: Typical low concentration Pressure-Time history in the primary vessel, connecting pipe and secondary vessel, with axial flame position for 14% (Φ = 0.48) hydrogen-air mixture within the primary vessel only. The adiabatic pressure rise expected for this explosion is shown.

During *phase 2*, the flame entered the connecting pipe and burned rapidly through the unburned turbulent gases. Figure 7-17 shows that it took around 3.6 ms to travel along the connecting pipe (measured between the first and last thermocouple T_6 and T_{11}) at an average flame-speed of 174 m/s. During this time, there was a major combustion event in the pipe which directed the flame front quickly into the second

vessel and also simultaneously back into the primary vessel. This accelerated the combustion of the remaining gas in the primary vessel, which had been pre-compressed by the expanding flame, contributing to the main explosion event in this vessel. The flame propagation along the pipe was fast, and the flame-speed recorded reached a peak towards the end of the pipe (between T_{10} and T_{11}).

Finally, during *phase 3*, the flame front entered the second vessel (predicted to be as a fast jet flame) and ignited the flammable gases pushed ahead of the flame before there was sufficient time for them to become diluted by the air in the second vessel. This fast event caused a large pressure rise, and it was at this point that the mechanism of pressure piling was observed in the secondary vessel, with the fastest rate of pressure rise for this vessel, followed by maximum pressures which were above the adiabatic threshold (as illustrated by the smoothed curves in Figure 7-17).

After this, an oscillating pressure differential (ΔP) between the two vessels was established creating an oscillating flow. This regular oscillating pressure pattern was observed on the pressure traces after the main explosion event, and it will be shown later that the frequency of this oscillation is consistent with the Helmholtz oscillations of this geometry. In addition, the flow interaction between the test vessel and the dump vessel was in agreement with that reported in literature for fully-filled vessels [3, 4].

Figure 7-18 displays a pressure trace obtained from the test vessel using 20% hydrogen-air (the trace is typical for concentrations of 18% and above). The flame position history indicates that the flame has passed through the connecting pipe, and was approximately half way along the dump vessel when a detonation-like peak appeared in the originating chamber (3ms after a flow reversal had occurred).

From the pressure trace on Figure 7-18, it may be seen that the pressure in the primary vessel actually increased to 2.5 barg before the detonation peak began. This pressure immediately prior to the detonation peak increased with mixture reactivity (1.6 barg to 2.7 barg for 18% and 22% H_2 respectively). In terms of time delay from the point of flow reversal to detonation, this decreased with increasing reactivity (4.9 ms to 2.2 ms for 18% and 22% H_2 respectively).

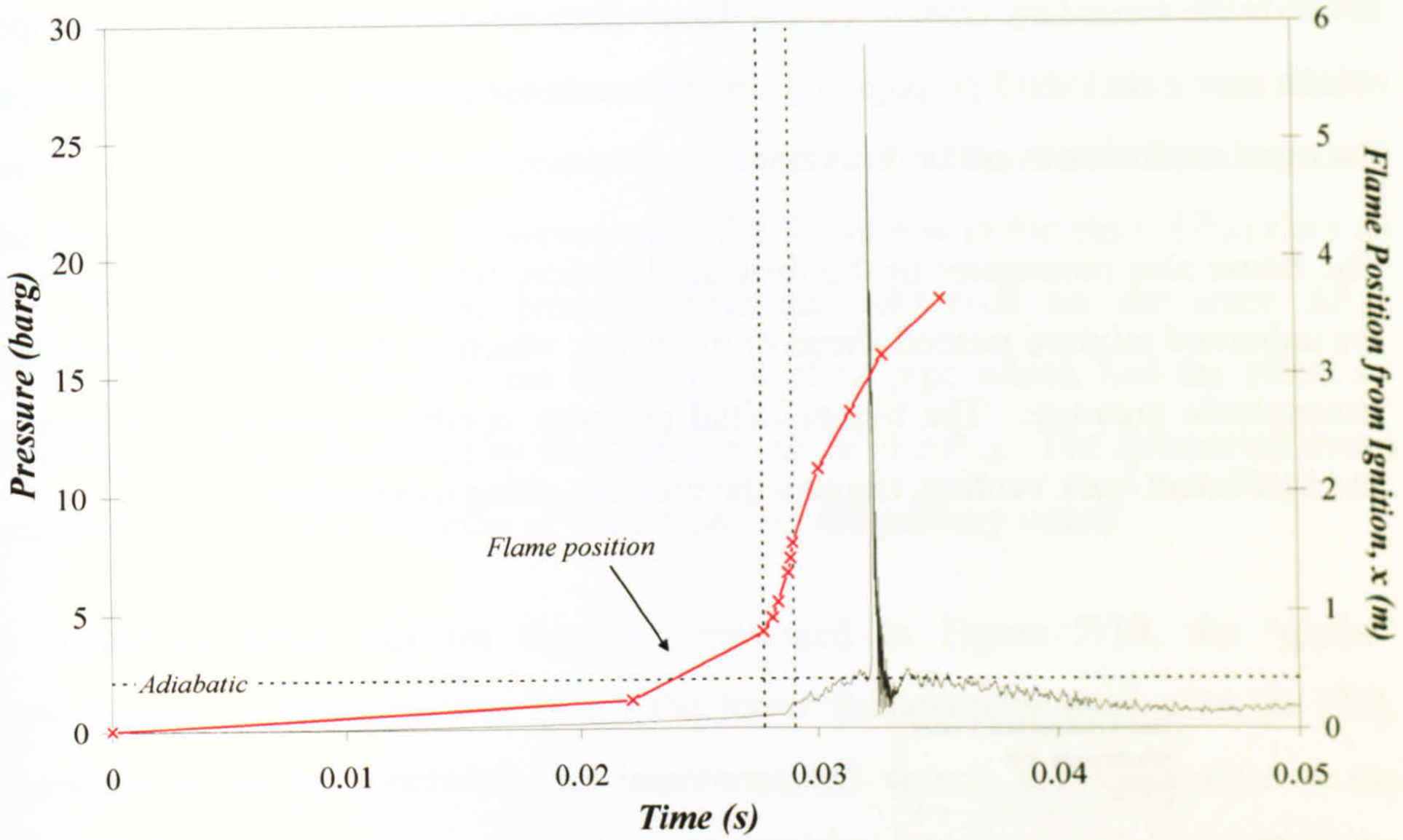

Figure 7-18: Typical Pressure-Time history in the primary vessel, connecting pipe and secondary vessel, with axial flame position for 20% (Φ = 0.68) hydrogen-air mixture within the primary vessel only. The adiabatic pressure rise expected for this explosion is shown.

Bjerketvedt *et al* [20] reported detonation pressures of typically 15-20 bar. However, at an elevated initial pressure (provided here by the pressure piling effect) this can effectively increase the expected maximum pressure. Using equations for prediction of a CJ detonation pressure given in Eq. 2.20, pressures of the order of 30 bar can be expected when an initial starting pressure is employed into the equation. This is consistent with that observed in this test vessel.

7.4.2. Pressure and Flow Analysis

Figure 7-19 displays the flow interaction in the vessel by considering the pressure differences between sections for (a) 14% and (b) 20% hydrogen-air mixtures. Illustrated are the pressure differences between the primary vessel and connecting pipe ($\Delta P_{1\text{-}2}$), and between the connecting pipe and the second vessel ($\Delta P_{2\text{-}3}$). This flow interaction clearly displays the three stages discussed above. Initially, the flow is relatively slow; once the flame enters the pipe, $\Delta P_{1\text{-}2}$ indicates a strong flow backwards into the primary vessel, while $\Delta P_{2\text{-}3}$ shows an amplification of the flow

towards the secondary vessel. This is due to a secondary explosion event in the pipe, which sent a backward propagating wave towards the primary vessel contributing to the main explosion event in this vessel.

The flame also propagates in the forward direction, into the second vessel, igniting the unburned mixture pushed ahead of the flame, which by this time is at higher than atmospheric pressure. The higher initial pressure, combined with the fast burning and inefficient back venting, triggers the pressure piling mechanism.

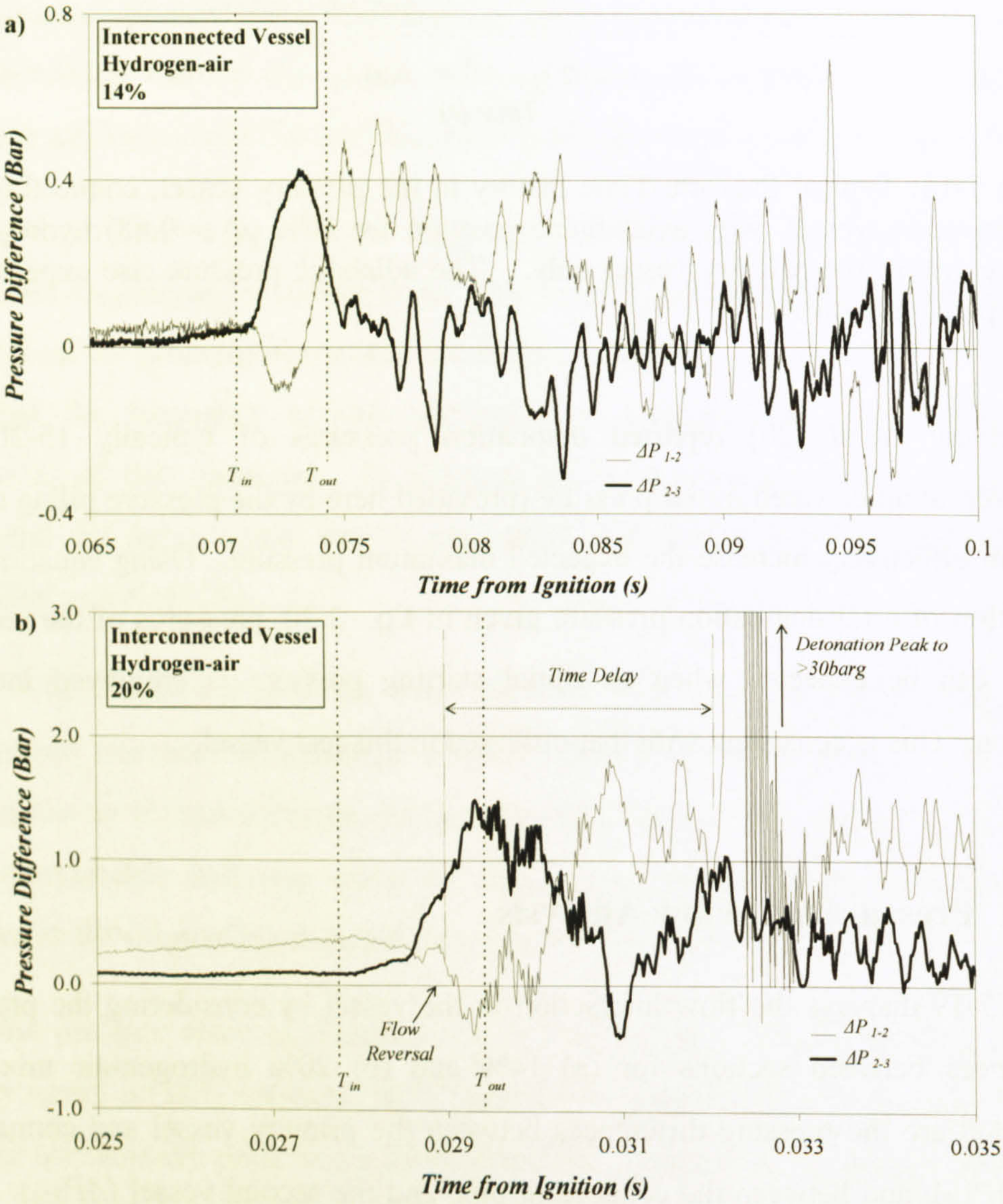

Figure 7-19: Flow interaction within the interconnected geometry for (a) 14% and (b) 20% hydrogen-air

Figure 7-19b shows the pressure differential for 20% hydrogen-air mixture in the primary vessel, for the same explosion test shown in Figure 7-18. This trace shows an initial slow pressure rise corresponding to the first phase, which lasted up until the flame entered the pipe. However, once the flame was in the pipe, $\Delta P_{2\text{-}3}$ rises as $\Delta P_{1\text{-}2}$ falls. The maximum pressure difference observed on the trace $\Delta P_{2\text{-}3}$ corresponds to the burn-up event in the connecting pipe which had the effect of reversing the flow, illustrated by the negative values of $\Delta P_{1\text{-}2}$. The detonation event occurred 3ms after the initiation of back flow into the primary vessel.

It should be noted that for the tests presented in Figure 7-19, the 'global' concentration of hydrogen was below the lower flammability limit of 4.1% [25]. Therefore it can be concluded that interconnected vessels are susceptible to the effects of pressure piling, even at concentrations which would be out of the flammability range if allowed to mix freely in the full geometry. In addition, as the concentration increases above 16% in the primary vessel, a detonation mechanism was displayed.

7.4.3. Maximum Pressure

In order to determine the mixture reactivity above which this phenomenon occurred, the maximum adiabatic pressure for this system was calculated. Again, the explosion was assumed to occur in the primary vessel only (the volume of the initial flammable mixture) which was then distributed throughout the whole system volume using Equation 7-1, adapted from Boyles Law.

Analysis of the results presented in Figure 7-20 clearly shows that pressure piling is a feature of partially-filled linked geometries – as it is for fully-filled systems – despite the dilution that the gas mixture may experience as it is pushed/mixed through the system. Pressure traces from the leaner concentrations (10-16%) consistently demonstrate higher maximum pressures in the second vessel (rather than in the ignition vessel). However only the maximum pressures produced in the range 12% to 16% are significant in terms of comparison to the adiabatic predicted pressure. Therefore, despite the second vessel having higher pressure than the primary for 10% mixtures, it cannot be argued that pressure piling is occurring in

these tests. The recorded pressures in the secondary vessel have been shown separately in Figure 7-20(b) for clarity. The results show the same trend with all explosion tests above 10% initial concentration providing final pressures above the expected system adiabatic.

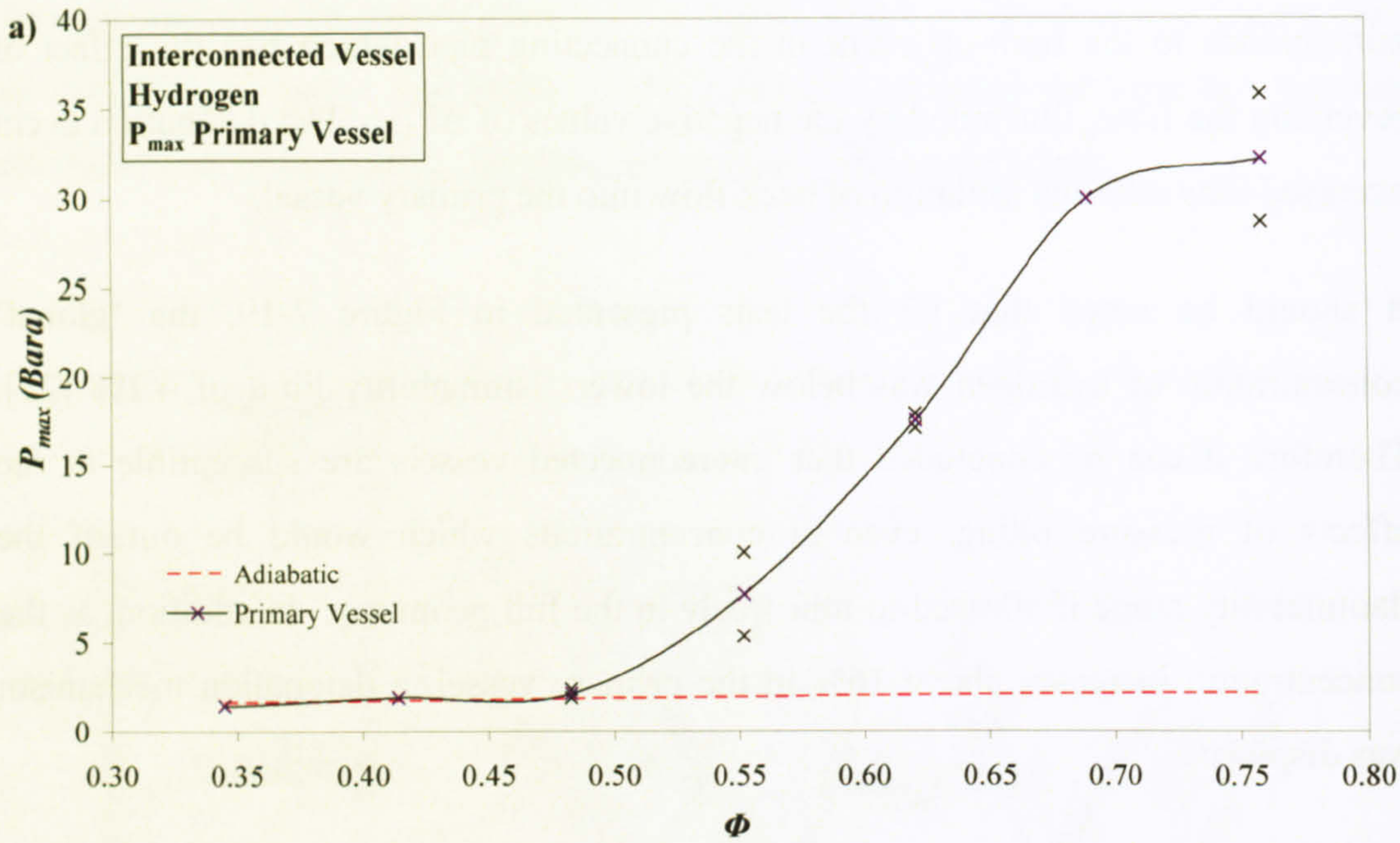

Figure 7-20: Comparison between maximum pressure and expected system adiabatic pressure measured in (a) the primary vessel and (b) the secondary vessel.

7.4.4. Flame Speed Analysis

In all tests, the maximum flame-speed measurements were observed as the flame passed through the connecting pipe. For H_2 concentration above 18% these speeds were consistent with a detonation event, with maximum values ranging between 900-1494m/s and associated pressures of 17-36 bara respectively. A pressure spike was also observed for H_2 at 16%, however the maximum pressure was close to 6 Bara, and with flame-speeds approaching 400 m/s this indicates a fast deflagration only (see Figure 7-21).

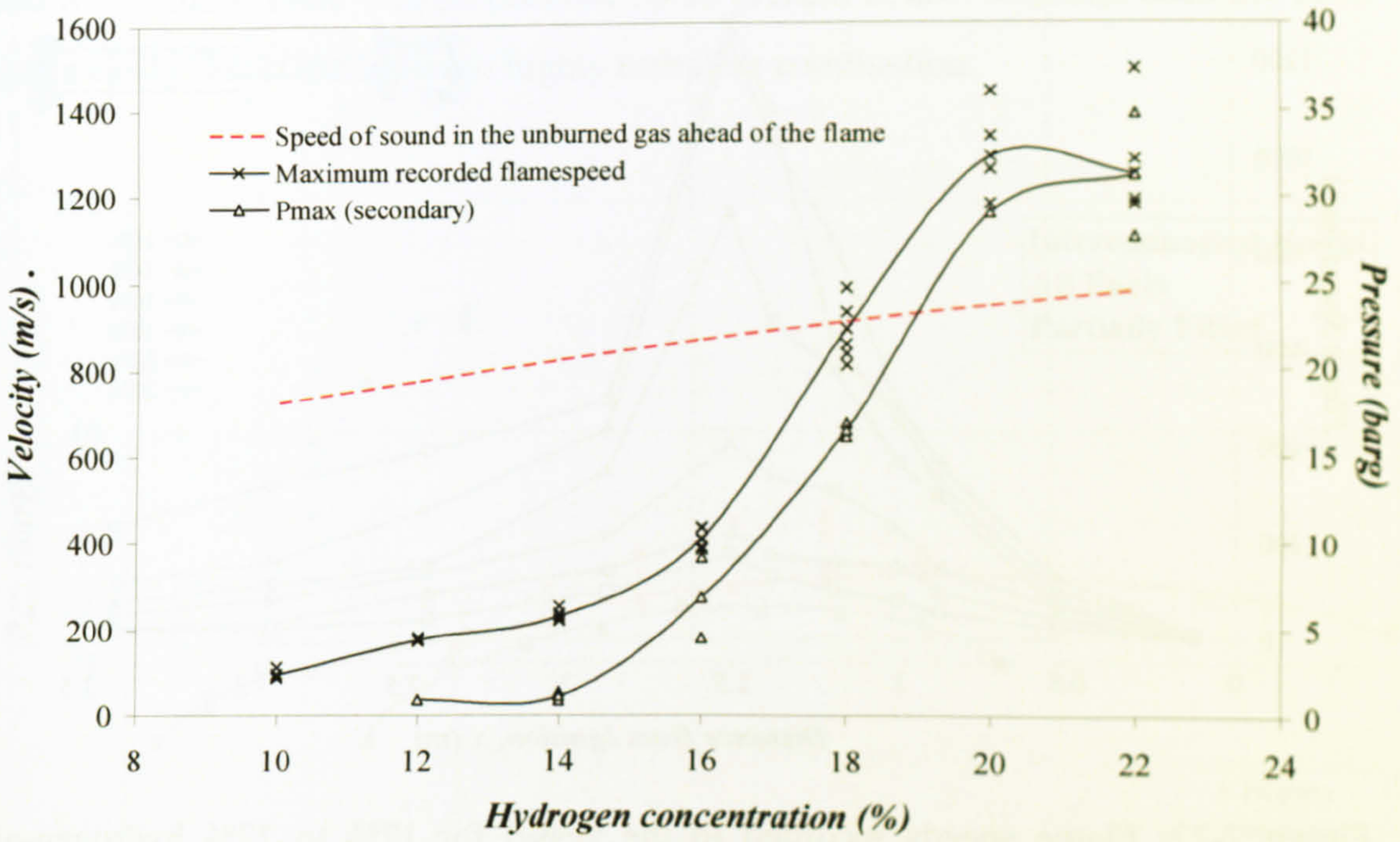

Figure 7-21: Maximum recorded flame-speed as a function of concentration

Figure 7-21 shows the maximum flame-speeds detected in the vessel. In each case this occurred at the last point in the connecting pipe (as illustrated in Figure 7-22). For H_2 concentrations less than 18% the maximum flame-speed was generally very repeatable, showing low velocities through the vessel. For the higher concentrations investigated the data spread was much greater (see Figure 7-21). These faster rates of burning are not only a function of concentration, but also of turbulence created in the initial stages of the explosion towards the end of phase 1, where the unburned gases were being pushed towards the connecting pipe. When the flow encountered the connecting pipe a sudden contraction occurred over the sharp orifice which

served to cause a pressure loss corresponding to the difference between the pressure in the primary vessel and a point downstream of the vent. For this vessel this would be the difference between the pressure traces P_1 and P_2 at the point where the flame enters the connecting pipe. However, the term pressure loss can be somewhat misleading; in fact the energy loss from the pressure is turned initially into turbulent motion which serves to increase the burning velocity and severity of the explosion.

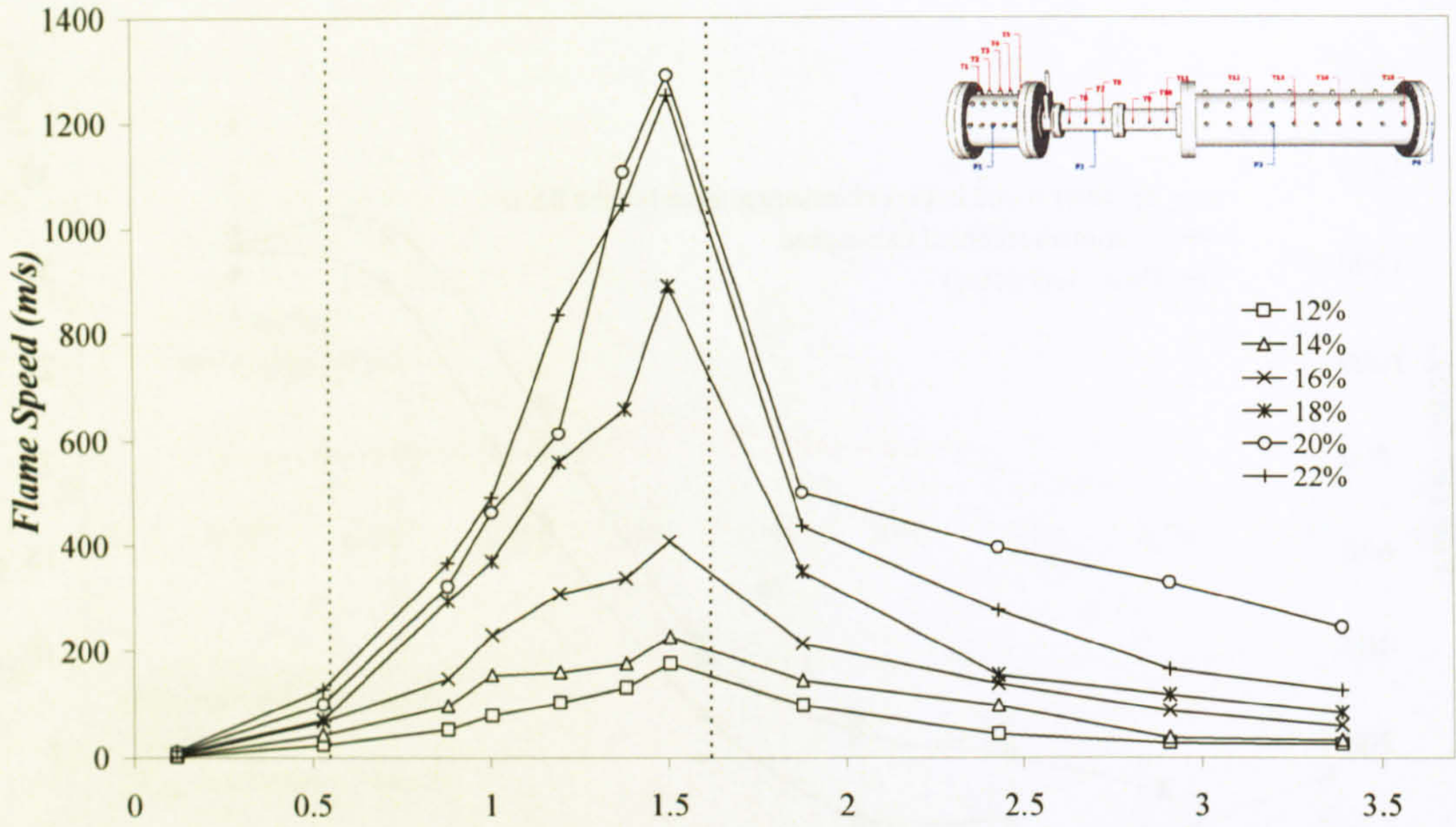

Figure 7-22: Flame speeds recorded in the vessel for 12% to 22% hydrogen-air mixtures. 10% hydrogen-air has been omitted due to the relatively small values involved, which were not well visible on the scale used.

A similar situation has been observed in the early work of Lewis and von Elbe [10], who discuss a situation in a closed ended tube where a detonation run is stopped when the flame encounters a shock which has been reflected from the closed end, meeting the flame before it developed into a detonation. In such cases, high velocities can be achieved without the detonation pressure record, which might explain the case here, where detonation velocities are observed in the connecting pipe, without the detonation becoming fully developed in terms of pressure.

7.5. Comparison of Peak Pressures for C_3H_8, CH_4 and H_2

Figure 7-23 illustrates the difference in magnitude of the peak pressure in the primary vessel as a function of equivalence ratio for partially filled mixtures of propane, methane and hydrogen as discussed in this chapter. For hydrogen and propane two peak pressure measurements have been plotted; the peak pressure 'spike' (dotted lines), and the underlying pressure from which the 'spike' has risen (solid lines). For hydrogen there was a very large difference, indicating a strong detonation-like event. For propane the difference was smaller, but still significant, and for methane there was no pressure spike present at all. Methane does not auto-ignite easily, but it can undergo highly turbulent combustion.

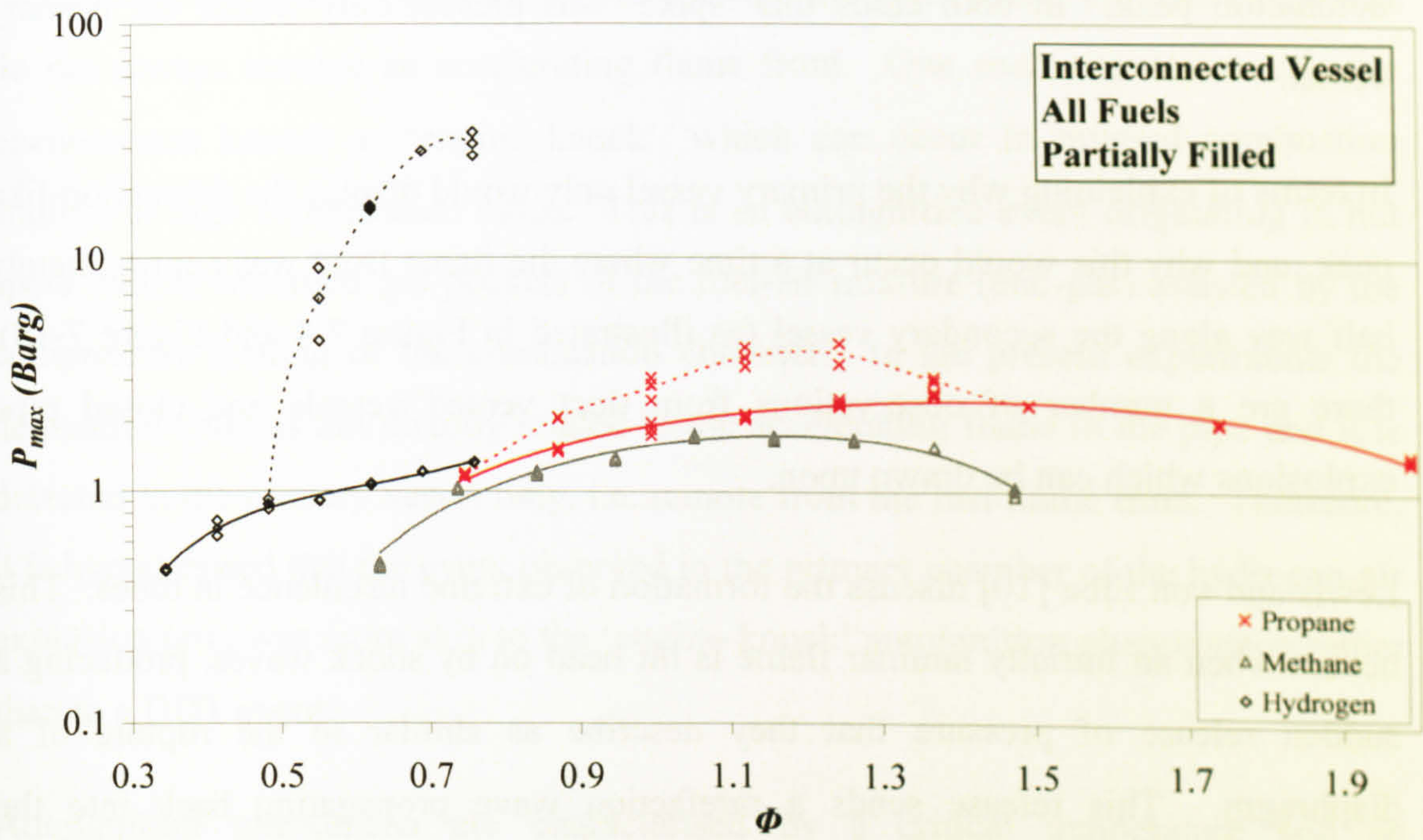

Figure 7-23: Comparison between maximum pressures observed in the primary vessel for propane, methane and hydrogen in the interconnected test vessel. Solid lines represent the average peak pressure, discounting any short duration spike, with the spike data illustrated with the dashed lines.

Similar to the short duration 'spike' observed in the current work, Bartknecht [11] has previously reported similar high pressure and rate of pressure rise irregularities for propane concentrations between 4.5 and 5.5%, however only for initial pressures above 2 bar. The research into the phenomenon in hydrogen-air mixtures could not

be completed due to constraints with the design pressure of the rig geometry. However, this is an interesting topic which allows the possibility of future work.

7.6. Determination of the Cause of the Detonation-Like Behaviour

As has been discussed in this chapter so far, several of the more reactive explosion tests have displayed severe unusual behaviour. In propane-air mixtures a short duration 'spike' has been observed on several pressure traces in the primary vessel between 3.2% and 5.5% ($\Phi = 0.80$ and 1.37). However, for hydrogen-air mixtures in the range 18% to at least 22% ($\Phi = 0.61$-0.75), the event manifested itself much more strongly, and indeed the resulting peak displayed was much more akin to a detonation peak. In both cases this 'spike' was present only within the primary vessel.

In terms of explaining why the primary vessel only would display the detonation-like peak, and why this would occur at a time where the flame front was approximately half way along the secondary vessel (as illustrated in Figure 7-4 and Figure 7-18), there are a number of observations from duct vented vessels and closed pipe explosions which can be drawn upon.

Lewis and von Elbe [10] discuss the formation of extreme turbulence in tubes. This occurs when an initially laminar flame is hit head on by shock waves, producing a sudden release of pressure that they describe as similar to the rupture of a diaphragm. This release sends a rarefaction wave propagating back into the unburned gas which creates an unburned gas jet, penetrating the burned gas and developing shear layers. This produces extreme turbulence, which causes a sudden increase in the burning rate whereby 'trains' of compressed waves are formed. They go on to describe work conducted by Karlovitz, who suggests that the wrinkling of the flame becomes so great that the pockets of trapped unburned gas preheat and collapse in a strong reaction burst. It is possible that such a reaction burst may form a single strong shock contributing to a detonation wave. This type of rarefaction initiated reaction was observed more recently by McCann *et al* [39] on a small scale vented vessel.

To the author's knowledge, a similar detonation-like spike has not been observed in any previous work on partially filled interconnected vessels, and while it was observed for hydrogen and to a lesser extent propane in the current work, no such behaviour was observed for methane-air mixtures.

Considering the hydrogen peak in confined or partially confined geometries, there is the possibility that hydrogen explosions may lead to detonations due to obstacles and changes in geometry (such as the connecting pipe here). Under these circumstances, detonation is associated with an accelerating flame coupling with the shock wave, and resulting in instantaneous heat release and a fast-propagating high pressure region over a transition distance known as DDT.

Some detonation-like events are reported in the literature under circumstances that do not always involve an accelerating flame front. One such circumstance is the phenomenon known as 'engine knock', which can occur in internal combustion engines at high compression ratios. This is an autoignition event originating in hot spots within unburned gas pockets of the fuel-air mixture (end-gas) assisted by the compressive heating of the combustion chamber. In the present experiments the detonation spike is not directly related to the accelerating flame in the pipe and it is detected in the primary vessel only, i.e. remote from the fast flame front. Therefore, it is hypothesised that the event observed in the primary chamber of the hydrogen-air explosion tests was more akin to the 'engine-knock' autoignition phenomenon rather than to a DDT event.

Autoignition phenomena are characterised by a critical temperature and an associated ignition delay. Mullins and Penner [14] report an experimental relationship between ignition delay and temperature (for hydrogen at 0.9 Atm) with about 100ms delay at 570°C, dropping to 0.2ms at 760°C. In the present experiments, the detonation-like event occurred at initial pressures ranging from 1.6 barg to 2.7 barg, which in themselves would have been insufficient to raise the temperature of the unburned mixture to the autoignition temperature. Therefore, the most likely heating mechanism in the present work is thought to be through the mixing of the burned and remaining unburned gases in the primary vessel. This mixing would have been the result of the pressure wave interaction with the flame

front (such pressure waves would have been produced by the accelerating flame in the pipe entrance and the subsequent rapid burning within the pipe). The flow reversal and jet discharge back into the primary vessel would have also resulted in entrainment and mixing of unburned gases, thus resulting in an increase in the temperature of the pockets of unburned gas and their subsequent autoignition.

Measurements of the time delay between the flow reversal and the recorded detonation (as shown in Figure 7-18) varied from 2.2ms to 4.9ms. Using the correlation proposed by Mullins and Penner [14], this would translate to an autoignition temperature requirement of 660°C for the 18% H_2 mixture, and of 700°C for the 22% mixture. Such temperatures are feasible for the heating mechanism of burned/unburned gas mixing proposed. These temperatures are close to the flame propagation temperatures for lean hydrogen mixtures, and consequently it may be feasible that the recirculation of the flow from the back venting may be sufficient to ignite these hot spot areas at the critical time delay.

In propane-air mixtures, the significant rapid pressure rise events or 'spikes' in the pressure traces for the primary vessel were also observed at a time where the leading flame front had already left the connecting pipe. The propane interconnected explosion results outlined above suggests that the auto-ignition phenomenon observed for lean hydrogen-air mixtures [37] also occurred for propane mixtures close to the stoichiometric, as shown in Figure 7-5. This was further demonstrated in Figure 7-9, which illustrates the time of flame arrival in the corner of the primary vessel at the spark end, where a flame arrival thermocouple was located. The results show that the time of flame arrival in this corner region was very close to the time of the pressure spike.

Bartknecht [11] describes irregular behaviour for concentrations slightly above stoichiometric, where the heat of the combustion is sufficient to increase the velocity of the explosion reaction after an acceleration path to a velocity close to the speed of sound, thereby creating a noticeable velocity (or ramming pressure). This is reported to cause additional heating of the mixture and increases the combustion process accordingly, therefore resulting in this unusual P_{max} and $(dP/dt)_{max}$. Bartknecht [11] argues that this mechanism is the initial stages of a detonation, and rationalises that

this can be the case since the limits for detonation are narrower than for ordinary explosion or flammability.

In the current work the initial conditions were always standard ambient conditions (~1.0132 bar and 20°C) and yet the phenomenon was still occurring, and as stated for the hydrogen work mentioned above, the run-up distance for detonation would be much longer than is available in the current work.

Such auto-ignition events did not occur in methane tests conducted on the same configuration [86, 134], since the auto-ignition temperature should be of the order of 1300K, with a much longer ignition delay, approaching 100ms [14]. Methane does not auto-ignite easily, but it can undergo highly turbulent combustion. It is considered that the corner regions of the primary vessel are not high turbulence zones, and hence autoignition was the most likely explanation for the observations.

While similar behaviour was not observed for methane-air mixtures, using a similar criterion for calculating the auto-ignition temperature it may be feasible that higher hydrocarbons may be susceptible to this same localised detonation event above that recorded for propane-air mixtures. However, the investigation of such a hypothesis is beyond the scope of this work, although such investigation would certainly be beneficial to plant and suppression systems which are understood not to account for the mitigation of such events.

7.7. Helmholtz Bulk Oscillations

Where the interaction of pressure differences between vessels ΔP_{1-4} is to be considered, it can be seen that once the main explosion event has subsided, and even as early as when the flame front is still travelling along the secondary vessel, pressure oscillations were present between the vessels showing a characteristic frequency. In all cases investigated, whether detonation coupled with pressure piling or pressure piling alone, the natural frequency of the geometry has been shown to be responsible for the 'bulk' wave propagating between vessels. From Eq. 7-2, [92] it is possible to calculate the natural frequency of an asymmetrical interconnected 2-vessel geometry:

$$F = \frac{c}{2\Pi}\left[\left(\frac{A}{L}\right)\left(\frac{1}{V_1}+\frac{1}{V_2}\right)\right]^{1/2} \qquad \text{Eq. 7-2}$$

where A is the area of the vent, L is the length of the connecting pipe, V_1 and V_2 are the volumes of the primary and secondary vessels respectively, and c is the speed of sound in the mixture Eq. 7-3:

$$\left(\frac{\gamma p}{\rho}\right)^{1/2} \qquad \text{Eq. 7-3}$$

or

$$\left(\frac{\gamma RT}{W}\right)^{1/2} \qquad \text{Eq. 7-4}$$

where γ is the ratio of specific heat at constant pressure to that at constant volume (taken to be 1.4), p is the mean pressure, ρ is the mass density, R is the gas constant (=8.314 J mol^{-1} K^{-1}), T is the temperature, and W is the molecular weight.

Using Eq. 7-2 and Eq. 7-3 for the burned gas, the characteristic frequency for this geometry was calculated to be 122 Hz, 122 Hz and 108 Hz for propane, methane and hydrogen respectively, assuming a speed of sound in the burned gases towards the lean flammability limits (which is a reasonable approximation of the diluted gases in the volume). The values obtained are in good agreement with the $\Delta P_{1\text{-}4}$ measured frequencies of 125Hz, 120 Hz and 110Hz respectively. There was actually little variation in the actual value of F in the range of concentration considered, which is unsurprising given that all of the combustion takes place at lean fuel-air mixtures.

Based upon the value of F calculated in Eq. 7-2, a good approximation can be gained of the frequency on oscillations in the secondary vessel by calculating the speed of sound in the burned gases. For hydrogen this calculation yields a frequency of 108 Hz, which predicts the pressure wave of the vessel with reasonable accuracy as displayed in Figure 7-24 based on an initial concentration of 18%. Where the speed of sound in the unburned gases is considered, the frequency becomes close to 60 Hz, which equates to the frequency of oscillations observed in the primary vessel.

It is consistent with the work of Razus *et al* (2003) that the two vessels have different acoustic frequencies.

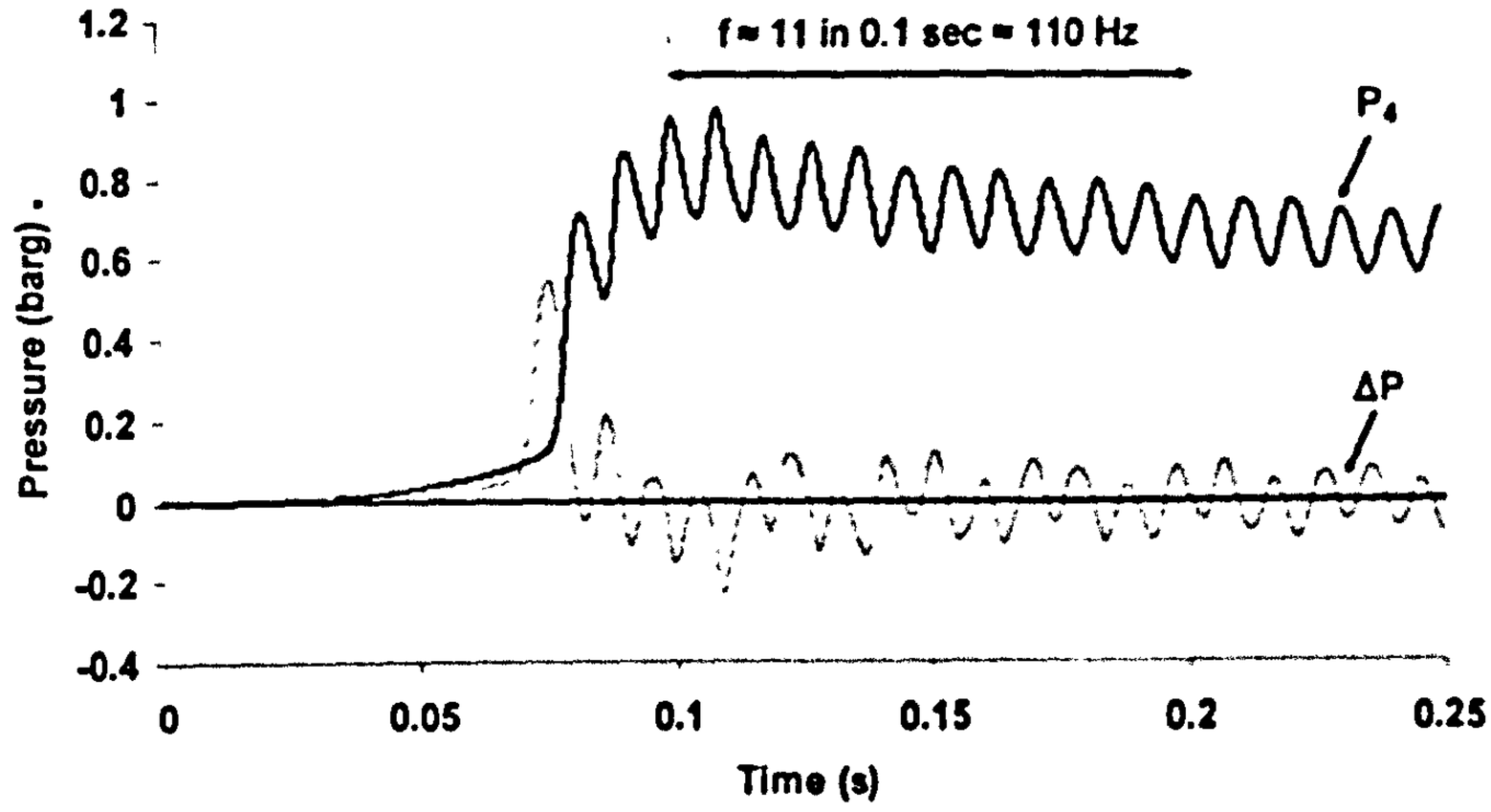

Figure 7-24: Oscillations observed in the pressure traces for primary and secondary vessels.

The Helmholtz bulk oscillations have also been linked to the onset of Taylor instabilities as the flame is driven in the unstable direction towards the denser medium in the vessel [39]. This effect will increase the surface area of the flame by enhancing the flame wrinkling, and will increase the severity of the explosion. In addition to this, the travelling shockwave ahead of the flame can be reflected by the rear wall and can potentially travel back to the main vessel to contribute to the onset of the detonation observed in the primary vessel, as discussed in the previous section.

The results presented here refer only to the bulk oscillations of the vessel. Many more high frequency oscillations are present in the raw pressure traces. However, a more in depth analysis of the acoustic interaction in the vessel is beyond the scope of this research.

7.8. Summary

In this chapter, the dynamics of explosion development in a partially filled interconnected vessel configuration have been discussed using propane-air, methane-

air, and hydrogen-air mixtures. Interconnected vessel explosions were studied with a 4:1 volume ratio, with the flammable mixture in the smaller primary vessel only. The 4:1 volume ratio ensured that the simulation of a leak in the primary vessel resulted in mixtures that were not flammable if the air in the secondary vessel mixed with the displaced unburned gases from the primary vessel. The duct between the two vessels was the same diameter as the vent, which had a K_V of 10.3 with respect to the primary vessel.

The results have shown the potential severity of a partially-filled interconnected vessel, and that the mechanisms of flame and pressure development were found to be similar to those reported in the literature for fully-filled systems. In particular, the mechanism of pressure piling was evident for all of the investigated fuels, despite the fact that the equivalent concentration – if averaged over the entire vessel, including the secondary vessel initially filled only with air – would be outside the normal flammable range, and so be deemed 'safe'. It was deemed that the very severe explosions observed in the secondary vessel occurred due to the displaced unburned gases from the primary vessel, which ignited before the gases could mix with the air in the secondary vessel, and this indicated fast turbulent combustion in the displaced flammable gases.

As an additional danger, certain propane-air and hydrogen-air mixtures were shown to produce a short detonation-like event upstream of the leading flame front propagation, in the primary vessel. This work found the cause of these pressure spikes to be due to auto-ignition of the unburned pockets of mixture in the primary vessel, at a time delay corresponding to the backward propagation of a secondary explosion or burn-up event in the duct. There was evidence of reverse flow from the secondary vessel explosion back into the primary vessel, and subsequent turbulence generation and fast flame development in the primary vessel. Further expansion of these fast primary flame gases into the secondary vessel eventually resulted in a further reverse flow into the primary vessel, followed by autoignition of the remaining unburned gases in the corner regions of the primary vessel, with a corresponding rapid pressure rise. These phenomena illustrate the difficulty in designing adequate protection for such interconnected geometries, since a relatively small pocket of weak methane-air mixture produced relatively severe explosions.

This can have implications for the safety design of inter-connected installations which are not intended to be subject to flammable mixtures.

PAGE NUMBERING AS ORIGINAL

CHAPTER 8:

CONCLUSIONS AND SUMMARY OF MAIN FINDINGS

8.1. Summary of Major Findings

Explosion tests were carried out in four medium-scale test-vessels incorporating closed, vented, duct vented and interconnected vessels. A systematic investigation into the influence of homogeneous and stratified mixtures was undertaken by varying mixture reactivity, ignition position, injection position and mixture composition.

A feature of this work has been the similarities in explosion phenomena between stratified and homogeneous explosions and between partially filled and fully filled geometries to the conclusion that the explosion severity recorded was in many cases much higher than the fuel concentration would normally provide.

Comparison of the pressure traces for homogeneous and stratified explosions in the closed vessel geometry revealed that the difference in maximum pressures between the two conditions was surprisingly small. The behaviour of stratified mixtures being similar in nature to that of homogeneous has been attributed to the mixing of the fuel-rich and air-rich portions of the unburned gas as the combustion progressed. Comparisons made with literature showed that the behaviour of the flame in the closed vessel seemed to conform more closely to that of longer vessels, with the occurrence of a 'tulip flame structure' which was attributed to the mixing in the vessel soon after ignition and before the flame attachment to the walls where the oscillatory combustion was initiated. It was concluded that the contact between the flame and the cylindrical walls of the vessel was the likely cause of the onset of oscillatory combustion, which was then amplified by growing perturbations of the flame front caused by other interactions such as returning shock waves causing inversion of the flame front in the unstable direction.

Results obtained from the vented vessel showed that both homogeneous and stratified mixtures mimicked the explosion phases set out in literature where an initially spherically expanding flame was drawn towards the vent as the result of an unburned gas flow field entraining the reaction zone in this direction. This was closely followed by a reduction in venting effectiveness as the flame reached the vent and ignited the unburned gas cloud formed directly outside the vent, which was then followed by the onset of venting once more as the flame continued to burn into the remaining unburned

mixture within the vessel. In some tests, mainly rich concentration propane, the onset of flame instabilities also triggered an oscillatory peak, which exhibited a much higher oscillatory frequency than expected for the fundamental harmonic frequency of the vessel. In such cases, the peak has been attributed to the interaction between the combustion of the remaining unburned mixture within the vessel, and the acoustic pressure waves generated by fluctuations in the heat release rate. Furthermore, it was concluded that the conditions satisfied the Rayleigh-Taylor criterion for flame instabilities within the vessel, which subsequently gave rise to the onset of Helmholtz oscillations. This occurred preferentially in central ignition over end ignition.

The results showed that while the near stoichiometric homogeneous concentrations generally represented the most severe overall explosion severity in each case, for propane-air mixtures towards the lower flammability limit, the stratified mixtures actually posed a more severe condition than the equivalent homogeneous. It was concluded that the main reason for the increased severity in stratified tests towards the lean limit is due to the concentration gradient in the vessel and the increased mixture reactivity at the ignition site, which would allow the explosion to initiate more quickly. In stratified mixtures, if the air lean and air rich portions of the unburned mixture were pushed through the vent differentially, the resulting mixture inside the vessel contributing to the main pressure peak could then be more reactive than the global concentration would suggest, and thereby account for the slightly elevated severity of the stratified mixtures towards the lower flammability limits.

Results obtained from the duct vented test series show that the same mechanisms which apply to the hydrocarbon mixtures in homogeneous explosions in a duct vented geometry, such as burn-up in the duct were also present for stratified mixtures. Similarly to the vented vessel explosions, the homogeneous tests provided the most severe overall condition, with the maximum pressures produced by the worst case stratified mixture being only about ¼ of the maximum produced by the worst case homogeneous mixtures. However, one of the most important points which has come from this research is that approaching both the lean flammability limit and the rich flammability limit, the stratified tests consistently provided the worst case for all ignition positions. This was consistent with the findings for vented explosions and showed that stratified propane-air explosions were more severe towards the

flammability limits. In addition, it has been shown that concentrations outside the flammability limits would ignite and produce measurable overpressures.

Pressures measured from the experimental data were compared with the simple layer fractions proposed by Tamanini in a large scale volume and were found to provide a significant correlation between the layer fraction ratio and the maximum recorded reduced pressure after venting (for central injection). Additional research in this area would determine the extent of the applicability of Tamanini's equation with the results obtained in this and smaller scale vessels.

Interconnected vessel explosions were studied with a 4:1 volume ratio, with the flammable mixture in the smaller primary vessel only. The 4:1 volume ratio ensured that the simulation of a leak in the primary vessel resulted in mixtures that were not flammable if the air in the secondary vessel mixed with the displaced unburned gases from the primary vessel.

The results have shown the potential severity of a partially-filled interconnected vessel, and that the mechanisms of flame and pressure development were found to be similar to those reported in the literature for fully-filled systems. In particular, the mechanism of pressure piling was evident for all of the investigated fuels, despite the fact that the equivalent concentration would be outside the normal flammable range, and so be considered safe. It was deemed that the very severe explosions observed in the secondary vessel occurred due to the displaced unburned gases from the primary vessel, which ignited before the gases could mix with the air in the secondary vessel, and this indicated fast turbulent combustion in the displaced flammable gases.

As an additional danger, certain propane-air and hydrogen-air mixtures were shown to produce a short detonation-like event upstream of the leading flame front propagation, in the primary vessel. This work found the cause of these pressure spikes to be due to auto-ignition of the unburned pockets of mixture in the primary vessel, at a time delay corresponding to the backward propagation of a secondary explosion or burn-up event in the duct. There was evidence of reverse flow from the secondary vessel explosion back into the primary vessel, and subsequent turbulence generation and fast flame development in the primary vessel. Further expansion of these fast primary flame gases into the secondary vessel eventually resulted in a further reverse flow into the primary

vessel, followed by autoignition of the remaining unburned gases in the corner regions of the primary vessel, with a corresponding rapid pressure rise.

This evidence poses an interesting problem for the design of safety vessels for near lean limit concentrations based on data obtained from homogeneous tests. The danger of under-designing on this basis is evident. If the mixture became stratified, higher $(dP/dt)_{max}$ would be observed and faster transmission of explosion could occur, so protection mechanisms may not be adequate if guided by homogeneous test data.

8.2. Recommendations for Future Work

Throughout the course of this research, several additional areas have presented themselves as potential points of interest for further investigation. Whilst ideally such areas would have been covered in the current work, restrictions of time have prevented all of the avenues being explored. Below are listed several possible directions through which to take this research forward.

The current research with its predominantly experimental nature lends itself well to the development and validation of computational modelling packages. In this regard, a pilot study has been undertaken using the explosion modelling package FLACS. Initial comparisons of results relating to gas dispersion and explosion parameters were quite good. However, further research in this area is clearly required. Furthermore, the results can and should be used to test correlations arising from the work of other researchers in the field which have been developed for other geometries. The development of a new correlation to fit the data obtained here is the next logical step in this direction.

In terms of further experimental works which could benefit the research, there are many avenues which could be explored, including the effect of scale, the addition of a vent burst disk to simulate an initially closed vent, the addition of a vent pipe with a diameter larger than that of the vent for vented explosions, additional gas-air mixtures.

The nature of the external explosion is one of great importance to the research in terms of safety data collation as it will give an indication of the distances that personnel and

sensitive equipment should be located away from the potential danger area to reduce cost and loss of life/injury. A more in depth investigation into the effect of the external explosion is possible in the current geometry since the vessel is connected to the dump vessel.

Furthermore, in vented vessels, it is not often the case that the vent would be open to the atmosphere, i.e. $P_{stat} = 0$. In this respect, the investigation of an explosion in a vented vessel protected by a vent with a low P_{stat} would beneficial to the progression of this research. Based on the current comparisons between stratified gas explosions in closed and vented vessels, it would be expected that the explosion severity of stratified mixtures increases where there is the addition of a vent burst disc. It would also be interesting to compare results obtained from such a test series with those obtained in literature for homogeneous mixtures where up to 4 pressure peaks are observed on the pressure trace, relating to (1) vent burst, which would have been followed by Taylor instabilities caused by the flame being accelerated in the unstable direction, (2) secondary ignition of the unburned gases forced ahead of the flame causing an external explosion followed by the onset of Helmholtz oscillations, which in turn can induce Taylor instabilities within the vessel as the flame is driven in the unsteady direction, particularly for central ignition, (3) flame interaction with the vessel walls, and finally (4) a high frequency acoustic peak linked to the coupling of the combustion process with the acoustic modes of the vessel thereby setting up sustained pressure oscillations satisfying the Rayleigh criterion [43]. It is not expected, however, that the severity will reach that of the homogeneous stoichiometric mixtures, and that homogeneous will still pose the overall worst case in most scenarios.

8.3. Final remarks

The phenomena discussed in this thesis illustrate the difficulty in designing adequate protection for such vented, duct vented and interconnected geometries, since even a relatively small pocket of weak fuel-air mixtures produced relatively severe explosions. This can have implications for the safety design of inter-connected installations which are not intended to be subject to flammable mixtures.

Stratified mixtures with global equivalence ratio around stoichiometric produced significantly lower pressures than their homogeneous equivalents. However, stratified (globally) near-limit mixtures produced overpressures that were several hundred mbar higher than those of the equivalent homogeneous mixtures. Even beyond the flammable range (globally) the stratified mixtures produced significant overpressures.

While it is an important conclusion from the work presented in this chapter that close to the flammability limits the stratified explosion severity was greater than its global concentration would normally indicate, it should be stressed that homogeneous stoichiometric tests still constitute the worst case tests. Therefore, it is not the suggestion of this work that the design of vented vessels should be modified to represent the maxima obtained in stratified work. However, the value of this research in the field of post-explosion investigation is clear.

REFERENCES

1. Cullen, W.D., *The public inquiry into the Piper Alpha disaster*. 1990, HMSO: London.

2. Kletz, T., *Piper alpha: latest chapter in a long story*. Journal of Loss Prevention in the Process Industries, 1991. 4(4): p. 277-278.

3. Phylaktou, H.N. and G.E. Andrews, *Gas explosions in linked vessels*. Journal of Loss Prevention in the Process Industries, 1993. 6(1): p. 15-19.

4. Razus, D., et al., *Transmission of an explosion between linked vessels*. Fire Safety Journal, 2003. 38: p. 147-163.

5. Maremonti, M., et al., *Numerical simulation of gas explosions in linked vessels*. Journal of Loss Prevention in the Process Industries, 1999. 12: p. 189-194.

6. NFPA 68, *Guide for Venting of Deflagration, National Fire Protection Association*. 2002, Quincy.

7. *prEN 14994:2004(E) Draft European Standard on Gas explosion venting protective systems*. 2004.

8. Ponizy, B. and J.C. Leyer, *Flame Dynamics in a Vented Vessel Connected to a Duct: 1. Mechanism of Vessel-Duct Interaction*. Combustion and Flame, 1999. 116: p. 259-271.

9. Lunn, G.A., *Venting Gas and Dust Explosions - A Review*. 1984: The Institution of Chemical Engineers.

10. Lewis, B. and G. von Elbe, *Combustion, Flames and Explosion of Gases*. 1951, New York: Academic Press Inc.

11. Bartknecht, W., *Explosions: Course, Prevention, Protection*. 1981, International: Springer-Verlag.

12. Hertzberg, M. *The flammability limits of gases, vapors and dusts: theory and experiment*. in *Proceedings of the International Conference of Fuel-Air Explosions*. 1982. Montreal, Canada.

13. Coward, H.F. and G.W. Jones, *Limits of flammability of gases and vapors*, in *US Bureau of Mines Report No. 503*. 1952, United States Government Printing Office: Washington.

14. Mullins, B.P. and S.S. Penner, *Explosions, Detonations, Flammability and Ignition*. 1959, International: Pergamon Press. 287.

15. Bartknecht, W., *Explosions: Course, Prevention, Protection*. 1980, International: Springer-Verlag.

16. Nettleton, M.A., *Gaseous detonations: Their nature, effects and control*. 1987, London: Chapman and Hall.

17. Phylaktou, H.N., G.E. Andrews, and P. Herath, *Fast flame speeds and rates of pressure rise in the initial period of gas explosions in large L/D cylindrical enclosures*. Journal of Loss Prevention in the Process Industries, 1990. **3**: p. 355-364.

18. Cashdollar, K.L. and e. al, *Flammability of methane, propane, and hydrogen gases*. Journal of Loss Prevention in the Process Industries, 2000. **13**: p. 327-340.

19. Zabetakis, M.G., *Flammability characteristics of combustible gases and vapors*, in *US Bureau of Mines Bulletin 627*. 1965, United States Bureau of the Interior: Washington.

20. Bjerketvedt, D., J.R. Bakke, and K. van Wingerden, *Gas Explosion Handbook*. Journal of Hazardous Materials, 1997. **52**: p. 1-150.

21. Phylaktou, H., *Important parameters in turbulent explosions*, in *CPD short course on gas, vapour and dust explosion hazards: Protection, mitigation and prediction*. 2006, University of Leeds (Unpublished).

22. Phylaktou, H., Y. Liu, and G.E. Andrews, *Turbulent explosions: A study of the influence of obstacle scale*. IChemE Symposium Series, 1994. **134**: p. 269-284.

23. Harris, R.J., *The Investigation and control of gas explosions in buildings and heating plants*. 1983, London: E & FN Spon. 194.

24. Bartknecht, W., *Explosions-Schultz*. 1993, Berlin: Springer-Verlag. Chapter 10 (854-868).

25. Bone, W.A. and D.T.A. Townend, *Flame and Combustion in Gases*. 1927, New York: Longmans, Green and Co. Ltd. 548.

26. Khitrin, L.N., *The Physics of Combustion and Explosion (Translated from Russian)*. 1962, London: Ann Arbor-Humphrey Science Publishers Ltd.

27. Williams, F.A., *Combustion Theory: The fundamental theory of chemically reacting flow systems*. 2nd ed. 1985, Wokingham, UK: The Benjamin/Cummings Publishing Company Inc.

28. Strehlow, R.A., *Combustion Fundamentals.* 1984, London: McGraw-Hill Book Company.

29. Strehlow, R.A., *Fundamentals of Combustion.* 1968, Scranton, Pennysylvania: International Textbook Company.

30. Markstein, G.H., ed. *Non-steady flame propagation.* 1964, Pergamon Press: Oxford.

31. Dorofeev, S.B., A.V. Bezmelnitsin, and V.P. Sidorov, *Brief Communication: Transition to detonation in vented hydrogen-air explosions.* Combustion and Flame, 1995. 103: p. 243-246.

32. Dorofeev, S.B., V.P. Didorov, and A.E. Dvinishnikov, *Deflagration to Detonation Transition in Large Confined Volume of Lean Hydrogen-Air Mixtures.* Combutstion and Flame, 1996. 104: p. 95-110.

33. Gelfand, B.E., et al., *Detonation and Deflagration Initiation at the Focusing of Shock Waves in Combustible Gaseous Mixture.* Shock Waves, 2000. 10: p. 197-204.

34. Alekseev, V.I., et al., *Experimental study of flame acceleration and the deflagration-to-detonation transition under conditions of transverse venting.* Journal of Loss Prevention in the Process Industries, 2001. 14: p. 591-596.

35. Smirnov, N.N. and V.F. Nitkin, *Effect of Channel Geometry and Mixture Temperature on Detonation-to-Deflagration Transition in Gases.* Combustion, Explosion and Shock Waves, 2004. 40(2): p. 186-199.

36. Lee, J.H. and I.O. Moen, *The mechanism of transition from deflagration to detonation in vapour cloud explosions.* Progress in Energy and Combustion Science, 1980. 6(4): p. 359-389.

37. Willacy, S.K., et al., *Detonation of Hydrogen in a Partially Filled Interconnecting Vessel Following an Initial Period of Pressure Piling.* Combustion Science and Technology, 2006. 178(10-11): p. 1911-1926.

38. NFPA, *68: Standard on explosion protection by deflagration venting.* 2007 Edition, Quincy.

39. McCann, D.P.J., G.O. Thomas, and D.H. Edwards, *Gasdynamics of vented explosions part I: Experimental studies.* Combustion and Flame, 1985. 59: p. 233-250.

40. Leyer, J.C. and N. Manson. *Development of vibratory flame propagation in short closed tubes and vessels.* in *13th Symposium (International) on combustion.* 1971. Salt Lake City, Utah, USA: The Combustion Institute.

41. Ferrara, G., et al. *Duct-vented propane/air explosions with central and rear ignition.* in *Proceedings of the International Association for Fire Safety Science Symposium.* 2005. Beijing, China.

42. Harris, G.F.P. and P.G. Briscoe, *The venting of pentane vapour/air explosions in a large vessel.* Combustion and Flame, 1967. **11**(4): p. 329-338.

43. Cooper, M.G., M. Fairweather, and J.P. Tite, *On the mechanisms of pressure generation in vented explosions.* Combustion and Flame, 1986. **65**: p. 1-14.

44. Solberg, D.M., J.A. Pappas, and E. Skramstad. *Observations of Flame Instabilities in Large Scale Vented Gas Explosions.* in *18th International Symposium on Combustion.* 1980. University of Waterloo, Canada.

45. Kordylewski, W. and J. Wach, *Influence of ducting on explosion pressure: Small scale experiments.* Combustion and Flame, 1988. **71**: p. 51-61.

46. van Wingerden, C.J.M. and J.P. Zeeuwen, *On the role of Acoustically Driven Flame Instabilities in Vented Gas Explosions and their Elimination.* Combustion and Flame, 1983. **51**: p. 109-111.

47. Batley, G.A., et al., *A numerical study of the vorticity field generated by the baroclinic effect due to the propagation of a planar pressure wave through a cylindrical premixed laminar flame.* Journal of Fluid Mechanics, 1994. **279**: p. 217-237.

48. McIntosh, A.C., *Deflagration fronts and compressibility.* Philosophical Transactions of the Royal Society, 1999. **357**: p. 3523-3538.

49. Van Wingerden, C.J.M. and J.P. Zeeuwen. *Venting of gas explosions in large rooms.* in *4th International Symposium on Loss Prevention and Safety Promotion in the Process Industries: Chemical Process Hazards.* 1983.

50. Ponizy, B. and J.C. Leyer, *Flame Dynamics in a Vented Vessel Connected to a Duct: 2. Influence of Ignition Site, Membrane Rupture and Turbulence.* Combustion and Flame, 1999. **116**: p. 272-281.

51. Bouhard, F., et al., *Explosion in a vented vessel connected to a duct.* Progress in Astronautics and Aeronautics, 1991. **134**: p. 85-103.

52. Medvedev, S.P., et al. *Initiation of upstream-directed detonation induced by the venting of gaseous explosion.* in *25th Symposium (International) on Combustion.* 1994: The Combustion Institute.

53. Wiekema, B.J., H.J. Pasman, and T.M. Groothuizen. *The effect of tubes connected with pressure relief vents.* in *2nd International Symposium on Loss Prevention and Safety Promotion in the Process Industries.* 1977.

54. Ponizy, B. and B. Veyssiere, *Mitigation of explosions in a vented vessel connected to a duct.* Combustion, Science and Technology, 2000. **158**: p. 167-182.

55. Liebman, I., J. Corry, and H.E. Perlee, *Flame propagation in layered methane-air systems.* Combustion Science and Technology, 1970. **1**: p. 257-267.

56. Rasbash, D.J., D.D. Drysdale, and N. Kemp. *Design of an explosion releif system for a building handling liquified gases.* in *IChemE Symoposium Series No. 47: Process Industry Hazards.* 1976.

57. NFPA, *68: Guide for Venting of Deflagration.* 2002 Edition, Quincy.

58. kumar, R.K., W.A. Dewit, and D.R. Greig, Combustion Science and Technology, 1989. **66**: p. 251-266.

59. Lunn, G.A., D. Crowhurst, and M. Hey, *The effect of vent ducts on the reduced explosion pressures of vented dust explosions.* Journal of Loss Prevention in the Process Industries, 1988. **1**: p. 182-196.

60. Ural, E.A., *A simplified method for predicting the effect of ducts connected to explosion vents.* Journal of Loss Prevention in the Process Industries, 1993. **6**(1): p. 3-10.

61. Singh, J., *Gas Explosions in inter-connected vessels: pressure piling.* IChemE Symposium Series, 1994. **134**: p. 195-212.

62. Alexiou, A., H. Phylaktou, and G.E. Andrews. *Gas explosions in three interlinked vessels.* in *Proceedings of the 1st international seminar on fire and explosion hazards of substances and venting of deflagrations.* 1995. Moscow, Russia.

63. Di Benedetto, A., E. Salzano, and G. Russo, *Predicting pressure piling by semi-empirical correlations.* Fire Safety Journal, 2005. **40**: p. 282-298.

64. Griffiths, J.F. and J.A. Barnard, *Flame and combustion.* Third ed. 1995, London: Blackie Academic and Professional.

65. Jimenéz, C., et al. *Numerical simulations of combustion into a lean stratified propane-air mixture.* in *Center for Turbulance Research Proceedings of the Summer Program 2000.* 2000.

66. Jimenéz, C., et al., *Numerical Simulation and Modeling for Lean Stratified Propane-Air Flames.* Combustion and Flame, 2002. **128**: p. 1-21.

67. Tamanini, F. *Partial-volume deflagrations – characteristics of explosions in layered fuel/air mixtures.* in *3rd International Seminar on Fire and Explosions Hazards of Substances.* 2000. Windermere, UK.

68. Tamanini, F., *Engineering Predictions of Explosive Layer Formation in Flammable-Liquid Spills.* Combustion and Flame, 2002. **174**(11&12): p. 223-239.

69. Hirano, T., et al. *Flame propagation through mixtures with a concentration gradient.* in *16th Symposium (International) on Combustion.* 1976.

70. Phillips, H. *Flame in a buoyant methane layer.* in *10th Symposium (International) on Combustion.* 1965.

71. Feng, C.C., S.H. Lam, and I. Glassman, *Flame propagation through layered fuel-air mixtures.* Combustion Science and Technology, 1975. **10**: p. 59-71.

72. Cleaver, R.P., M.R. Marshall, and P.F. Linden, *The build-up of concentration within a single enclosed volume following a release of natural gas.* Journal of Hazardous Materials, 1994. **36**: p. 209-226.

73. DeHaan, J.D., et al., *Deflagrations involving stratified heavier-than-air vapor/air mixtures.* Fire Safety Journal, 2001. **36**: p. 693-710.

74. Whitehouse, D.R., D.R. Greig, and G.W. Koroll, *Combustion of stratified hydrogen-air mixtures in the 10.7 m^3 Combustion Test Facility Cylinder.* Nuclear Engineering and Design, 1996. **166**: p. 453-462.

75. Girard, P., et al. *Flame propagation through unconfined and confined hemispherical stratified gaseous mixtures.* in *17th Symposium (International) on Combustion.* 1978. University of Leeds, UK.: The Combustion Institute.

76. Furuno, S., S. Iguchi, and T. Inoue, *Lean Combustion Characteristics of Locally Stratified Charge Mixture: Basic Studies Of In-Vessel Combustion Ignited By Laser.* JSAE Review, 1995. **16**
p. 357-361.

77. Ishikawa, N., *Flame Propagation in Time-Independent Concentration Gradient Fields.* Combustion Science and Technology, 1983. **35**: p. 207-213.

78. Kaptein, M. and C.E. Hermance. *Horizontal propagation of laminar flames through vertically diffusing mixtures above a ground plane.* in *16th Symposium (International) on Combustion.* 1976.

79. Tamanini, F. and J.L. Chaffee. *Combustion behavior of stratified propane/air layers simulating flammable liquid spills.* in *Mediterranean Symposium on Combustion.* 1999. Antalya, Turkey: The Combustion Institute & ICHMT.

80. Tamanini, F. *Progress Towards the Development of Scenario-Specific Explosion Protection Design Guidelines.* in *Proceedings of the 2nd International Seminar on Fire-and-Explosion Hazard of Substances and Venting of Deflagrations.* 1997. Moscow, Russia: All-Russian Institute for Fire Protection.

81. Ishikawa, N., *Flame Structure and Propagation Through an Interface of Layered Gases.* Combustion Science and Technology, 1983. **31**: p. 109-117.

82. Tamanini, F. and J.L. Chaffee, *Mixture reactivity in explosions of stratified fuel/air layers.* Process Safety Progress, 2000. **19**(4): p. 219-227.

83. Hartley, L.J. and J.W. Dold, *Flame propagation in a nonuniform mixture: analysis of a propagating triple-flame.* Combustion Science and Technology, 1991. **80**: p. 23-46.

84. Dold, J.W., *Flame propagation in a nonuniform mixture: analysis of a slowly varying triple flame.* Combustion and Flame, 1989. **76**: p. 71-88.

85. van Oijen, J.A. and L.P.H. de Goey, *A numericla study of confined triple flames using a flamelet-generated manifold.* Combustion Theory and Modelling, 2004. **8**: p. 141-163.

86. Willacy, S.K., et al. *Medium scale duct vented explosions of stratified propane-air mixtures.* in *Proceedings of the European Combustion Meeting (CD format).* 2005. Louvain-la-Neuve, Belgium.

87. Gardner, C.L., *Turbulent combustion in obstacle-accelerated gas explosions - the influence of scale.* 1998, University of Leeds: Leeds.

88. Phylaktou, H.N., *Gas explosions in long closed vessels with obstacles*, in *Department of Fuel and Energy.* 1993, University of Leeds: Leeds.

89. Herath, P., *Closed vessel explosions: the influence of baffles*, in *Fuel and Energy.* 1986, University of Leeds: Leeds.

90. Starke, R. and P. Roth, *An experimental investigation of flame behaviour during cylindrical vessel explosions.* Combustion and flame, 1986. **66**: p. 249-259.

91. Ellis, O.C.d.C., *A history of fire and flame.* 1st Edition ed. 1932, United Kingdom: The poetry lovers fellowship.

92. Blevins, R.D., *Formulas for natural frequencycombustion frequency and shape.* 1979, London: van nostr and Reinhold Company.

93. Strehlow, R.A., A.J. Crooker, and R.E. Cusey, *Detonation initiation behind an accelerating shock wave.* Combustion and Flame, 1967. **11**: p. 339-351.

94. DeGood, R. and K. Chatrathi, *Comparative analysis of test work studying factors influencing pressures developed in vented deflagrations.* Journal of Loss Prevention in the Process Industries, 1991. **4**: p. 297-304.

95. Swift, I. and e. al, *Venting Deflagrations-Theory and Practice.* Plant/Operations Progress, 1984. 3(2): p. 89-93.

96. Molkov, V.V. *Theoretical generalization of international experimental data on vented gas explosion dynamics.* in *First International Seminar on Fire-and-Explosion Hazard of Substances and Venting of Deflagrations*. 1995.

97. Alexiou, A., H. Phylaktou, and G.E. Andrews, *The effect of vent size on pressure generation in explosions in large L/D vessels.* Combustion, Science and Technology, 1996. **113-114**.

98. Molkov, V., A. Baratov, and A. Korolchenko, *Dynamics of gas explosions in vented vessels: Review and progress.* Progress in Astronautics and Aeronautics, 1993. **154**: p. 117-131.

99. Molkov, V.V. *Venting of Gaseous Explosions: Turbulization Aspect*. in *Proceedings of the 1st Asian Conference on Fire Science*. 1992.

100. Pappas, J.A. *Venting of large-scale volumes*. in *The control and prevention of gas explosions: Conference transcripts*. 1983: Oyez Scientific andd Technical Services.

101. Bradley, D. and A. Mitcheson, *The venting of gaseous explosions in spherical vessels. I - Theory.* Combustion and Flame, 1978. **32**: p. 221-236.

102. Bradley, D. and A. Mitcheson, *The venting of gaseous explosions in spherical vessels. II - Theory and experiment.* Combustion and Flame, 1978. **32**: p. 237-255.

103. Catlin, C.A., *Scale effects on the external combustion caused by venting of a confined explosion.* Combustion and Flame, 1991. **83**: p. 399-411.

104. Chow, S.K., et al., *An Experimental Study of Vented Explosions in a 3:1 Aspect Ratio Cylindrical Vessel.* IChemE B: Process Safety and Environmental Protection, 2000. **78**(B6): p. 425-433.

105. Kumar, R.K., T. Skraba, and D.R. Greig, *Vented combustion of hydrogen-air mixtures in large volumes.* Nuclear Engineering and Design, 1987. **99**: p. 305-315.

106. Hu, J., Y. Pu, and F. Jia, *Study of gas combusiton in a vented cylindrical vessel.* Combustion Science and Technology, 2005. **177**: p. 323-346.

107. McCann, D.P.J., G.O. Thomas, and D.H. Edwards, *Gasdynamics of Vented Explosions. Part II: One-Dimensional Wave Interaction Model.* Combustion and Flame, 1985. **60**: p. 63-70.

108. Tamanini, F. and J.L. Chaffee. *Turbulent vented gas explosions with and without acoustically-induced instabilities*. in *24th Symposium (International) on Combustion*. 1992: The Combustion Institute.

109. Chippett, S., *Modelling of vented deflagrations.* Combustion and Flame, 1984. **55**: p. 127-140.

110. Du, Z., et al., *The investigation of correlated factors of external explosion during the venting process.* Journal of Loss Prevention in the Process Industries, 2006. **19**: p. 326-333.

111. Forcier, T. and R. Zalosh, *External pressures generated by vented gas and dust explosions.* Journal of Loss Prevention in the Process Industries, 2000. **13**: p. 411-417.

112. Jiang, X., et al., *Experimental investigations on the external pressure during venting.* Journal of Loss Prevention in the Process Industries, 2005. **18**: p. 21-26.

113. Molkov, V., *Unified correlations for vent sizing of enclosures at atmospheric and elevated pressures.* Journal of Loss Prevention in the Process Industries, 2001(14): p. 567-574.

114. Molkov, V. and e. al, *Modeling of vented hydrogen-air deflagrations and correlations for vent sizing.* Journal of Loss Prevention in the Process Industries, 1999. **12**: p. 147-156.

115. Palmer, K.N. and P.S. Tonkin. *External pressures caused by venting gas explosions in a large chamber*. in *3rd International Symposium on Loss Prevention and Safety Promotion in the Process Industries*. 1980. Basel, Switzerland.

116. Singh, J., *Sizing vents for gas explosions.* Chemical Engineering, 1979: p. 103-109.

117. Hjertager, B.H., M. Bjørhghaug, and K. Fuhre, *Explosion propagation of non-homogeneous methane-air clouds inside an obstructed 50 m3 vented vessel.* Journal of Hazardous Materials, 1988. **19**: p. 139-153.

118. Kitagawa, T., et al., *Flame propagation into lean region in stratified methane mixture.* SAE Transactions, 2002. **111**(4): p. 1221-28.

119. Badr, O. and G. Karim, *Flame propagation in stratified methane-air mixtures.* Journal of Fire Sciences, 1984. **2**: p. 415-426.

120. Bakke, P. and S.J. Leach, *Methane roof layers*, in *Safety in Mines Research Establishment Research Report*. 1960, Ministry of Power. p. 1-62.

121. Kang, T. and D.C. Kyritsis, *Methane flame propagation in compositionally stratified gases.* Combustion Science and Technology, 2005. **177**: p. 2191-2210.

122. Ishikawa, N., *Combustion of stratified methane/air layers.* Combustion Science and Technology, 1983. **30**: p. 311-325.

123. Ishikawa, N., *A diffusion combustor and methane-air flame propagation in concentration gradient fields.* Combustion Science and Technology, 1983. **30**: p. 185-203.

124. Tamanini, F., *Vent sizing in partial-volume deflagrations and its application to the case of spray dryers.* Journal of Loss Prevention in the Process Industries, 1996. **9**(5): p. 339-350.

125. Fairweather, M. and M.W. Vasey. *A mathematical model for the prediction of overpressures generated in totally confined and vented explosions*. in *Nineteenth Symposium (International) on Combustion*. 1982: The Combustion Institute.

126. Iida, N., O. Kawaguchi, and G. Takeshi Sato, *Premixed flame propagating into a narrow channel at high speed, Part 1: Flame behaviours in the channel.* Combustion and Flame, 1985. **60**: p. 245-255.

127. Willacy, S.K., et al. *Stratified Propane-Air Explosions of Global Concentration Outside Normal Flammability Limits*. in *Proceedings of the 2nd International Conference on Safety & Environment in Process Industry*. 2006. Naples, Italy.

128. Ferrara, G., et al. *Venting of premixed gas explosions with a releif pipe the same area as the vent*. in *Procedings of the European Combustion Meeting (CD format)*. 2005. Louvain-la-Neuve, Belgium.

129. Willacy, S.K., et al., *Ignition of Stratified Propane-Air Explosions in a Duct Vented Geometry: Effect of Concentration, Ignition and Injection Position.* IChemE B: Process Safety and Environmental Protection, 2006. **85**(B2): p. [Article in Press].

130. Kanzleiter, T.F. and K.O. Fischer, *Multi-compartment Hydrogen Deflagration Experiments and Model Development.* Nuclear Engineering and Design, 1994. **146**: p. 417-426.

131. Lunn, G.A., et al., *Dust explosions in totally enclosed interconnected vessel systems.* Journal of Loss Prevention in the Process Industries, 1996. **9**(1): p. 45-58.

132. Holbrow, P., S. Andrews, and G.A. Lunn, *Dust explosions in interconnected vented vessels.* Journal of Loss Prevention in the Process Industries, 1996. **9**(1): p. 91-103.

133. Roser, M., et al., *Investigations of flame front propagation between interconnected process vessels. Development of a new flame front propagation time prediction model.* Journal of Loss Prevention in the Process Industries, 1999. **12**: p. 421-436.

134. Willacy, S.K., et al., *Partially Filled Interconnected Vessel Explosions: Methane-Air in the Lean to Stoichiometric Range.* Journal of the Energy Institute, 2006. **73**(3): p. 152-157.

135. Willacy, S.K., et al. *Explosions in a partially filled interconnected vessel using methane-air in the lean to stoichiometric range.* in *Proceedings of the European Combustion Meeting ECM2005 (CD format).* 2005. Louvain-la-Neuve, Belgium.

136. Willacy, S.K., et al. *Propane-air explosions in a partially filled interconnected vessel.* in *Proceedings of the 5th International Seminar on Fire and Explosion Hazards.* 2007. Edinburgh.

137. Morley, C. *GASEQ Version 0.78 [Online].* 2004 January 2005]; Available from: http://www.gaseq.co.uk/.

Appendix 1

1. The power was switched on to the test equipment, data logger and computers (the data logger was switched on prior to the computer otherwise the connection would not be registered);
2. Pre-test audible check of spark;
3. The pipes connecting the fuel line and barocel were connected to the test vessel and ambient conditions were recorded on the test sheet;
4. All valves in the system were closed and checked, including those in the piping;
5. The test vessel was evacuated to < 30 mbar using Vac B, and monitored using the barocel;
6. When adequate vacuum pressure was achieved, the valve connecting the rig to the pump was closed, the vac was stopped and the vacuum integrity was checked to be < 2 mbar/min leak rate;
7. The fuel line was made live by opening all of the valves between the fuel cylinder to the test vessel;
8. The required mixture was prepared using either the homogeneous or stratified technique as described in sections 3.7.1 and 3.7.2;
9. Once fuel filling was complete, all of the valves connecting the fuel bottle to the rig were closed and the connection removed (and connected to the ignition safety circuit);
10. If the ambient pressure was higher than 1013.3 mbar (test vessels 1 & 4 only) the valves were closed prior to reaching this pressure and air slowly allowed in to test pressure, if the ambient pressure was lower than 1013.3 mbar, the valves to the ambient were closed and the vessel was topped up with air to 1013.3 mbar. For test vessels 2&3, the volume of the dump vessel and mixture preparation method for the stratified mixtures meant that tests were conducted at 'day ambient' pressure, therefore valves were left open to equalise with the ambient air;

11. the barocel was used to monitor the pressure in the test vessel and dump volume/secondary vessel until both were equal and fluctuations had ceased, for stratified mixtures;
12. at t = 4 min post injection, samples were taken from the test vessel using the procedure described in Chapter 3;
13. All valves were closed, in both the primary and secondary/dump vessels, barocel connection removed ;
14. The test room was checked to ensure no personnel remained and the partition doors were closed and locked from the test room side,
15. The data-logging system was activated and armed to trigger in coincidence with the ignition, ensuring that sufficient time-base had been selected to capture the full explosion (this varied dependent upon concentration);
16. At t = 5 minutes post injection, the gate valve was activated (where connected) and once fully opened (indicated on the ignition safety circuit light board) the 'FIRE' button was pressed firmly once;
17. At the end of data-logging the data-file generated was saved with a unique test number;
18. The partition door was unlocked (severing the ignition circuit) and the test room was safe to enter;
19. The system was purged dependent upon configuration (see below)

Purging of the system

1. The large valve connecting Vacuum B to the dump vessel was opened;
2. Vacuum pump B was started;
3. The barocel pipe was connected and the separating valve opened slowly to allow slow equalisation of pressure across the valve;
4. The pressure was monitored to ensure that it was below ambient day pressure, then one valve was opened in the test vessel, a large 2" valve half opened in the main section of the dump volume and another smaller valve on the far end of the 6m extension arm to the dump volume;
5. The vacuum was left running for > 10 minutes pulling the contaminated air through the pump, to be replaced with clean ambient air;

6. After the 10 minute purge, the valve connecting the vacuum pump to the dump vessel was closed and all the ambient valves opened fully to allow the vessel to return to ambient conditions;
7. The gate valve and all valves in the test volume were closed,
8. The valve connecting Vacuum pump B to the test volume was opened, and the pump started;
9. Pressure was monitored to below 50 mbar, then the valve closed and the pump stopped;
10. All valves to the ambient were opened and the vessel allowed to equalise to ambient pressure;
11. Steps 7-11 were repeated
12. The vessel was made safe by leaving at least one valve in each section open to the ambient to prevent subsequent pressure difference between the vessel and the ambient air on the test room.